MICROSTRUCTURE AND PROPERTIES OF TRANSPARENT GLASS - CERAMICS

by

ANDREW J. STRYJAK B.Sc.

A thesis submitted for the degree of

Doctor of Philosophy

of the University of Warwick

Department of Physics
University of Warwick

February, 1977

CONTENTS

ACKNOWLEDGEMENTS

I would like to thank Professor A.J.Forty for making available to me the facilities of the Department of Physics at the University of Warwick. I should like to thank Dr. P.W. McMillan for his continued interest and encouragement throughout the course of this work, and for the careful reading of the manuscript. I am grateful to all those members of the academic and technical staff who have assisted me during the course of this work and in particular Mr. A.A.Draper for introducing me to the art of glass-making.

My thanks are due to the Science Research Council and to Thorn Lighting Ltd. for the provision of a CAPS Research Studentship.

Finally, I wish to thank my wife for her unfailing understanding and encouragement throughout the period of this work, and for her care and attention in typing this thesis.

MEMORANDUM

This dissertation is submitted to the University of Warwick in support of my application for admission to the degree of Doctor of Philosophy. It contains an account of my work carried out at the Department of Physics of the University of Warwick in the period October 1973 to October 1976 under the general supervision of Dr. P.W. McMillan. No part of it has been used previously in a degree thesis submitted to this or any other University. The work described is the result of my own independent research except where specifically acknowledged in the text.

February, 1977 Andrew J.Stryjak

To my wife and my parents

whose encouragement and support were invaluable.

List of Figures

List of Tables

ABSTRACT

The overall aim of the research programme was to produce a transparent glass-ceramic suitable for high temperature lamp applications, and to correlate microstructural parameters with physical properties.

The experimental study included a detailed analysis of the microstructure of a transparent glass-ceramic comprising tetragonal zirconia and zinc aluminate (gahnite) crystals in a high glassy phase.

Thermal expansion coefficients were measured for a selection of glass-ceramics and found to be compatible with the expansion coefficients of certain metals used as current leads in lamp construction.

Density, microhardness and mechanical strength measurements were determined and correlated with the particle size, volume fraction and mean free path of the crystalline species.

The degree of transparency was investigated by optical transmission techniques in the visible and near infra-red ranges.

An investigation into the chemical compatibility in selected lamp vapours and at high temperatures was undertaken with good stability occurring for bromine, and sodium iodide and scandium iodide lamps.

Electron spin resonance was used to investigate colour centre formation due to sodium vapour exposure, and was also shown to be an invaluable tool in monitoring the crystallization process.

CHAPTER 1

General Introduction

1.1. Introduction

Glass-ceramics, which are polycrystalline materials produced by the controlled nucleation and crystallization of special glass compositions and which have outstanding physical properties, are now well known. The first practical glass-ceramics were developed by Corning Glass Works and were derived from glasses of the lithium aluminosilicate type.

In recent years the border between traditional ceramics on the one hand and glass technology on the other hand has become more and more vague. In the past the highest ideal of the glassmaker and the glass technologist has been to compound and to manufacture transparent glass, if possible without heterogeneities (crystallizations, bubbles) and without inhomogeneities (striae), and a great deal of effort has been spent on trying to realise this ideal.

However, it has been found in the past twenty five years that partially crystallized vitreous systems have quite interesting properties. Once the glass scientist had succeeded in controlling the crystallization of vitreous systems, as far as grain size and chemical composition of the crystals were concerned, materials with very remarkable properties were obtained, and these materials are known as glass-ceramics (McMillan, 1964).

The preparation of a satisfactory glass-ceramic depends on devitrifying or crystallizing a suitable glass composition under strictly controlled conditions in order to provide a closely interlocking microcrystalline structure and a smooth uncrazed surface. In order to do this it has generally been necessary to include in the glass a material which will provide nuclei for subsequent crystal growth or control of crystal formation in such a manner that many crystals of the desired form grow simultaneously in the glass.

In glass-ceramics, the crystalline phases are produced entirely by crystal growth from a glass phase which is homogeneous. This distinguishes these materials from traditional ceramics where most of the crystalline material is introduced when the ceramic composition is prepared. Some recrystallization may occur or new crystal phases may arise due to solid state reactions. Glass-ceramics are distinguished from glasses by the presence of major amounts of crystals, since glasses are non-crystalline or amorphous.

The production of glass-crystalline materials is possible because of the discovery of the catalytic crystallization method, the essence of which is the simultaneous growth of crystals from a large number of nuclei which are uniformly distributed in the pre-shaped glass article. Crystallization produces a very fine-grained and uniform structure, resulting in very good mechanical, thermal and electrical properties of these materials.

1.2. History and Development

For centuries the glassmaker has been trying to avoid crystallization, because it degraded his product, and because he did not know how to control it. Morey (1954) described devitrification as "the chief factor which limits the composition range of practical glasses, and is an ever-present danger in all glass manufacture and working".

A few researchers, however, thought otherwise. One of the earliest references to an attempt to use the crystallization of glass to advantage was made by Réaumur (1739), who attempted to crystallize soda-lime-silica bottles. He showed that if glass bottles were packed into a mixture of sand and gypsum and subjected to red heat for several days they were converted into opaque porcelain-like objects. Although Réaumur was able to convert glass into a polycrystalline ceramic, he was unable to achieve the control of the crystallization process which is necessary for the production of true glass-ceramics. The materials produced by his process

had low mechanical strengths, and distortion of the articles during the heat-treatment process occurred.

Little further work was done until the early 1900's. At this time Tammann(1925) investigated crystallization in detail and through theoretical and experimental investigations supplied the basis for much of our present understanding of the nucleation and crystallization process. Blau (1933) illustrated the importance of controlled crystallization, and in the 1950's and 1960's there was accelerated interest in controlled crystallization aided by nucleation promoters.

About two hundred years after Réaumur's work, research carried out at the Corning Glass Works led to a development of glass-ceramics in their present form. The first important step was the discovery of photosensitive glasses. These contain small amounts of copper, silver or gold, which can be precipitated in the form of very small crystals during heat-treatment of the glasses. The precipitation process occurs much more readily if the glasses are irradiated with ultra-violet light before heat-treatment and , by selective irradiation using a suitable mask or negative, a photographic image can be produced in the glass. Further work showed that photosensitive glasses could be made opaque in the irradiated regions by the precipitation of further crystals on the original metallic crystals.

Stookey (1953) made an important discovery when he heated the photosensitively opacified glass to a higher temperature than that normally employed in the heat-treatment process. He found that,instead of melting, the glass was converted into an opaque polycrystalline ceramic material. This material had a much higher mechanical strength than the original glass and much improved electrical insulation characteristics. The conversion from glass to glass-ceramic was accomplished without distortion of the articles and with only minor changes in dimensions. This material represented the first true glass-ceramic. Apparently, the small metallic crystals acted as nucleation sites for the crystallization of major phases

from the glass. The large number of nuclei present and their uniform distribution throughout the glass ensured that crystal growth proceeded uniformly and that a skeleton of crystals was produced to maintain the rigidity of the glass article as its temperature was raised.

In the manufacturing process of a glass-ceramic the initial step is the preparation of a glass which is shaped in its molten state to produce the article of the required form. The glassware is next subjected to a controlled heat-treatment cycle bringing about nucleation and crystallization of various crystal phases to produce the final polycrystalline ceramic. Since molten glass can be obtained in the homogeneous condition, uniformity of chemical composition can easily be achieved for glass-ceramics. The homogeneity of the parent glass and the control of the heat-treatment result in a glass-ceramic having a very fine-grained uniform structure free from porosity.

An important feature of the glass-ceramic process is that it is applicable to a wide range of compositions and many variations can be applied in the heat-treatment process. Therefore, various crystal types can be developed in controlled proportions. As a result, the physical characteristics of glass-ceramics can be varied in a controlled manner. This has a significant bearing upon the practical applications of glass-ceramics.

1.3. Nucleation and Crystallization

A glass exists in a state of metastable equilibrium and this metastable condition has a free energy higher than that of the corresponding mixture of crystalline phases of the same composition. In order to be transformed from the metastable to the stable state it must undergo two types of reaction, namely nucleation and crystal growth.

When a liquid is cooled below its melting point, crystallization does not occur by an instantaneous and homogeneous transformation of the material from liquid to solid. It occurs by the growth of crystals at a finite

rate from a finite number of centres or nuclei. For many materials the rate of crystal growth is high and the number of nuclei formed per unit volume is large; these materials do not form glasses. Glass-forming materials are those which do not readily crystallize on cooling. Glass formation may be attributed to a low rate of crystal growth, a low rate of formation of nuclei or to a combination of the two.

At the melting point the free energy of a given quantity of a material is the same whether the material is crystalline or liquid. At lower temperatures, the crystalline form has the lower free energy and the liquid will crystallize if nuclei are available. Suitable nuclei may have been present in the liquid even above the melting point. They could be particles of foreign material, minute fragments of incompletely melted crystal or favourable sites on the wall of the containing vessel. In the absence of nuclei of this nature it is necessary to consider the rate at which they form spontaneously in the liquid. The formation of a nucleus in a liquid clearly involves the creation of a crystal-liquid interface. Although there is a decrease in free energy when the material forming the nucleus transforms from the liquid to the crystalline state, the formation of a crystal-liquid interface at the nucleus surface involves a free energy increase, which may in fact be greater than the free energy decrease associated with crystallization. If this occurs, the nucleus will be unstable. Stable nuclei only form at a detectable rate when the liquid is supercooled to below a critical temperature, the degree of supercooling required depending on the relative magnitudes of the interfacial free energy and the free energy of crystallization. The rate of nucleus formation is given by

$$I = A \exp(-\Delta G/kT) \qquad (1.1)$$

The exponential term in ΔG describes the thermodynamic barrier to nucleation, where ΔG is the free energy of formation of a nucleus of critical size; for the case of formation of a spherical nucleus

$$\Delta G = \frac{16\pi (\Delta f_s)^3}{3 (\Delta f_v)^2} \qquad (1.2)$$

where Δf_s is the energy per unit area of surface between the two phases, and can be equated to the interfacial tension, σ, and Δf_v is the change of free energy per unit volume resulting from the transformation from one phase to the other. Equation (1.2) in fact is very similar to the Gibbs equation for W, the work done to form a spherical mass of a new phase B within the mother phase A,

$$W = \frac{16\pi\sigma^3}{3(p''-p')^2} \qquad (1.3)$$

where σ is the interfacial energy

p' is the pressure within the phase A

p'' is the pressure within the phase B

The pre-exponential factor A, in equation (1.1) represents the kinetic probability of a molecule crossing the interface from the matrix to the particle,

$$A = n \nu \exp (-\Delta G'/kT) \qquad (1.4)$$

where $\Delta G'$ is the free energy of activation for the motion of molecules across the matrix-nucleus interface, n is the number of molecules of the nucleating species per unit volume , and ν is the vibrational frequency of molecules at the nucleus-liquid interface.

Hence combining equations (1.1) and (1.4) the rate of nucleus formation is

$$I = n \nu \exp (-\Delta G /kT) \exp (-\Delta G'/kT) \qquad (1.5)$$

The equation predicts that the rate of nucleus formation should be very sensitive to variations in temperature, since it depends on ΔG which varies rapidly with temperature. The rate of nucleus formation does not increase indefinitely as the temperature falls. Eventually the second exponential factor, called the kinetic barrier to nucleation, begins to exert a con-

trolling influence.

The application of the above classical theory has several disadvantages. It is unsafe to assume that the interfacial energy for a flat interface can be applied to particles of very small radius,i.e. to particles containing only a small number of molecules. As the radius increases, the interfacial tension,σ, becomes a function of size. Furthermore, for small clusters of molecules, the concept of a surface breaks down particularly in glasses with network structures.

Once a stable nucleus has formed, it will continue to grow at a rate determined by the rate at which the atoms necessary for its growth can diffuse to the surface of the crystal, and by the ease with which they can free themselves from the attractions of their neighbours in the liquid phase and form new bonds in positions determined by the structure of the growing crystal. Early treatments of the kinetics of crystal growth were based on a model which involved the building up of a crystal plane by plane. When one plane of atoms was complete, it was necessary to form a two-dimensional nucleus on the surface of the completed plane before the next could begin to grow. The equations governing the temperature dependence of the rate of crystal growth based on this model were very similar to equation (1.5.) for the rate of nucleus formation, (Stanworth, 1950). It is now recognised that two-dimensional nucleation is not an essential feature of the process. All real crystals contain spiral dislocations, which make possible the continuing growth of a crystal without any need for the repeated nucleation of new crystal planes.

The full mathematical treatment of homogeneous and heterogeneous nucleation and crystallization is well developed, with excellent reviews given by McMillan (1964), Rawson (1967), Rogers (1970), Uhlmann (1971), Doremus (1973), Jackson (1974), Hopper et al. (1974), James (1974), Vreeswijk et al. (1974), Cotterill et al. (1975), Scholes et al. (1975), Scholes (1975), Amato et al. (1975), Ookawa (1975) and Binder & Stauffer (1976).

These authors have pointed out that the controlling factor, which

allows one to make conventional glasses without crystallization, is the very slow nucleation rate which implies the presence of a large energy barrier to nucleation. One cannot hope to develop a generalized picture of the nucleation mechanism, since it differs from nucleant to nucleant, It is, however, probably safe to say that, by one means or another, the nucleant causes a disproportion of the binding forces, which in turn introduce sites of lower thermodynamic stability.

Stookey (1954) has listed several important characteristics of an effective nucleating agent, since it is the nucleation process which is more critical than crystal growth in determining whether a satisfactory microcrystalline glass-ceramic can be produced:

(i) The nucleating agent should be readily soluble at melting and forming temperatures but only sparingly soluble at low temperatures.

(ii) It should have a low free energy of activation for homogeneous nucleation.

(iii) The nucleant atoms or ions must diffuse rapidly at low temperatures, unlike the major components of the glass.

(iv) The interfacial energy between the glass and nucleant must be low.

(v) The crystal structure and lattice parameters of the nucleant and the crystal phase to be developed should be as nearly the same as possible.

The first three factors govern the formation of the nucleus, the latter two govern the effectiveness of the nucleant as a crystal growth promoter. Factor (v) is not necessarily a requirement for all modes of nucleation.

With the expansion in new materials and therefore new compositions, new theories are constantly being proposed for nucleation and crystallization of glass systems.

1.4. Properties of Glass-ceramics.

Glass-ceramics are non-porous and generally have an opaque white appearance in the finished state, although some compositions may also be transparent (section 1.5.). Ceramics made by conventional techniques are often quite impermeable to liquids or gases, so that their porosity is effectively zero and they are vacuum tight.They are, however, rarely completely free from closed pores, e.g. 5 to 10% in a high-alumina ceramic. Glass-ceramics are entirely free from any type of porosity, which cannot develop during conversion from the glass to glass-ceramic because the overall volume changes are small. Quite often the volume change is a shrinkage, but even when the conversion is accompanied by a volume increase due to the production of crystals with a lower density than the original glass, voids do not develop within the material. The complete absence of pores in glass-ceramics is a characteristic which favours the development of good properties, since pores will reduce mechanical strength by diminishing the useful cross-section of the material. In addition, they may act as flaws at which internal fractures could originate.

Glass-ceramics resemble glasses in their ability to resist chemical attack and they compare favourably in this respect with other ceramic-type materials.

Generally speaking, glass-ceramics are strong compared with ordinary glasses and with most conventional ceramics. The complete absence of pores in a glass-ceramic contributes to high strength. In addition, the high abrasion resistance of glass-ceramics compared with ordinary glasses makes them less susceptible to the type of surface damage which produces stress-raising flaws. In comparison with glasses, it is possible that fractures are propagated with greater difficulty in glass-ceramics since a crack travelling through the material can be slowed down, diverted, or even stopped as it crosses boundaries between crystalline and vitreous phases. In a homogeneous glass there would be an uninterrupted fracture

path. The very fine grain size of glass-ceramics undoubtedly plays an important role in determining their mechanical strength. For conventional ceramics, it is known that a reduction in grain size leads to a significant increase in mechanical strength (Hayden et al., 1965). One of the reasons for the dependence of strength upon grain size is the existence of boundary stresses between adjacent crystalline or glass phases, which can be generated as the result of differential thermal contraction of the phases or due to the presence of a phase which exhibits marked differences in thermal expansion coefficients in different crystallographic directions e.g. quartz, aluminium oxide, and many others (McMillan, 1964).

The thermal expansion coefficients of glass-ceramics range from negative values, through zero, to positive values of around 110 x $10^{-7}{}^{o}C^{-1}$. Extreme heat-shock resistance and dimensional stability with temperature are available by choice of composition to provide coefficients of expansion near zero. The expansion characteristics of a glass-ceramic are markedly affected by the heat-treatment schedule, since this determines the properties and nature of the crystal phases present.

The moduli of elasticity for glass-ceramics are higher than those of ordinary glasses and some conventional ceramics, but they are lower than those of sintered pure oxide ceramics. For glasses, the modulus of elasticity,E, shows a roughly additive relationship with chemical composition. For glass-ceramics it is expected that the modulus of elasticity will be determined primarily by the elastic constants of the major crystalline phase, although the presence in the glass phase of oxides which promote the development of high values of E must be allowed for; in particular, calcium oxide, magnesium oxide and aluminium oxide appear to exert a marked influence upon the elastic moduli of glasses.

Glass-ceramics are electrical insulators and some types are characterised by exceptionally low values of dielectric loss factor at high frequencies and high temperatures, and a dielectric constant ranging from

5 to 10 at high frequencies. With regard to their electrical insulating properties, glass-ceramics are comparable to the better ceramic dielectrics.

Owing to their dense microstructure and absence of pores, glass-ceramics have a high electric strength at increased temperatures and high frequencies. According to Partridge and McMillan (1963), the electric strength of phosphate-containing glass-ceramics at increased frequencies and room temperature is higher than that for conventional ceramics, and is comparable to the electric strength of glass.

Glass-ceramics are heat-insulating materials. Glass has a low heat conductivity, which increases with temperature, whereas non-porous ceramics have a heat conductivity which is higher than that of glasses, and which decreases with increasing temperature. The heat conductivity of glass-ceramics is also greater than that of glasses, but lower than that of pure oxide ceramics, and it varies only slightly with temperature.

1.5. Transparent Glass-ceramics

1.5.1. Introduction

For the most part, glass-ceramics are non-transparent, i.e. opaque. However, a number of glass-ceramics containing not less than two crystalline phases have been prepared which are transparent, due to the absence of voids, and also due to the small crystal size and the absence of light scattering at the crystal boundaries which require good matching between the indices of refraction for the crystals and the glassy phase. In transparent glass-ceramics, the crystals are so small and so close in their indices of refraction that the material is as transparent as sheet glass, except that it may have a coloured tint.

1.5.2. Light Scattering Theory

Light energy can be attenuated or removed by a medium in two ways; atomic absorption which converts the light energy into heat in

the medium, or light scattering which involves the absorption and simultaneous re-radiation of energy by atomic, molecular or ionic species.

The scattering phenomenon is essentially due to the radiation of secondary waves caused by oscillating dipoles induced in heterogeneities in the medium through which the light is passing (Bleaney & Bleaney, 1968; Longhurst, 1970).

A light wave is constituted by electronic and magnetic vibrations in planes perpendicular to the direction of wave propagation. When an aggregate of atoms or ions such as the molecules in a gas or small crystallites in a glass-ceramic are subjected to an external electric field, dipoles which are induced by the field are formed in each element of volume. When the electric field is due to an electromagnetic wave, the induced dipoles themselves become radiators of electromagnetic waves and scattered light results.

The dependence of small particle scattering on the wavelength of light was first investigated by Rayleigh (1871,1881,1899). He considered an incident electromagnetic wave to be monochromatic and linearly polarized with the electric vector along the x-axis and the direction of propagation in the z-direction. The field at a scattering particle is then given by

$$E_x = e^{-j\omega t}$$
$$E_y = 0 = E_z \qquad (1.6)$$

Rayleigh assumed the scattering particle was small in comparison to the wavelength of light. The result was that the net scattered wave caused by the sinusoidal oscillations at a frequency ω of each of its elastically bound electrons was just that which would be radiated by a single dipole oscillator with some specific dipole moment.

The scattering cross-section for these particles as given by Rayleigh (1899) is

$$\sigma_s = \frac{8}{3\pi}\left(\frac{2\pi}{\lambda}\right)^4 \left|\beta\right|^2 \qquad (1.7)$$

where λ is the wavelength and β is the polarizability of the scattering material. Assuming independent spherical particles $|\beta|^2$ is given by

$$|\beta|^2 = \alpha^6 \left| \frac{M^2 - 1}{M^2 + 2} \right|^2 \qquad (1.8)$$

where α is the radius of the particle

M is the ratio of refractive index of the particle to that of the surrounding medium.

The angular intensive distribution of scattered light can therefore be written as

$$I(\theta) = \left(\frac{1 + \cos^2\theta}{r^2} \right) \frac{8\pi^4}{\lambda^4} \alpha^6 \left| \frac{M^2 - 1}{M^2 + 2} \right|^2 I_o \qquad (1.9)$$

where I is the specific intensity

θ is the scattering angle

r is the distance from the scattering centre

I_o is the intensity of the incident beam

From equation (1.9) it can be seen that the magnitude of Rayleigh (small-particle) scattering is inversely proportional to the fourth power of the wavelength. This form of scattering is characterized by a sharp scattering in the lower wavelengths.

From equation (1.9) it can also be seen that the criteria for complete transparency of a light transmitting material are twofold: (a) $\alpha \ll \lambda$, where the particles are very much smaller than the wavelength of light, or (b) $M \approx 1$, where the refractive indices of the particles and the surrounding medium approach equality. In addition, as a general condition for transparency, even in a homogeneous medium, absorption effects should be minimized.

The more general scattering problem, that of an isolated sphere of any diameter in an electromagnetic field of any character, has been investigated by Mie (1908). Detailed discussions of the theory may be found in Stratton (1944) and Orr and Dallavalle (1959). The theory finds major

applications where the simpler Rayleigh theory breaks down, i.e. where the size of the scattering particle is about the same size or larger than the wavelength of the incident radiation.

1.5.3. Systems

The first transparent glass-ceramics were prepared from titanium-containing lithium aluminosilicates at Corning Glass Works (1960), approximate composition in weight percent $68SiO_2 - 6TiO_2 - 5Li_2O - 21Al_2O_3$. If the heat treatment of these glasses does not exceed 900°C, then glass-ceramics are formed which are transparent with respect to visible wavelengths and which differ from the original transparent glasses only in having a lower thermal expansion coefficient (less than $10 \times 10^{-7}\ °C^{-1}$ as compared to greater than $30 \times 10^{-7}\ °C^{-1}$ for glass), by the presence of β-eucryptite and β-spodumene, and by the absence of deformation at temperatures below 1200°C. Herbert (1963) transformed a glass (composition in weight percent: $70{\cdot}9SiO_2 - 23{\cdot}3Al_2O_3 - 5Li_2O - 0{\cdot}IB_2O_3 - 0{\cdot}8TiO_2$) into a transparent glass-ceramic by crystallizing at 925°C for 12 hours.

Janakiramao (1964) prepared transparent glass-ceramics from glasses of the $K_2O - SiO_2 - TiO_2$ and $Bi_2O_3 - B_2O_3 - PbO$ systems. Here, glass of the composition (in weight percent) $30SiO_2 - 25K_2O - 45TiO_2$ with a thermal expansion coefficient, $\alpha = 110 \times 10^{-7}\ °C^{-1}$ was transformed into a transparent glass-ceramic with $\alpha = 94 \times 10^{-7}\ °C^{-1}$, whereas glass of the composition $35SiO_2 - 20K_2O - 45TiO_2$ with $\alpha = 94 \times 10^{-7}\ °C^{-1}$ was transformed into a semi-transparent glass ceramic with $\alpha = 92 \times 10^{-7}\ °C^{-1}$. Transparent glass-ceramics have also been prepared in the $MgO - Al_2O_3 - SiO_2$ system by Kalinin and Podushko (1964) based on cordierite, and in the $Li_2O - Ga_2O_3 - SiO_2$ system by Petrovski et al. (1964).

Kondrat'ev (1965) studied the dual role of TiO_2 in the formation of the structure of transparent crystalline glass materials in the $Li_2O - Al_2O_3 - SiO_2 - TiO_2$ systems.

Petrovski et al. (1965) performed a structural interpretation of the possibility of formation of transparent glass-ceramics in the systems $SiO_2 - Bi_2O_3 - SrTiO_3$ ($BaTiO_3$, $PbTiO_3$).

Corning Glass Works (1965) produced a transparent semi-crystalline ceramic body from the system $SiO_2 - Al_2O_3 - XO$ (where XO is $MgO + Li_2O + ZnO$) with ZrO_2 as the nucleating agent, resulting in β-quartz as the main crystalline phase. Duke et al. (1967) chemically strengthened various aluminosilicate transparent glass-ceramics by an ion exchange process in which the crystalline structure at the surface of the body was modified to produce a compressive layer. Beall et al.(1967) strengthened by ion exchange transparent glass-ceramics with β - quartz structure which was crystallized from most glasses in the systems $SiO_2 - Mg(AlO_2)_2 - LiAlO_2$ as well as from many containing additional components $Zn(AlO_2)_2$, $Al(AlO_2)_3$, Li_2ZnO_2 and Li_2BeO_2 nucleated with TiO_2 and ZrO_2.

Schleifer et al. (1968) succeeded in strengthening transparent glass-ceramics in the system $SiO_2 - Al_2O_3 - Na_2O - TiO_2$ by ion exchange of Na^+ for Li^+ to promote surface crystallization of β-eucryptite.

Vargin and Milyukov (1968) studied phase separation and crystallization in the $ZnO - Al_2O_3 - SiO_2$ system nucleated with TiO_2, and produced a transparent glass-ceramic with a gahnite phase ($ZnO - Al_2O_3$) when the amount of TiO_2 present was 5 mole percent.

Very important further work was performed by Beall and Duke (1968) on three main systems:

(i) That in which the major crystal phase is of the stuffed β -quartz type. This is based on $Li_2O - MgO - Al_2O_3 - SiO_2$ and $ZnO - MgO - Al_2O_3 - SiO_2$ glasses nucleated with ZrO_2. Buerger (1954) recognised that certain aluminosilicate crystals composed of three-dimensional networks of SiO_4 and AlO_4 tetrahedra are similar in structure to one or another of the crystalline forms of pure silica. These aluminosilicates were termed stuffed derivatives because they may be thought of as formed from a silica structure by network replacement of Si^{4+} by Al^{3+}, accompanied by a filling of

interstitial vacancies by larger cations to preserve electrical neutrality. As would be expected, considerable solid solution normally occurs between these derivatives and pure silica.

(ii) That in which the major crystalline phase is a spinel of the general formula AB_2O_4 where A is a tetrahedrally coordinated, generally divalent ion, and B is octahedrally coordinated, generally trivalent ion. The glass-ceramics are based on glasses of the $MgO - ZnO - Al_2O_3 - SiO_2$ type nucleated with ZrO_2. Up to 10% of an alkali metal oxide, such as K_2O or Cs_2O, can be added to prevent devitrification of the residual glass phase. This provides an example of a glass-ceramic where the crystallization is deliberately limited.

(iii) That in which the major crystalline phase is mullite. This is based on $Al_2O_3 - SiO_2$ glasses which can be heat-treated to precipitate the mullite in a finely divided form. Oxides such as BaO, Na_2O, K_2O, Rb_2O and Cs_2O are added in amounts up to 10% to prevent the siliceous residual glass from devitrifying to cristobalite.

Transparency in glass-ceramics of type (i) results from the optical isotropy of β-quartz and from satisfactory matching of the refractive indices of the crystals and residual glass. Thus, although the crystals are generally small, they can approach one micron without causing light scattering.

In the cases of spinel and mullite glass-ceramics, types (ii) and (iii), the crystals have to be very small (less than the wavelength of visible light, as mentioned in section 1.4.1.) to achieve good transparency. Both types contain a considerable proportion of residual glass and show gradual softening with an increase in temperature, but remain transparent when held at temperatures in excess of 1000°C.

In conjunction with type (iii), MacDowell and Beall (1969) observed immiscibility and crystallization in $Al_2O_3 - SiO_2$ glasses, and produced transparent glass-ceramics with mullite as the dominant crystalline phase.

Petzoldt(1970) studied transparent glass-ceramics in the system Li_2O - MgO - ZnO - Al_2O_3 - SiO_2 - P_2O_5 whereby β-quartz was the main crystalline phase produced.

From the above review, it can be seen that most of the transparent glass-ceramics are based on the aluminosilicate system. With these, depending on the crystalline phase present, a vast number of differing properties can be achieved.

1.5.4. Applications

The ultra-low thermal expansion of lithium stuffed β - quartz transparent glass-ceramics in lithium aluminosilicate systems as discussed by Duke and Chase (1968) could be used as mirror blank materials for high precision reflective-optic applications. It was found that when the grain size was kept smaller than the wavelength of visible light, an optical finish could be obtained with no evidence of relief polishing, due to the differential hardness between the phases. The transparent nature of these glass-ceramics allows inspection of the mirror blank for residual stress and quality.

The properties of magnesium - lithium - stuffed transparent β-quartz glass-ceramics (Beall and Duke, 1968) ranging from low thermal expansion, excellent chemical durability, thermal stability above 900°C and excellent transparency over all visible light wavelengths make them very useful for refractory applications such as high temperature lamp envelopes and oven windows.

Similarly, magnesium-zinc-stuffed glass-ceramics have been produced but with a slightly higher thermal expansion coefficient, excellent chemical durability combined with high temperature resistivity, and superior dielectric properties allow the consideration of these materials for a wide range of high temperature applications where low electrical losses are required.

Beall and Duke (1968) also investigated spinel and mullite transparent glass-ceramics (type (ii) and (iii); section 1.4.3). They found a moderate thermal expansion coefficient and excellent transparency when the glass-ceramics were heated in excess of 1000°C. High temperature lamp applications may therefore be considered where sealing to tungsten elements is necessary for expansion matching. These glass-ceramics are largely amorphous with only a small volume fraction of crystals. Considerable deformation occurs at higher temperatures, ruling out high temperature rigidity applications.

Beall (1972) produced transparent glass-ceramic articles comprising zinc spinel, and doping them with Cr_2O_3 resulted in red transparent materials which exhibited photoluminescence.

Neuroth (1975) produced transparent glass-ceramic laserable articles from the base glass system Li_2O - ZnO - Al_2O_3 - SiO_2 containing neodymium.

1.6. Choice of system

In choosing a glass-ceramic system for transparency, the requirements of extremely small particle size or complete optical isotropy must be combined with the desired physical characteristics which are defined by the application. For high temperature lamp applications a material is needed which has a high hardness and mechanical strength, good chemical and high temperature stability, and a moderate thermal expansion for sealing to metals used as filaments or supports in the lamps.

A degree of compositional flexibility is generally desired in order to minimise the grain size or to match the refractive index of an optically isotropic crystalline phase to that of the residual glass, and still produce such desired properties as a moderate thermal expansion coefficient and high mechanical strength.

One system of glasses with this flexibility, studied by Beall and Duke (1968), contains the basic oxides SiO_2 - Al_2O_3 - ZnO - ZrO_2.

In these the high index phase of spinel is the major crystalline phase. Transparency is therefore achieved by producing extremely fine crystals, much smaller than the wavelength of light. All the materials present, including the addition of alkaline earth metal oxides, can combine to produce a refractory material with a moderate thermal expansion suitable for sealing to tungsten. Excellent transparency can be achieved despite a large proportion of low-index siliceous residual glass.

This system was therefore chosen as the basis for the study of transparent glass-ceramics, with the aim of modifying the composition to achieve the high temperature lamp requirements, and of investigating the relationship between the microstructure and the physical properties.

1.7. Choice of Experiments

For the investigation of microstructure the usual methods of X-ray diffraction and electron microscopy were employed. A Differential Thermal Analysis apparatus was used to determine certain heat-treatment characteristics. Electron spin resonance was used, as a result of colour centre investigations, to study the crystallization process.

From the point of view of physical properties, experiments were chosen so as to be able to relate these properties with the microstructure and to determine properties necessary for the production of lamp envelopes. Such experiments were density, thermal expansion, hardness and mechanical strength measurements. The chemical stability was investigated in various lamp vapours. Electron spin resonance was again used to monitor the effect of colour centre formation due to sodium vapour attack.

The range of wavelengths and the degree of transparency over which the material transmitted was measured by visible and infra-red spectroscopy.

Finally, high temperature stability was investigated.

1.8. Plan of Thesis

The thesis is divided into seven chapters. Chapter II describes the general methods of investigating the physical properties of glass-ceramics, including methods of glass preparation.

Chapter III contains a description of the microstructural investigation techniques mentioned in section 1.6. together with a discussion of the quantitative and statistical analysis of volume fraction and particle size measurements.

Chapter IV accounts for the microstructure results. The X-ray diffraction section monitors the selection of compositions and their alteration in finding the correct crystalline phase. A detailed account is given of electron microscopy work, and of electron spin resonance investigations on the crystallization process.

Chapter V describes the physical property results with an attempt being made to relate the microstructure properties with the physical properties studied.

Chapter VI discussed the chemical stability of glass-ceramics with an outline of the experimental techniques. It was felt that these techniques would be incorporated in this chapter so as to keep the subject of chemical stability as a distinct unit. Electron spin resonance analysis of colour centre formation is described with optical transmission results and thermal bleaching. A brief section is given on the high temperature stability.

Chapter VII summarizes all the results, with a special emphasis put on unifying the physical and microstructural properties, with general comments on the successes and failures of the work.

A section is devoted to suggestions for future work in this field.

A list of references cited, in alphabetical order is given at the end of the thesis.

CHAPTER II

Physical Property Techniques

2.1. Introduction

In this chapter details are presented of the experimental techniques and apparatus used in the measurement of the physical properties of the transparent glass-ceramic under investigation.

The preparation of the parent glass and its crystallization into a glass-ceramic is described.

The apparatus and experimental procedures used in measuring the annealing and crystallization points, density, thermal expansion coefficients, hardness, modulus of rupture, and optical properties are reviewed.

2.2. Glass Preparation

The compositions of the glasses studied are given in Table 2.1.. These were chosen on the basis that they were expected to yield transparent glass-ceramics having thermal expansion coefficients in the medium range and thus suitable for sealing to tungsten for lamp construction. Also their melting temperatures were high and therefore they would be likely to produce refractory glass-ceramics.

The initial compositions were taken from a paper by Beall and Duke (1968).

All glasses were made up from batch materials of greater than 99·6% purity. The glasses were prepared from Brazilian quartz, ground so as to pass through a 30 mesh sieve, aluminium oxide, zinc oxide, magnesium oxide, calcium oxide (or calcium carbonate), barium oxide, and zirconium dioxide.

The starting materials were thoroughly dried, weighed and mixed in a rotary ball-mill for two hours. The batch was melted in a

	SiO_2	Al_2O_3	ZnO	MgO	CaO	BaO	ZrO_2	P_2O_5	other oxides
Glass 1	64·8	17·6	5·6	4·6	-	-	7·4	-	-
Glass 2	64·2	17·5	5·5	4·6	-	-	7·3	0·9	-
Glass 3	63·6	15·5	11·8	-	-	-	5·5	-	3·6 K_2O
Glass 4	50·0	40·0	-	-	-	10·0	-	-	-
Glass 5	62·5	17·6	5·5	7·0	-	-	7·4	-	-
Glass 6	60·2	17·6	5·5	9·3	-	-	7·4	-	-
Glass 7	61·1	20·4	5·5	5·5	-	-	7·4	-	-
Glass 8	63·6	17·3	5·5	4·5	-	-	9·1	-	-
Glass 9	63·1	17·1	5·4	4·5	-	-	9·0	0·9	-
Glass 10	64·2	17·4	5·5	4·6	-	-	8·3	-	-
Glass 11	63·6	17·3	-	10·0	-	-	9·1	-	-
Glass 12	63·6	17·3	5·5	-	4·5	-	9·1	-	-
Glass 12A	63·6	17·3	5·5	-	4·5	-	9·1	-	0·08 Fe_2O_3
Glass 13	63·6	17·3	5·5	-	-	4·5	9·1	-	-

Table 2.1. Glass compositions (wt.%).
(Glass 4 - Beall and Duke (1968) and glass 11 were initially made up but further work on these was halted).

platinum crucible at 1650°C in an electrically heated furnace until bubble-free, quenched in a melting mixture of ice and water and then crushed and dried. This process was repeated twice, with the object of achieving good homogeneity. The glasses were melted for approximately twenty hours and poured into slabs on a cast iron plate coated with a graphite suspension 'Aquadag' to prevent adhesion of the glass. In some cases, the plate was heated up to a temperature of 200°C to prevent thermal shock occurring, and in other cases the plate was initially cooled with liquid nitrogen to cool the glass rapidly to prevent phase separation.

The glasses were annealed at 780°C and subsequently heat-treated in static air in an electric furnace, employing Pt/Pt13% Rh thermocouples to control the temperature.

The range of temperatures over which the glass was annealed and then devitrified was that employed by Beall and Duke (1968).

2.3. Density

2.3.1. Introduction

The density of a glass-ceramic will be an additive function of the densities of the various crystal and glass phases present. Since the volume change occurring during conversion from a glass state to the glass-ceramic is usually small it would be expected that the effects of various oxides upon the densities of glass-ceramics would be similar to those observed with conventional glasses.

2.3.2. Experimental

Archimedes' method was used to measure the density with distilled water as the immersion liquid. For specimens of a regular shape, e.g. square or rectangular beams, the densities were measured by the direct method of mass divided by volume, and these results were compared with those of Archimedes' method. For each material six specimens were measured.

2.4. Thermal Expansion

2.4.1. Introduction

The dimensional changes which occur in a material with change in

temperature are of great importance. From a technological viewpoint, the themal expansivity is the most important thermal characteristic and for many applications, the ability to produce glasses and glass-ceramics with accurately controlled expansivities is vital. For example if a glass-ceramic is required to have a high thermal shock resistance, the coefficient of thermal expansion should be as low as possible to minimise strains resulting from temperature gradients within the material. Also, if the glass-ceramic is to be sealed or otherwise rigidly joined to another material, such as a metal, as in the case of envelopes for lamp bulbs or vacuum tubes, close-matching of the thermal expansion coefficients of not only the glass-ceramic, but also of the parent glass is necessary to prevent the generation of high stresses when the composite article is heated or cooled. Otherwise fracture of the glass or glass-ceramic will be encountered.

In certain applications, dimensional stability with change in temperature may be important and a glass-ceramic of near zero expansion coefficient would be required for this.

Glass-ceramics are remarkable for the wide range of thermal expansion coefficients which can be attained. At one extreme, materials having negative expansion coefficients are available while for other compositions very high positive coefficients are observed. Between these two extremes there exist glass-ceramics having expansion coefficients practically equal to zero and others, the expansion coefficients of which are similar to those of ordinary glasses or ceramics, or to those of certain metals or alloys.

As well as knowing the physical properties of the crystal phases present in a glass-ceramic, it is worthwhile also to be able to note the properties of the glassy matrix. Properties like thermal expansion, density and microhardness all follow an additive relation of the form

$$A = C_1X_1 + C_2X_2 + C_3X_3 \cdots \qquad (2.1)$$

where A is the complete glass-ceramic property parameter, C_i is the volume fraction of a particular phase, and X_i is the absolute value of the property under investigation for that phase.

2.4.2. Measurement of Thermal Expansion

The coefficients of thermal expansion of the glasses and transparent glass-ceramics were measured on a silica dilatometer. This consisted of a fused silica specimen holder and a linear variable differential transformer (L.V.D.T.). The L.V.D.T. produced an electrical signal proportional to the linear displacement of its core. The specimen holder was positioned vertically in a furnace and the expansion of the specimen was transmitted via a silica push rod to the core of the L.V.D.T.. The L.V.D.T. and the top of the push rod were kept at a constant temperature by passing water at 25°C around the system.

The specimen tube could reach a temperature of 1000°C and the L.V.D.T. sensitivity was 4·32mV per micron displacement of the push rod. The temperature of the specimen was measured with a chromel-alumel (T_1 versus T_2) thermocouple. The rate of rise of temperature of the furnace used was 1·73°C per minute by means of a cam.

The apparatus was designed to measure the expansion of specimens of up to approximately 6cm in length. In the present work, specimens approximately 5cm in length were used. For shorter specimens, it was found necessary to use silica spacers in the specimen holder. Output from the L.V.D.T. and the thermocouple e.m.f. of the specimen temperature were recorded against time on a two-pen chart recorder.

In the ideal case, whereby the specimen was of silica, the expansion would be independent of the temperature, i.e. the expansions of the holder and specimen would cancel each other. The expansion, therefore, of a glass or glass-ceramic specimen would then be measured relative to that of silica. In the apparatus used, it was found that the expansion of the silica spacers was a function

of holder temperature, probably due to temperature gradients across the holder. This expansion was accounted for in evaluating the expansion of a specimen. Five specimens of each material were measured.

If L_o is the length of the specimen at a temperature T_o, and L is the specimen length at a temperature T, the coefficient of thermal expansion, α, is given by

$$L = L_o\left[1 + \alpha(T - T_o)\right] \qquad (2.2)$$

2.5. Mechanical Properties.

2.5.1. Introduction

The mechanical strength of a material is one of its most important properties because it is often the major factor in determining the suitability of the material for a particular application. At room temperature, glass-ceramics, like ordinary glasses and ceramics, are brittle materials. They exhibit no region of ductility or plasticity and show perfectly elastic behaviour up to the load which causes critical failure.

In the present work, microhardness and three-point bending experiments were performed on several transparent glass-ceramics made.

2.5.2. Microhardness Measurements.

Hardness is not a fundamental physical property of a material, but rather it is a complex function of a number of physical properties which are combined in different degrees, depending on the method of test. In a sense, the hardness of a material can be equated with its resistance to abrasion or wear. For example, if a material which is to be used to build some mechanical apparatus is being selected, particular attention is paid to its behaviour under

load. The material of suitable shape and size must be strong enough to support any expected loads and stiff enough to prevent any elastic deflections. Although perhaps not quite so obvious, it is true that the mechanical properties are often a major factor in the selection of a material for many applications which are not primarily structural.

Glass is often preferred to transparent plastics for most windows and lenses because of its much greater resistance to scratching. Thus, the resistance of a material to abrasion under closely specified conditions may be taken as one measure of hardness.

A measure of hardness can be represented by the resistance to scratching of a material by other materials, or by depth of penetration of a loaded pyramid (usually diamond) into the material.

Indentation hardness has been widely applied in the metallurgical field, and this method has been used to study glasses and similar materials. Under suitable conditions, the point of a diamond pyramid will penetrate a glass surface, leaving a permanent indentation.

The mechanism by which the indentation is formed is complex and not fully understood. The fact that glass flows during indentation, resulting in a permanent impression, indicates plastic flow analagous to that which occurs in metals. Ernsberger (1961), however, believes that the yielding results from localised densification of the glass around the indenter, due to the extremely high stresses around the diamond tip. Douglas (1958) has shown that the indentation hardness is a function of the fictive temperature and viscosity of the glass.

In a glass-ceramic the flow mechanism which occurs when a surface is indented will be impeded by the presence of closely spaced phase particles. This will lead to a higher hardness than in the parent glass. This dependence of microhardness on crystalline

phase morphology present in the glass-ceramic has been reported by Watanabe et al. (1962), Tashiro and Sakka (1964), and Toropov and Sirazhiddinov (1966).

In the present work, values of the 'deformation hardness' were measured by the Vickers pyramid hardness test for glass and glass-ceramics specimens. This method was chosen because it is one of the most commonly used to measure the property generally defined as 'diamond pyramid hardness' or 'indentation strength '.

The Vickers Hardness Number, H_V, is a number related to the applied load and the surface area of the permanent impression made by a square-based pyramidal diamond indenter having face angles of 136 degrees.

The hardness, H_V, is defined as

$$H_V = \frac{2P \sin \alpha/2}{D^2} = \frac{1854P}{D^2} \text{ kg mm}^{-2} \qquad (2.3)$$

where P is the indenting load in grams

D is the mean value of the impression diagonal in microns

α is the 136° angle between opposite indenter faces.

The diamond indenter was incorporated in a McCrone microhardness apparatus mounted on an inverted optical microscope. Indentations were made on the surfaces of glass and glass-ceramic specimens polished to a one micron diamond paste finish.

A 1000 gram load was found to give easily measurable indentations. From equation (2.3) it can be seen that if the load is proportional to the square of the diagonal, the same hardness number is obtained whatever the load. This in fact has been investigated by Ainsworth (1954), Prod'homme (1968), and Turchinovich and Adler (1973), who concluded that the hardness was independent of load.

Ten indentations were made for each specimen with a time of 15 seconds at full load of the 1000 gram weight.

The diagonal lengths of the impression were measured with a calibrated eyepiece graticule. From the mean of each pair of diagonals of one indentation, the average and standard error of the whole series were calculated.

2.5.3. Three-Point Bending Measurements.

The three-point bend technique was used to determine the modulus of rupture and Young's modulus in bending of glass and glass-ceramic specimens.

In this method, a beam of the material of rectangular cross-section is placed across two parallel knife edges. A third knife edge is positioned exactly between and parallel to these knife edges and is lowered onto the specimen at a constant rate.

The modulus of rupture σ_F, of a rectangular bar for centre loading is determined from the expression

$$\sigma_F = \frac{3P_F L}{2bd^2} \qquad (2.4)$$

where P_F is the load to fracture

L is the distance between the outer knife edges

b is the width of the sample

d is the thickness of the sample

Young's modulus in bending, E_b, is determined from the force-deflection curve using the expression

$$E_b = \frac{PL^3}{4bd^3y} \qquad (2.5)$$

where y is the deflection corresponding to a load P.

A three-point bending jig with a 2cm. span between the outer knife edges was used on an Instron universal testing machine operating at room temperature and at a cross-head speed of

0·02cm min^{-1} to load the specimen. On average eight specimens were used for each strength determination.

The load was applied at a constant rate by a cross-head and was monitored against time on a chart recorder. This could then be used to draw a graph of load against displacement of the cross-head.

The effect of the condition of the surface on the mechanical strength of glasses and glass-ceramics has been investigated by Gordon et al. (1958), Brearley and Holloway (1963), Ray and Stacey (1969), McMillan et al. (1969), and Kay and Doremus (1974). Their investigations showed that a glass-ceramic which had been heat-treated to achieve a desired strength was weakened by a standard abrasion treatment.

In this present work the specimens for mechanical strength measurements were initially given a standard surface abrasion to reduce scatter in the results. This did not prove very satisfactory, therefore some glass-ceramics were given milder abrasion before heat-treatment, and others received no abrasion at all.

The specimens which were abraded received the standard abrasion treatment of 60 minutes in a rotary ball mill containing ≤ 100 mesh Carborundum powder in an amount corresponding to 20 times the weight of the specimens. The samples abraded before heat-treatment received the above treatment for 5 minutes.

The typical size of the specimens used was 25mm x 5mm x 3mm.

2.6. Optical Properties

2.6.1. Introduction

When a material is termed transparent, vagueness arises in the definition of the word transparent, since no strict rules

are applied for distinguishing between transparent and translucent. Similarly, if a material is called transparent, no mention is given of the wavelength range over which it transmits.

In general terms, for transparent glass-ceramics, the wavelength range is in the optical region from approximately 300nm to 700nm., and the transparency can mean that the material can transmit over approximately 70% of the incident light over most of the visible region.

In recent years many papers have been published on the near infra-red absorption bands in glasses. Most of the work has been performed on silicate, borate and phosphate glasses, although at the present time, more and more unusual compositions are being considered in the search for glasses with better infra-red transmissions.

2.6.2. Experimental Techniques

Optical transmission spectra were recorded in the ultra-violet range (250nm to 400nm) and in the visible region (350nm to 750nm) on a Perkin Elmer III spectrometer, and in the infra-red region (0.5 micron to 6 micron) on a Grubb Parsons Infra-red spectrometer.

Samples approximately 1mm in thickness were prepared by mounting in Specifix and polishing both sides with 600 grit Carborundum paper, and then on 6 micron and 1 micron diamond pasted pads. The specimens were then separated from Specifix and thoroughly cleaned.

Differences in thickness were recorded, due to different polishing rateson the rough 600 grit paper.

CHAPTER III

Structure and Microstructure Analysis

3.1. Introduction

In this chapter details are presented of the techniques used to investigate the microstructure of transparent glass-ceramic materials. The crystalline phases were commonly identified by conventional X-ray diffraction techniques. Transmission electron microscopy was used to study crystal morphology and the microstructure of samples removed at various stages in the crystallization sequence.

Methods of specimen preparation for X-ray diffraction, transmission and scanning electron microscopy are also described. A modified technique has been outlined for rapid mechanical thinning of specimens for transmission electron microscopy.

A review is given of the quantitative analysis of crystal phase parameters namely, particle size and volume fraction determinations.

Details are presented of basic electron spin resonance theory, and experimental techniques used in the study of the crystallization process utilising the presence of impurity ions in the glass systems.

3.2. X-Ray Diffraction

3.2.1. Preparation of Samples

The crystalline phases present in the glass-ceramics studied were determined by the evaluation of Debye-Scherrer powder X-ray photographs.

Debye-Scherrer samples were prepared by crushing the material into a fine powder and attaching it to a very thin Pyrex glass fibre, using a solution of Sellotape adhesive dissolved in chloroform. The Pyrex fibre alone produced a very diffuse halo, which was allowed

for in all X-ray photographs. The fibre with the powdered sample was attached to a Debye-Scherrer camera and was rotated in a beam of Copper K_{α} X-rays using a Phillips X-ray set. Standard operating conditions were employed, 40kV and 15mA, with an exposure time of four hours on Kodak X-ray film.

The position of the lines on the powder photograph was measured from a Joyce Loebl Mk.IIIc automatic recording densitometer trace of the film density along the photograph. Crystalline phases were identified from the calculated d-spacings and the ASTM X-ray powder data file.

Where broadening of the Debye rings occurred owing to the extremely fine crystal size, the diameter D of these crystals was estimated from the Scherrer formula for spherical particles (Cullity 1959, Guinier 1963)

$$\frac{0{\cdot}9\,\lambda}{(B^2-b^2)^{1/2}\cos\theta} \qquad (3.1)$$

where λ is the X-ray wavelength

θ is the Bragg angle

B is the observed line width at half-maximum intensity

b is the same with only instrumental boradening involved.

This formula is essentially valid when the particle size is less than 100nm. All diffraction lines have a measurable breadth, even when the crystal size exceeds 100nm, due to the divergence of the incident beam and size of the sample in Debye cameras.

The breadth $(B^2-b^2) = B_1^2$ refers to the extra breadth or broadening, due to the particle size effect above. In other words, B_1 is essentially zero when the particle size exceeds 100nm.

The best method of determining B_1 is to use a standard material which has a particle size much greater than 100nm, and which produces a diffraction line near to the line from the unknown. In practice

the method is useful only if the standard line is narrow compared with the line under investigation.

In the present case, the standard chosen was Brazilian quartz used in the preparation of the glasses. When quenched, the material consists of large crystals of α-quartz. The diffraction lines of the α-quartz were extremely narrow and measurements were performed on a strong line at $2\theta = 50{\cdot}1^{\circ}$, very close to another strong line, for example, in the case of tetragonal zirconia crystals, to $2\theta = 50{\cdot}6^{\circ}$.

The half-maximum width was evaluated from a microdensitometer trace.

3.3. Differential Thermal Analysis.

3.3.1. Introduction

In glassy or crystalline materials chemical reactions and structural changes are accompanied by an exothermic or endothermic effect. When a substance crystallizes, an exothermic effect occurs, since the free energy of the regular crystal lattice is less than that of the disordered liquid state.Conversely, the melting of a crystal gives rise to an endothermic effect. Differential Thermal Analysis (D.T.A.) enables these reactions or phase transformations to be investigated (Matusita et al. 1975, Briggs and Carruthers 1976).
In the case of a glass-ceramic, D.T.A. can be used to determine the transformation temperature T_g, crystallization temperature , and the temperature at which melting of the material occurs (Smothers and Chiang, 1958, Tudorovskaya and Sherstyuk, 1964).

In a D.T.A. apparatus, thermocouples are placed in close contact with two crucibles, each filled with a finely powdered and compressed sample, one of which is the substance under investigation, the other an inert reference material, the thermal properties of which are known. The thermocouples are connected with their e.m.f.'s opposed, so that the net e.m.f. represents the temperature difference between the sample and the reference material.

3.3.2. D.T.A. Apparatus

A D.T.A. apparatus was constructed to measure the differential e.m.f. between the reference material and the sample, and the temperature of one of these. Aluminium oxide was used as the reference material, as it is generally inert over the temperature range encountered. The two samples were contained in small platinum crucibles approximately 10mm high and 7mm in diameter. The sample and reference material were thoroughly crushed into powder in a pestle and mortar, and passed through a 300 mesh sieve, to ensure even particle size of both. A dimple was formed at the bottom of each crucible which then sat on the thermocouple assembly (McIntosh et al. 1974).

The temperature and differential e.m.f. were measured with a Pt/Pt13% Rh thermocouple. The crucibles were positioned close together in a special D.T.A. assembly (Thermal Syndicate Ltd.) made from recrystallized alumina, to ensure an identical rise in temperature for both crucibles. Fig. 3.1. illustrates the assembly with the crucibles positioned in place.

Preliminary experiments were carried out on sodium chloride to check the sensitivity of the instrument. Sodium chloride has a melting temperature of 804°C. This was used as a calibration of the apparatus. In some cases distilled water was added to the sample crucible to detect any peaks occurring at 100°C.

The differential e.m.f. was mechanically chopped and amplified with a low noise A.C. amplifier. This signal was detected and rectified by a phase sensitive detector. The mechanical chopper operated at 77 Hz. and was placed in the circuit so that the A.C. amplifier was never in open circuit. All electrical wiring was shielded from electrical interference. The rate of rise of the furnace temperature was chosen to be 5°C per minute. Fig. 3.2 shows a block diagram of the experimental arrangement and fig. 3.3. shows a photograph of the complete apparatus.

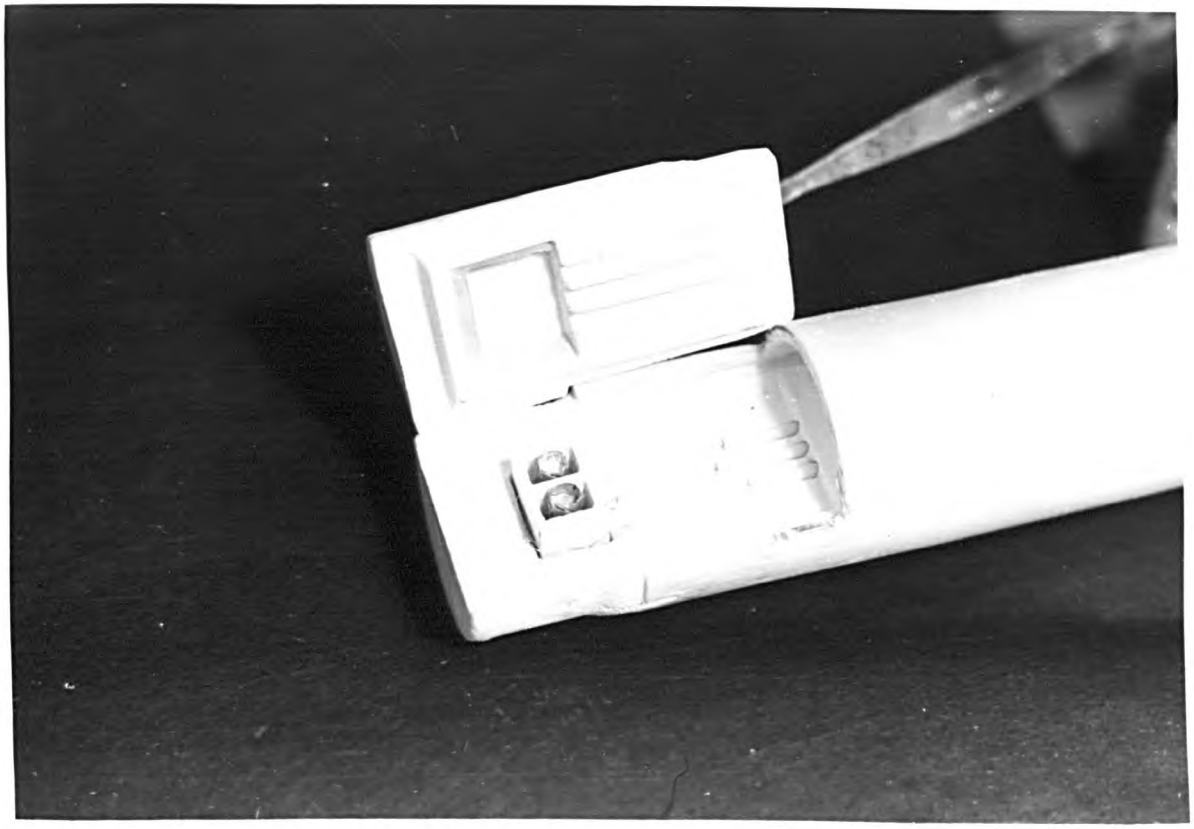

Fig. 3.1 D.T.A. assembly with crucibles.

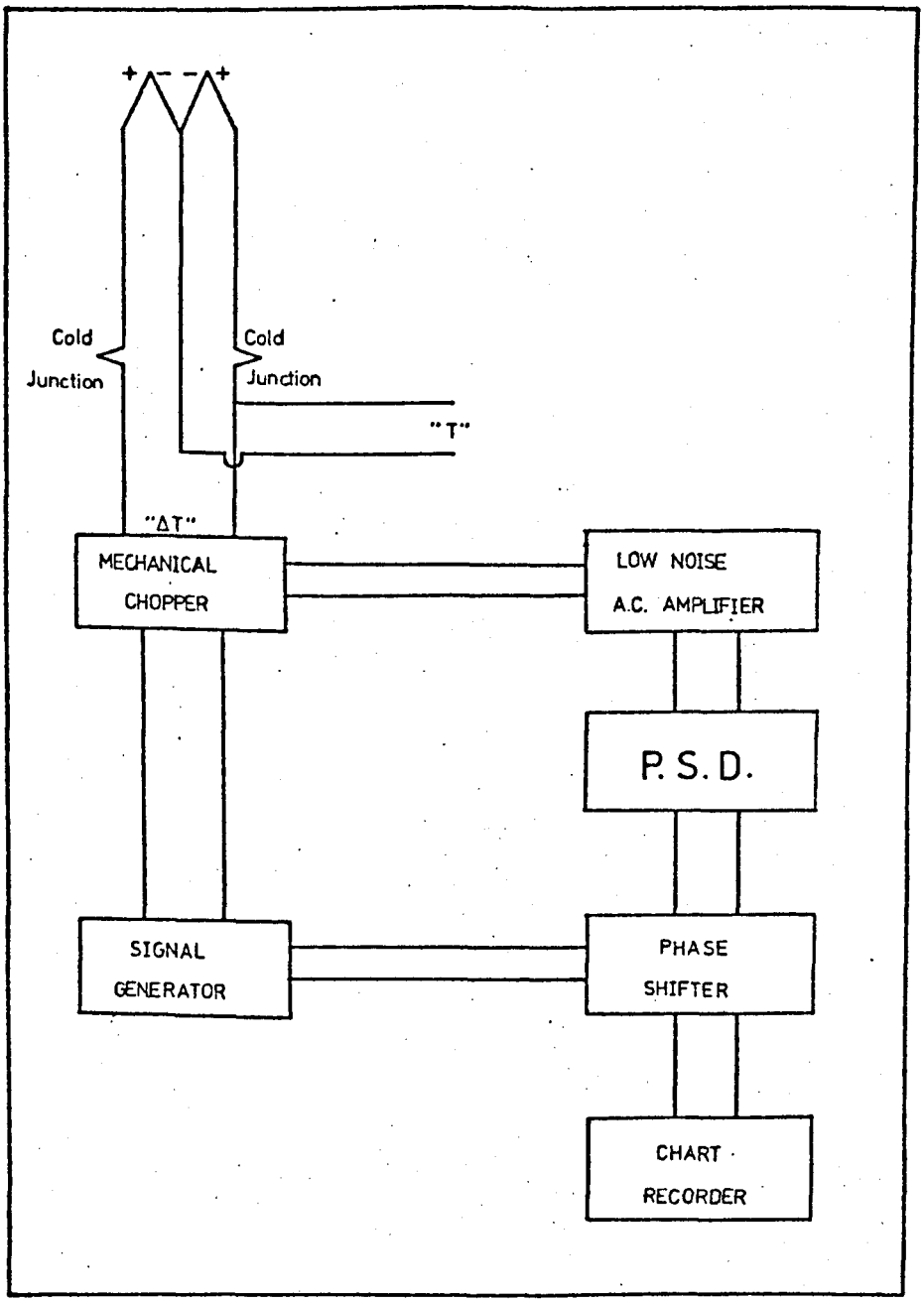

Fig. 3.2. Block diagram of D.T.A. apparatus.

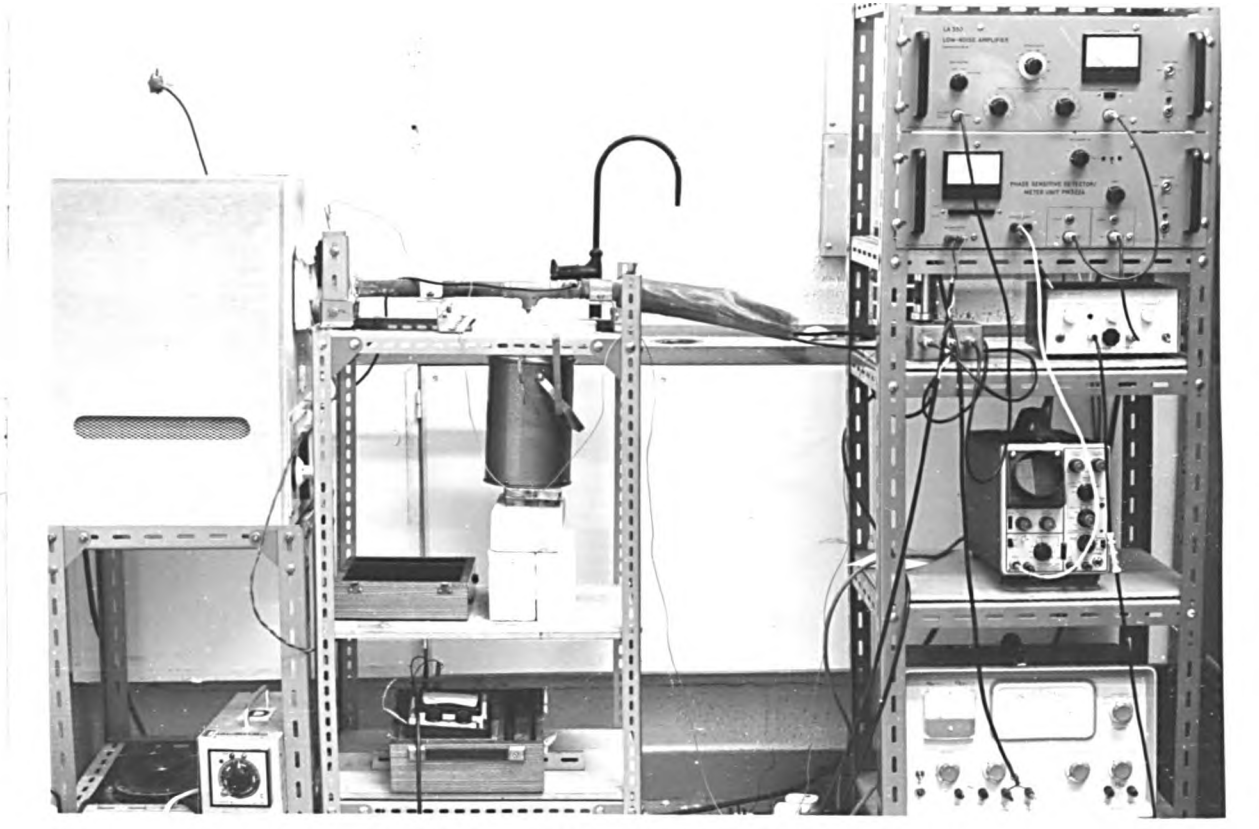

Fig. 3.3. D.T.A. apparatus.

Fig. 3.4. shows a typical D.T.A. curve. As the temperature increases, a dip A can be seen, due to the absorption of heat occuring when the glass transformation is reached. With a further temperature increase, a sharp exothermic peak B can be seen, corresponding to the presence of a crystal phase. A second exothermic peak C may occur at higher temperatures if any secondary crystalline phase appears.

Raising the temperature even further results in an endothermic effect D, representing the first melting of the crystalline phases.

Two glasses were studied by D.T.A., namely glass 1, giving the β-quartz crystalline phase, and glass 12 with the gahnite phase. Several interesting peaks were recorded which will be discussed in detail in chapter IV.

The D.T.A. curve can yield a great deal of useful information which is of assistance in devising heat-treatment schedules for glass-ceramics, since it not only indicates the temperature ranges in which crystallization occurs, but it also indicates the maximum temperature to which the glass-ceramics could be heated without encountering deformation due to melting of crystal phases. Having determined the D.T.A. curve, the exothermic peaks can be assigned to the crystallization of various phases. For this, glass specimens are heated in turn to maximum temperatures corresponding to the exothermic peaks and are then subjected to X-ray diffraction analysis. Unfortunately, many factors play a role in D.T.A. e.g. the rate of rise of the temperature and the particle size of the powdered samples (the smaller particles having a much higher specific surface area and hence surface nucleation plays a dominant role), so that D.T.A. is only an initial guide for subsequent heat-treatment schedules.

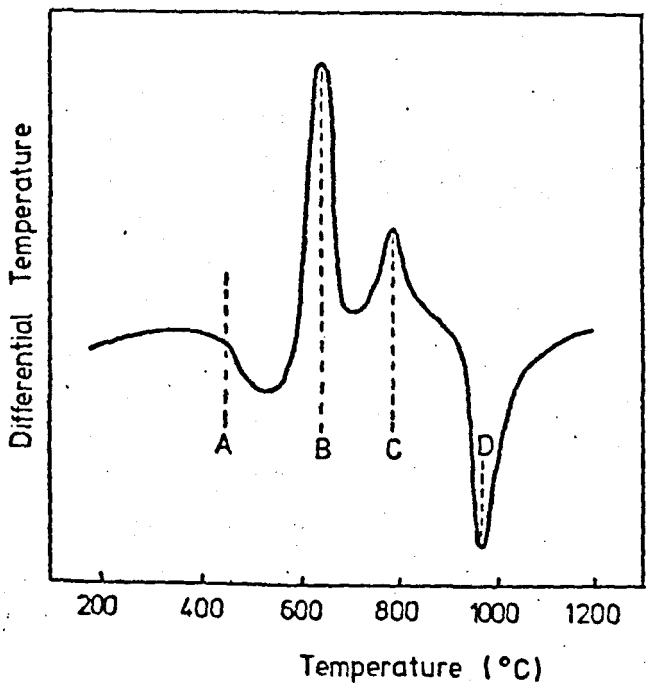

Fig. 3.4. Typical D.T.A. curve.

3.4. Transmission Electron Microscopy

3.4.1. Introduction

Transmission Electron Microscopy is one of the most useful techniques when studying the extremely fine nature of crystals in glass-ceramics. The main difficulty, though, in the investigation of glass-ceramic microstructures, especially transparent glass-ceramics, whereby crystals are found to be less than 100nm in size, is the preparation of sections, thin enough (less than 100nm) to transmit the electron beam. Several preparation methods have been investigated. The microscopes employed were a JEM 7 electron microscope operating at 100kV, a JEM 200 microscope operating at 200kV, and a JEM 100 C operating ar 100kV, fitted with an EDAX (Energy Dispersive Analysis of X-rays) attachment.

Most specimens were mounted in a $\pm$ 15° tilting stage.

3.4.2. Fragmentation

A relatively simple and quick method for producing thin areas for the study of brittle materials was found by Seward et al. (1967) and Turkalo (1968) to be the fragmentation technique.

Here a sample of the material to be studied was initially crushed in a percussion mortar and then ground into a fine powder, using an agate pestle and mortar. The powdered material was tapped out onto a clean microscope slide. A 100 mesh copper electron microscope grid, previously dipped in a solution of Sello-tape adhesive dissolved in chloroform, was pressed onto the finest fragments. The grid was inverted and gently tapped to remove any loose excess particles, and placed in the electron microscope specimen

holder. The grid was subsequently examined, and the positions of those chips containing regions thin enough for investigation were noted.

This method of specimen preparation was found to give only small areas that were thin enough to transmit the electron beam, and few particles were produced with such thin areas. Specimen charging was found to be a problem. This could be reduced by coating the specimen and grid with a thin layer of less than 30nm of evaporated carbon, or by using a copper grid, previously coated with a carbon film, before tapping the powdered specimen onto it. The latter method proved difficult, since Sellotape adhesive could not be used, because this would damage the carbon film, and hence the particles of powdered glass were lost during transportation to the microscope.

Fig. 3.5. shows a typical micrograph of a thin area prepared by this technique.

An advantage of the fragmentation technique is that it permits dark field image micrographs and selected area diffraction to be performed.

3.4.3. Carbon Replication

Much of the early microscopic work in materials science was performed on replicas of the specimen surface. While obviously giving very little insight into the internal structure of the specimen, replica techniques have several clear-cut advantages; firstly that the specimen need not be thinned to electron transparency, therefore requiring either no pre-treatment, or merely an established etch; secondly that the specimen itself need not be placed in the electron microscope; and thirdly, surface detail may be accentuated by shadowing.

Fig. 3.5. Typical transmission electron micrograph of glass-ceramic 1, prepared by the fragmentation technique.
(Mag. 100,000 : 1cm = 100nm).

The main limitations, however, are twofold; the internal microstructure cannot be examined and the surface, being replicated, must usually be destroyed to remove the replica.

The surface of the specimen to be replicated, approximately one square centimetre, was polished with 6 micron, followed by one micron diamond paste, and etched in a standard 5% solution of hydrofluoric acid. A 60 second etch with quite vigorous agitation was found to give the best results. The etching solution attacked the glass phase of the glass-ceramic, producing a surface topography.

According to Bradley (1954) and Vaisfeld (1971), it was found that to increase the contrast in the microsccpe, platinum had to be pre-shadowed onto the specimen (less than 10^{-4} torr). This was performed by making a solution of chloroplatinic acid dissolved in hydrochloric acid, and dipping a carbon rod into the solution, and gently heating in order to leave a deposit of platinum on the rod. Hence, during evaporation in vacuo at approximately 45° to the normal, the platinum evaporated first, followed by a layer of carbon onto the specimen surface.

Areas approximately 3mm square were scratched onto the surface of the specimen, and the replica was removed from the surface by slowly immersing the sample at an angle into a solution of 5% hydrofluoric acid (Siddall, 1960). After the immersions, the carbon film remained on the liquid surface. Each square was lifted onto a copper grid and refloated in distilled water in order to remove the acid solution. The replica was floated onto a copper grid, dried around the edges with filter paper, and finally dried under a lamp.

Fig.3.6. shows a typical pre-shadowed replica of a glass-ceramic surface.

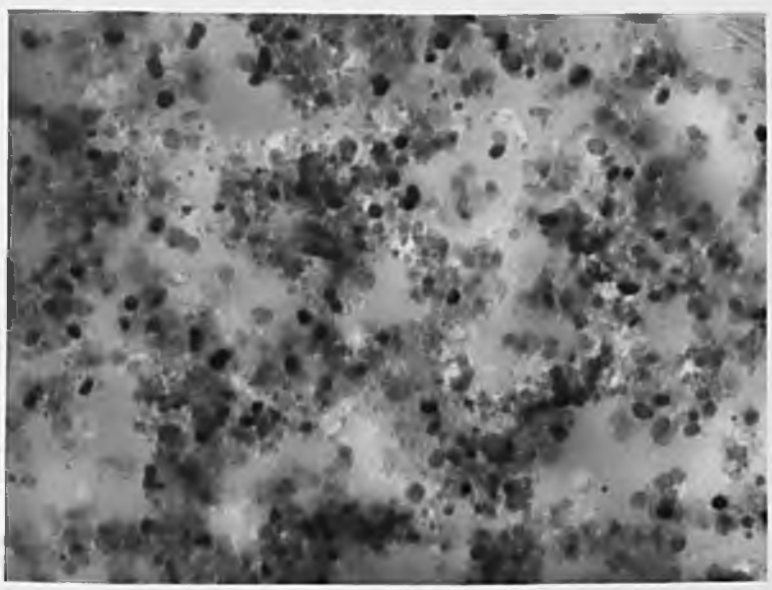

Fig. 3.6. Typical transmission electron micrograph of pre-shadowed carbon replica of glass-ceramic 1 (Mag. 120,000 : 1cm = 83nm.)

This technique for preparing specimens was found to be relatively simple. No information, however, can be obtained about the replicated material from selected area diffraction or dark field imaging. The observed microstructure can also depend on the precise etching treatment and care must therefore be taken in the interpretation of the micrograph.

3.4.4. Chemical Thinning.

This method enables thin sections to be obtained when the bulk material contains a single phase. Extended work has been done on chemical thinning by James and McMillan (1968, 1971), Harper et al. (1970), Hing and McMillan (1973) and James and Keown (1974).

Thin slices approximately 200 microns in thickness were cut, using a diamond saw, from the specimen. Both surfaces of the slice were polished flat with 6 micron, followed by a one micron diamond paste. Each specimen was held by the edges with a pair of fine tweezers and the rim was covered with a thin coating of a material resistant to chemical attack (Lacomit varnish was found suitable). The slice was then immersed in an etching solution of 5% HF - 2% HCl - 93% H_2O after Hing and McMillan (1973). The specimen was frequently agitated until a perforation of the slice occurred. The slice was then carefully washed in distilled water and methanol and a small piece of the specimen was broken off from an area near to the edge of the hole, and mounted in a double copper grid.

Fig. 3.7. shows a typical chemically thinned area of a phase separated glass.

Chemical thinning is a powerful method for preparing specimens for the electron microscope from single phase materials, or multiphase materials where the different phases present are etched at the same rate. In glass-ceramics it was found that the glass phase etched faster than the crystalline phase, resulting in the loss of some crystals which is unsuitable for the study of volume fraction of the crystal phase.

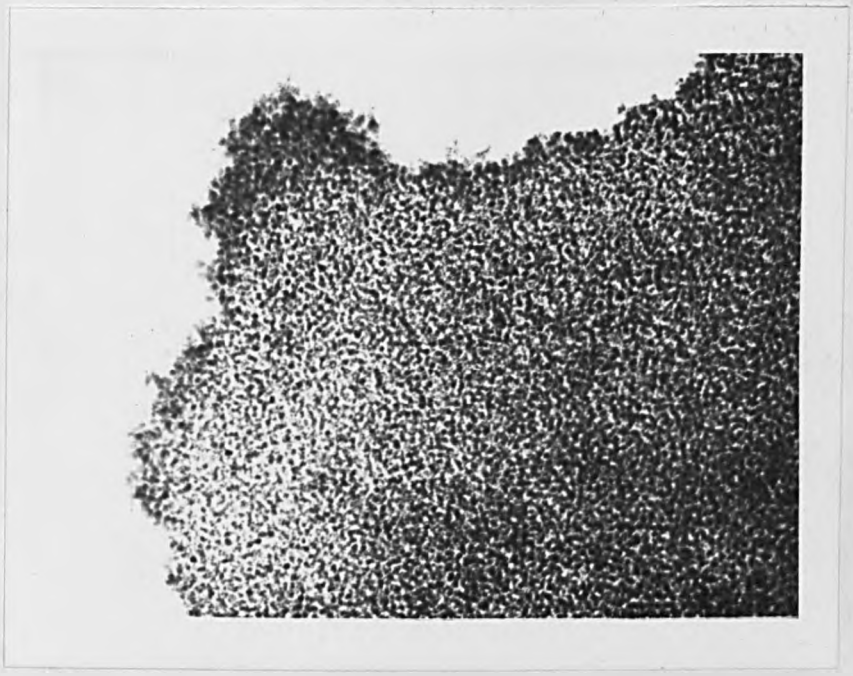

Fig. 3.7. Typical transmission electron micrograph of glass 1, nucleated at 800°C for one hour, prepared by chemical thinning (Mag. 26,000 : 1cm = 380nm).

Surface artefacts can also be present due to the choice of the wrong etching solution, causing a reaction between the solution and the glass surface.

3.4.5. Ion-beam Machining

This method, although slightly more involved than the previous ones mentioned, proved to be the most successful for the study of glass-ceramics where the crystals present are extremely small (less than 50nm).

Preliminary thinning was initially performed by mounting thin plates of the sample onto a glass slide and polishing them down, using 6 micron and one micron polishing pads as described by Doherty and Leombruno (1964) and Clinton (1972) but proved to be unsuccessful due to fracture of the specimens.

Following this, a new technique was devised. Cylinders of glass 3mm in diameter were cut from a bulk sample using an ultrasonic drill with a stainless steel drill tip fed with 220 mesh silicon carbide (Carborundum) powder. The cylinders were subsequently sliced into discs, approximately 250 microns in thickness on a diamond saw. The discs were then heat-treated at the required temperature for the required time. These heat-treated discs were airbraded using a stream of gas-borne particles as described by Rampley (1973). The powder employed was alumina which was carried in a stream of nitrogen gas. It was found that a 10 micron particle size was the best for thinning the specimens, giving a more uniform finish than larger 30 micron particles.

The sample was held by the edges, using a pair of tweezers and the jet of gas-borne particles allowed the thinning of the centres of both sides of the disc. Thinning was complete when a small perforation occurred through the disc.

The samples were then thoroughly washed with trichloroethylene, ether and methanol, to remove all excess dirt and dust, and transferred to an Edwards ion-beam machining equipment. The discs were

mounted at an angle of 20° and sputtering with argon ions was continued for a period of 8 hours. Suitable operating conditions were found to comprise a total current density of 100 μA cm^{-2} at a voltage of 6kV. Finally the specimen was thinned at an angle of 10°, with liquid nitrogen cooling the specimen to prevent sputtering atoms re-depositing on it. This was continued for about 4 to 6 hours until interference fringes could be observed in an optical microscope. The samples were again thoroughly washed and mounted into the specimen holder of the electron microscope.

One of the greatest concerns of electron microscopists is whether the microscopically observed structure is exactly representative of the bulk structure. Not only is it possible to miss seeing a level of structure by going straight from low to high magnification, but there is the added problem of not knowing whether any artefact has been introduced by the preparation technique. The production of artefacts is the more worrying of the two problems, since in most cases it is difficult to check an electron microscope observation by another technique. An obvious danger is that of changing the structure by heating the specimen during the preparation and even by heating due to the electron beam in the microscope. Almost all methods of thinning put an appreciable amount of energy into the specimen, and this manifests itself by heat. Similarly, charging due to poor conduction can also be a problem in the microscope. While in a metal specimen this is easily conducted away, the problem is more acute for non-conductors.

In the glass-ceramics studied it was found that very little, in fact no, damage had occurred during ion-beam thinning, since micrographs of nucleated specimens prepared in this way corresponded exactly to those produced by chemical thinning. Charging in the electron microscope was reduced by coating the area around the hole, but not the thinned area, of the ion-beam thinned samples with a conducting 'silver dag' paint.

3.4.6. Electron Diffraction

Electron diffraction was performed on most specimens to verify results from X-ray diffraction techniques. In order to analyse the diffraction rings produced, it was necessary to have an accurate value of the camera constant, L. From the geometry of the microscope (Glavert, 1974)

$$\tan 2\theta = \frac{R}{L} \qquad (3.2)$$

where R is the radius of the diffraction ring

L is the distance between the specimen and photographic plate

θ is the angle subtended between the specimen and the ring to be measured.

Bragg's law states that

$$\lambda = 2d \sin\theta \qquad (3.3)$$

and since the angles θ, through which the electrons are diffracted are very small, only 1°-2°, the approximation

$$\tan 2\theta = 2 \sin\theta$$

can be made with very little error. Then

$$\frac{R}{L} = \frac{\lambda}{d}$$

or

$$Rd = \lambda L \qquad (3.4)$$

So, if R,L, and λ for a particular diffraction ring or spot can be measured, then the d-spacing of the set of lattice planes giving rise to that ring or spot can be determined.

Since λ is dependent on the accelerating voltage, and this voltage fluctuates in the microscope, the instrument has to be calibrated wherever electron diffraction photographs are taken. This was done by introducing a grid with some thallous chloride powder sprinkled on it.

This produced very narrow intense rings, the spacings of which are known accurately. Hence the camera constant could be determined, and therefore the d-spacings could be deduced from the glass-ceramic specimens.

3.5. Scanning Electron Microscopy.

3.5.1. Introduction

The scanning electron microscope surmounts most of the difficulties encountered with conventional transmission electron microscopy, in that specimen surfaces can be viewed directly because of the much greater depth of focus. In this instrument a beam of electrons is focused onto a specimen surface and, in the normal mode of operation, secondary electrons generated at the surface are detected with an electron multiplier system. The signal from this detector is used to modulate the brightness of a cathode-ray oscilloscope. The one drawback with commercially available scanning electron microscopes is that the resolution is, at the very best, approximately 20nm.

3.5.2. Experimental

This method did not prove very successful for the study of the surface microstructure of transparent glass-ceramics. A number of reasons are attributed to this, the main one being that the crystals were too small for the microscope to resolve. Another reason is that difficulty was found in choosing a suitable etching solution. Microscopy only becomes successful if the etching treatment is performed satisfactorily, without damaging or altering the microstructure.

The experimental preparation of samples for scanning microscopy was performed by choosing a sample of glass approximately 8mm. cube. The sample was set in Specifix and one side was polished down to a one micron finish. The specifix was dissolved in acetone, and the sample was thoroughly washed in ether, distilled water and methanol. Etching

was subsequently performed, using a solution of 8% HF, 2% HCl and 90% H_2O. This produced an etch residue on the surface which could not be removed by washing. Part of this surface was removed with a razor blade and an X-ray diffraction photograph was taken. Too many reflections were present, which could not be identified, but it was thought that the etching residue was some form of aluminium fluosilicate. Many different etching solutions and etching times were attempted, and only one gave a reasonable micrograph, namely a solution of 5% HF with an etching time of 60 seconds. After washing the surface was vacuum coated with a thin layer of Gold-Palladium to prevent charging in the electron beam.

Difficulty, however, was still encountered in obtaining good micrographs of the glass-ceramics, due to the extremely small size of the crystals present. It was therefore considered unnecessary to pursue scanning eletron microscopy much further in this direction.

Scanning microscopy was employed quite extensively in observing the surfaces of chemically attacked samples. (Chapter VI).

The samples, after exposure to the chemical vapours, were gently washed, dried, and coated with Gold-Palladium. No effort was made to remove any surface layer, even for surfaces where vapours had condensed, since it was difficult to distinguish these from actual chemically attacked glass surfaces.

3.6. Quantitative Analysis.

3.6.1. Introduction

Two main principles of quantitative analysis are considered: a) grain size determinations, and b) assessment of phase proportions.

For grain size determinations, a brief review is given of the measurements of spherical particles and rod-shaped particles commonly encountered in glass-ceramics.

The relative amounts of crystal phases can be measured by the classical methods of areal, lineal, and point counting analysis.

Each method is discussed.

3.6.2. Grain Size Determinations

The particle size was measured for glass-ceramics 1,8,12 and 13 (Table 2.1.) using a Carl-Zeiss Particle Size Analyser (Model TGZ3). Here a circular beam of light is adjusted so that its circumference aligns with the edge of the particle to be measured, if it is spherical, or with the ends of the rod-shaped particles, if the lengths are to be determined. The diameter of this beam and hence the particle diameter, or length, are recorded on one of the recording meters. The diameter varies linearly from 0•5mm to 9•2mm on the 48 meters. The meter recordings were then scaled down corresponding to the magnification of the micrograph used. The micrographs were printed so that the average particle size fell half-way on the meter scale, i.e. about 5mm on the full print. Approximately ten photographs were analysed for each specimen, with about 300 counts on each micrograph (Sellars and Smith, 1967).

As expected, no difficulty arose in measuring the average size of the spherical particles, or near-spherical particles as found in glass-ceramics 1,8, and 13. The main difficulty was encountered in measuring the average size of the rod-shaped particles in glass-ceramic 12.

Since the rod-shaped particles in this glass-ceramic are randomly oriented, the problem of determining the average particle length arises. Measuring lengths of rods as they appear in a two-dimensional micrograph could indicate the projection of long particles at various angles.

Fullman (1953) attempted to analyse the measurement of randomly oriented rods, but determined that the usual types of observation do not permit the measurements of the length of these rods.

Analysis was, however, performed on the rod-shaped particles. Since a small percentage of particles would be expected to lie in the plane of the micrograph, these would indicate the maximum size of particles present in the glass-ceramic.

Since absolute values of particle size were impossible to calculate, the relative average length of the particles resulting from each heat-treatment was determined.

Histograms were drawn corresponding to each heat-treatment and the errors were calculated as the half-value width.

3.6.3. Volume Fraction.

The basic principles involved in the determination of phase proportions were studied by Thomson (1930), Howard and Cohen (1947) and Gladman (1963). The most important factor to note is that in multiphase materials, such as glass-ceramics, the volume fraction of a phase is equal to the area fraction in a random planar section, and is equal to the linear fraction in a random linear intercept through the solid. The volume fraction is also equal to the fraction of randomly distributed points which lie within that particular phase.

The three methods of areal, lineal and point counting analysis are discussed.

It should be pointed out that the measurements were carried out on transmission electron micrographs of thin foils and not two-dimensional sections, as strictly required. Nevertheless, the measurements obtained still provide a reliable guide to the relationship between the properties and the microstructure of the materials.

Areal Analysis.

This method is not normally used as a quantitative method because it is often long and tedious. The simplest application is to be found in a comparative method of estimating the areal fraction of a phase. The comparative method utilises a set of prepared charts, showing various phase proportions and each field of view is compared with the standard charts. This process is repeated a number of times, and the average fraction is determined. This method has the disadvantage of being subjective, i.e. susceptible to personal bias and may become unreliable when the shapes of the second phase in the standard chart are different from the shapes of the second phase in the microstructure. This method is not in common use and little is known of its accuracy.

Relative areas can be determined from tracings or photo-

micrographs by a planimeter, or by cutting out the phase of interest and weighing all the pieces, then comparing this weight to the total weight. Again, the determination of areas is very time consuming.

Lineal Analysis.

The principle involved in lineal analysis is that the fractional length of a line which occurs in a particular phase in a microstructure is equal to the volume fraction of that phase,

$$P_\alpha = \frac{l_\alpha}{L} \qquad (3.5)$$

where l_α is the length of the intercept in the α-phase and L is the total length of the intercept.

The standard deviation of the proportion of the α-phase, P_α, in a microstructure was calculated by Gladman (1963) to be,

$$\sigma_{p_\alpha} = P_\alpha (1-P_\alpha) \left(\frac{2}{n}\right)^{1/2} \qquad (3.6)$$

where n is the number of α-phase particles intercepted.

This method, however, is better employed with microstructural features that are aggregated into relatively large areas, rather than those which are finely dispersed (Weinberg, 1970).

Point Counting

This method depends on the fact that the proportion of a random array of points which are placed on a micrograph and which will fall on a specific phase is equal to the proportion by volume (or area) of that phase. In order to meet this requirement, points would have to be projected onto the micrograph at random, the volume fraction of α-phase being given by the proportion of the points which occupy positions in the α-phase.

In practice, it is generally found to be inconvenient

to project a random array of points onto a microstructure. A regular array of points is used and it is assumed that the micro- constituents are randomly distributed. This assumption is generally valid for most of the common microstructures found in glass-ceramics.

It is important that the spacing of the points on the grid be large with respect to the microstructural features. If the spacing of the points is very small compared to the features, then the condition for random spacing with respect to the grid is invalidated, and therefore the error in the phase proportion could be considerably larger than expected.

The volume fraction P_α of the α-phase is thus given by,

$$P_\alpha = \frac{n_\alpha}{n} \qquad (3.7)$$

where n_α is the number of points occurring in the α-phase

and n is the total number of points on the test grid.

The standard deviation of the volume fraction in relation to the number of points used in the points counting method has been considered by Hilliard and Cahn (1964). Their equation, however, is thought to be incorrect because the error associated with the determination of a volume fraction of 10% is suggested to be different from the error associated with the determination of a volume fraction of 90%.

In a two-phase structure this is obviously incorrect, and the equation by Gladman and Woodhead (1960) is thought to be more appropriate. This is,

$$\sigma_{P_\alpha} = \left(\frac{P_\alpha(1-P_\alpha)}{n} \right)^{1/2} \qquad (3.8)$$

This method of point counting was found to be the most suitable for the microstructures in the transparent glass-ceramics. A test grid was constructed from Perspex by drilling a regular array of 1mm holes at 1cm intervals. The test grid itself measured 15cm by 15cm.

3.6.4. Mean Free Path

A spatial parameter of great importance in particulate systems is the mean free path, λ, between particles, for example, of α-phase.

As defined by Fullman (1953)

$$\lambda = \frac{1 - (V_f)_\alpha}{N_L} \tag{3.9}$$

where (V_f) refers to the volume fraction of α-particles, or second phase regions in a two-phase aggregate

and N_L is the number of intersections per unit length of test lines with the particles.

The above equation is valid regardless of size, shape, or distribution of particles or other separated volume elements.

The relation derives simply from the fact that the number of interceptions with α-particles is the same as the number of interceptions with the matrix. Thus the lineal fraction occupied by the matrix is λN_L, which is also equal to its volume fraction, $1 - (V_f)_\alpha$.

It can be seen that the mean free distance, λ, is essentially a mean edge-to-edge distance. It represents the uninterrupted interparticle distance through the matrix. Although λ is measured on random section planes, it gives the true three-dimensional distance between particles.

The mean particle size, d, is related to N_L by (Underwood, 1970)

$$d = \frac{1}{N_L} \tag{3.10}$$

For isolated α-particles in a matrix

$$d = \frac{(V_f)_\alpha}{N_L} \tag{3.11}$$

Substituting this into equation (3.9) yields the relationship between the mean free path and the average α-particle size and volume fraction of the α-phase

$$\lambda = d \left[\frac{1 - (V_f)_\alpha}{(V_f)_\alpha} \right] \tag{3.12}$$

3.7. Electron Spin Resonance

3.7.1. Introduction

The striking success of electron spin resonance in determining the structure of numerous paramagnetic centres has poised the question of whether it could not also be applied to the study of glasses and glass-ceramics.

Electron spin (or paramagnetic) resonance studies are particularly concerned with the structure and localisation of paramagnetic centres produced either by high-energy radiations (X-rays, γ-rays, fast neutrons) or by the presence of paramagnetic impurities (e.g. 3d ions). At the same time, the centres act as a probe for their surroundings and so provide information about the glass structure.

Most of the work on glass in the past twenty years has been mainly concerned with looking at the effect of ionising radiation on glass and the effect of transition metal ion impurities.

The first report of E.S.R. in glasses was by Sands (1955), who obtained spectra of a number of transition metal and rare-earth ions in various soda-lime silica base glasses. The paramagnetic ions were introduced as oxides in amounts ranging from 0·4 to 0·005 wt %. It was noted that in all cases, including the undoped base-glass materials, there existed resonances which have apparent anisotropic g-values of 4 and 6 belonging to a specific (then unknown)impurity. These resonances were later shown by Castner et al. (1960) to be due to Fe^{3+} ions, which were probably present as an intrinsic impurity in the base material of Sands' study.

In recent years the role of Fe^{3+} ions in glasses has been extensively researched, particularly by Tucker (1962)., Karapetyan (1963), Steele and Douglas (1965), Kurkjian and Sigety (1968), Barry (1968) and Loveridge and Parke (1971). Similarly, work has been performed by E.S.R. on the role of manganese in glasses by Lunter et al. (1968) and Shaffer et al.(1976).

Very little study of colour centre formation in glasses has been reported. The only work has been performed on radiation damage in glasses by van Wieringen and Kats (1957), Lee and Bray (1962) Bishay (1970), Sidorov and Tyul'kin (1971), Akhmad-zade et al. (1974) and Griscom (1975).

Very little work has also been done on the E.S.R. of glass-ceramics. Karapetyan et al. (1964), Garif'yanov and Tokareva (1964), Arafa et al. (1975), and Pavlushkin et al. (1974) have studied the crystallization process by monitoring the change in the resonance spectra due to the presence of TiO_2.

The main interest in the present work lay in the colouration of a transparent glass-ceramic when exposed to sodium vapour in a low pressure discharge lamp. This is described in detail in Chapter VI. The colour centres which were thought to be involved, were considered appropriate for study by E.S.R.. In the course of this work certain interesting resonances were observed which unfolded the possibility of using E.S.R. as a valuable tool for looking at the impurities present in glass-ceramics. These impurities could be used to monitor the devitrification process.

3.7.2. The Resonance Condition.

If an atomic system, which possesses a resultant spin angular momentum and therefore a magnetic moment, is placed in a magnetic field, the spin degeneracy is lifted and a splitting of the energy levels is produced. Transitions between the energy levels created by the magnetic field may then be induced by an oscillating magnetic field of suitable frequency.

The simplest system consists of a simple unpaired eletron with an angular momentum $\frac{Sh}{2\pi}$ ($S = \pm 1/2$) and a magnetic moment of $2\sqrt{S(S+1)}\beta$, where h is Planck's constant and β is the Bohr magneton. The magnetic field produces two levels with an energy separation $g\beta B$, where g is the spectroscopic splitting factor and B is the magnitude of the applied steady

magnetic field. The two energy levels correspond to the electron precessing about the positive and negative directions of B. If an oscillating magnetic field of frequency ν is applied in a plane normal to the steady magnetic field, transitions can be induced between the levels when

$$h\nu = g\beta B \tag{3.13}$$

For the single electron system the spin of the electron provides the only contribution to the angular momentum; g is equal to 2·0023 and the resonance condition is satisfied for a steady magnetic field of 3308 G (0·3308T) when ν = 9·270 GHz. Therefore, ν occurs in the microwave region of the electromagnetic spectrum.

In a sample which contains many unpaired electron systems, the thermal equilibrium distribution of the unpaired electrons between the energy levels created by the applied magnetic field is described by the Maxwell-Boltzmann expression. For the group of single electron systems, the ratio of the number of unpaired electrons in the higher energy state, n_2, to the number in the lower energy state, n_1, is given by

$$\frac{n_2}{n_1} = e^{-\left(\frac{h\nu}{kT}\right)} \tag{3.14}$$

where k is Boltzmann's constant and T is the absolute temperature. At all but the lowest temperatures, $h\nu \ll kT$ and to a good approximation

$$\Delta n = \frac{n_o h\nu}{2kT} \tag{3.15}$$

where $\Delta n = n_1 - n_2$

and $n_o = n_1 + n_2$

Transitions between the two energy levels are induced by the applied radiation and occur with equal probability in either direction. As the number changing state per second is proportional to the probability per second of a change and to the population of the state, there is a net

migration of electron spins from the lower to the higher level.

E.S.R., therefore, involves measuring microwave transitions within a small group of energy levels. Frequently only two energy levels are involved and only rarely is the number larger than eight. In a formal way it is possible to regard the ground state levels as an isolated set the properties of which may be described without reference to other levels. This method of description uses the so-called spin-Hamiltonian. No further mention will be made here of the spin-Hamiltonian, since the present work is mainly quantitative. Excellent theories of E.S.R., including the spin-Hamiltonian, are given by Abragam and Pryce (1951), Bowers and Owen (1955), Lancaster (1967), Orton (1968), and Barry (1968).

3.7.3. E.S.R. Experimental

As described in Chapter VI, no specific preparation of samples was necessary for E.S.R. investigations. Samples of glass, glass-ceramic, and materials exposed to lamp vapours and ionising radiations, were inserted into a clean silica tube and then placed into the resonant cavity between the poles of the magnet of the spectrometer. Typical sizes of samples were 8mm x 3mm x 1mm.

Eletron spin resonance spectra were run on a Decca spectrometer, at room temperature, operating in the X-band at a frequency of 9·270 GHz. Carbon (coke) was used as a g-marker, producing a sharp resonance at g = 2·0023.

The effective g-value was calculated from the magnetic field where the centre of the resonance of the first derivative curve crossed the horizontal base line. All the measurements were the mean of approximately five single sweeps.

Initial runs produced spectra which were rather puzzling in that a certain resonance (g = 4·38) did not correspond to one quoted in the literature for the Fe^{3+} impurity ion resonance in a soda-lime silica

glass at g = 4•27. It was assumed that the magnetic field was linear and that at the beginning of each sweep the field was zero. Calibration, using a proton resonance magnetometer, showed that the field was linear, but that a small remnant field was present at the beginning of the sweep when the current to the coils was zero. According to this, the resonance at g = 4•38 was in fact at g = 4•27, which correlated with published results.

Where deemed necessary, samples were run at various temperatures, and so a special liquid nitrogen attachment was fitted, running from -200°C to +300°C.

All investigations were performed concurrently with chemical stability experiments, details of which are given in Chapter VI.

CHAPTER IV

Microstructure Results.

4.1. Introduction

In this chapter details are presented of the microstructural characteristics of transparent glass-ceramics investigated by X-ray diffraction, Differential Thermal Analysis, electron microscopy, electron diffraction and electron spin resonance.

In the X-ray diffraction section a detailed discussion is presented of the series of glasses studied, starting from initial compositions and leading to the final glasses chosen.

Results are also given of quantitative analysis of particle size and volume fraction of certain glasses selected for detailed investigations.

4.2. X-Ray Diffraction

The initial glass was prepared from a composition given by Beall and Duke (1968), glass 1 in Table 4.1.. Glass 2 was also prepared with 0•9% P_2O_5 to determine whether in these compositions the P_2O_5 would enhance micro-phase separation, as suggested by Partridge and McMillan (1963), and therefore promote the growth of extremely fine crystallites.

The heat-treatment by Beall and Duke of glass 1 at 800°C for 4 hours produced the initial crystalline phase of tetragonal ZrO_2, followed by the growth of a spinel solid solution, (s.s) $MgAl_2O_4$ after a crystallization treatment of 950°C for 4 hours.

This was not the case for the final crystalline species when glass 1, prepared in the present study was subjected to the same heat-treatment. The initial minor crystalline phase, after the nucleation heat-treatment at 800°C for one hour, was

	SiO_2	Al_2O_3	ZnO	MgO	ZrO_2	P_2O_5
Glass 1	64,8	17,6	5,6	4,6	7,4	-
Glass 2	64,2	17,5	5,5	4,6	7,3	0,9

Table 4.1. Compositions of glasses 1 and 2.

tentatively assigned as tetragonal zirconia, since there was close agreement of the observed d-spacings of the four most intense reflections with those reported in the ASTM card index for this structure, but there were large differences in the relative intensities of these reflections from those reported. The reflections of the tetragonal zirconia phase appeared very broad, indicative of small crystallite size. This phase was quite difficult to distinguish from the cubic zirconia phase, except for two reflections at 1·29Å and 2·57Å which were present in the tetragonal zirconia phase. For the crystallization heat-treatment of 950°C for 4 hours, a β-quartz solid solution was formed for glasses 1 and 2. Fig.4.1. shows a densitometer trace of both the tetragonal zirconia and β-quartz phases of glass 1.

The crystalline phases present were very similar to those formed in another composition given by Beall and Duke (1968), namely, 74% SiO_2, 16·5% Al_2O_3, 3·5% MgO, 6% ZnO and an excess of 4% ZrO_2, with a heat-treatment of 750°C for 4 hours followed by 860°C for 4 hours.

To establish a microstructure comprising spinel ($MgAl_2O_4$) as the main crystalline phase, it was decided to change the composition of glass 1 by introducing more MgO at the expense of SiO_2 (glasses 5 and 6 in Table 4.2.), and then more Al_2O_3 also at the expense of SiO_2 (glass 7). X-ray analyses of these glasses, however, showed the same results as for glass 1 and 2, i.e. after a heat-treatment of 800°C for 4 to 6 hours and 950°C for 4 hours, tetragonal zirconia and β-quartz s.s. crystals were formed.

Further attempts to produce the spinel phase by heat-treating the glasses at 800°C and then at different crystallization temperatures of 950°C, 975°C, and 1000°C for periods of 4 to 6 hours still resulted in the formation of a β-quartz s.s.. It was

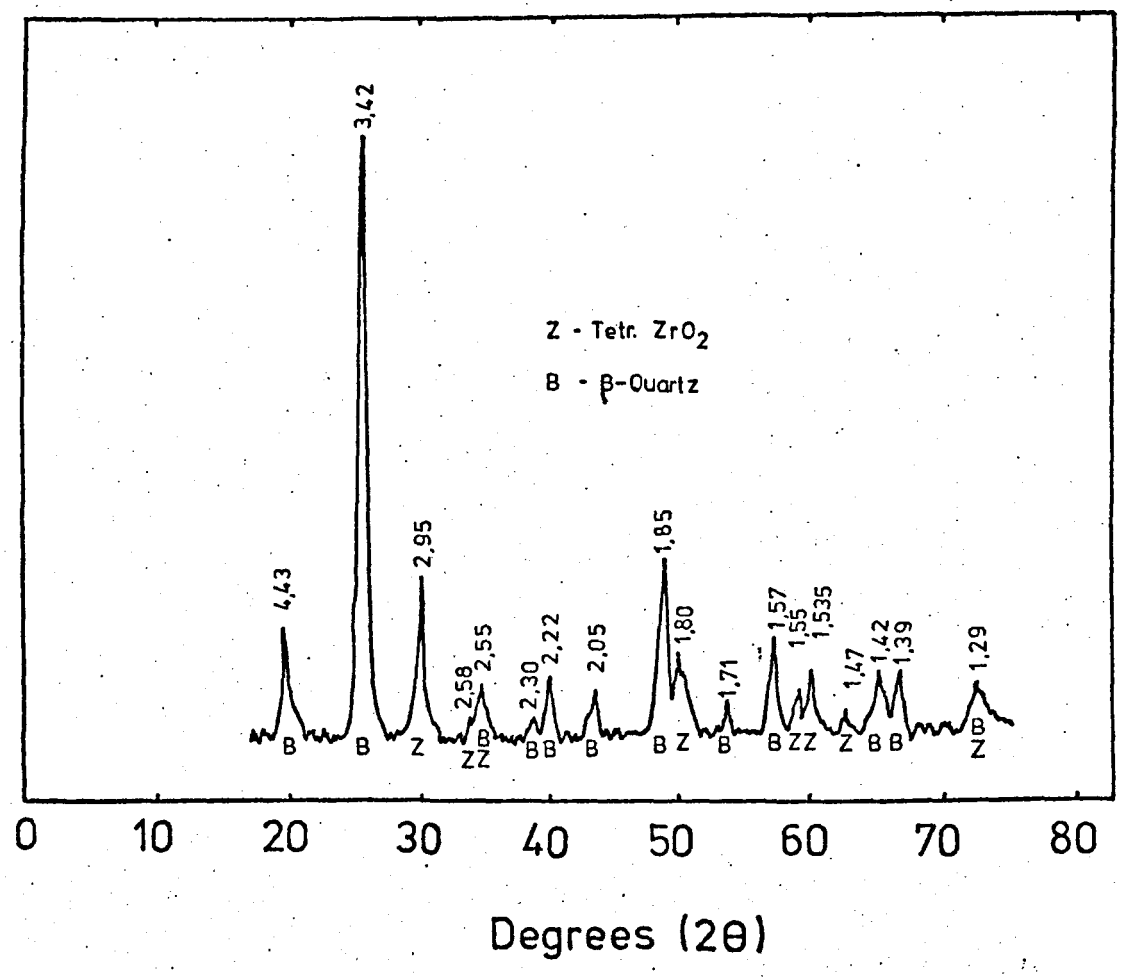

Fig. 4.1. Densitometer trace of glass-ceramic 1.

	SiO_2	Al_2O_3	ZnO	MgO	ZrO_2
Glass 5	62,5	17,6	5,5	7,0	7,4
Glass 6	60,2	17,6	5,5	9,3	7,4
Glass 7	61,1	20,4	5,5	5,5	7,4

Table 4.2. Compositions of glasses 5, 6 and 7.

concluded, therefore, that for the particular compositions, the only crystalline species formed were tetragonal zirconia and a β-quartz s.s., and that the temperatures necessary for nucleation and crystal growth were 800°C and 950°C respectively.

The next step was to investigate the role of the nucleating agent ZrO_2. Nucleation is supposedly accomplished in these materials by the addition of zirconia which produces uniform internal nucleation. The mechanism of the nucleation by zirconia has been discussed by Neilson (1970(a), 1970(b), 1971, 1972) using SAXS studies. He found that upon a heat-treatment at 791°C of an $MgO - Al_2O_3 - 3SiO_2$ base glass, an amorphous phase separation of ZrO_2-enriched regions occurred. Pavlushkin et al. (1971), Conrad (1972), Pavlushkin and Ellern (1974) and Babosova et al (1974), drew parallel conclusions on an investigation of similar compositions. Neilson found that upon heat-treatment of his glass at 850°C, spherical particles containing excess ZrO_2 were formed, although it could not be established whether or not they were amorphous at early times of treatment. For treatments at 903°C and 977°C no evidence was shown of an initial glass-in-glass separation in the material prior to the formation of ZrO_2 crystallites. The data indicated the continuous formation and growth of these crystals until crystallization of the glass occurred, at which time these processes were abruptly halted.

Even though in the previous glasses 1 to 7 tetragonal zirconia crystals were present, it was thought that maybe too few nuclei were available to promote the growth of spinel crystals, and that the presence of the zirconia was essential for the growth of these spinel crystals. Neilson (1970(a)), however, found that no cause-and-effect relationship could be established between the formation and growth of the ZrO_2-rich phase and the subsequent crystallization

process.

In proposing a further addition of ZrO_2 to the base glasses, note was made of research performed by Pavlushkin and Ellern (1974), who found that in a Li_2O - MgO - Al_2O_3 - SiO_2 glass, 5 wt % ZrO_2 was the minimum concentration inducing crystallization, and 6 wt % ZrO_2 was the maximum solubility.

Considering all the above studies, glasses were prepared with an addition of more ZrO_2. Glasses 8,9, and 10 (Table 4.3.) were prepared with an increase in the amount of ZrO_2 i.e. an excess of 10% ZrO_2 in glasses 8 and 9, and an excess of 9% ZrO_2 in glass 10.

These glasses were given the same heat-treatment as the previous ones, i.e. 800°C for 4 hours and 950°C for 4 hours. X-ray diffraction photographs of these showed that during the nucleation stage, fine crystals of tetragonal ZrO_2 were present, due to the broad reflections obtained. After the crystallization heat-treatment glasses 8 and 9 had spinel-type crystals. Glass 10, however, showed the β-quartz s.s. phase, as in glasses 1 to 7.

From the above investigation, it can be seen that for the particular system under study, there appears to be a minimum amount of the nucleating agent ZrO_2 needed to induce the growth of spinel crystals. This amount is 9% ZrO_2 (or 10% excess ZrO_2 added to the base composition).

At this stage, it could not be deduced whether this spinel phase was spinel s.s. $(Zn,Mg)Al_2O_4$ or gahnite $ZnAl_2O_4$, since both gave very similar X-ray diffraction reflections. A glass-ceramic known to have gahnite as the main phase, according to Beall and Duke (1968), was prepared (Glass 3 in Table 2.1.). The composition, in weight percent, was 70% SiO_2, 17% Al_2O_3, 13% ZnO, 6% excess ZrO_2 and 4% excess K_2O. The X-ray diffraction of this glass, heat-treated at 800°C for 4 hours and 1000°C for 4 hours, produced exactly the same

	SiO_2	Al_2O_3	ZnO	MgO	ZrO_2	P_2O_5
Glass 8	63,6	17,3	5,5	4,5	9,1	-
Glass 9	63,1	17,1	5,4	4,5	9,0	0,9
Glass 10	64,2	17,4	5,5	4,6	8,3	-

Table 4.3. Compositions of glasses 8, 9 and 10.

reflections as glass-ceramics 8 and 9, Fig.4.2.. The result, however, was still inconclusive for glasses 8 and 9.

To determine whether the dominant phase was a spinel s.s. or gahnite phase, the assumption was made that if the MgO in glasses 8 and 9 took part in the crystal formation to produce spinel $MgAl_2O_4$, then a completely different phase would be obtained on replacement of the MgO by another alkaline earth metal oxide. If, however, the MgO did not take part in the crystal formation, with the Mg^{2+} ion acting as an interstitial ion in the residual glass phase, then gahnite, $ZnAl_2O_4$ would be formed. This was performed by replacing the MgO present in the glasses by another alkaline earth metal oxide e.g. CaO or BaO, since, if the X-ray diffraction patterns proved to be the same as those of glasses 8 and 9, then this would indicate that gahnite was the dominant crystalline phase and not a spinel s.s..

Glasses 12 and 13 were prepared; Table 4.4.. The same heat-treatments were employed as for previous glasses; 800°C for 4 hours and 950°C for 4 hours. The same X-ray diffraction reflections were produced as for glasses 8 and 9, indicating that the main crystalline phase was in fact gahnite. Fig.4.3. shows a densitometer trace of the diffraction pattern of glass 12. The alkaline earth metal oxides do not, therefore, take part in the crystal formation, and the ions must reside in interstitial positions in the glass network. X-ray patterns were taken of the complete nucleation stage, and it was noticed that tetragonal zirconia appeared within a few minutes of the glass being held at 800°C, and was even present after annealing of the glass. Over the complete nucleation treatment, it appears that the optimum number of tetragonal zirconia crystals had developed to induce subsequent growth of gahnite crystals. The structural similarity between tetragonal zirconia and gahnite as deduced from X-ray diffraction investigations appears to be in accordance with crystal growth theories of Stookey (1954), Berezhnoi (1970), and Zdaniewski (1975),

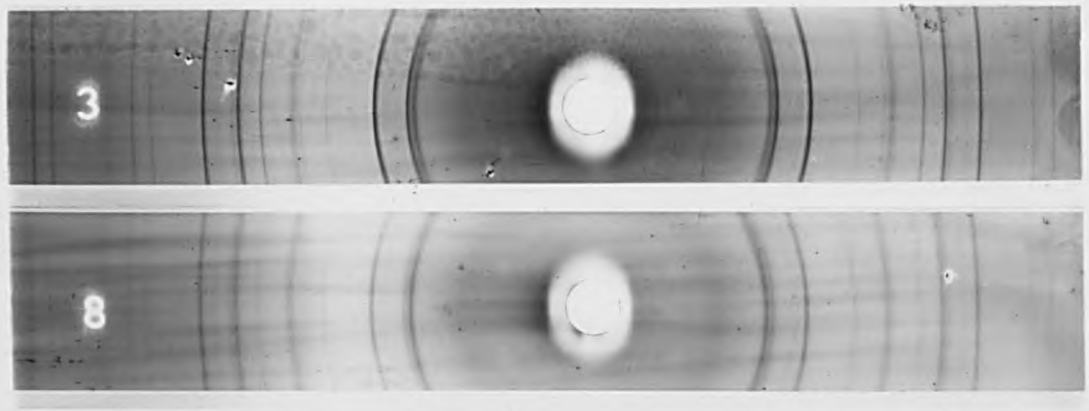

Fig. 4.2. X-ray diffraction photographs of glass-ceramics 3 and 8.

	SiO_2	Al_2O_3	ZnO	CaO	BaO	ZrO_2
Glass 12	63,6	17,3	5,5	4,5	-	9,1
Glass 13	63,6	17,3	5,5	-	4,5	9,1

Table 4.4. Compositions of glasses 12 and 13.

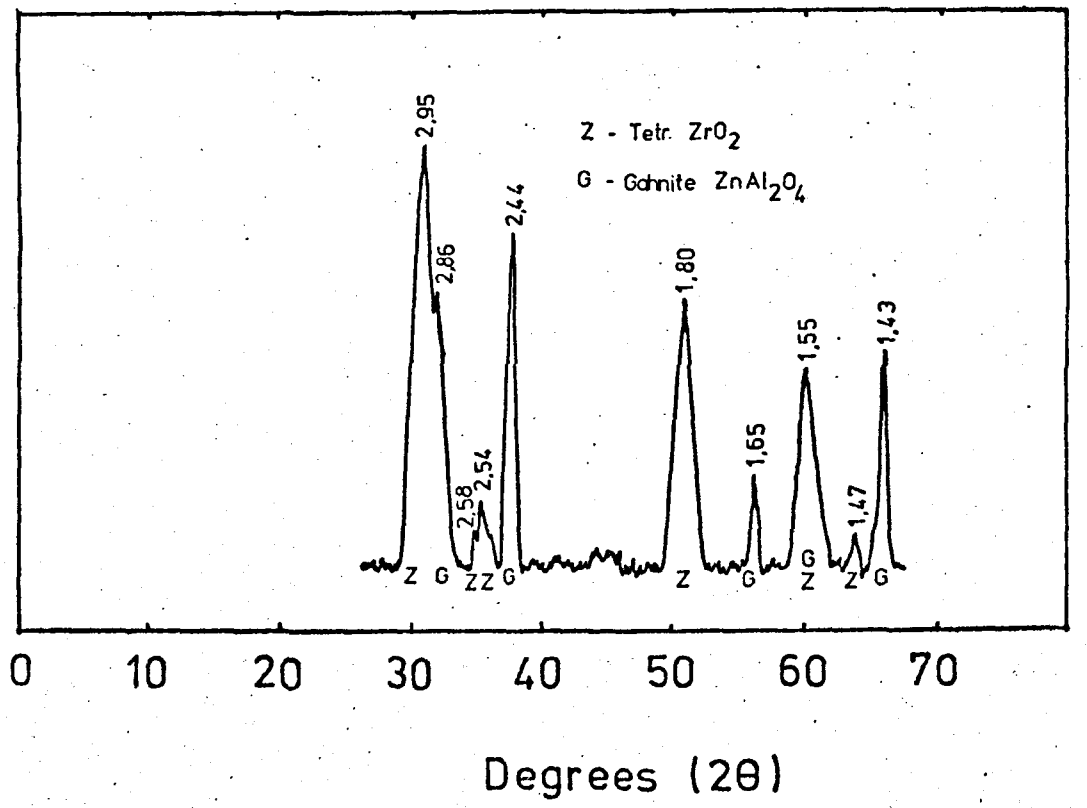

Fig. 4.3. Densitometer trace of glass-ceramic 12.

who suggested that the capacity of nuclei to catalyze heterogeneous crystallization depends on the closeness of structures between the nucleating agent and the precipitating phases.

To determine whether any change would occur in the X-ray reflections at temperatures above that used for nucleation, glass 12 was heat-treated at 850°C for 4 hours and also at 900°C for 4 hours. Both treatments produced the same diffraction reflections as the 800°C treatment, but the reflections were sharper for the 900°C schedule, indicating larger crystals. A heat-treatment at 925°C for 4 hours, besides revealing the tetragonal zirconia, also produced extremely faint gahnite reflections.

An X-ray broadening analysis of the tetragonal zirconia line in glass 12, heat-treated at 800°C for 4 hours and 950°C for one hour, indicated that the tetragonal zirconia crystals had an average size of 11•3 ± 3•4nm. It must be remembered, however, that these measurements were performed using the line broadening of reflections produced in a Debye-Scherrer camera, and that more accurate results would have been obtained using a diffractometer. The description of X-ray broadening analysis was described in Chapter III section 3.2.

Glass 13 again heat-treated at the same temperature and the same time as glass 12 produced the same diffraction peaks as glasses 8,9 and 12.

Since in glass 12 the appearance of tetragonal zirconia crystals occurred quite spontaneously at 800°C, the nucleation temperature, it was wondered whether this treatment could be omitted and the glass heat-treated at 950°C only. An X-ray diffraction pattern of this glass, heat-treated at 950°C for 1 to 6 hours, produced exactly the same reflections as those of the two stage heat-treatment. Obviously, as the sample temperature reached and passed 800°C, enough time was allowed for the precipitation of the tetragonal zirconia

crystals to promote the growth of gahnite crystals, apparently without change in microstructure, as will be seen in section 4.4..

4.3. Glass Appearance.

All glasses when poured, had good transparency but with a slight yellowish appearance when viewed in reflected light. The glass-ceramics varied in transparency with glass-ceramic 8 being more translucent than transparent. Glass-ceramics with the β-quartz s.s. phase produced a good transparent material, as did glass-ceramics 12 and 13, which had the gahnite phase. Glass-ceramic 12, after heat-treatment, had a slight bluish appearance in reflected light, and a slight brownish appearance in transmitted light. The glasses were heat-treated without polishing after slicing into suitably sized specimens ready for crystallization. All the glass-ceramics had surfaces with a similar appearance to those of the untreated glasses. Glass-ceramic 12, however, had an unusual surface topography. The sliced glass had a rough surface after slicing on the diamond saw, and during the crystallization heat-treatment, the surface appeared to soften and become smooth, as if polished. Fig.4.4. shows the appearance of the glass-ceramic before and after heat-treatment.

The overall transparency of certain glasses will be discussed in the optical properties' section.

4.4. Differential Thermal Analysis.

A D.T.A. curve of glass 1 is shown in fig 4.5.. No exothermic peak can be seen which distinguishes the crystallization of the tetragonal zirconia phase at 800°C. The general pattern of the curve, however, tends to show a rough annealing temperature at around 800°C, with a dip which rises to 950°C, showing the crystallization of the β-quartz phase. This corresponds to the X-ray diffraction results of the presence of β-quartz at 950°C. It is curious, though,

generally around 800° C.
initial crystalline precipitate is inv
nal zirconia, which begins to form
urs at the phase separation temp
n increase in temperature to about
begins to crystallise, presumabl
onia nuclei. The spinel is generally
O_4) or a spinel ss – (Zn, Mg)Al_2O_4
gahnite composition. The spinel cry
y fine-grained, and judging from

Fig. 4.4. Appearance of glass 12 before and after heat-treatment. (The sample on the left is the untreated glass and on the right the glass-ceramic).

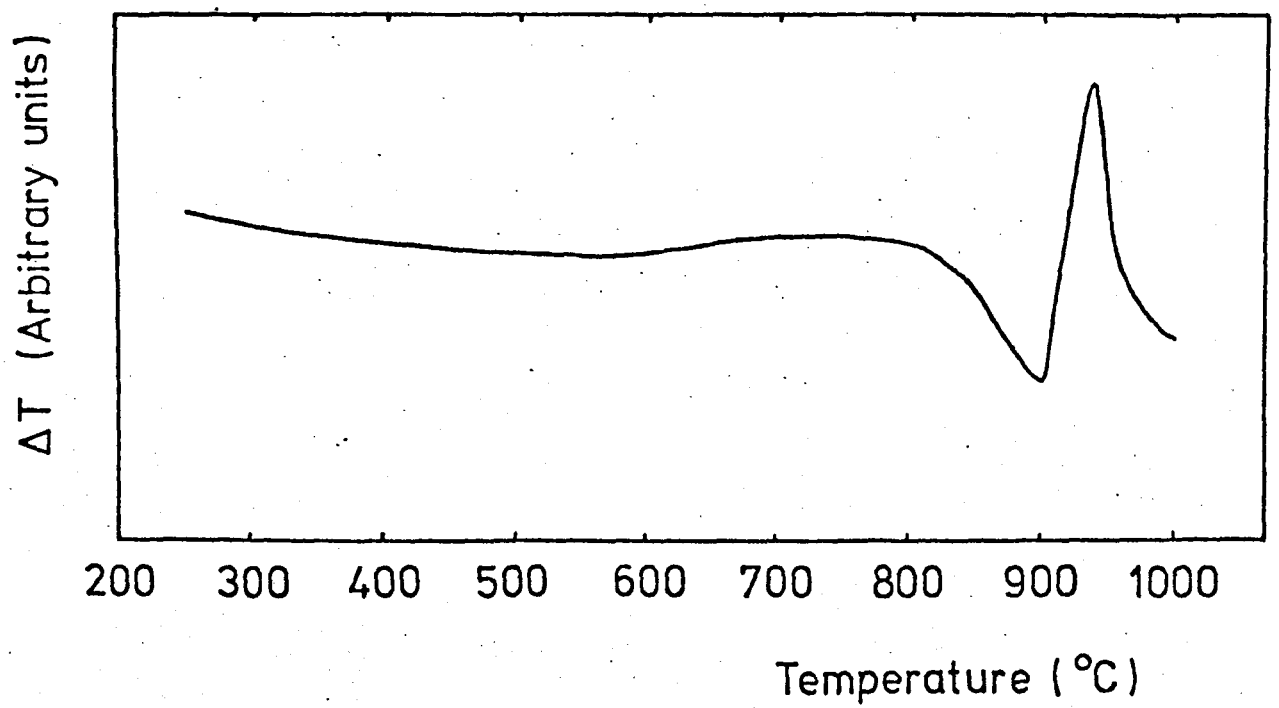

Fig. 4.5. D.T.A. curve of glass 1.

that no peak was present at the tetragonal zirconia crystallization temperature. X-ray diffraction results (and electron microscopy) showed that tetragonal zirconia had started to grow during annealing of the glass and ,since D.T.A. was performed on the powdered annealed glass, no peak was observed for the crystallization of the tetragonal zirconia phase.

For glass 12, fig.4.6., no indication is given of the crystallization of gahnite, but peaks do appear for crystallization of the tetragonal zirconia which correspond quite closely to theories by Neilson (1970(a), 1970(b)) who studied the crystallization of zirconia in $MgO - Al_2O_3 - SiO_2$ glasses in some detail.

The D.T.A. curve of glass 12 shows somewhat contradictory results from those observed by X-ray diffraction. The nucleation temperature of 800°C,to which glass 12 was subjected, produced fine tetragonal zirconia crystals. According to the D.T.A. results, however, a small endotherm at around 840°C is present, followed by an exothermic peak at 906°C.

SAXS results by Conrad (1972) and Neilson (1970(a), 1971) on $MgO - Al_2O_3 - 3SiO_2$ glasses indicated that phase separation occurred at 791°C, the annealing point, and crystallization of zirconia occurred at 838°C, as reported by Conrad, and 850°C, as reported by Neilson. Following this at 903°C, crystallization of zirconia is complete with secondary crystallization occurring at 977°C.

The crystallization peaks at 838°C and 903°C by Neilson and Conrad correspond to the exothermic peaks in the D.T.A. traces of glass 12 at 844°C and 906°C, but the X-ray diffraction of glass 12 indicated nucleation at 800°C and crystallization at 950°C. Even an X-ray diffraction photograph of glass 12, heat-treated at 906°C alone, produced the tetragonal zirconia phase, just as for the

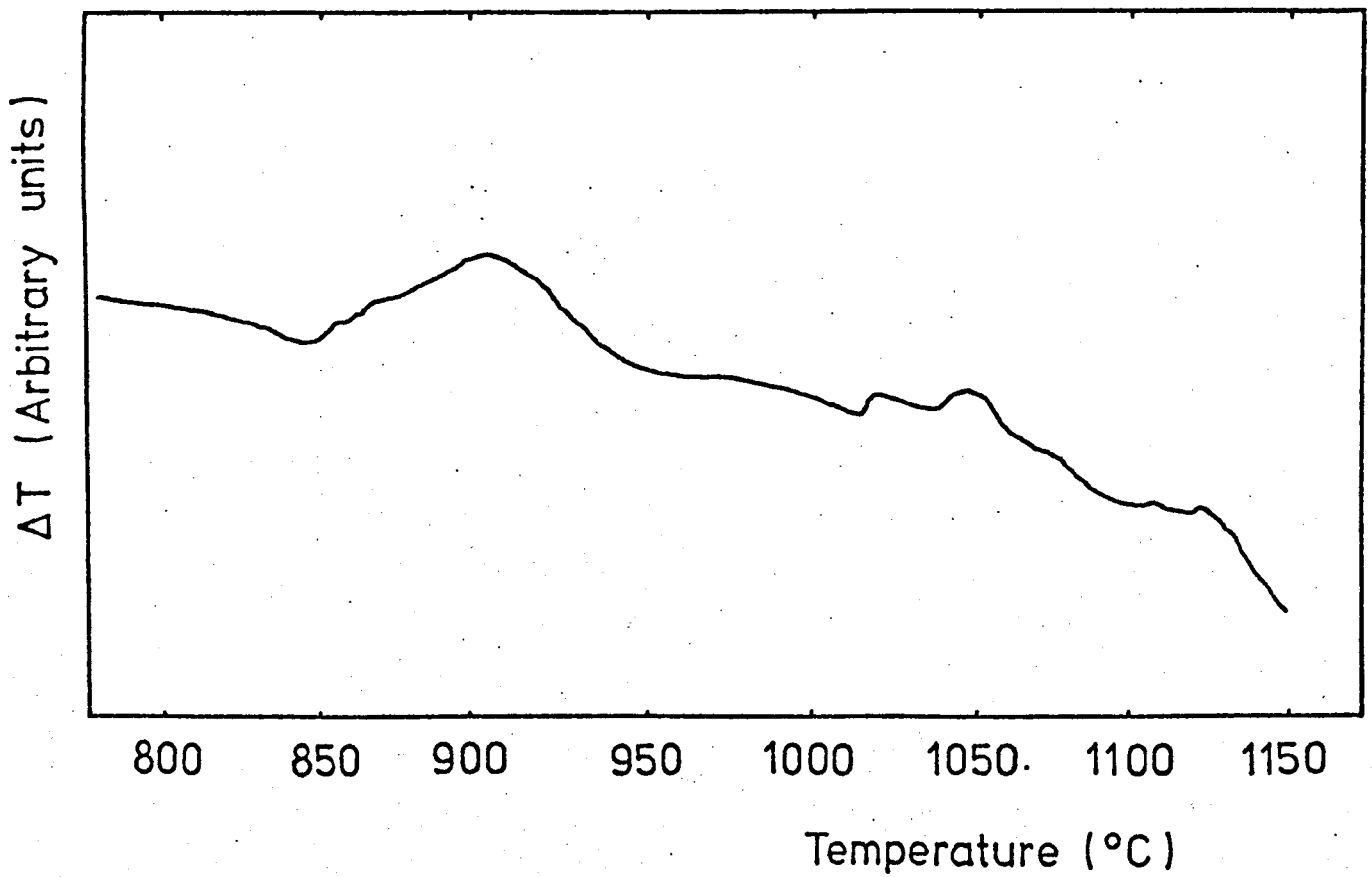

Fig. 4.6. D.T.A. curve of glass 12.

800°C treatment.

For glass 12, in the region of 1020°C to 1050°C, some exothermic effects are present which could again be associated with the nucleating agent, related to 1060°C for secondary crystallization of α-cordierite and cristobalite, as observed by Conrad. Following this, the glass began to fuse at 1133°C, producing an opaque, slightly sintered residue, probably indicating secondary crystallization. According to Conrad, secondary crystallization occurred at 1155°C.

Zdaniewski (1975) performed D.T.A. and X-ray analyses of nucleation and crystallization of $MgO - Al_2O_3 - SiO_2$ glasses containing ZrO_2, TiO_2 and CeO_2. For ZrO_2 nucleated glasses, he found a shallow endotherm present at 840°C, which he claimed was the M_g point of the glass. Following this, no exothermic peaks were observed until 1050°C and 1170°C, corresponding to secondary crystallization of quartz.

The surprising phenomenon is the fact that no exothermic peaks were recorded for the crystallization of gahnite.

The occurrence of crystallization peaks at lower temperatures is possible, because the samples used in the D.T.A. measurements were of a powdered form, and so nucleation, especially at the surface, and crystallization could occur at these lower temperatures. This reasoning would, however, alter the positions of the zirconia peaks which would be different from the results obtained by Neilson. The heat-treatment of samples for microstructural and physical property analyses were performed in the bulk form and so no comparison could be made between the D.T.A. results and, for example, X-ray diffraction.

An attempt was made to explain the absence of the gahnite crystallization peak in terms of heats of formation, but this proved inconclusive when considering crystal growth onto

the nucleated phase in a glass matrix.

4.5. Microscopy

From the forthcoming discussion it will be apparent that in most of the glasses three mechanisms are involved during the crystallization period to form a transparent glass-ceramic.

Investigations began on glass 1. The initial mechanism involved during the formation of a glass-ceramic was a phase separation, initiated during annealing of the glass at 780°C. This annealing temperature could not be determined with a great degree of precision. D.T.A. results and points of inflexion on dilatometric curves gave a temperature of around 780°C, although this was very close to the nucleation temperature of 800°C. Stresses in the glass were removed after annealing at 780°C, as observed in a strain-viewer.

No structure was seen in the quenched glass under the electron microscope, and electron diffraction revealed only amorphous halos. The annealed samples also showed no diffraction (X-ray or electron) peaks.

The phase separation is generally believed to be caused by the diffusion of zirconium ions into zirconium rich regions as studied by Neilson (1970(a), 1970(b), 1971, 1972), Conrad (1972), and Pavlushkin and Ellern (1974) in aluminosilicate syatems.

During the nucleation stage of glass 1 at 800°C, electron (as well as X-ray) diffraction showed the presence of tetragonal zirconia crystals; fig.4.7.. Fig.4.8. shows the regions where the tetragonal zirconia crystals were formed. Following this at the crystallization temperature of 950°C, β-quartz crystals were identified. As seen in fig.4.8., it was not until the 3 hour stage that distinct crystals of β-quartz began to appear, although X-ray diffraction showed the presence of these crystals even after the one hour treat-

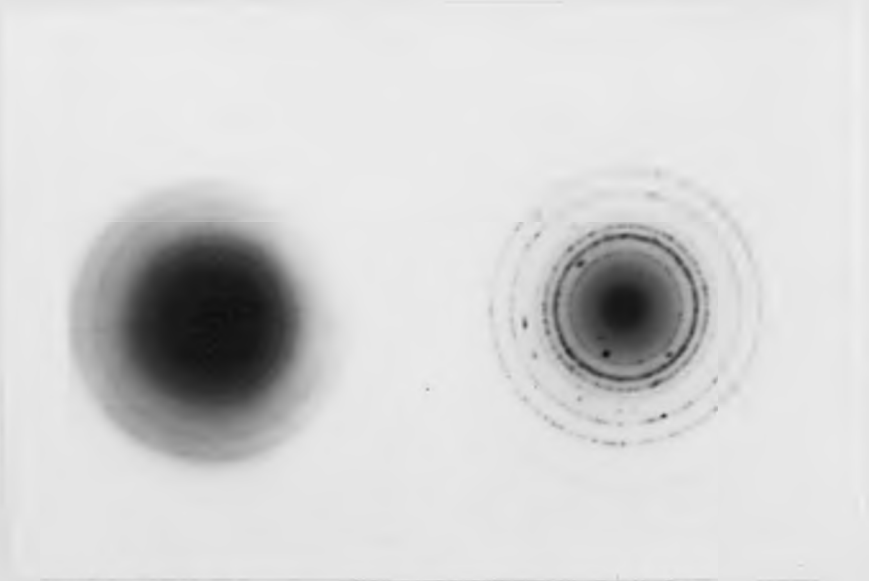

800°C 1 hr.

800°C 4 hours
950°C 4 hours

Fig. 4.7. Electron diffraction photographs of nucleated and crystallized glass 1.

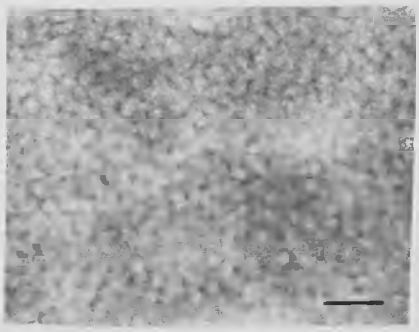

Annealed glass

800°C 1hr.

800°C 2hrs.

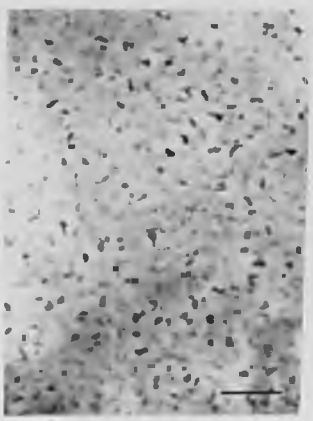

800°C 3hrs.

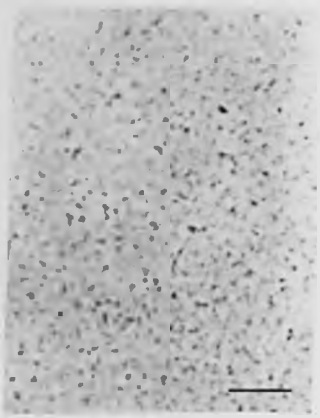

800°C 4hrs.

800°C 4hrs.
950°C 1hr.

800°C 4hrs.
950°C 2hrs.

800°C 4hrs.
950°C 3hrs.

800°C 4hrs.
950°C 4hrs.

(Bar : 100nm)

Fig. 4.8 Transmission electron micrographs of annealed, nucleated and crystallized glass 1.

ment. The β-quartz crystals had a spherical morphology and were randomly distributed throughout the glassy matrix. After the full heat-treatment of 800°C for 4 hours and 950°C for 4 hours, the glass-ceramic showed excellent transparency.

No difference in the microstructure was observed in glass-ceramics 1 and 2, indicating that the presence of P_2O_5 was not necessary to enhance phase separation and so produce extremely small crystals. The microstructure of glasses 5,6 and 7 was not studied, since the main phase produced was again β-quartz and the object was to produce a spinel s.s.

Glasses 8 and 9 showed a uniform dispersion of gahnite crystals in a glassy matrix. Figs.4.9.and 4.10. show the microstructure of these materials. As in glass 1, the annealed glasses showed a phase separation thought to be due to the diffusion of zirconium ions into zirconium rich regions. Nucleation at 800°C developed finely dispersed spherical crystals or nuclei of tetragonal zirconia, confirmed by X-ray and electron diffraction (fig.4.11.). Crystallization at 950°C resulted in the growth of spherical particles of gahnite, which began to appear within one hour.

No difference was encountered in the microstructure of glasses 8 and 9, indicating that the P_2O_5 presence in glass 9 did not affect phase separation.

A detailed analysis was performed on glass 12, which produced some slightly different results. The quenched glass showed no structure, but the annealed glass revealed that tetragonal zirconia had started to grow, with signs of very small background phase separation, as seen in fig.4.12.. It will be remembered from section 4.2. that X-ray diffraction reflections were obtained for the annealed glass. This is in accordance with electron diffraction results. Fig.4.13. shows the diffraction rings present for the

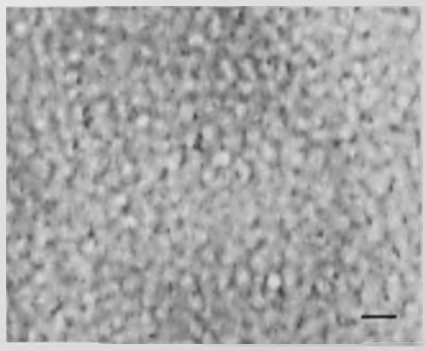

Annealed glass

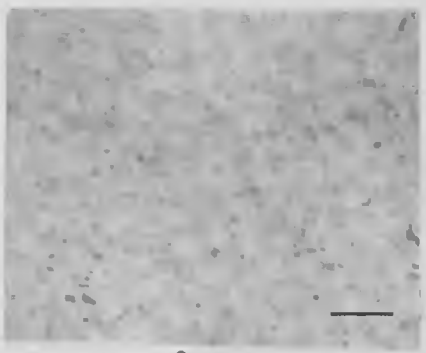

800°C 1hr.

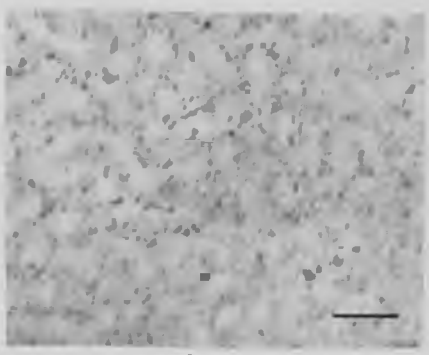

800°C 4hrs.

800°C 4hrs.
950°C 1hr.

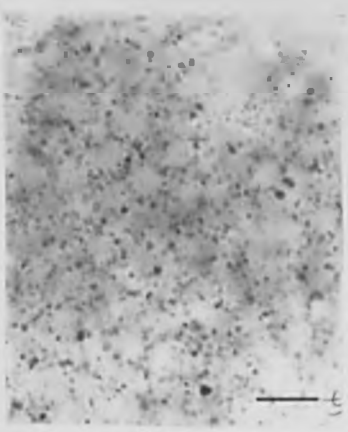

800°C 4hrs.
950°C 2hrs.

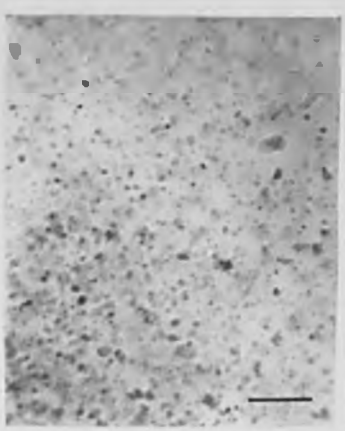

800°C 4hrs.
950°C 3hrs.

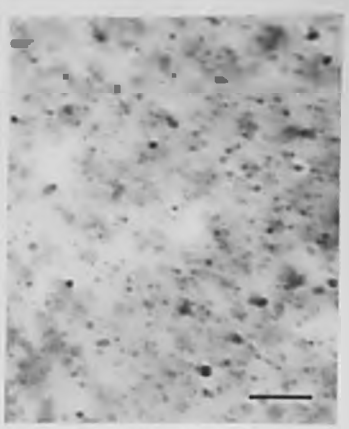

800°C 4hrs.
950°C 4hrs.

(Bar : 100 nm)

Fig. 4.9 Transmission electron micrographs of annealed nucleated and crystallized glass 8.

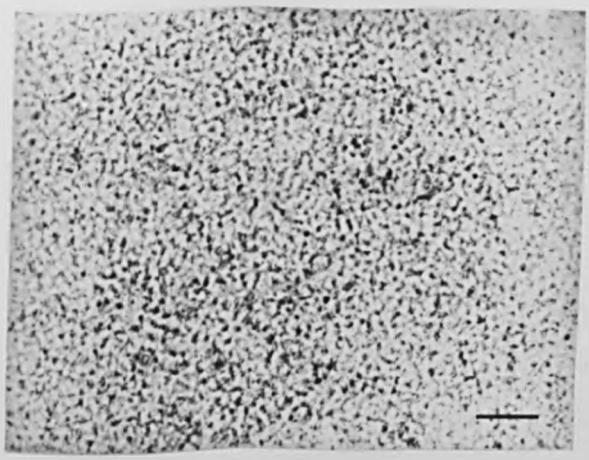

Annealed glass

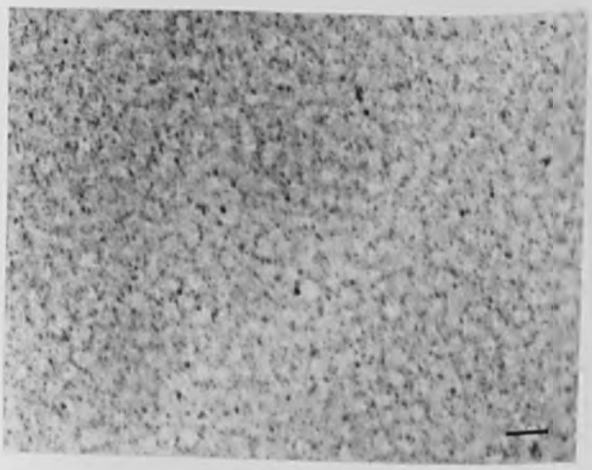

800°C 1hr.

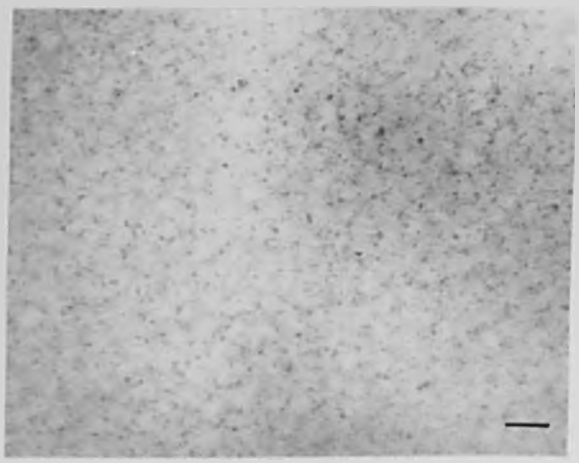

800°C 4hrs.

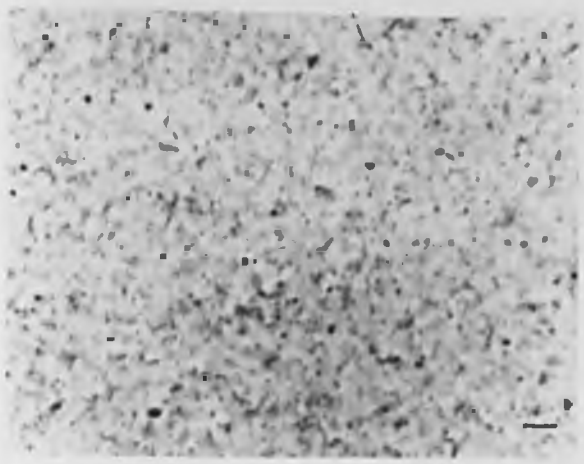

800°C 4hrs.
950°C 1hr.

800°C 4hrs.
950°C 4hrs.

(Bar : 100 nm)

Fig. 4.10 Transmission electron micrographs of annealed, nucleated and crystallized glass 9.

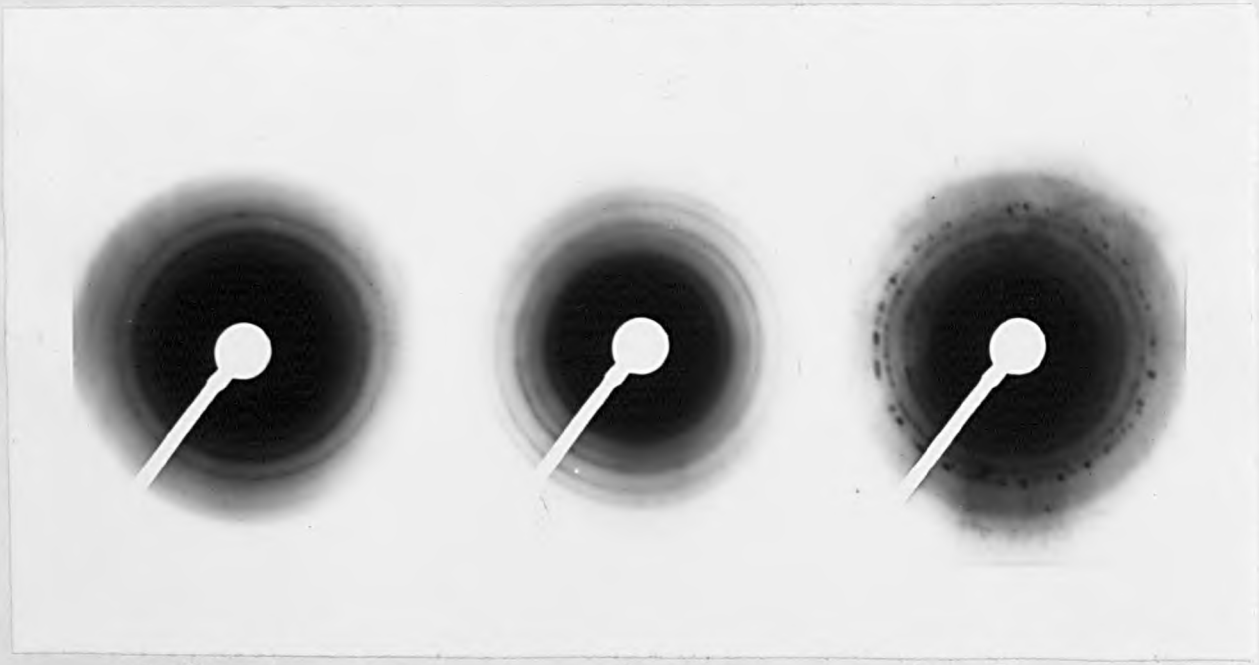

800°C 1 hr

800°C 4 hrs
950°C 2 hrs

800°C 4 hrs
950°C 4 hrs

Fig. 4.11. Electron diffraction photographs of nucleated and crystallized glass 8.

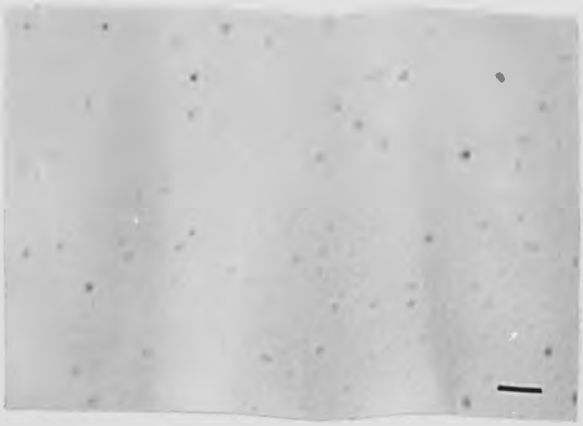

Annealed glass

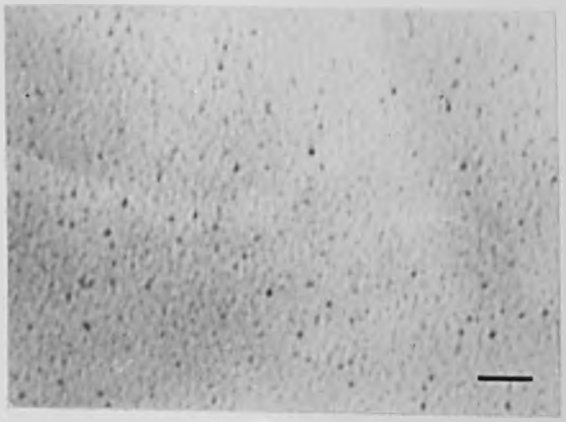

800°C 1hr.

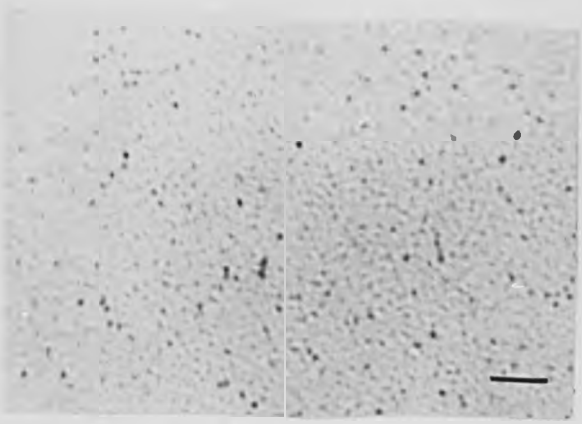

800°C 2hrs.

800°C 3hrs.

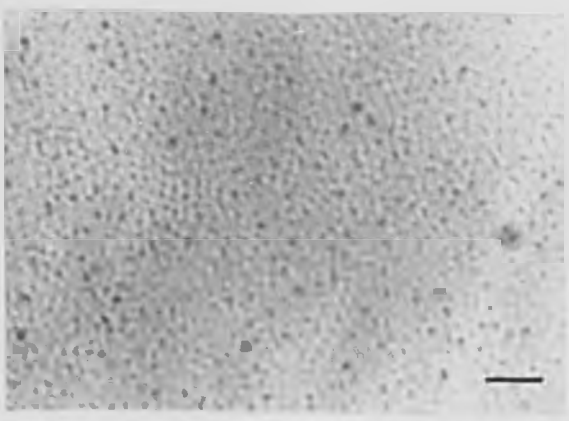

800°C 4hrs.

800°C 5hrs.

(Bar : 50 nm)

Fig. 4.12 Transmission electron micrographs of annealed and nucleated glass 12.

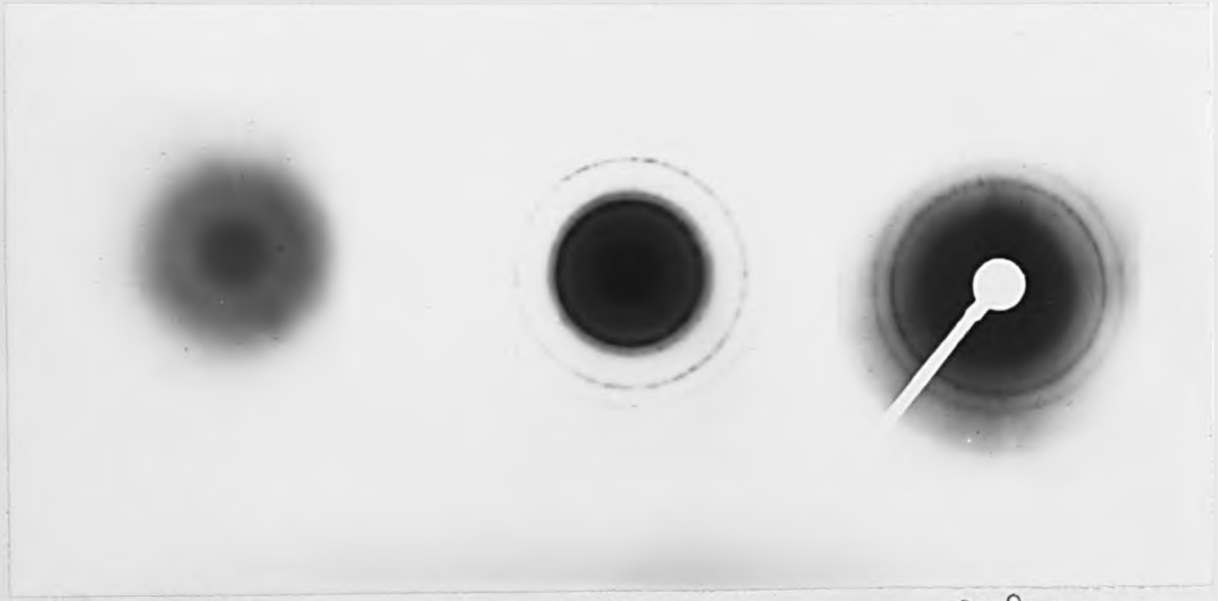

Fig. 4.13. Electron diffraction photographs of quenched, annealed and nucleated glass 12.

annealed glass and the nucleated glass, as well as very diffuse amorphous halos present in the quenched glass. Fig.4.12. also shows the nucleation heat-treatment at 800°C. No change is obviously apparent in the particle size or volume fraction of the tetragonal zirconia crystals throughout the heat-treatment.

An increase in temperature to 950°C resulted in the growth of gahnite crystals. Even after 15 minutes at this temperature, the crystals began to appear. Fig 4.14. shows the electron diffraction rings obtained from the fully developed glass-ceramic. Both tetragonal zirconia and gahnite can be identified.

The gahnite crystals initially took the form of spherical particles, but structural changes caused the particles to take on a rod-shaped formation after a one hour treatment. This can be seen in fig.4.15. Subsequent times at the crystallization temperature resulted in an increase in the length of the rod-shaped gahnite crystals, until a maximum length is achieved at around the six hour treatment. Fig.4.16. shows the microstructure of the glass heat-treated at 800°C for 4 hours and 950°C for 24 hours. No noticeable change in microstructure is observed.

Since the nucleation of glass 12 appeared quite spontaneously, it was wondered whether gahnite crystals would grow when the temperature was taken directly to 950°C, through the nucleation temperature of 800°C. Fig.4.17. shows the micrographs of glass 12 heat-treated at 950°C only. X-ray diffraction patterns showed exactly the same reflections as for the two-stage treated specimens, and electron microscopy again showed no difference in the microstructure from the two-stage heat-treatment. It can be seen that rod-shaped gahnite crystals are present.

Fig 4.18. shows the microstructure of glasses 1, 8, 12 and 13, heat-treated at 800°C for 4 hours and 950°C for

Fig. 4.14. Electron diffraction photograph of crystallized glass 12 (z = tetragonal zirconia, g = gahnite).

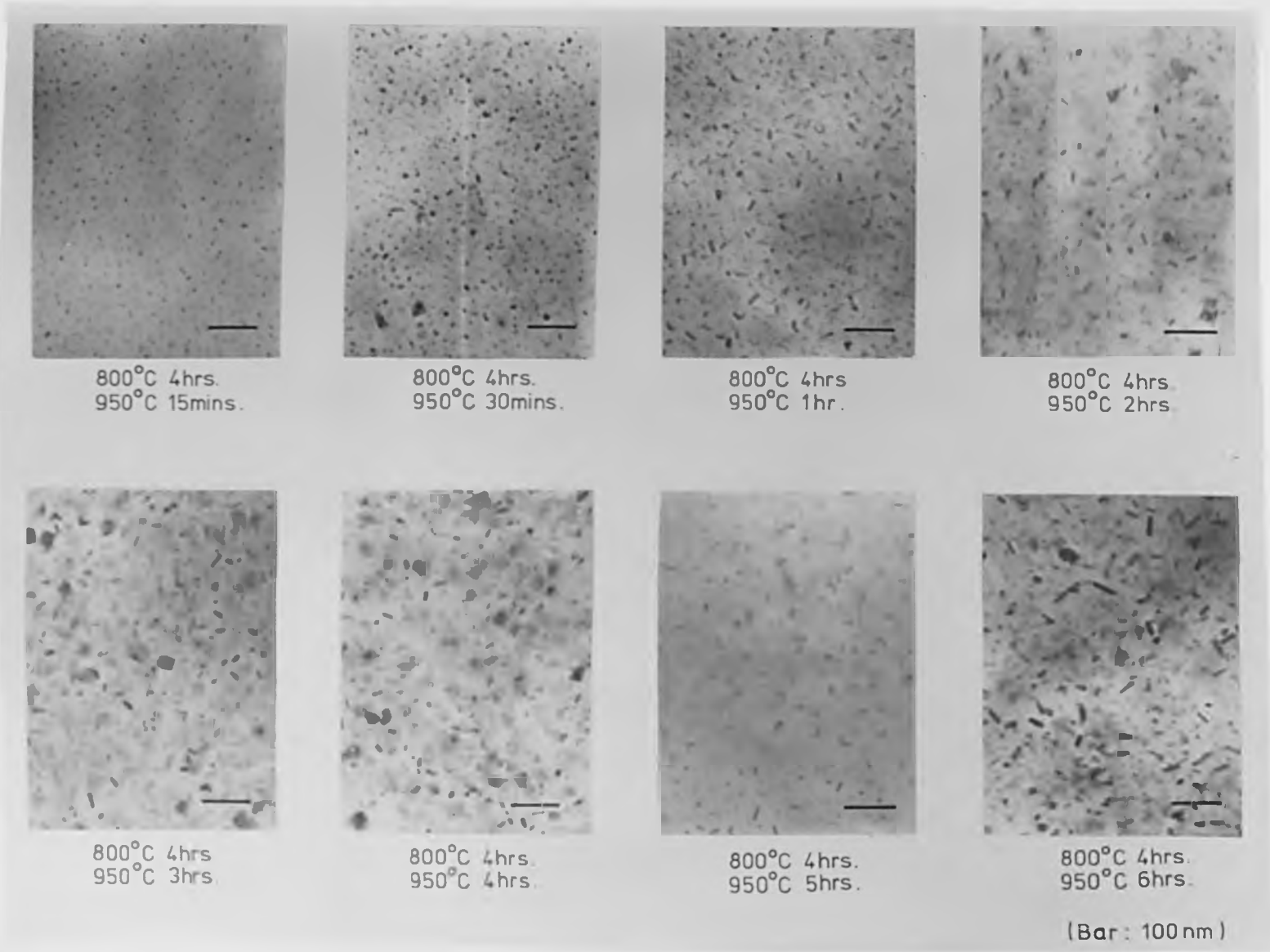

Fig 4.15 Transmission electron micrographs of *crystallized glass 12*

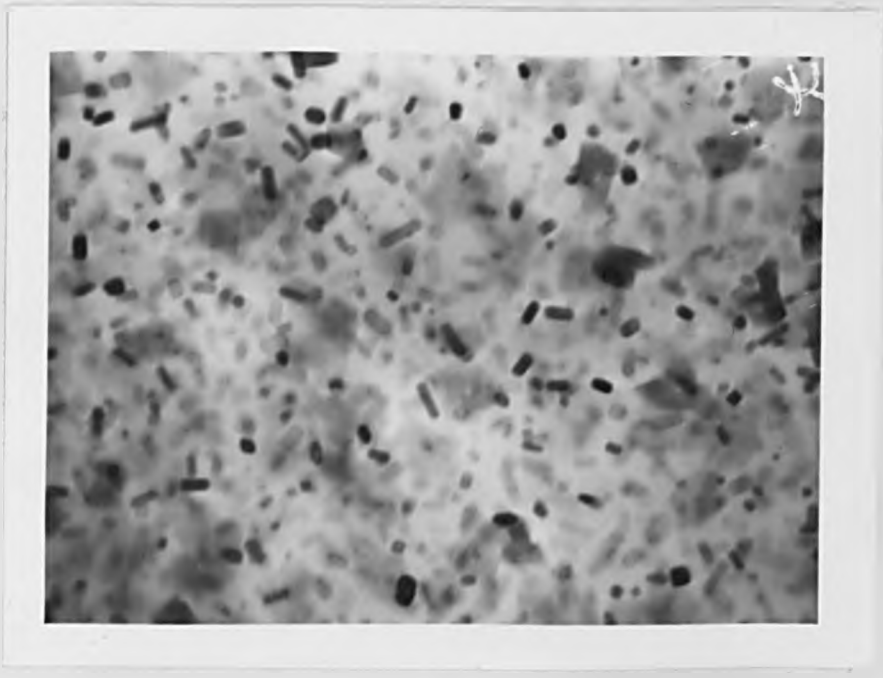

Fig. 4.16. Transmission electron micrograph of glass 12 heat-treated at 800°C for 4 hours and 950°C for 24 hours (Mag. 150,000 :1cm = 66nm).

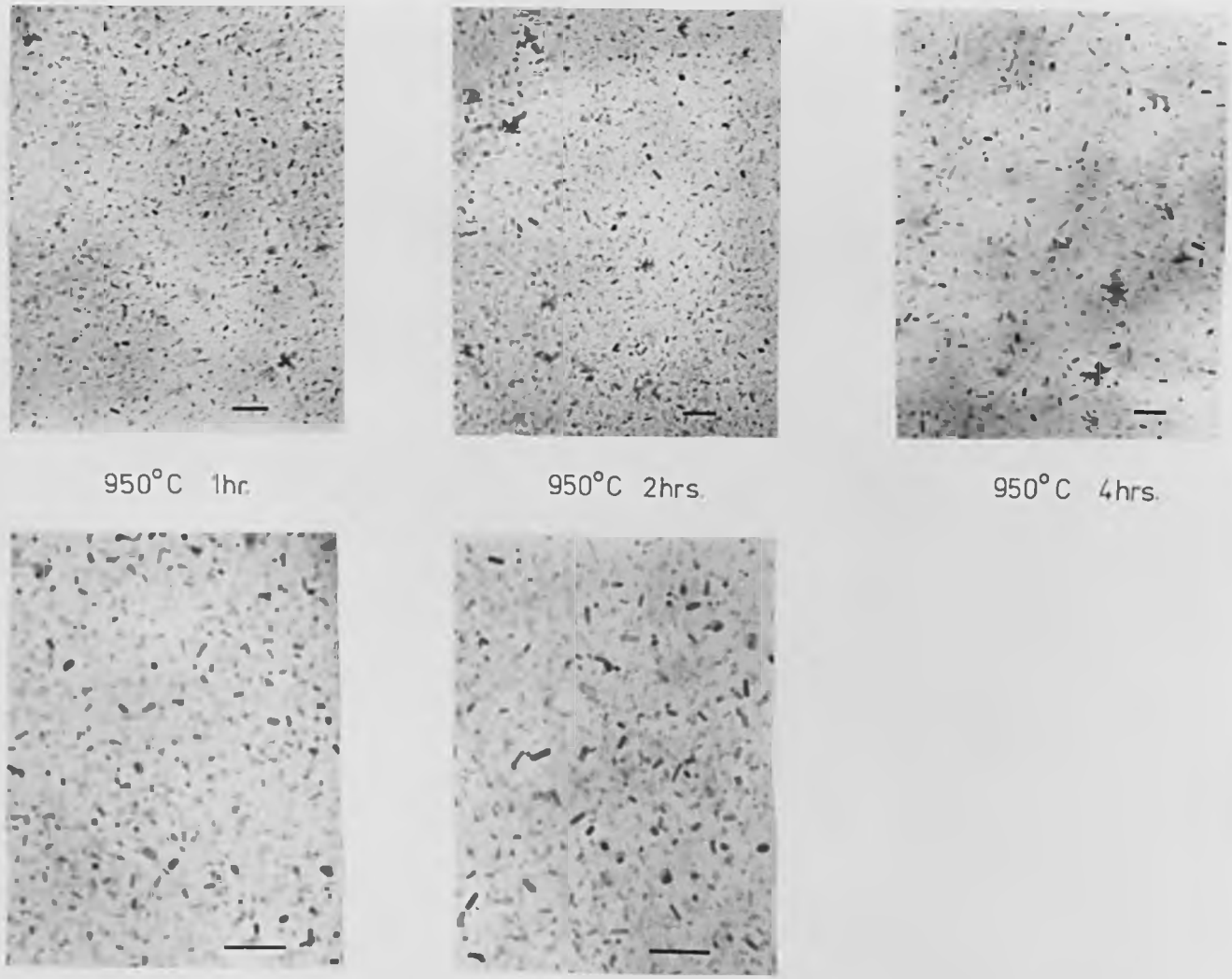

Fig. 4.17 Transmission electron micrographs of crystallized glass 12.

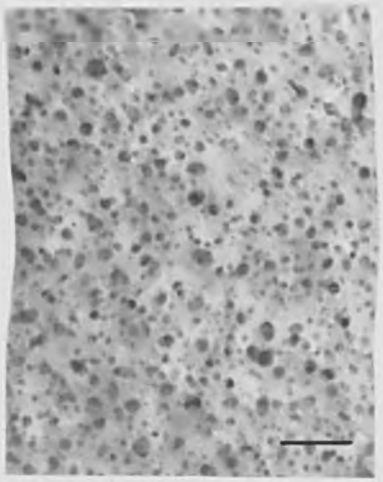

GLASS 1
800°C 4hrs.
950°C 4hrs.

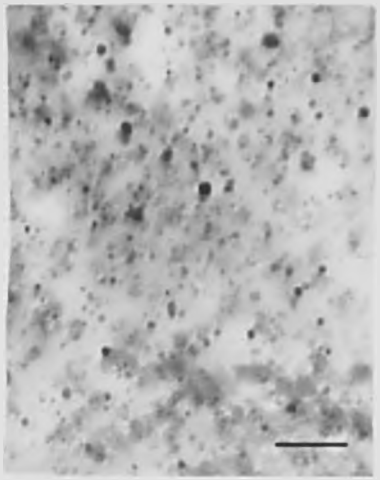

GLASS 8
800°C 4hrs.
950°C 4hrs.

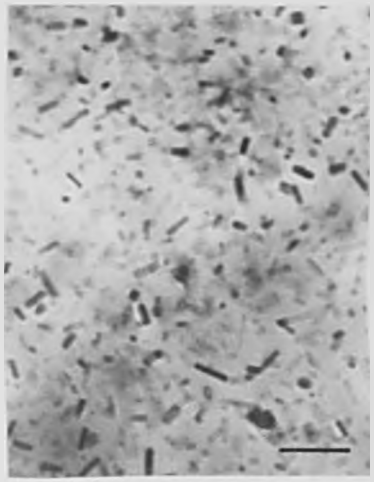

GLASS 12
800°C 4hrs.
950°C 6hrs.

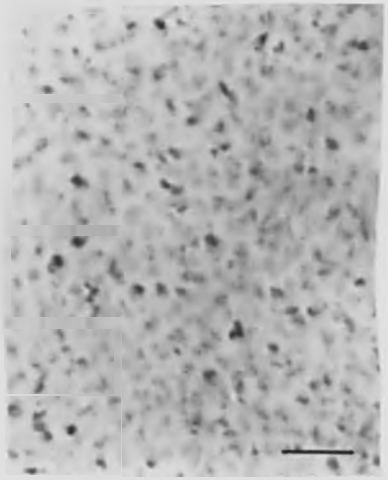

GLASS 13
800°C 4hrs.
950°C 4hrs.

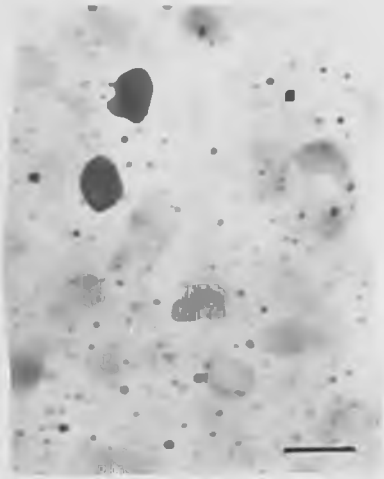

GLASS 3
800°C 4hrs.
1000°C 4hrs.

(Bar : 100 nm)

Fig 4.18 Transmission electron micrographs of crystallized glasses 1, 8, 12, 13 and 3.

4 hours, and also glass 3 (Table 2.1.) which is the glass-ceramic where the gahnite phase was known to be present. This glass was heat-treated at 800°C for 4 hours and 1000°C for 4 hours. It can be seen that the microstructures of glass-ceramics 1, 8, 12, and 13 are slightly different, in the sense that the morphology of the gahnite crystals appears different in glass-ceramics 8, 12, and 13, but the volume fraction and particle size are approximately the same. Glass-ceramic 1 has a larger volume fraction, but of course the crystals present here are a β-quartz s.s.. For glass-ceramic 3, X-ray and electron diffraction showed that the phases present were tetragonal zirconia and gahnite. Fig 4.18. illustrates these two crystalline phases. A larger volume fraction of crystals is present but of a smaller diameter, approximately 9·5nm, and a lower volume fraction of crystals, but of a larger diameter, approximately 53nm, is also present. The smallest aperture selected for electron diffraction was too large even to select the large crystals and so the phases could not be identified individually. A transmission electron micrograph of this glass, heat-treated at 800°C for 4 hours, showed the same microstructure as for the nucleated glass 12. It can be assumed, however, that the small crystals are tetragonal zirconia and the large crystals are gahnite.

4.6. Quantitative Microstructural Analysis.

The particle size analysis of the glass-ceramics 1, 8, 12, and 13 showed that the overall grain size did not exceed 30nm. Similarly, the volume fraction of crystalline phases was low, not exceeding 40% for the β-quartz glass-ceramic and not exceeding 25% for the gahnite glass-ceramics.

Table 4.5. summarises the complete analysis of particle size, volume fraction and intercrystalline spacing of the

Glass-ceramic	Particle size (nm)	Volume fraction (%)	Mean free path (nm)
1-800°C 4 hrs-950°C 3 hrs	10·0 ± 1·5	-	-
1-800°C 4 hrs-950°C 4 hrs	12·5 ± 2·0	34 ± 2	-
8-800°C 4 hrs-950°C 4 hrs	10·0 ± 1·5	22 ± 2	-
13-800°C 4 hrs-950°C 4 hrs	15·5 ± 8	22 ± 2	-
3-800°C 4 hrs-1000°C 4 hrs	9·5 ± 2→53 ± 5	-	-
12-annealed 780°C	5·0 ± 0·5	4·0 ± 0·8	-
12-nucleated 800°C 1 - 4 hrs	7·0 ± 0·8	9·0 ± 1·0	-
12-800°C 4 hrs-950°C 15 mins	8·0 ± 1·0	10·0 ± 1·0	-
12-800°C 4 hrs-950°C 30 mins	8·5 ± 1·5	11·0 ± 1·0	-
12-800°C 4 hrs-950°C 1 hr	19·5 ± 2·5	12·0 ± 2·0	143 ± 7
12-800°C 4 hrs-950°C 2 hrs	21·0 ± 3·0	14·0 ± 2·0	129 ± 7
12-800°C 4 hrs-950°C 3 hrs	22·0 ± 4·0	17·0 ± 2·5	107 ± 8
12-800°C 4 hrs-950°C 4 hrs	23·0 ± 4·0	18·0 ± 1·8	105 ± 8
12-800°C 4 hrs-950°C 5 hrs	24·0 ± 4·0	20·0 ± 1.5	96 ± 8
12-800°C 4 hrs-950°C 6 hrs	28·0 ± 4·0	21·0 ± 1·5	105 ± 8

Table 4.5. Particle size, volume fraction and mean free path of selected transparent glass-ceramics after various heat-treatments.

glass-ceramics studied. No measurements were performed on nucleated glasses 1, 8, 13, and 3, since the nucleation stage provided a phase separated structure, making it difficult to pursue quantitative analysis.

For glass-ceramic 1, the spherical β-quartz s.s. particles reached a maximum size of 12·5 ± 2nm and a volume fraction of 34 ± 2%. For glass-ceramics 8 and 13 the volume fraction was the same; 22 ± 2%. The average particle size varied only slightly from 100 ± 1·5nm for glass-ceramic 8 to 15·5 ± 0·8nm for glass-ceramic 13. For glass-ceramic 3, as mentioned in the previous section, two sets of crystals are present; one assumed to be tetragonal zirconia with a particle size of 9·5 ± 2·0nm and the other gahnite of average size 53 ± 5nm.

For the nucleated glass 12, the average size of the tetragonal zirconia crystals was found to be 7·0 ± 0·8nm with a volume fraction of 9 ± 1%. These values remained constant over the whole nucleation treatment. Quantitative analysis of the annealed glass 12 revealed that here the tetragonal zirconia crystals were 5·0 ± 0·5nm in diameter, with a volume fraction of 4·0 ± 0·8%

Fig.4.19. shows the results of the particle size analysis performed on the crystallized glass 12. The initial size of the spherical gahnite crystals after a 15 minute treatment was 8nm. During the course of crystallization the spherical particles transformed into rod-shaped particles and the length of these rods reached a value of 28 ± 4nm for the 6 hour treatment. Owing to the large errors associated with the measurements of particle size, it was expected that the particle size would stabilize, since no difference in microstructure was observed between the samples treated for 6 hours and those treated for 24 hours. (fig.4.13.)

Fig.4.20. illustrates the change in volume

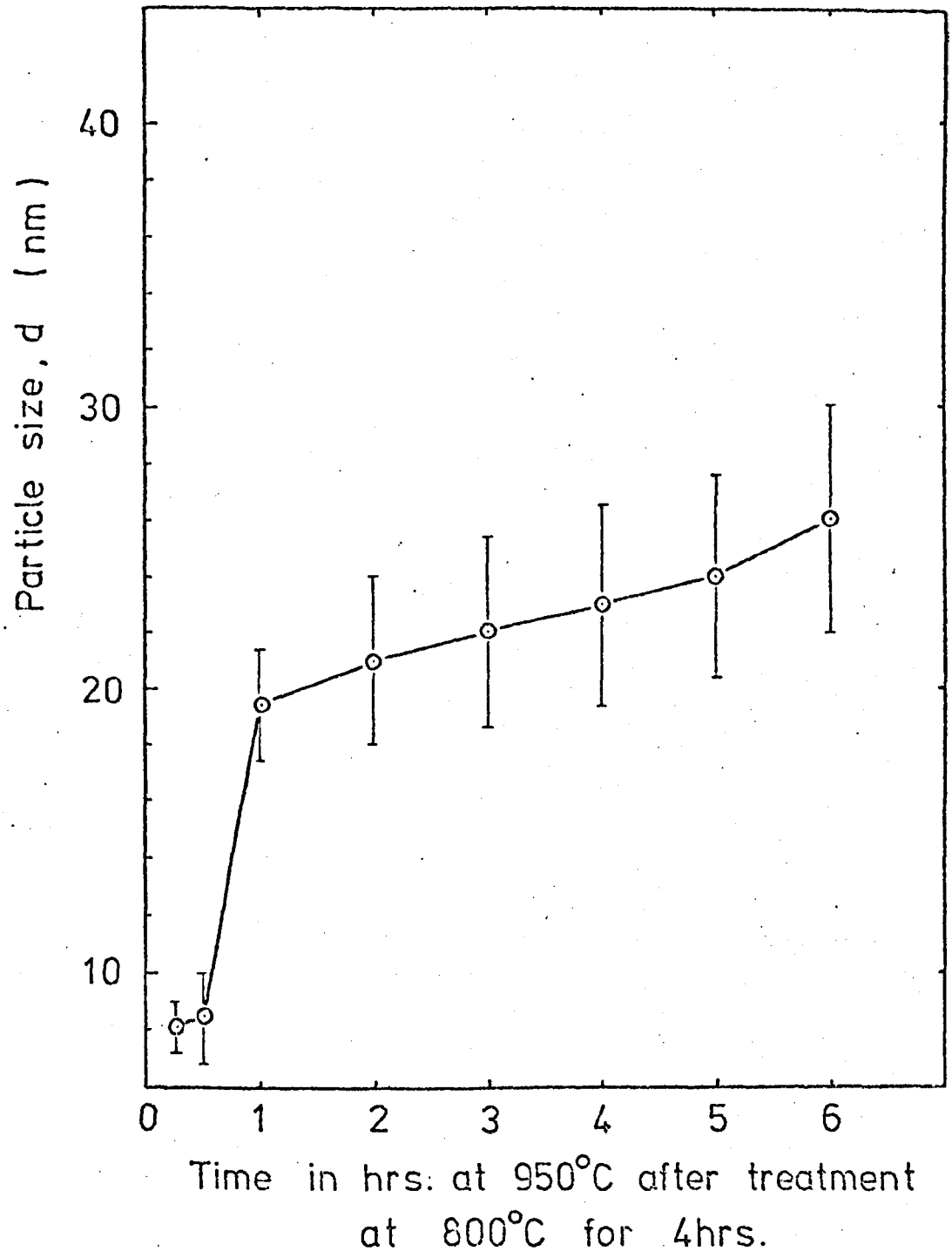

Fig. 4.19. Variation of particle size, d, with heat-treatment for glass-ceramic 12.

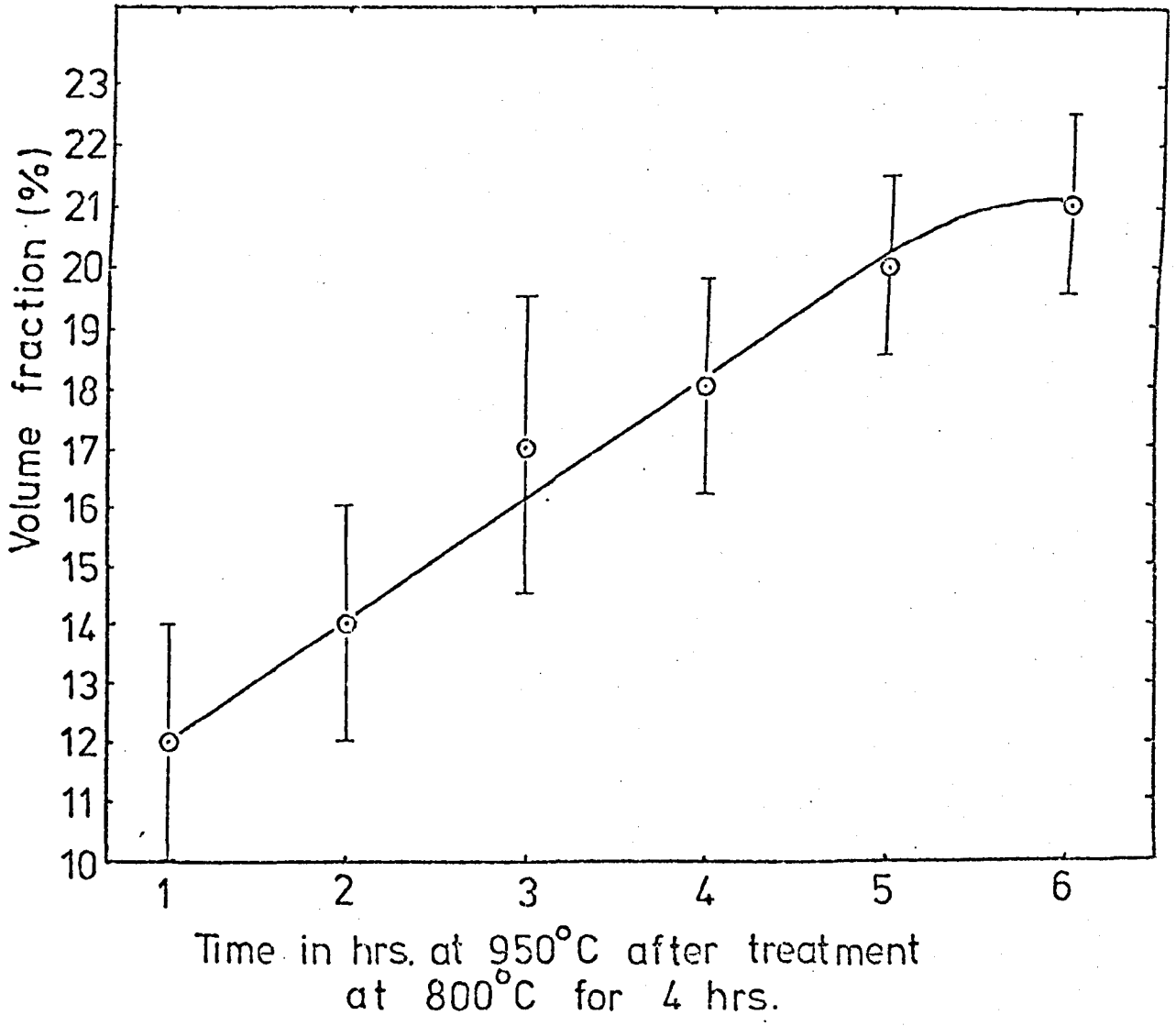

Fig. 4.20. Variation of volume fraction, V_f, with heat-treatment for glass-ceramic 12.

fraction with crystallization heat-treatment of glass 12. Again the errors present are fairly large due to the difficulty of obtaining good micrographs for this kind of analysis. It can be seen, however, that the volume fraction increases uniformly and levels off after the 5 hour treatment at a value of around 20%.

For mean free path or intercrystalline spacing measurements of the rod-shaped particles in glass-ceramic 12, the value of mean particle size was taken to be the average particle length. For the microscopy investigations, no measurements were performed on the average width or diameter of the rods, since no difference was apparent between samples heat-treated for different lengths of time. Since the rod length changed with heat-treatment and the values measured were only relative to each other, this was used in the equation for mean free path. (section 3).

The mean free path, λ, as seen in fig 4.21. decreases until a minimum occurs after the 5 hour treatment.

4.7. E.S.R. Studies.

The spectrum obtained of glass 12, heat-treated at 800°C for 4 hours and 950°C for 6 hours, is shown in fig.4.22.. Several interesting resonances are present; two asymmetric resonances at $g = 4.27 \pm 0.03$ and $g = 3.92 \pm 0.02$, and six symmetric lines around $g = 2$ with $\Delta B = 83.0$ Gauss (0.00830 T). The untreated glass 12, however, produced only the $g = 4.27$ resonance. Literature references were obtained to determine the nature of these resonances.

Firstly, the six small resonances centred around $g = 2$ were identified as the hyperfine structure of Mn^{2+} ions present in the glass as an impurity, following work by Tucker (1962), Barry (1968), Lunter et al (1968), Ja (1969), Loveridge and Parke (1971), Wong and Angell (1971), Moon et al. (1973) and Shaffer et al.(1976).

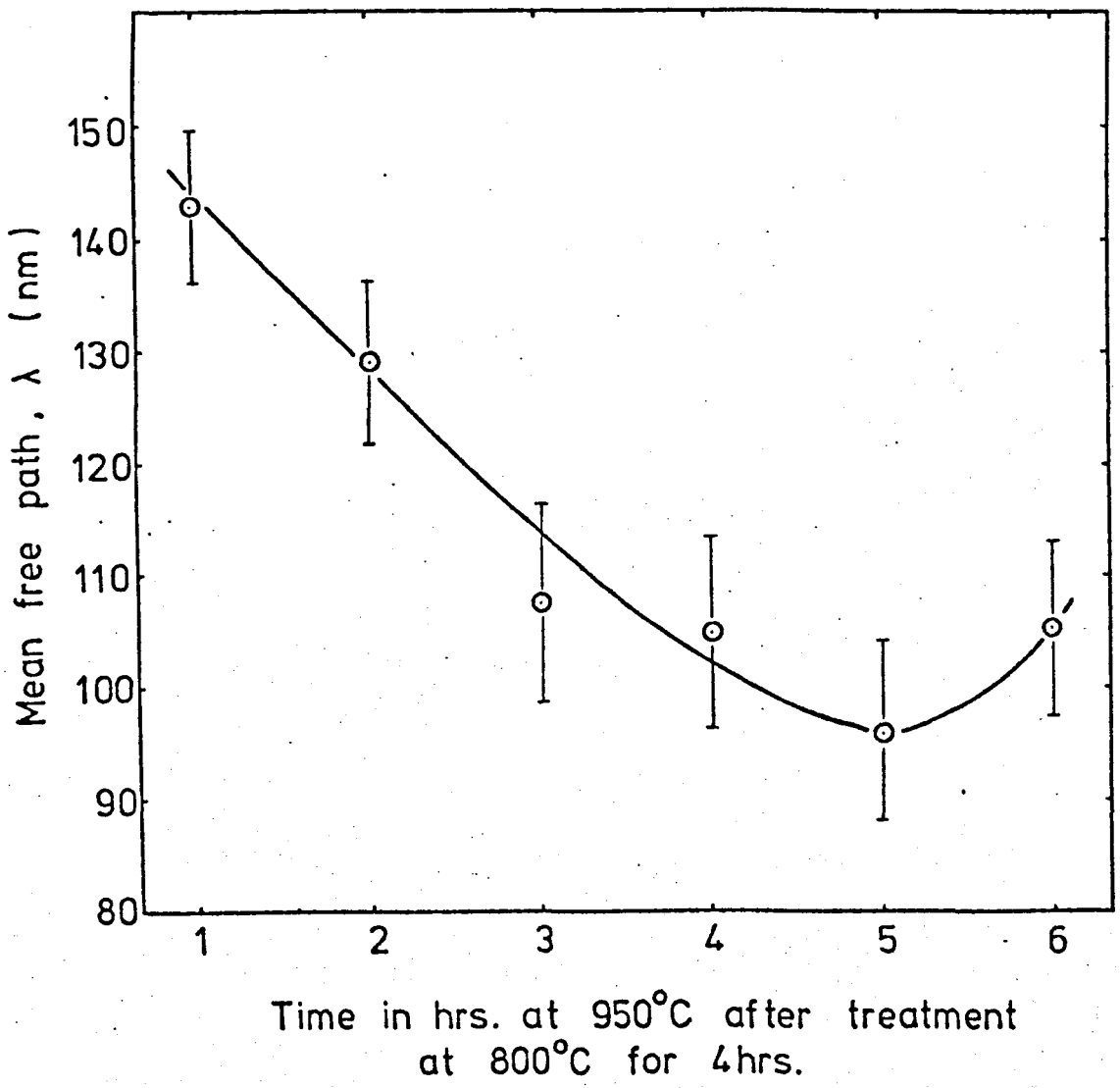

Fig. 4.21. Variation of mean free path, λ, with heat-treatment for glass-ceramic 12.

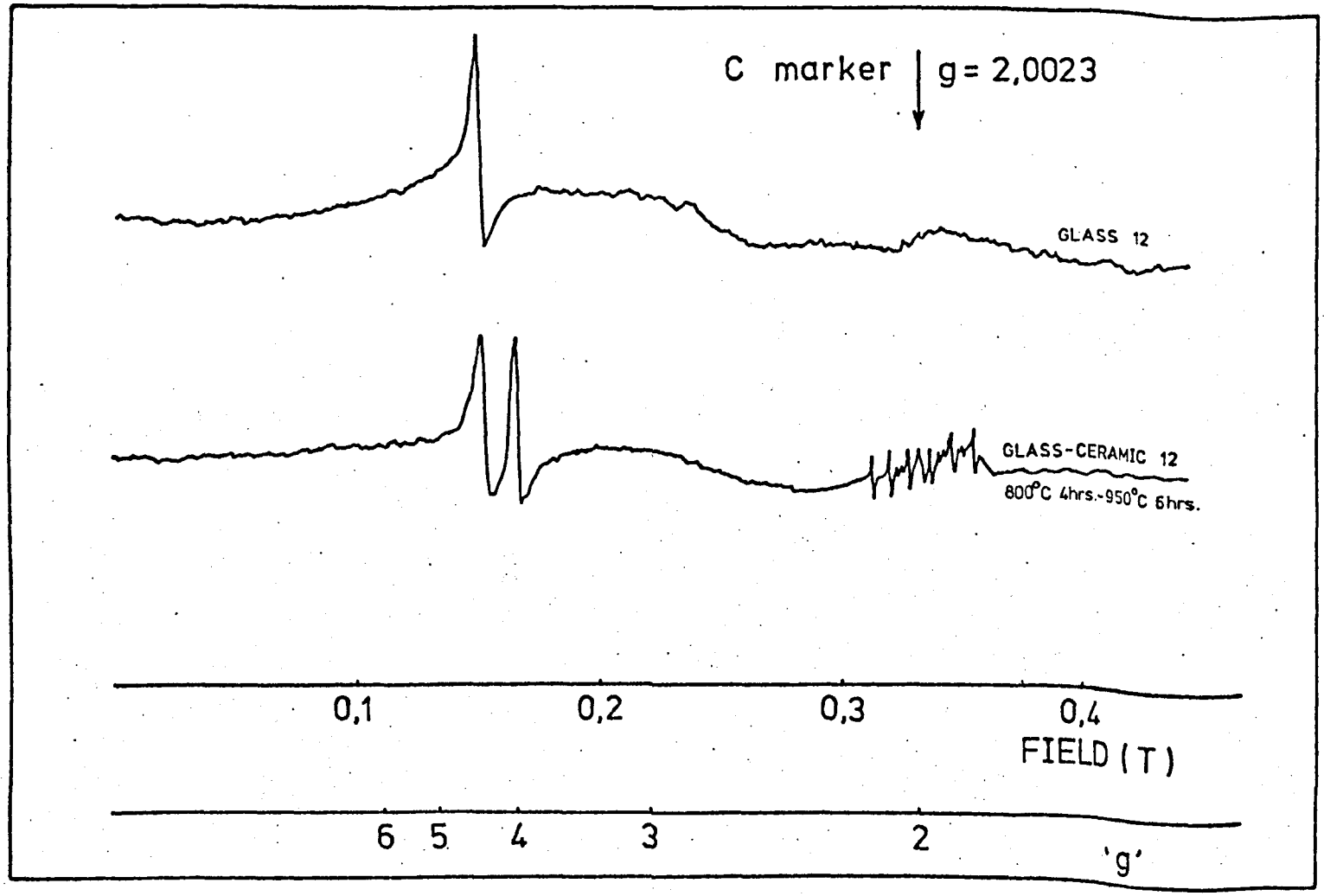

Fig. 4.22. E.S.R. spectra of glass and glass-ceramic 12.

The other two resonances at g = 4·27 and g = 3·92 were more difficult to interpret. It was thought that one or both of these could be due to iron, Fe^{3+}, again present as an impurity, because of previous work on the role of iron in glass systems. It was believed that the main source of iron impurity was the Brazilian quartz used in making up the batch compositions.

Castner et al. (1960) identified unknown resonances at g = 4·27 and g = 6 determined by Sands (1955), as being due to Fe^{3+} ions. Castner considered the most general Hamiltonian which does not involve powers higher than the second,

$$\mathcal{H} = g_o \beta B S_{z'} + D S_z^2 + E(S_x^2 - S_y^2) \qquad (4.1)$$

where D and E are constants, S_x, S_y, S_z are components of spin along three mutually perpendicular crystalline axes x, y, z (chosen so that no terms such as $S_x S_y$ occur in $\mathcal{H}$), z′ is the axis of the static field B, and g_o is the g-value observed if D and E were zero. When considering the importance of tetrahedra in glass, Castner proposed that if the Fe^{3+} ion was at the centre of a tetrahedron and all four corners contained equal charges, then D = 0 = E. A single charge on one corner (or a single corner without a charge) leads to $D \neq 0$, E = 0, the S_z^2 or g = 6 case. Equal charges on two corners (or any charge distribution obtained by superposing 4 charges equal to each other but not necessarily equal to the first two) give the $(S_x^2 - S_y^2)$ or g = 4·28 case.

Kurkjian and Sigety (1968) investigated the E.S.R., optical and Mössbauer spectra of Fe^{3+} in silicate and phosphate glasses. They found that in silicate glasses the Fe^{3+} was four coordinated and in phosphate glasses it was six coordinated. Two resonances were observed, one at g = 4·3 when a low concentration of Fe^{3+} was present, and g = 2 with a high concentration of Fe^{3+}. No resonance is expected

for the Fe^{2+} ion at temperatures above the liquid nitrogen range.

Tucker (1962), in his study of Fe^{3+} in sodium silicates, found that the g = 2 resonance indicated the Fe^{3+} to be in a network modifier position and that the g = 4·28 resonance showed the Fe^{3+} to be in a network former position. This was supported by Kurkjian and Sigety, and Hirayama et al. (1968) who combined Mössbauer, optical and E.S.R. measurements on iron in alkaline earth phosphate glasses to infer the resonances at g = 2 and g = 4·3 to arise from Fe^{3+} in six- and four-fold coordination respectively.

Karapetyan et al. (1963) studied Fe^{3+} in barium and lead silicates, and concluded that the resonance with g = 4·3 belonged to the iron ion in the role of a lattice former in tetrahedral coordination, and that the g = 2 resonance was due to six-fold coordinated iron. Similar results on the coordination of iron with resonances at g = 2 and g = 4·3 were found by Bishay and Makar (1968) in calcium phosphates, Ja (1970) in petalite, $LiAlSi_4O_{10}$, Loveridge and Parke (1971) in sodium borates and sodium silicates, Wong and Angell (1971) in soda-lime silicates, Moon et al.(1975) in barium borates, and Navarro(1976) in alkali silicate, borate and phosphate glasses.

Even in non-glassy systems, Folen (1962) and Schmocker et al.(1972) have shown that Fe^{3+} in ordered $LiAl_5O_8$ goes completely into the tetrahedral site,and Wickman et al.(1965) observed a g = 4·3 resonance for Fe^{3+} in a biological fungus.

A piece of investigation relevant to the present work was performed by Dickson and Srivastava (1976) on the Mössbauer hyperfine spectra of dilute Fe^{3+} in synthetic $MgAl_2O_4$ spinel. Ferric ions introduced into spinel should be able to enter the octrahedral (mainly Al) sites or tetrahedral (Mg) sites. In low concentrations, the iron has a strong preference to enter the tetrahedral site.

Birchall and Reid (1973), however, in a study on the Mössbauer spectra, and Low and Offenbacher (1965) on E.S.R. spectra, of dilute Fe^{3+} in spinel suggested that the iron entered only the octrahedral site. Dickson and Srivastava (1976) re-examined their work and confirmed their initial findings.

From the above survey, it was now thought that the two resonances at g = 4•27 and g = 3•92 were due to Fe^{3+} ions present as an impurity in the glass.

Atomic absorption measurements (Varian Techtron Model 1000 atomic absorption spectrophotometer - Thorn Lighting Ltd.) were obtained on a powdered sample of glass 12. Emphasis was put on the amount of iron and manganese in the glass. The amount of iron was determined to be 130ppm and of manganese to be 3•1ppm. Fig.4.23. shows an EDAX photograph of glass-ceramic 12 and iron is seen to be present in a very small quantity.

The E.S.R. resonance of manganese observed was therefore real, but direct evidence was still required in order to prove that the two g = 4 peaks were due to iron. Glass 12A was prepared. This involved adding an excess of 0·08% Fe^{3+} (800ppm), in the form of ferric oxide Fe_2O_3, to glass 12 and melting the batch in the usual way.

Fig.4.24. shows the resulting spectrum of glass 12A. There is a marked increase in the g = 4•27 resonance, and also present is an additional asymmetric resonance at g = 2•075 $\pm$ 0•002 which could not be identified.

Crystallization of this glass resulted in the appearance of the resonance at g = 3•92. Further heat-treatment increased the peak-to-peak height of this resonance while at the same time decreasing the intensity of the g = 2•075 resonance and also of the g = 4•27 resonance. This will be discussed presently. In the

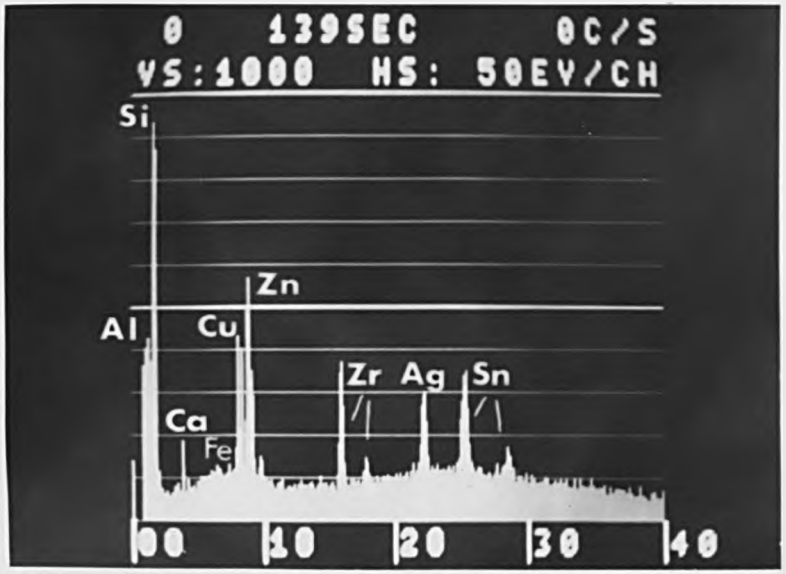

Fig. 4.23. EDAX photograph of glass-ceramic 12.

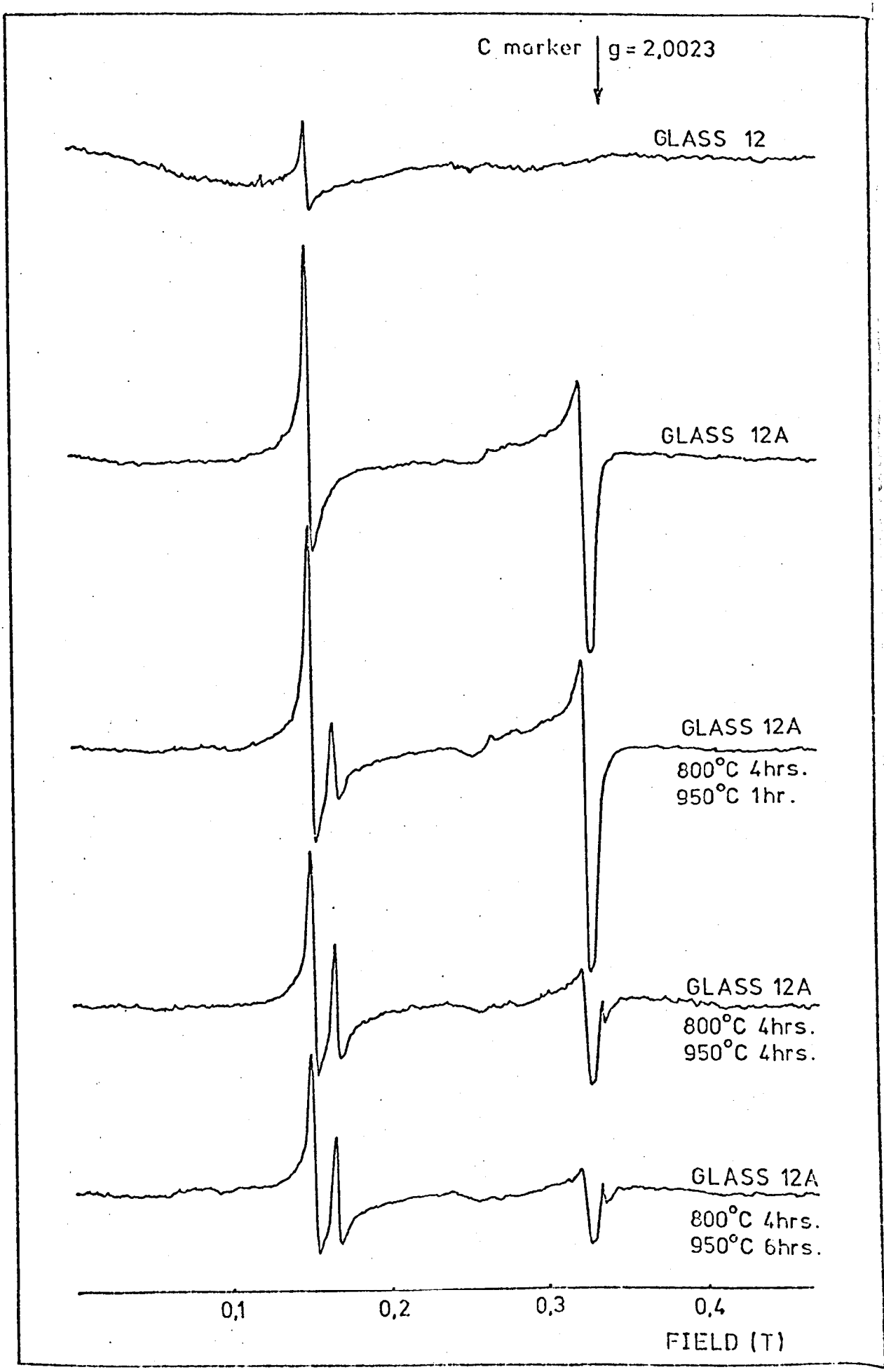

Fig. 4.24. E.S.R. spectra of glass and glass-ceramic 12A.

later stages of crystallization a small free electron resonance appeared at g = 2·00.

Both the g = 4·27 and g = 3·92 resonances produced in glass and glass-ceramic 12A were of a greater intensity than those of glass and glass-ceramic 12, indicating that these resonances must be due to the presence of iron, Fe^{3+}. On this basis, glass 12 was analysed in more detail. Fig.4.25. shows the spectra of glass and glass-ceramic 12 for varying crystallization heat-treatments. It is clear that the resonance at g = 3·92 increases in intensity as the glass crystallizes. Nucleated glasses showed only the g = 4·27 resonance. Similarly, the Mn^{2+} peaks tend to increase in intensity, indicating some structural arrangement as the heat-treatment proceeds.

From the preceding results, it was thought that the iron could possibly change its state of coordination as the glass crystallized, taking on a four-fold coordination in the glass as a network former, and changing to six-fold coordination during the growth of gahnite crystals. This could well be the case for glass 12A, where it is apparent that the g = 4·27 resonance decreases in intensity as crystallization proceeds, but for glass 12, no change in peak-to-peak is recorded for this resonance.

According to Dickson and Srivastava (1976), ferric ions introduced into spinel should be able to enter the octahedral (mainly Al) sites or the tetrahedral (Zn or Mg) sites, although in low concentrations, the iron would have a strong preference to enter the tetrahedral site. Sugiura (1960) and Drumheller et al.(1964) studied the paramagnetic resonance of Fe^{3+} in $MgAl_2O_4$ and $ZnAl_2O_4$ spinel and assumed that in gahnite $ZnAl_2O_4$ the Fe^{3+} ions occupy B-sites in place of Al^{3+} ions, i.e. they can take up a six-fold coordination. In $MgAl_2O_4$ spinel, the Fe^{3+} ions can occupy both of the A- or B-sites, i.e. either four-fold or six-fold coordination. Bishay and

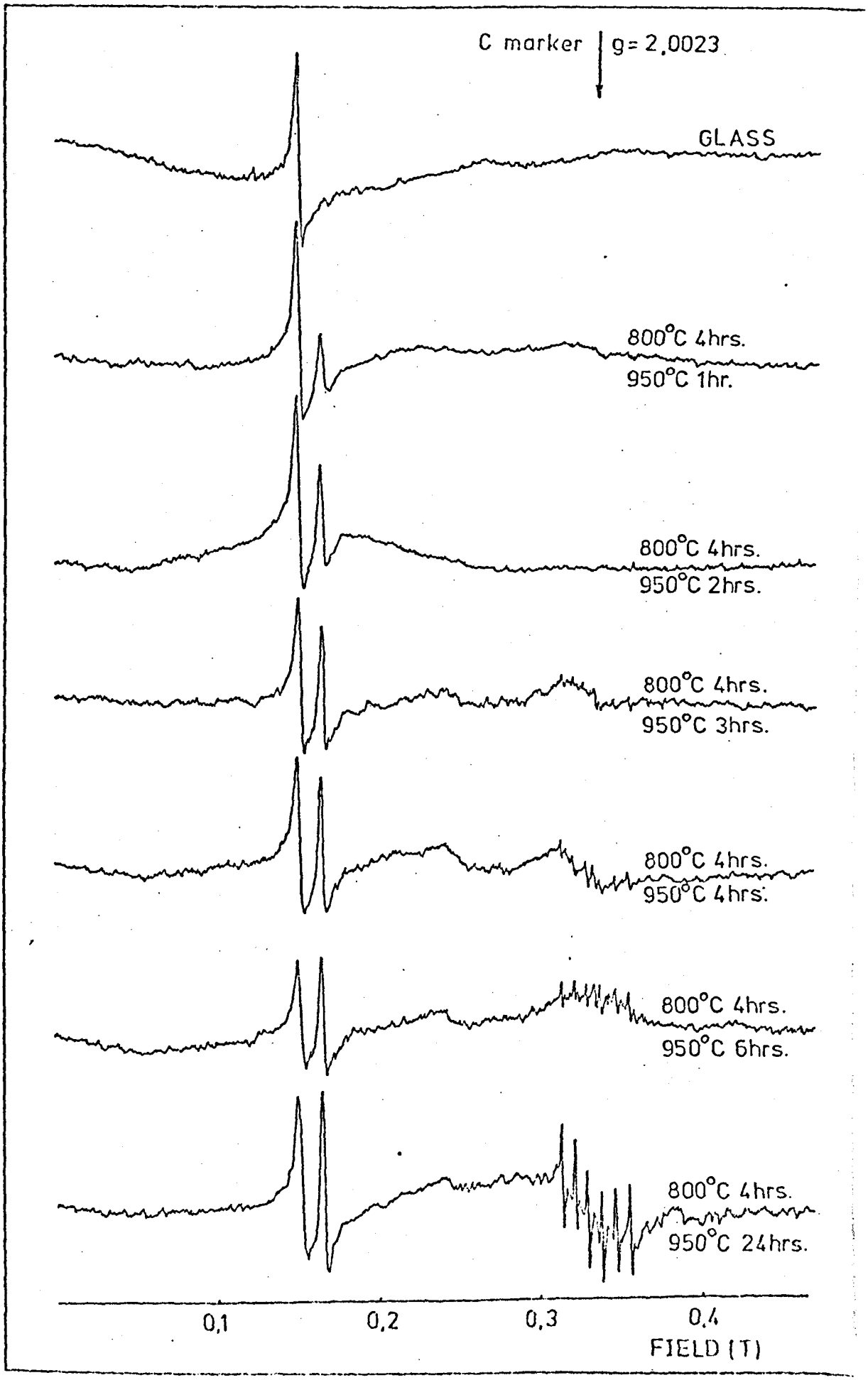

Fig. 4.25. E.S.R spectra of glass 12 for various heat-treatments.

Makar (1968) confirmed by E.S.R. that in calcium phosphate glasses containing 26 mole percent Fe_2O_3, the Fe^{3+} ions existed in both four- and six-fold coordination. Bishay and Hassan (1967) also suggested, on the basis of irradiation studies, that the g = 4•3 resonance is associated with four-coordinated ferric ions in natural silica glass.

In the glasses studied, it can be assumed that the g = 4•27 resonance is due to Fe^{3+} in four-fold coordination, and that once the glass crystallizes, the Fe^{3+} ions in six-fold coordination can be detected at the value of g = 3•92. The resonance observed by previous workers at g = 2 could have been shifted to a higher value, due to the crystal field splitting. It is known that the zinc in the gahnite is present in four-fold coordination, and the aluminium is in six-fold coordination, whereas in the glass, aluminium can take up a four or a six-fold coordination. The iron could, therefore, play a very similar role to that of aluminium.

Since the resonance of glass 12, which in fact was annealed and showed signs of phase separation (section 4.5.), produced an asymmetric feature, it could be established that the Fe^{3+} ions reside fairly closely to an asymmetric crystal field which in this case would be tetragonal zirconia nuclei or even zirconia-rich regions. Similarly, the appearance of the asymmetric six-fold coordinated Fe^{3+} ion resonance at g = 3•92 during heat-treatment might indicate that the gahnite crystals grow very close to, or even around, the tetragonal zirconia nuclei, since the gahnite itself is cubic and would lead to a symmetric resonance.

A plot of the ratio of intensities of the right hand (g = 3•92) peaks to the left hand (g = 4•27) peaks of the crystallization series, (to normalize the height of the g = 4•27 peak) leads to a smooth curve, pictured in fig.4.26., tailing off after the

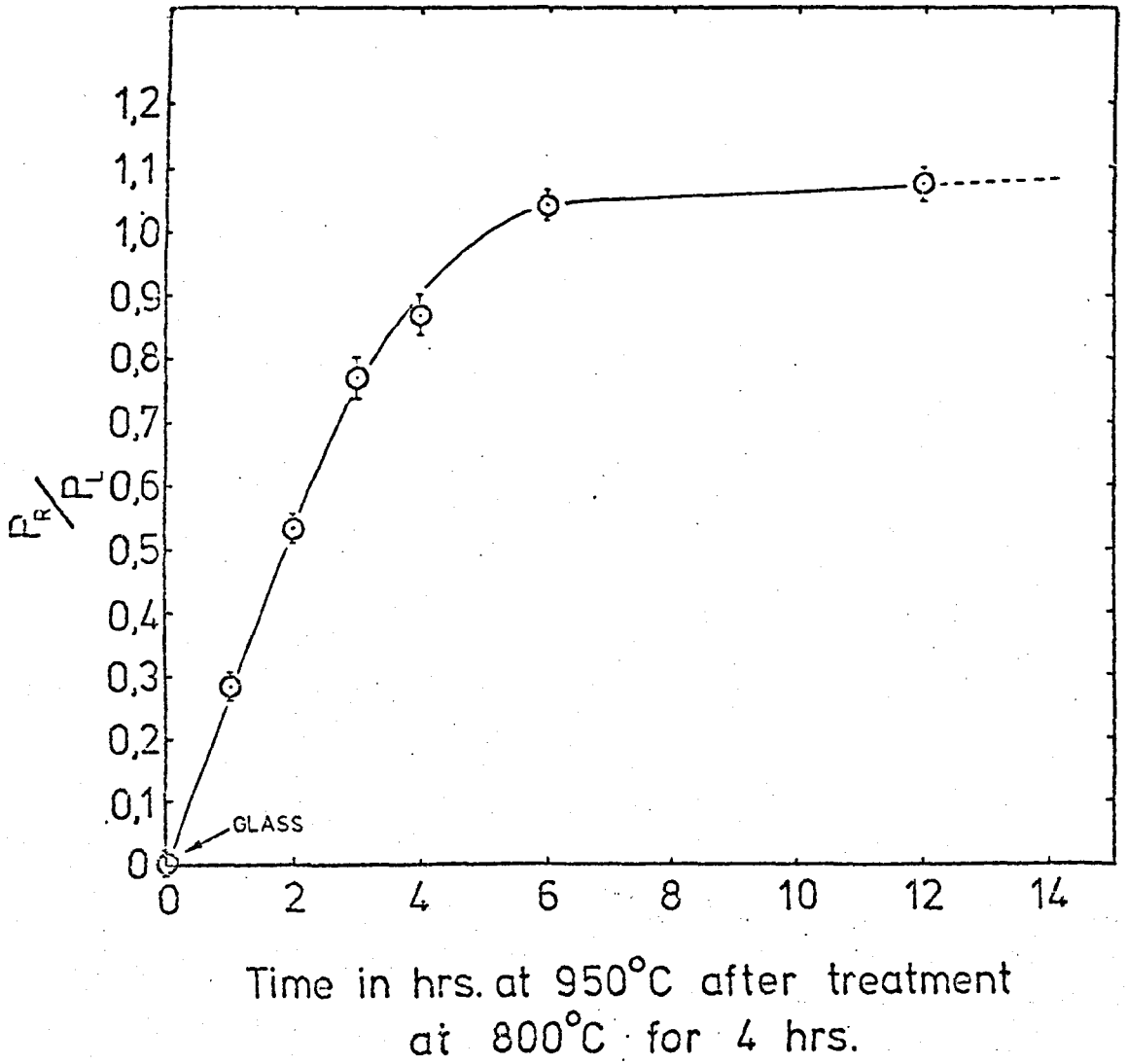

Fig. 4.26. Variations in ratio of the intensities of the two Fe^{3+} peaks with heat-treatment of glass-ceramic 12.

six hour heat-treatment, presumably indicating that maximum crystallization has occurred, since no more six coordinated Fe^{3+} ions in gahnite are developed.

Spectra were run on all available glasses and glass-ceramics prepared, i.e. glasses 1, 3, 5, 7, 8, 12, 13, and these produced similar results for the iron resonances of glass 12 described above. Fig 4.27. shows the resulting spectra. In all the glasses there is present the g = 4•27 resonance of approximately the same intensity. In the heat-treated glasses it is apparent that the g = 4•27 resonance has been reduced in intensity, indicating some transfer from the four coordinated to the six coordinated state. This is not necessarily meaningful, since samples of all glasses, except glass 12, varied somewhat in size and the g = 4•27 peaks could be of the same height for the glass-ceramics and parent glasses. In glass 12, where the heat-treated samples were identical in size, no difference in peak-to-peak height was observed.

The resonances at g = 3•92 all vary in size and appear in glass-ceramics where the phase is a β-quartz s.s., as well as in glass-ceramics where the main phase is gahnite. It is not known whether iron in β-quartz could take up a six-fold coordination.

4.8. Discussion.

The microstructure of the transparent glass-ceramics produced was identified by the usual techniques of X-ray and electron diffraction, D.T.A., and transmission electron microscopy.

The investigations showed that a zirconia nucleated glass-ceramic, derived from the $ZnO - Al_2O_3 - SiO_2$ system could be converted to an extremely fine-grained glass-ceramic by a two-stage heat-treatment in the temperature range of 800°C to 950°C.

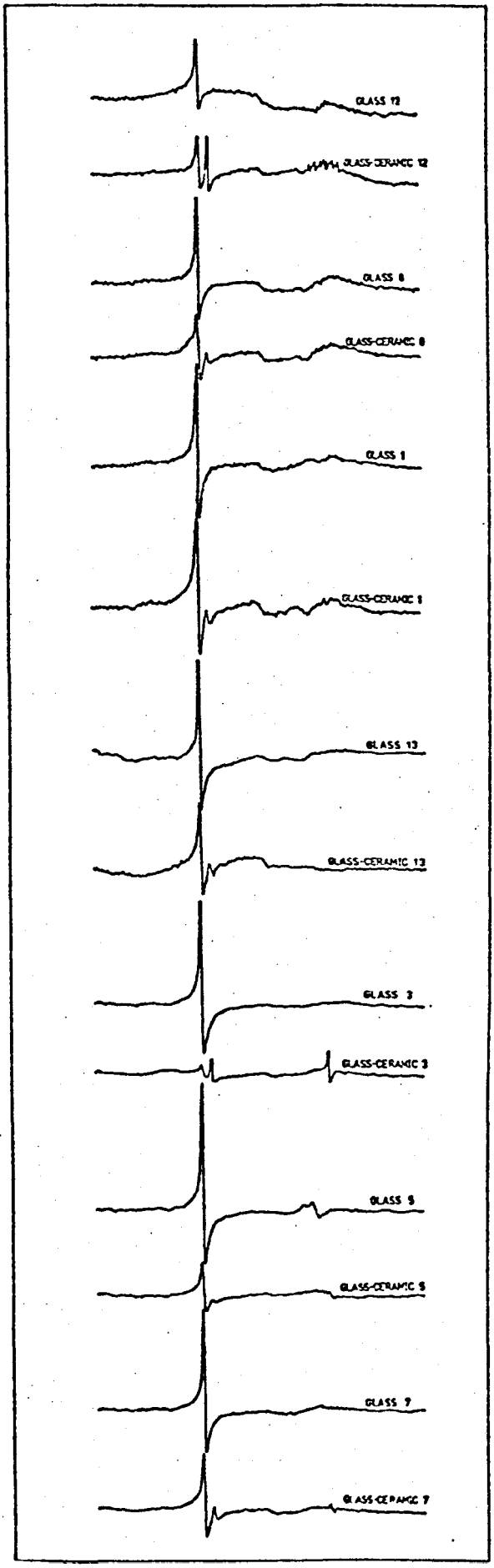

Fig. 4.27. E.S.R spectra of glasses and glass-ceramics 1, 3, 5, 7, 8, 12 and 13.

In all materials the initial crystalline phase was identified as a tetragonal zirconia phase, preceded by a phase separation, which was thought to involve the diffusion of zirconium ions into zirconium rich regions. The phase separation occurred during annealing of the glasses at 780°C, with growth of tetragonal zirconia nuclei during nucleation at 800°C. In all the glasses the tetragonal zirconia crystals were spherical in shape and reached a maximum size of 9nm and a maximum volume fraction of 9%. For glasses where the amount of nucleating agent present was too low for the development of a spinel type crystalline phase, a β-quartz solid solution was formed after crystallization at 950°C. The β-quartz s.s. crystals were spherical in shape with a maximum size, developed after treatment at 800°C for 4 hours and 950°C for 4 hours, of 12·5nm and a volume fraction of 34%. The minimum amount of nucleating agent, ZrO_2, needed for the development of the spinel phase was 9·1% and this produced gahnite, $ZnAl_2O_4$, with the alkaline earth metal ions present in the materials residing in interstitial positions in the glass network. Similar microstructures were observed for glass-ceramics with differing alkaline earth metal oxides, namely MgO, CaO and BaO. Glass-ceramics with MgO and BaO produced spherical or near spherical gahnite crystals, whilst the glass-ceramic with CaO produced spherical crystals in the early stages of crystallization, which transformed to rod-shaped particles at a later stage. For glass-ceramics with MgO and BaO the crystal sizes were 10.0 and 15·5nm respectively with volume fractions of 22%. The glass-ceramic with CaO produced crystals with a maximum length of 28nm and a maximum volume fraction of 21%.

Investigations of microstructural parameters of glass-ceramic 12 (the material with CaO) as a function of heat-treatment, showed that the volume fraction and particle size were

sensitive to heat-treatment, with a flattened maximum occurring after a heat-treatment of 800°C for 4 hours and 950°C for 5 hours.

The mean intercrystalline spacing, λ, appears to be a very sensitive parameter for monitoring the microstructural changes and a distinct minimum occurred at 96nm, for a heat-treatment of 800°C for 4 hours and 950°C for 5 hours.

It is concluded that the optimum microstructure in the sense of maximum volume fraction of the crystalline phase, combined with minimum interparticle spacing was developed by a heat-treatment at 800°C for 4 hours and 950°C for 5 hours.

For the particular systems under investigation, electron spin resonance proved invaluable also in monitoring the heat-treatment schedule, especially when impurities, such as iron or manganese, are present. In the particular investigation, it was found that iron produced the much surveyed resonance at $g = 4{\cdot}27$, indicating that Fe^{3+} ions take up a tetrahedral coordination as a network former. Crystallization led to the introduction of Fe^{3+} into the crystal phase gahnite and to a lesser extent β-quartz, which take up a six-fold coordination, giving the resonance at $g = 3{\cdot}92$. The height of this resonance increased with increasing time at the crystallization temperature and reached a maximum after 5 hours, just as did the volume fraction, indicating that no more iron can be introduced into the six-fold coordination. This shows that the maximum volume fraction of crystals has been reached.

CHAPTER V

Physical Property Results

5.1. Introduction

In this chapter details are presented of results of measurements of physical properties of transparent glass-ceramics, namely thermal expansion, density, hardness, mechanical strength and optical properties. For certain physical properties a relationship is discussed between these properties and the microstructural parameters mentioned in the previous chapter.

5.2. Thermal Expansion

Thermal expansion measurements were performed on glasses and glass-ceramics 1, 8, 12 and 13 (Tables 5.1. and 5.2.), i.e. of compositions giving the β-quartz s.s. crystalline phase or gahnite with different alkaline earth metal oxides.

Table 5.1. gives a summary of thermal expansion coefficients of these glasses and glass-ceramics. It can be seen that glass 1 has an expansion coefficient of $21{\cdot}4 \times 10^{-7}{}^{\circ}C^{-1}$, whereas the glass heat-treated at 800°C for 4 hours and 950°C for 4 hours has an expansion coefficient of $12{\cdot}4 \times 10^{-7}{}^{\circ}C^{-1}$. It is known that a β-quartz s.s. has a very low expansion coefficient; $\sim 5 \times 10^{-7}{}^{\circ}C^{-1}$, (Bailar et al. 1973a), indicating that overall the glass-ceramic should produce a lower expansion than the parent glass, even though there is present a low volume fraction of tetragonal zirconia crystals having a high expansion coefficient of $\sim 128 \times 10^{-7}{}^{\circ}C^{-1}$, (Bailar et al, 1973b). Owing to the inaccuracy of the values of expansion coefficients for the two crystal phases present and the high error in volume fraction measurements, the additive relationship gave only a very approximate value for the expan-

Composition N°	α ($\times 10^{-7} {}^{\circ}C^{-1}$) Base glass	α ($\times 10^{-7} {}^{\circ}C^{-1}$) Glass-ceramic 800°C 4 hrs - 950°C 4 hrs
1	21•4 ± 0•2	12•4 ± 0•2
8	23•1 ± 0•2	26•6 ± 0•2
12	25•5 ± 0•1	31•0 ± 0•1
13	26•9 ± 0•3	38•1 ± 0•3

Table 5.1. Thermal expansion coefficients of glasses and glass-ceramics (20°C - 800°C).

Glass 12	α ($\times 10^{-7} {}^{\circ}C^{-1}$) 20°C - 800°C	α ($\times 10^{-7} {}^{\circ}C^{-1}$) 400°C - 800°C
Base glass	24.4 ± 0.1	28.9 ± 0.1
800°C 4 hrs - 950°C 1 hr	24.5 ± 0.2	25.9 ± 0.2
800°C 4 hrs - 950°C 2 hrs	27.9 ± 0.1	29.3 ± 0.1
800°C 4 hrs - 950°C 3 hrs	28.8 ± 0.3	30.3 ± 0.3
800°C 4 hrs - 950°C 4 hrs	31.0 ± 0.1	33.1 ± 0.1
800°C 4 hrs - 950°C 5 hrs	31.7 ± 0.09	33.8 ± 0.09
800°C 4 hrs - 950°C 6 hrs	31.5 ± 0.3	33.6 ± 0.3

Table 5.2. Thermal expansion coefficients of glass 12 after various heat-treatments.

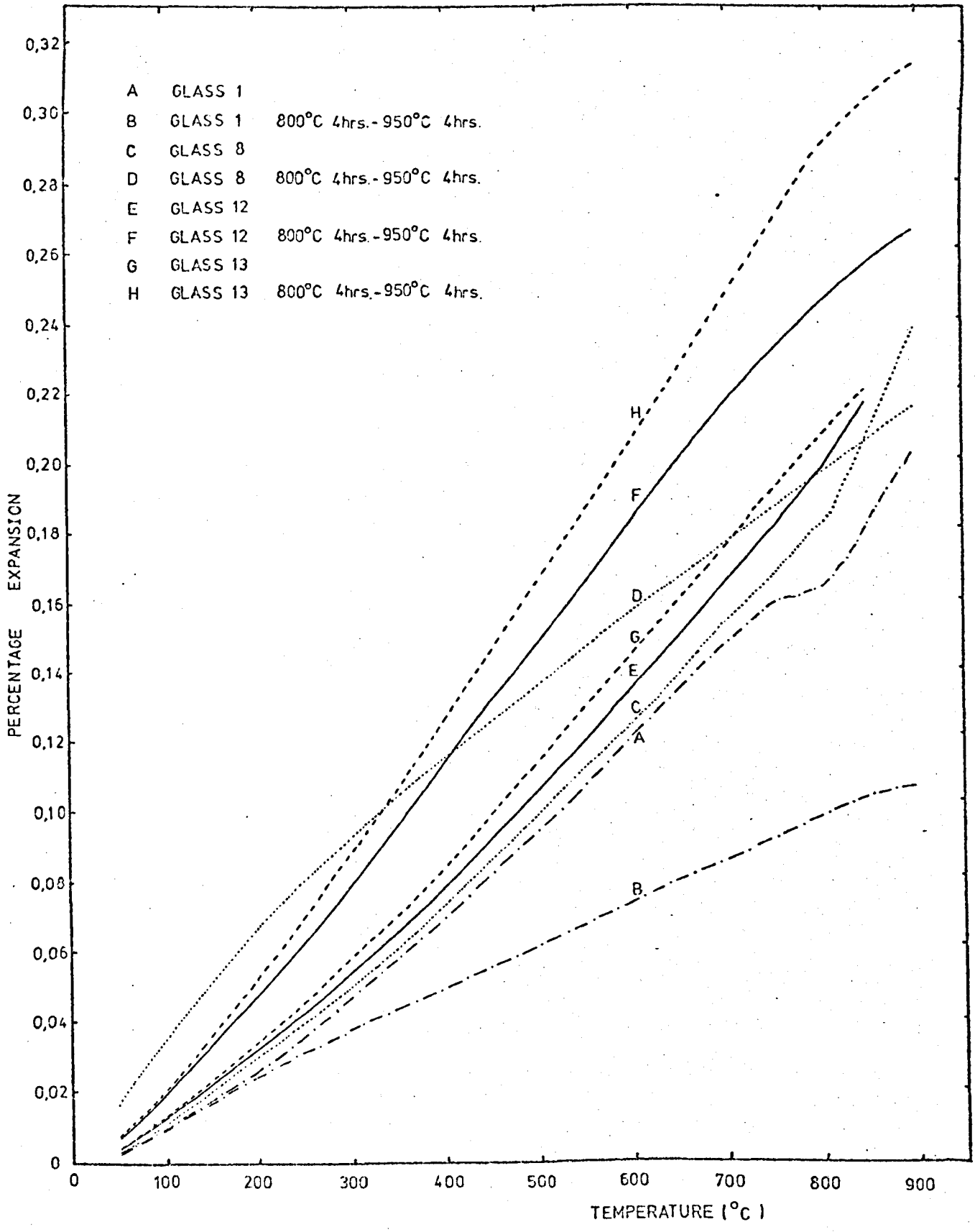

Fig. 5.1. Percentage expansion curves of glasses and glass-ceramics 1, 8, 12 and 13.

sion coefficient of the residual glass phase. This was approximately $2 \times 10^{-7} {}^{o}C^{-1}$.

Fig 5.1. shows percentage expansion curves of glasses 1, 8, 12 and 13 and their corresponding glass-ceramics. The expansion increases from glass 1 to 8 to 12 to 13. For glass 1 to have a lower expansion than the others would be expected, since the extra amount of ZrO_2 in glass 8 would increase the overall expansion. The increase in expansion from glass 8 to 12 to 13 is also expected due to the presence of larger alkaline earth metal ions. The size of the ions increases from Mg^{++} to Ca^{++} to Ba^{++} with a corresponding decrease in ionic field strength, and hence the overall expansion would tend to increase. It must be remembered, however, that a weight by weight substitution of the alkaline earth metal oxides was made. A molecular substitution would show a greater expansion difference. The molecular percentage of the oxides used was MgO 7·5%, CaO 5·5%, and BaO 2·1%.

Since the volume occupied by the oxygen ions is large compared with the volume occupied by all the cations in the glass, the closeness of packing can be expressed in terms of the number of oxygen ions contained within unit volume of glass, or in terms of the volume of glass which contains some definite weight of oxygen (Stevels, 1948, Moore and McMillan, 1956, Weyl and Marboe, 1962). Since the chemical composition of the glasses is known, the weight of glass which contains one gram atom of oxygen can be calculated. This weight divided by the density of the glass, ρ, gives the volume V_o, which contains one gram atom of oxygen, and this provides a measure of the closeness or compactness of the glass structure. The values of V_o can be expressed in the form;

$$V_o = \frac{100}{\rho \sum\left(\frac{Pn}{W}\right)} \qquad (5.1.)$$

V_o and ρ are defined as above

P is the weight percent of any one of the constituent oxides, represented by A_mO_n.

n is the number of oxygen ions in one molecule of the oxide A_mO_n.

W is the molecular weight of the oxide A_mO_n.

The value of V_o was calculated for glasses 8, 12, and 13, and was found to be 13·12c.c., 13·13c.c. and 13·29c.c. respectively. Large ions with low field strengths will exert only weak forces on the neighbouring oxygen ions, and the separation between such cations and their neighbouring oxygen ions will increase with a rise in temperature. The thermal expansion of complex glasses will depend on the binding forces of all cations on their neighbouring oxygen ions. If the proportion of large cations of low field strength is large, giving a high value of V_o, the coefficient of thermal expansion of the glass will also be high, while a high proportion of small cations of high field strength, giving a low V_o value, will tend to keep the expansion coefficient low. Hence from these theoretical considerations, the expansion would increase from glass 8 to 12 to 13. This is confirmed by experimental evidence.

Fig. 5.2. shows the percentage expansion of glass 12 during crystallization. The steady increase in expansion is due to the growth of gahnite crystals, gahnite having an expansion coefficient of approximately $77 \times 10^{-7}{}^{o}C^{-1}$, (National Research Council, 1926). The maximum expansion appears to be attained after approximately 4 hours at the crystallization temperature, when the maximum size and volume fraction of gahnite crystals has been reached, as described in section 4.6.. According to the additive relationship, equation (2.1), the expansion of the residual glass phase is approximately $5 \times 10^{-7}{}^{o}C^{-1}$, which is the value for fused silica. Fig 5.3. shows the change in thermal expansion coefficient with the volume fraction of gahnite crystals present in the glass-ceramic.

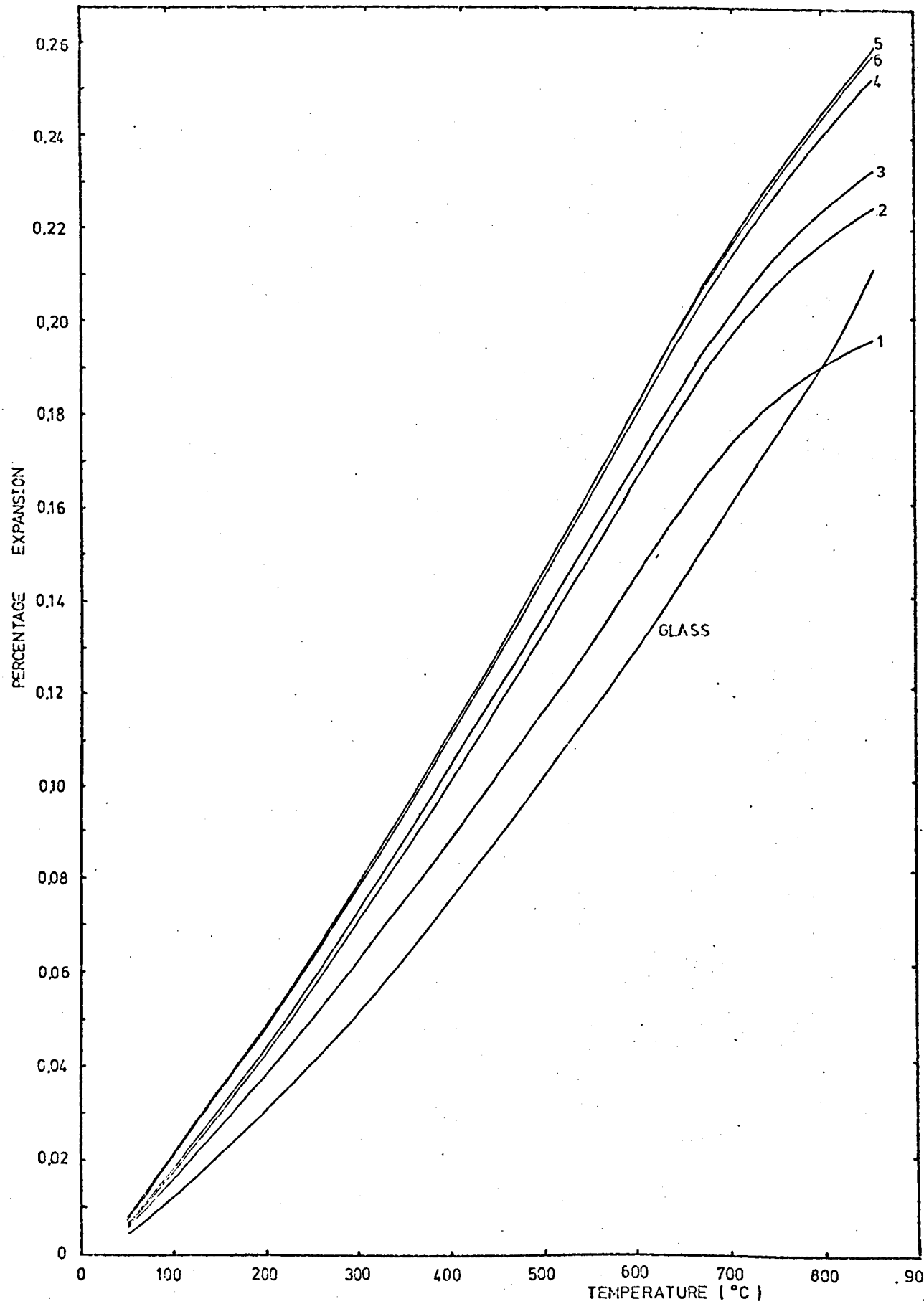

Fig. 5.2. Percentage expansion curves of glass 12 after various heat-treatment times (the numbers on the right of the curve refer to the number of hours the samples had been heat-treated at 950°C after a nucleation treatment of 800°C for 4 hours.

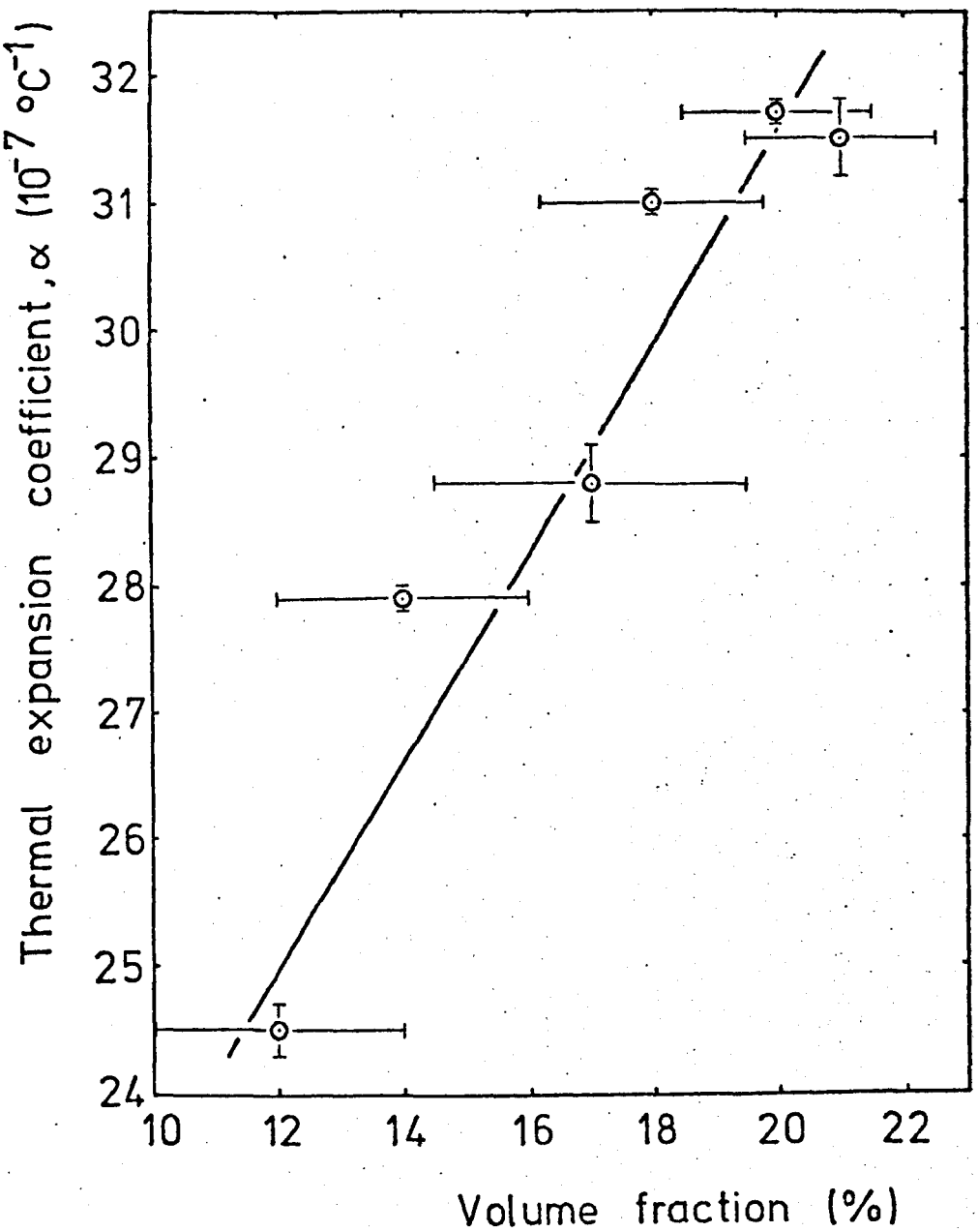

Fig. 5.3. Variation of expansion coefficient, α, with volume fraction, V_f, of gahnite crystals in glass-ceramic 12.

Glass 12 was selected for detailed investigations of other physical properties, because of the possibility of sealing the glass to tungsten, due to reasonable compatibility of thermal expansions.

5.2.1. Sealing to Tungsten

Tungsten has a thermal expansion coefficient of $45 \times 10^{-7} {}^{o}C^{-1}$, and so the question arose as to whether the glass itself (expansion coefficient $28{\cdot}9 \times 10^{-7} {}^{o}C^{-1}$) would be sealed to the tungsten. An attempt was made to seal glass 12 to the tungsten by taking a 1mm diameter and 3cm long tungsten wire, spinning it in a lathe and melting a fragment of glass onto the wire, using a hydrogen-oxygen torch, to produce a thin sleeve of glass on the tungsten. The strong oxidising nature of the hydrogen-oxygen flame resulted in crystallization of the glass, producing a white opaque material. The crystalline phase was analysed by X-ray diffraction, which showed narrow reflections of tetragonal zirconia. Blowing nitrogen gas onto the glass and tungsten wire whilst sealing with the hydrogen-oxygen flame eliminated the crystallization.

After sleeving of the tungsten wire with the glass, more glass was sealed onto the wire to form a bead, which again did not crystallize as long as nitrogen gas was blown onto the glass. Fig. 5.4. shows the glass sealed to the tungsten. No noticeable straining or cracking was observed after the glass had been sealed to the tungsten.

The wire and glass were then sealed in an evacuated silica tube, and heat-treated at 800°C for 4 hours and 950°C for 6 hours in order to produce the transparent glass-ceramic. Again no sign of stressing was noticed, thus indicating a good rigid seal. A piece of the glass-ceramic was broken off and analysed by X-ray diffraction, and produced the usual tetragonal zirconia and gahnite phases.

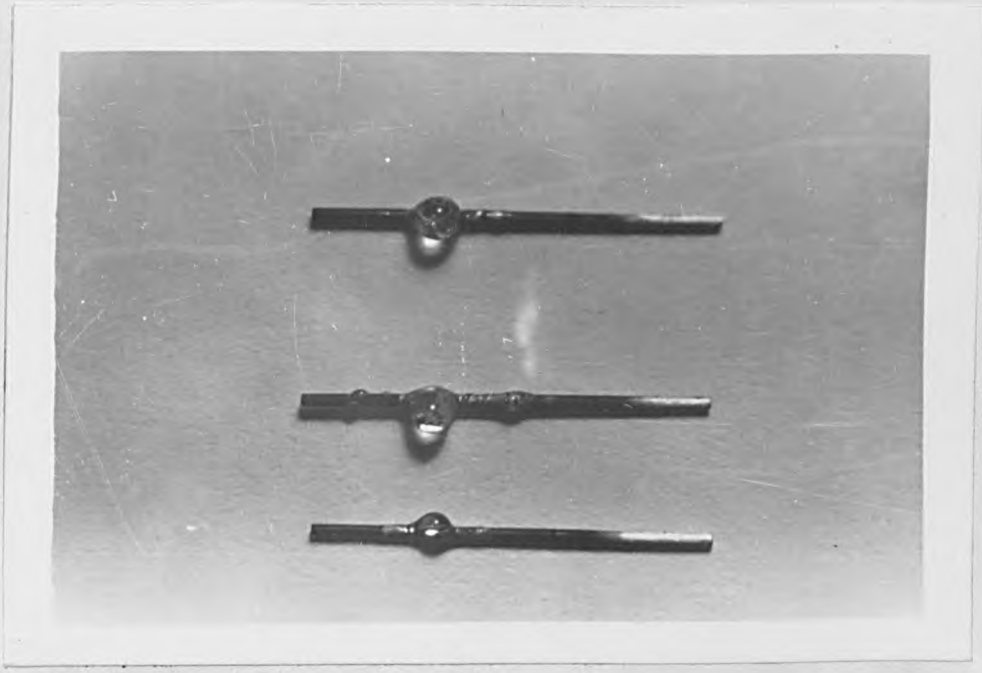

Fig. 5.4. Photograph of glass 12 sealed to tungsten wire.

5.3. Density

Densities were measured for glasses 1, 8, 12 and 13 and their corresponding glass-ceramics. All show a density in the region of 2·5 to 2·7 gm cc^{-1}.

Table 5.3. shows the measured densities of the above glasses. All, except glass 12, show an increase in the density which is expected, due to the presence of tetragonal zirconia (density 6·16 gm cc^{-1}, Bailar et al. 1973b), gahnite (density 4·58 gm cc^{-1}, National Research Council, 1926), and β-quartz (density approximately 2·63 gm cc^{-1}, Bailar et al, 1973a).

Theoretical densities of glasses were obtained from the specific volume V_s estimated by the weight fraction, W_{xo}, and the volume fraction V_{xo}, given by Huggins and Sun (1943). For the case of glasses 1, 8, 12 and 13, the density is related to the empirical expression

$$\frac{1}{\rho} = V_s = V_{SiO_2} W_{SiO_2} + V_{Al_2O_3} W_{Al_2O_3} + V_{RO} W_{RO} + V_{ZnO} W_{ZnO} + V_{ZrO_2} W_{ZrO_2} \quad (5.2.)$$

where RO is the corresponding alkaline earth metal oxide MgO, CaO or BaO.

According to the above equation the theoretical densities are

Glass 1	2·547 gm cc^{-1}
Glass 8	2·571 gm cc^{-1}
Glass 12	2·601 gm cc^{-1}
Glass 13	2·641 gm cc^{-1}

which tie in fairly well with the experimental values in Table 5·3. Glass 12 was studied in greater detail and density measurements were performed on heat-treated samples. Table 5.4. and fig. 5.5. show the results. The density after the initial crystallization treatment at 800°C for 4 hours and 950°C for 1 hour drops to a value of 2·546 gm cc^{-1}. This could well be expected because the nucleation temperature, being

Composition N°	Density ρ (gm cc^{-1}) Base glass	Density ρ (gm cc^{-1}) Glass-ceramic 800°C 4hrs - 950°C 4 hrs
1	2·539 ± 0·007	2·573 ± 0·008
8	2·580 ± 0·007	2·712 ± 0·008
12	2·605 ± 0·003	2·576 ± 0·004
13	2·622 ± 0·009	2·648 ± 0·009

Table 5.3. Densities of glasses and glass-ceramics.

Glass 12	Density ρ (gm cc^{-1})
Base glass	2·605 ± 0·003
800°C 4 hrs - 950°C 1 hr	2·546 ± 0·004
800°C 4 hrs - 950°C 2 hrs	2·555 ± 0·002
800°C 4 hrs - 950°C 3 hrs	2·570 ± 0·003
800°C 4 hrs - 950°C 4 hrs	2·576 ± 0·004
800°C 4 hrs - 950°C 5 hrs	2·580 ± 0·002
800°C 4 hrs - 950°C 6 hrs	2·582 ± 0·004

Table 5.4. Densities of glass 12 after various heat-treatments.

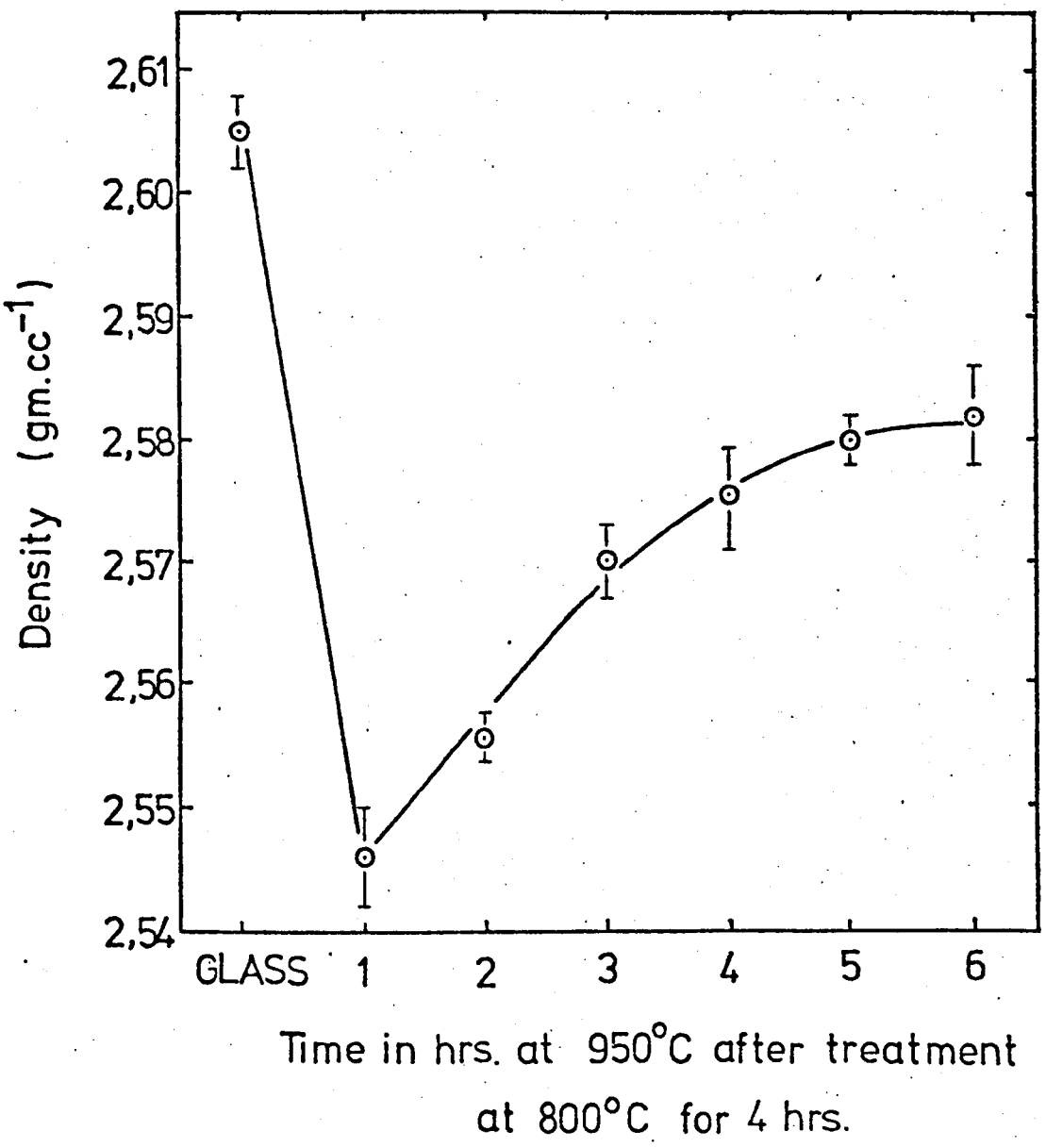

Fig. 5.5. Density of glass 12 after various heat-treatment times.

higher than the annealing temperature, would introduce structural changes into the glass, allowing relaxation of the network to occur at the higher temperature. This is also what generally occurs when a quenched glass is annealed.

Further crystallization results in a steady and gradual increase in density until a levelling off occurs after the five hour treatment. The density itself does not, however, reach the previous level of the glass itself, but it can be seen that the overall change in density is very small.

Fig. 5.6. shows the relationship between the density and volume fraction of gahnite crystals present in glass-ceramic 12.

5.4. Microhardness.

Hardness measurements were performed on glasses 1, 8, 12 and 13 before and after various heat-treatments. Experimental details are described in section 2.5.2.

Table 5.5. and fig. 5.7. show the results of hardness measurements on glass and glass-ceramic 12, subjected to both nucleation and crystallization heat-treatments. Two facts are apparent from the figure:

(1) The nucleated glasses have a lower hardness than the parent glass. The hardness rises to a maximum after three hours and then decreases again. This effect appears real, because the errors are small, but no explanation can be given for it. In the nucleation stage, no microstructural changes are observable by electron microscopy and so no change is expected in the microhardness of these glasses. The decrease in hardness of the nucleated glasses may arise from the crystallization of tetragonal zirconia which

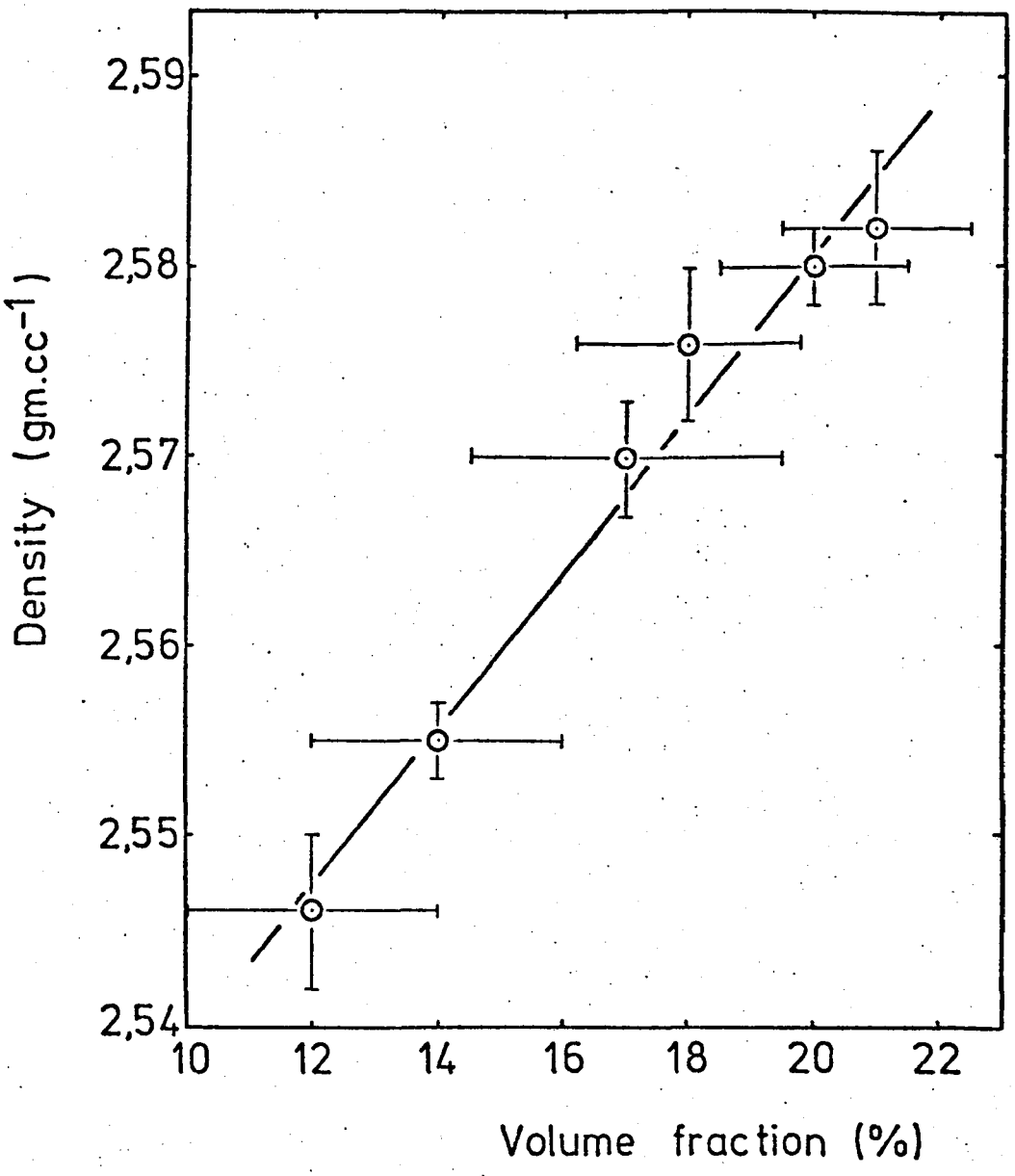

Fig. 5.6. Variation of density, ρ, with volume fraction, V_f, of gahnite crystals in glass-ceramic 12.

		VHN $kg\ mm^{-2}$	$10^9\ Nm^{-2}$
GLASS 12	Base glass	669 ± 3	6·56 ± 0·03
	800°C 1 hr	646 ± 5	6·34 ± 0·05
	800°C 2 hrs	658 ± 10	6·45 ± 0·09
	800°C 3 hrs	660 ± 8	6·47 ± 0·08
	800°C 4 hrs	658 ± 6	6·45 ± 0·06
	800°C 5 hrs	641 ± 4	6·29 ± 0·04
	800°C 4 hrs - 950°C 1 hr	655 ± 5	6·42 ± 0·05
	800°C 4 hrs - 950°C 2 hrs	673 ± 6	6·60 ± 0·06
	800°C 4 hrs - 950°C 3 hrs	704 ± 5	6·90 ± 0·05
	800°C 4 hrs - 950°C 4 hrs	709 ± 6	6·95 ± 0·06
	800°C 4 hrs - 950°C 5 hrs	718 ± 6	7·04 ± 0·06
	800°C 4 hrs - 950°C 6 hrs	716 ± 4	7·02 ± 0·04
GLASS 1	Base glass	666 ± 17	6·53 ± 0·17
	800°C 4 hrs - 950°C 1 hr	790 ± 12	7·75 ± 0·12
	800°C 4 hrs - 950°C 2 hrs	813 ± 9	7·97 ± 0·09
	800°C 4 hrs - 950°C 3 hrs	861 ± 12	8.44 ± 0·12
	800°C 4 hrs - 950°C 4 hrs	883 ± 12	8·66 ± 0·10
	800°C 4 hrs - 950°C 5 hrs	933 ± 21	9·15 ± 0·21

Table 5.5. Vicker's Hardness of glasses 1 and 12 after various heat-treatments.

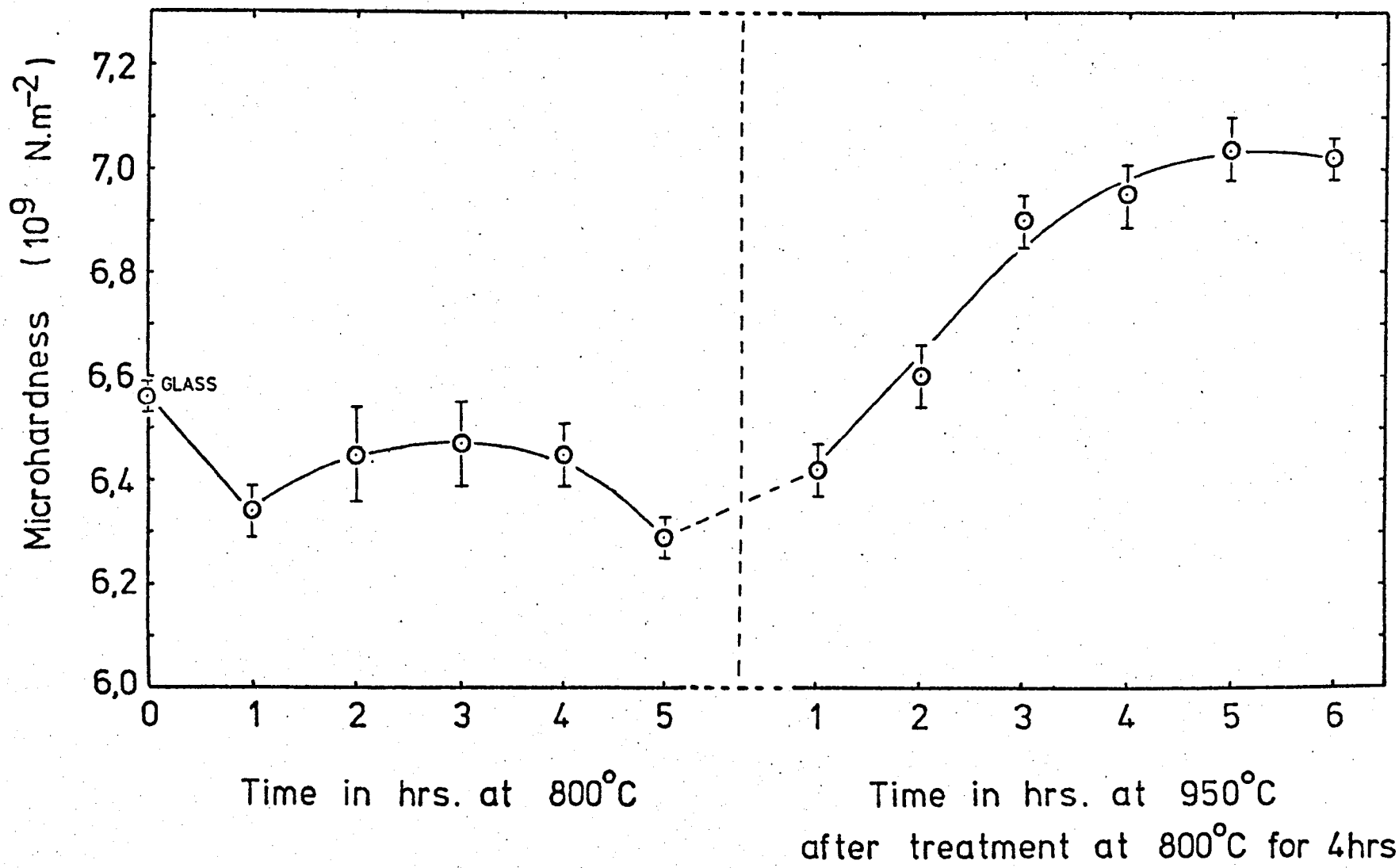

Fig. 5.7. Microhardness of glass 12 after various heat-treatment times.

shows a high hardness of approximately 1100 VHN ($kgmm^{-2}$), (Landolt-Börnstein, 1950), resulting in a decrease in the hardness of the glassy matrix. The volume fraction of tetragonal zirconia being only 9% would not generally be sufficient to raise the overall hardness. The additive relationship would indicate that the glassy matrix has a hardness of around 616 VHN ($kgmm^{-2}$).

(2) In the crystallization region, the micro-hardness rises linearly up to a 4 hour treatment and subsequently levels off after a 5 to 6 hour treatment. The increase is, as would be expected, due to the high hardness of gahnite, which is approximately 1300 VHN ($kgmm^{-2}$) (Landolt-Börnstein, 1950).

Table 5.6. shows the hardness measurements of glasses 1, 8, 12 and 13 and their corresponding glass-ceramics, heat-treated at 800°C for 4 hours and 950°C for 4 hours. The base glasses all fall within a narrow range, but the glass-ceramics show a wide trend. Fig. 5.8. relates the microhardness of glass-ceramic 12 to glass-ceramic 1. It is apparent that the high hardness of glass-ceramic 1 is due to the high volume fraction of β-quartz crystals.

Theoretical calculations were made of the Vicker's Hardness by using an equation derived by Yamane and Mackenzie (1974).

$$H_V = 0{\cdot}051\left(\frac{\alpha}{0{\cdot}462 + 0{\cdot}09V - V^2}\right)^{1/2} E \quad (5.3.)$$

where α is the ratio of the average single bond strength to the Si-O bond strength,

E is Young's Modulus

V is the ionic volume fraction.

α is calculated using the equation:

Composition N°	Base glass		Glass-ceramic 800°C 4 hrs-950°C 4 hrs	
	VHN ($kgmm^{-2}$)	$10^9 Nm^{-2}$	VHN ($kgmm^{-2}$)	$10^9 Nm^{-2}$
1	666 ± 17	6·53 ± 0·17	883 ± 10	8·66 ± 0·10
8	688 ± 5	6·75 ± 0·05	789 ± 7	7·74 ± 0·07
12	669 ± 3	6·56 ± 0·03	709 ± 6	6·95 ± 0·06
13	642 ± 8	6·30 ± 0·08	749 ± 6	7·35 ± 0·06

Table 5.6. Vicker's Hardness of glasses and glass-ceramics.

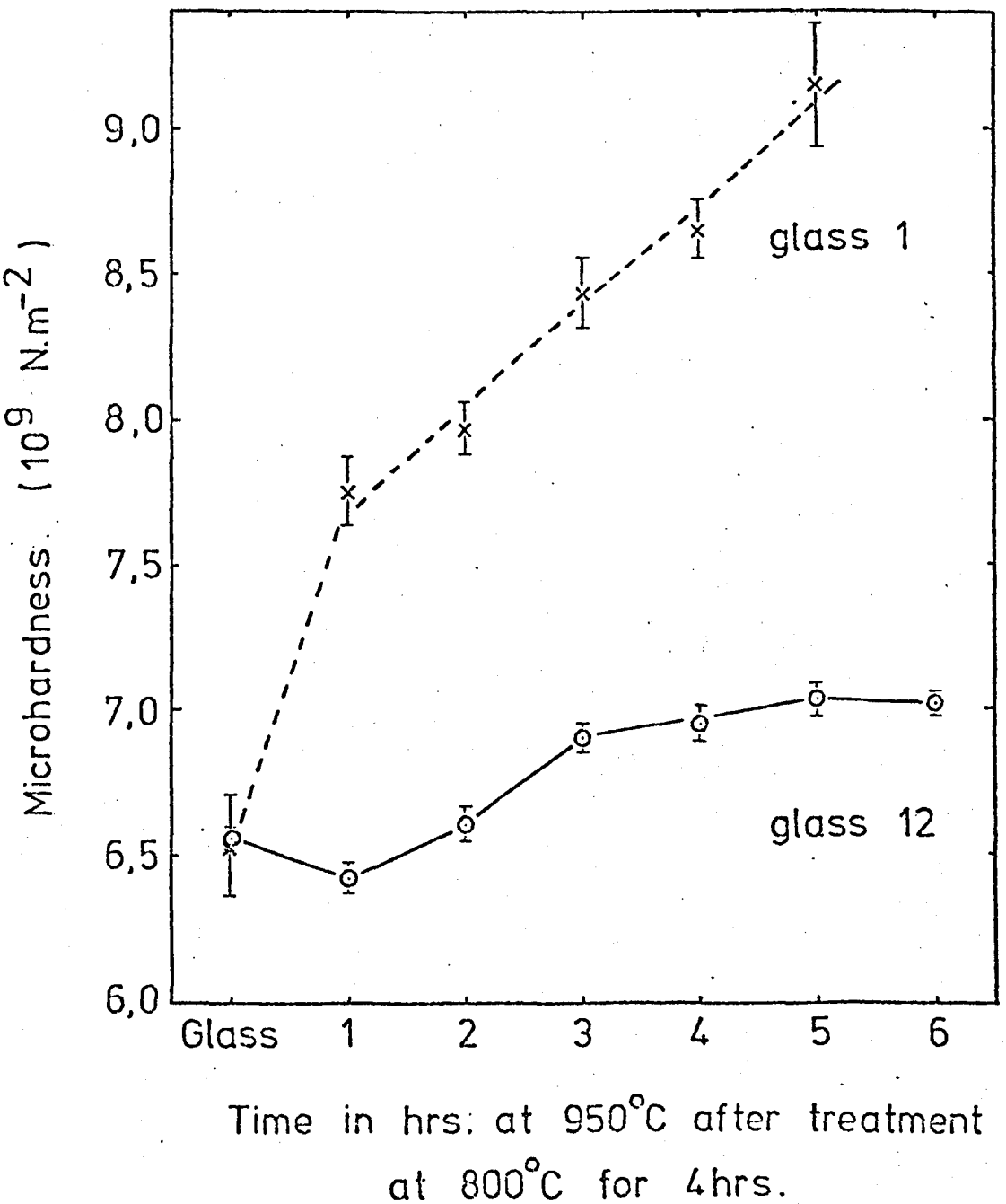

Fig. 5.8. Comparison of microhardness of glasses 1 and 12 after various heat-treatment times.

$$\alpha = \frac{\sum | f_j n_j \epsilon_j |}{\epsilon_{Si} \sum | f_j n_j |} \qquad (5.4.)$$

where f_j is the number of cations, j, in one mole weight of glass

n_j is the coordination number of the cation j

ϵ_j is the single bond strength of cation j to the oxygen band

ϵ_{Si} is the single bond strength of the Si-O bond

The ionic volume fraction is determined using the relation:

$$V = \frac{\rho}{M} \sum_i \left[\frac{4}{3} \pi r_i^3 f_i \right] \qquad (5.5.)$$

where ρ is the density of the glass

M is the molecular weight of the glass

r_i is the radius of ion i

f_i is the number of ions, i, in one mole weight of glass

The density, ρ, as mentioned in section 5.3., is obtained from the specific volume, V_s, established by the weight fraction, W_{xo}, and the volume fraction, V_{xo}, given by Huggins and Sun (1943). Young's Modulus is calculated from the empirical expression:

$$E = X_{SiO_2} E_{SiO_2} + X_{Al_2O_3} E_{Al_2O_3} + X_{RO} E_{RO} + X_{ZnO} E_{ZnO} + X_{ZrO_2} E_{ZrO_2} \qquad (5.6.)$$

where E_{SiO_2}, $E_{Al_2O_3}$, E_{RO}, E_{ZnO}, and E_{ZrO_2} are the Young's Modulus coefficients in kbars/mole%.

X_{SiO_2}, $X_{Al_2O_3}$, X_{RO}, X_{ZnO} and X_{ZrO_2} are the molar percentages in the glass

and RO is the corresponding alkaline earth metal oxide MgO, CaO, or BaO.

According to the above relations, the Vicker's Hardness was obtained for glasses 1, 8, 12 and 13 and the results are as follows;

glass 1 : $\rho = 2{\cdot}547$ gm cc^{-1}

$E = 7729{\cdot}6$ Kg mm^{-2}

$H_v = 659{\cdot}7$ Kg mm^{-2}

glass 8 : $\rho = 2{\cdot}571$ gm cc^{-1}

$E = 7643{\cdot}1$ Kg mm^{-2}

$H_v = 658{\cdot}4$ Kg mm^{-2}

glass 12: $\rho = 2{\cdot}610$ gm cc^{-1}

$E = 7578{\cdot}3$ Kg mm^{-2}

$H_v = 649{\cdot}3$ Kg mm^{-2}

glass 13: $\rho = 2{\cdot}641$ gm cc^{-1}

$E = 7362{\cdot}8$ Kg mm^{-2}

$H_v = 647{\cdot}8$ Kg mm^{-2}

Another method of determining Young's Modulus, E, was devised by Yamane and Sakaino (1974):

$$E = 9{\cdot}3 \frac{\rho}{M} \sum \left[T_{m_i} X_i \right] \qquad (5.7.)$$

where ρ is the density in gm cc^{-1}

M is the molecular weight of the glass in gm $mole^{-1}$

T_{m_i} is the melting point of oxide i in degrees Kelvin

X_i is the mole fraction of oxide i

E is Young's Modulus in Kbars.

According to this equation the values of E and H_v for glasses 8, 12 and 13 are:

Glass 1 : $E = 7386{\cdot}4 \text{ Kg mm}^{-2}$

$H_v = 630{\cdot}4 \text{ Kg mm}^{-2}$

Glass 8 : $E = 7555{\cdot}7 \text{ Kg mm}^{-2}$

$H_v = 650{\cdot}8 \text{ Kg mm}^{-2}$

Glass 12: $E = 7365{\cdot}05 \text{ Kg mm}^{-2}$

$H_v = 631{\cdot}0 \text{ Kg mm}^{-2}$

Glass 13: $E = 7067{\cdot}2 \text{ Kg mm}^{-2}$

$H_v = 621{\cdot}8 \text{ Kg mm}^{-2}$

The experimental values of Vicker's Hardness are:

Glass 1 : $H_v = 666 \pm 17 \text{ Kg mm}^{-2}$

Glass 8 : $H_v = 688 \pm 5 \text{ Kg mm}^{-2}$

Glass 12: $H_v = 669 \pm 3 \text{ Kg mm}^{-2}$

Glass 13: $H_v = 642 \pm 8 \text{ Kg mm}^{-2}$

The experimental values appear to be in good agreement with the theoretical calculations, especially where equation (5.7.) has been used to calculate Young's Modulus, E. According to this relation, the relative order of microhardness increases from glass 13 to glass 1 to glass 12 to glass 8, which is in accordance with the experimental values. Where equation (5.6.) was used in the determining of E, it was thought that the values of E for the individual components in the glass where inaccurate.

Fig. 5.9 shows the relationship between the microhardness

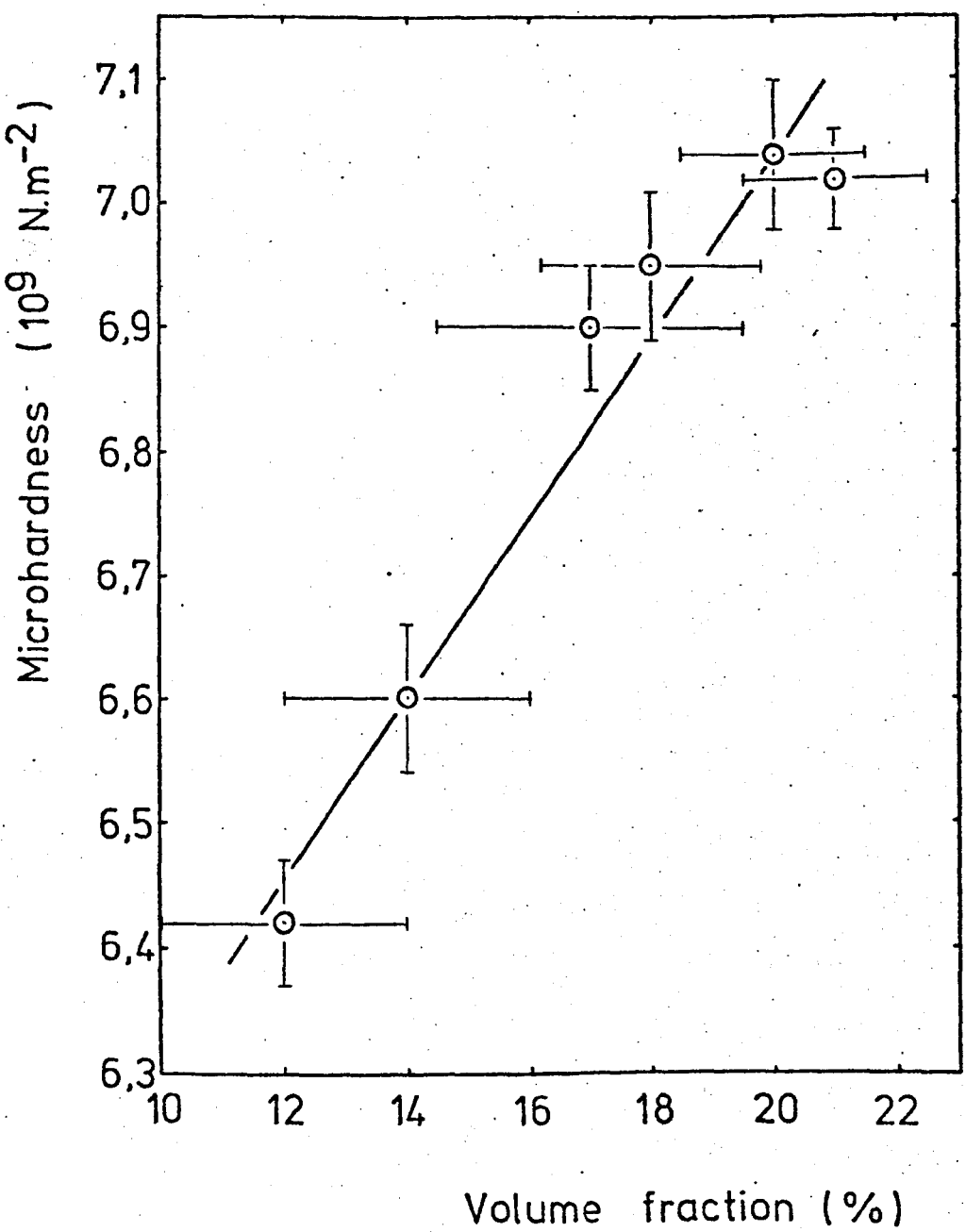

Fig. 5.9. Variations of microhardness, H_v, with volume fraction, V_f, of gahnite crystals in glass-ceramic 12.

and volume fraction of gahnite crystals in glass-ceramic 12.

In relation to the crystal microstructure, it is apparent that some relationship exists between the hardness and crystal size. A theoretical relationship derived by Stroh (1955) assumes a hardness proportional to $d^{-1/2}$, where d is the average particle size, if the deformation in a polycrystalline aggregate is caused by slip within grains. If a slip occurs at grain boundaries, however, Zener (1952) revised the equation to H_v = constant d^{+1}, because in this case the tendency for slipping increases in proportion to the total area of the grain boundaries.

Fig. 5.10. indicates that the measured values of hardness of glass-ceramic 12 for various heat-treatments are proportional to the average particle size. This would indicate that the fracture mechanism occurs at grain boundaries. This conclusion was hard to justify due to the large errors associated with the measurement of the small particle size. The line of best fit was drawn after a least squares calculation.

5.5. Mechanical Strength.

5.5.1. General Strength Theories.

Theoretical work by Hall (1951), Petch (1953), Tashiro and Sakka (1964), Hasselman and Fulrath (1966) and Zarzycki (1973) has been aimed at analysing the effect of both particle size and volume fraction of dispersed phases on the mechanical strength. Hard crystalline inclusions in the glassy matrix are taken to limit the size of the Griffith flaws. This diminishes the probability of rupture of the glassy phase and thus increases the overall strength of the composite. With this approach, the fracture strength, σ, of the composite, as a function of volume fraction V_f and the radius R of the dispersed particles is given by:

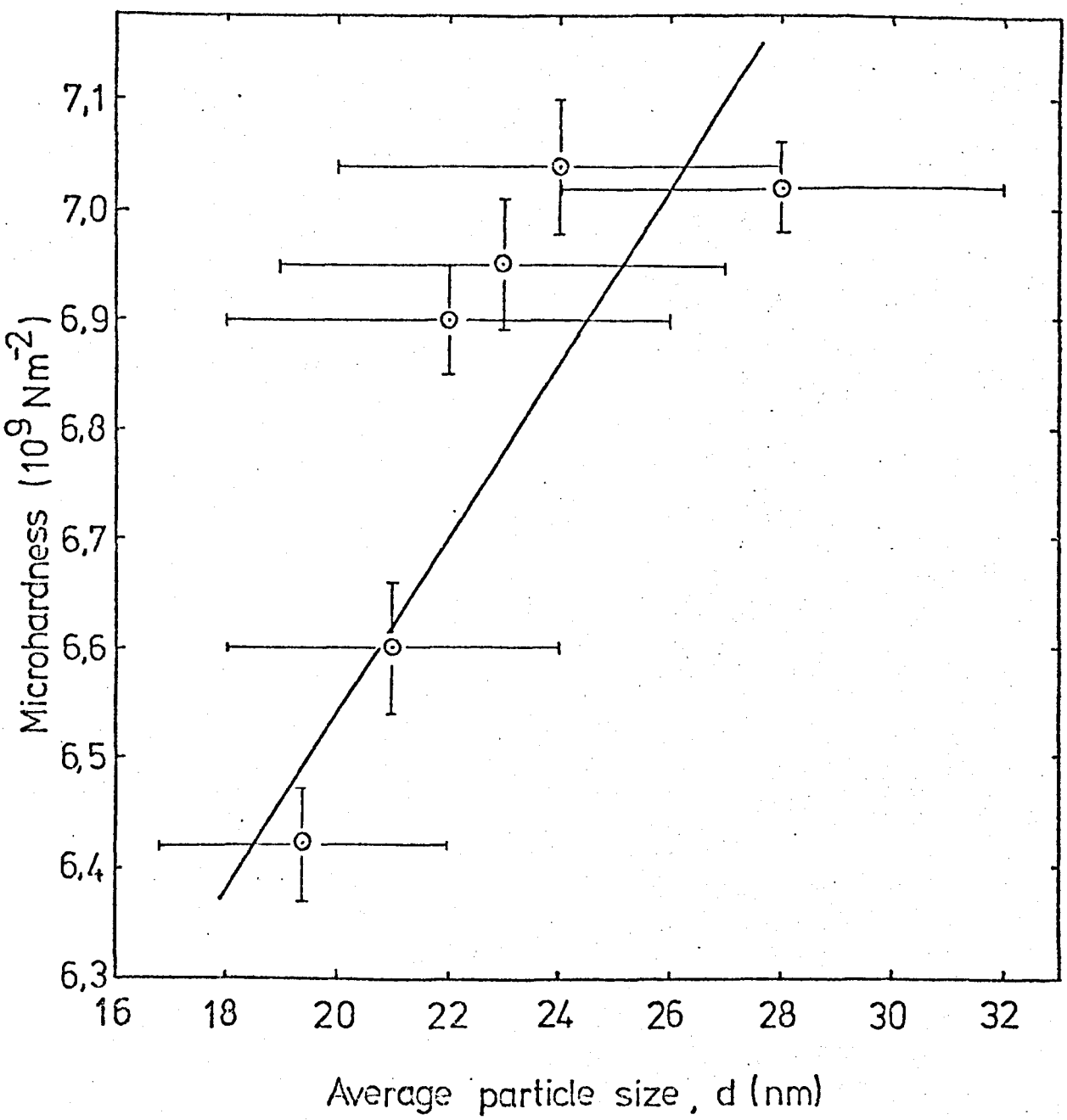

Fig. 5.10. Dependence of microhardness upon the average particle size, d, for glass-ceramic 12.

$$\sigma = \sigma_o (1 - V_f)^{1/2} \qquad (5.8.)$$

for lower values of V_f or large particles (i.e. when the flaws are smaller than the average distance between particles), σ_o being the fracture strength of the glassy matrix; or

$$\sigma = \left[\frac{3E \gamma V_f}{\pi R(1 - V_f)}\right]^{1/2} \qquad (5.9.)$$

for higher values of V_f, or small particle size (where the flaw size depends on the average distance between the particles). E and γ are Young's Modulus and the surface energy of the glass matrix respectively.

It has also been suggested by Orowan (1949), and Utsumi and Sakka (1970) that the mechanical strength, σ, of a polycrystalline aggregate is related to the mean grain diameter, d, by the relationship:

$$\sigma = K_1 d^{-1/2} \qquad (5.10)$$

where K_1 is a constant.

This equation implies that the crack length, c, in the Griffith equation

$$\sigma = \left(\frac{2E\gamma}{\pi c}\right)^{1/2} \qquad (5.11.)$$

is proportional to the grain diameter, d. In the Griffith equation, E is Young's Modulus of the material and γ is the effective surface energy for crack initiation.

Tashiro and Sakka (1964), and Utsumi and Sakka (1970) have shown that equation (5.10) holds for glass-ceramics. Hall (1951) and Petch (1953) have also verified this for metals. This suggests that the critical flaws are present within the crystal grains and do not extend into the glass phase, or that they exist at the glass-crystal

interface and are, therefore, proportional to the surface area of the grains.

Hasselman and Fulrath (1960), Freiman and Hench (1972) and Hing and McMillan (1973) have observed a relationship between the strength and the mean free path, λ. In a glass-crystal composite such as a glass-ceramic containing a relatively strong crystalline dispersion, fracture could be initiated within the glass matrix. For such composites, at sufficiently high volume fractions of the crystalline phase, the maximum flaw size in the glass is restricted by the presence of the dispersion. This implies that the flaws present in the glass are terminated at the crystal-glass boundaries and the spacing between the crystals or mean free path in the glass phase will be a critical parameter in determining the mechanical strength of the composite. This suggests that equation (5.10) can be modified to:

$$\sigma = K_2 \lambda^{-1/2} \qquad (5.12.)$$

where K_2 is a constant and λ is the mean free path in the glass phase.

In order to produce glass-ceramics having a maximum strength, Stookey (1962) believed that it would be of considerable interest to study the effect on strength of a decrease to very small crystal sizes, such as molecular sizes. It was not clear what degree of strength could be attained by reducing the crystal size to such small dimensions, and at the same time preventing the structure from becoming amorphous. Work by Kingery (1958) showed that the strength of a ceramic with grain size greater than 20 microns is inversely proportional to the square root of its grain size and is independent of surface cracks. The internal stress was assumed to be more than 70,000 Kg cm^{-2} (6,865 MNm^{-2}); however, under the influence of surface cracks, this is reduced to between 400 and 700 Kg cm^{-2} (39 and 69 MNm^{-2}). The strength of glass-ceramics must increase considerably with decreasing crystal

size to a point where phase boundaries practically disappear. However, this is accompanied by a simultaneous effect of surface microcracks on the strength of such glass-ceramics as stated by Stookey (1962).

5.5.2. Modulus of Rupture.

In the present work the modulus of rupture by three-point bending of abraded samples of heat-treated glass 12 gave very scattered results, as shown in fig. 5.11., with no apparent dependence on the microstructure. Samples here were given the standard abrasion treatment for 60 minutes as mentioned in section 2.5.3..

With abraded specimens it is possible to obtain reproducible results even though cracks and flaws are introduced. This is assuming that exactly the same abrasion treatment has been given to each specimen.

It is suspected that the lack of dependence on the microstructure of glass-ceramic 12 can be attributed to the introduction of cracks and flaws which are larger than the average particle size.

Further work on selected heat-treatments of glasses 1, 8 and 12 produced the results of fig. 5.11.. The samples here were abraded for a much shorter time than the initial tests, i.e. 5 minutes instead of 60 minutes. It can be seen that the moduli of rupture of the parent glasses all lie within the range 108 to 110 MNm^{-2}. Subsequent crystallization led to a large increase in the modulus of rupture, which then appeared to stabilize. The large errors involved in the measurements of the modulus of rupture again made it impossible to achieve a relationship with respect to the microstructural parameters.

Comparing the results of three-point bending to those of the microhardness, Tashiro and Sakka (1964) related the Vicker's Hardness Number H_v, to the yield strength σ by

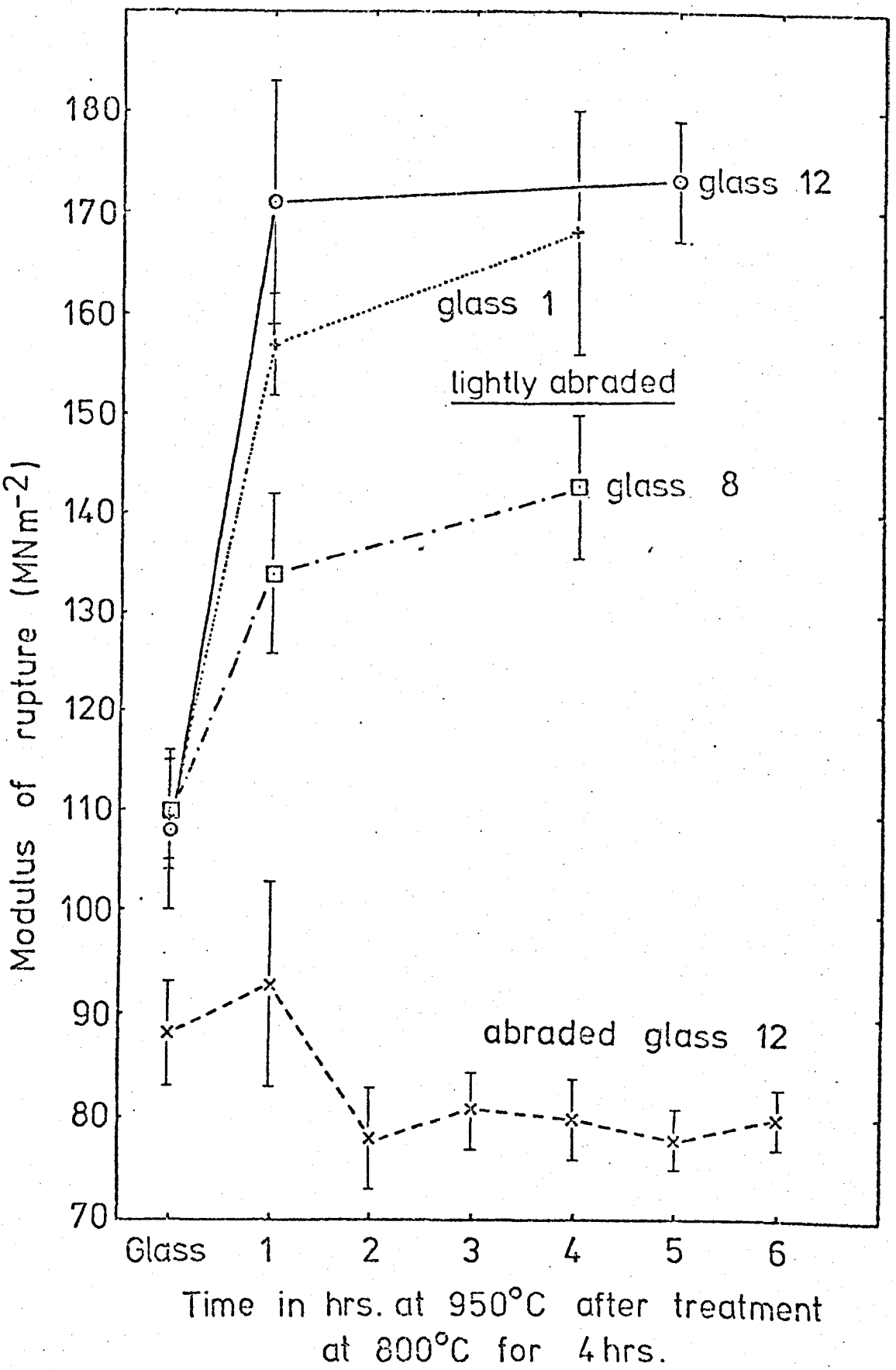

Fig. 5.11. Modulus of rupture, σ_f, of abraded glass 12 and lightly abraded glasses 1, 8 and 12 for various heat-treatment times.

$$H_v = 2{\cdot}68\,\sigma \qquad (5.13.)$$

With this relationship, it would be expected that the mechanical strength would increase from glass-ceramic 12 to 8 to 1, as in the case of microhardness. It appears, however, that glass-ceramic 12 is stronger than glass-ceramic 1. A possible reason for this could be that the smoothing of the surface during heat-treatment, as mentioned in section 4.3., could mean that less flaws are present prior to the abrasion treatment, and hence no standard surface was produced on all the glass-ceramics 1, 8 and 12.

It was realized from work performed by Haward (1949) that samples in the form of beams must be long in comparison with the thickness, otherwise shearing forces must be considered. In general, it seems that the effect of shearing forces is small when the span-to-depth (length-to-thickness) ratio is greater than 10 : 1, and beams may even be regarded as long when the span-to-depth ratio is above 6 : 1.

Since the span-to-depth ratio of previously measured samples was of the order of 4 : 1, it was considered necessary to perform tests on samples with a larger span-to-depth ratio. The abrasion process was also eliminated, because it was thought that previously abraded samples did not produce a standard surface on all the heat-treated samples due to the greater abrasion resistance (from hardness measurements) as the crystallization times increase.

Samples were, therefore, cut with a depth of approximately 3mm. The span of the outer knife edges used was 2cm, giving a span-to-depth ratio greater than 6 : 1.

The detailed analysis of unabraded samples of glass 12, heat-treated simultanecusly at 800°C for 4 hours and 950°C from 1 to 6 hours, produced the results of fig. 5.12.. Note that the parent glass has been omitted. The overall strength of the glass-ceramic can be seen to decrease, even though the errors are again quite large.

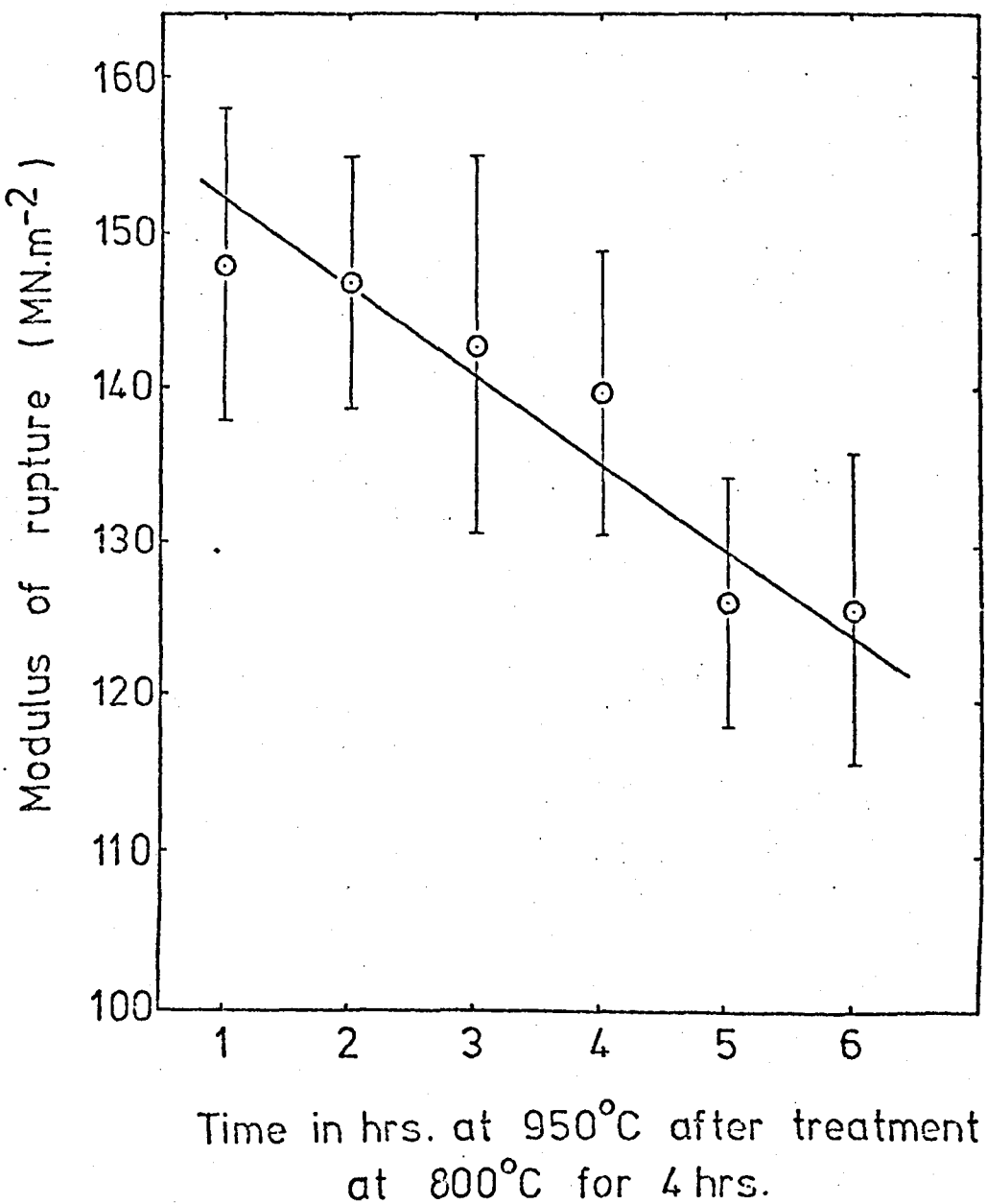

Fig. 5.12. Modulus of rupture, σ_f, of unabraded glass 12 after various heat-treatment times (Note that the parent glass has been omitted).

Comparing figs. 5.11. and 5.12., it can be seen that there is a difference between the overall strength of the abraded and unabraded crystallized glass 12, especially the glass heat-treated at 800°C for 4 hours and 950°C for 1 hour, although for this particular heat-treatment the errors in the modulus of rupture overlap. It would be expected for the unabraded samples to have a higher strength than the abraded ones, because of the larger number of flaws introduced onto the surface during the abrasion process. It must be remembered, however, that shearing forces could have given a higher value to the strength in the samples with the smaller span-to-depth ratio, which in fact were also the abraded specimens. It can be concluded, therefore, that the results of fig. 5.11. are invalid.

Fig. 5.13. shows the relationship between the strength of glass-ceramic 12 and the square root of the particle size, the line of best fit being drawn in after a least squares calculation. The large errors associated with both the strength and particle size measurements make it difficult to establish this relation.

The relationship that strength is proportional to $d^{-1/2}$ would indicate that the critical flaws are present at the glass-crystal interface, because of stresses introduced at these boundaries, due to the thermal expansion difference between the glass and crystal phases. Tashiro and Sakka (1966) pointed out the interdependence between the modulus of rupture, σ_f, of the glass-ceramic and the thermal expansion coefficient of the primary crystal phase. McMillan (1974) has pointed out that where the thermal expansion coefficient of the crystal phase is very much lower than that of the glass phase, the stresses in the glass phase around a crystal will be tensile in the circumferential direction and compressive in the radial direction. In such a material, microcracks aligned with their major axes in the radial direction, are likely to be most critical, and thus predicts

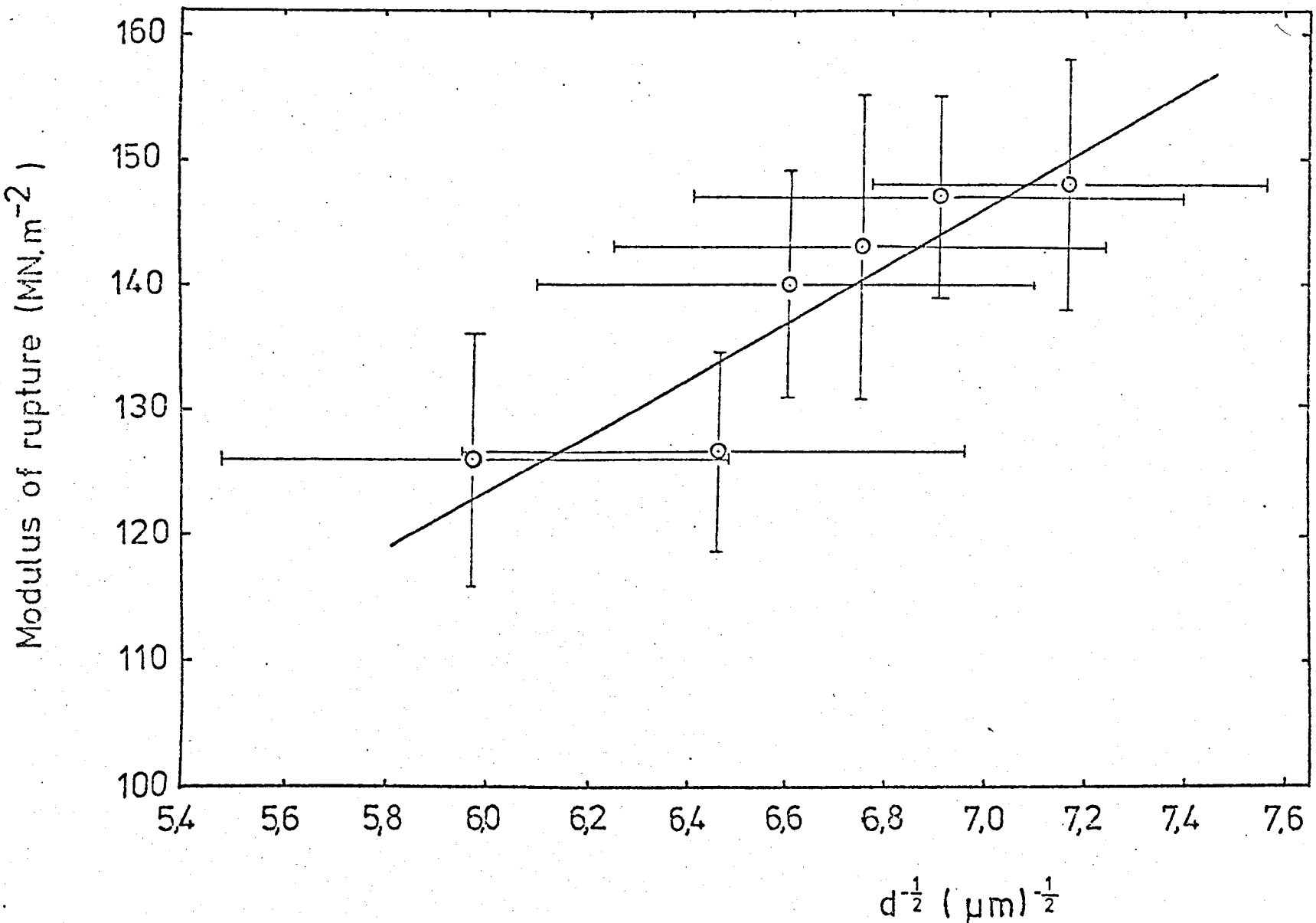

Fig. 5.13. Dependence of the modulus of rupture, σ_f, upon the square root of the mean crystal size of glass-ceramic 12.

that the dependence of strength on $\lambda^{-1/2}$ is likely to be applicable, where λ is the mean free path. Where the thermal expansion coefficient of the crystal phase is higher than that of the glass, which is the case in the present study, the stresses in the glass immediately surrounding the crystal will be compressive in the circumferential direction and tensile in the radial direction. Thus microflaws having their major axes aligned in the circumferential direction are likely to be more critical in this case. For such materials, therefore, microcracks formed at the grain boundaries rather than those traversing the glass phase may be the controlling factor. The lengths of these flaws will be proportional to the crystal diameter, d, and hence a dependence of the strength upon $d^{-1/2}$ might be expected.

Agreement, therefore, exists between the present work and the results of McMillan, whereby the expansion coefficient of the gahnite phase was much higher than the residual glass phase leading to the dependence of strength and $d^{-1/2}$.

5.5.3. Young's Modulus

From the series of tests performed on the unabraded samples of glass-ceramic 12, load-deflection curves were analysed to determine Young's Modulus. Fig. 5.14. shows that the parent glass has a Young's Modulus of $(4{\cdot}1 \pm 0{\cdot}2) \times 10^{10}$ Nm^{-2}, with a sharp increase for the crystallized material to $(5{\cdot}6 \pm 0{\cdot}9) \times 10^{10}$ Nm^{-2}. This value then remains constant for the remainder of the heat-treatment schedule. Although the modulus of elasticity is an additive function of the individual characteristics of the crystalline and glassy phases, there appears to be no change in value of E during the crystallization process, evidently because of the small change in the volume fraction of the crystal species.

Table 5.7. gives a summary of all the mechanical

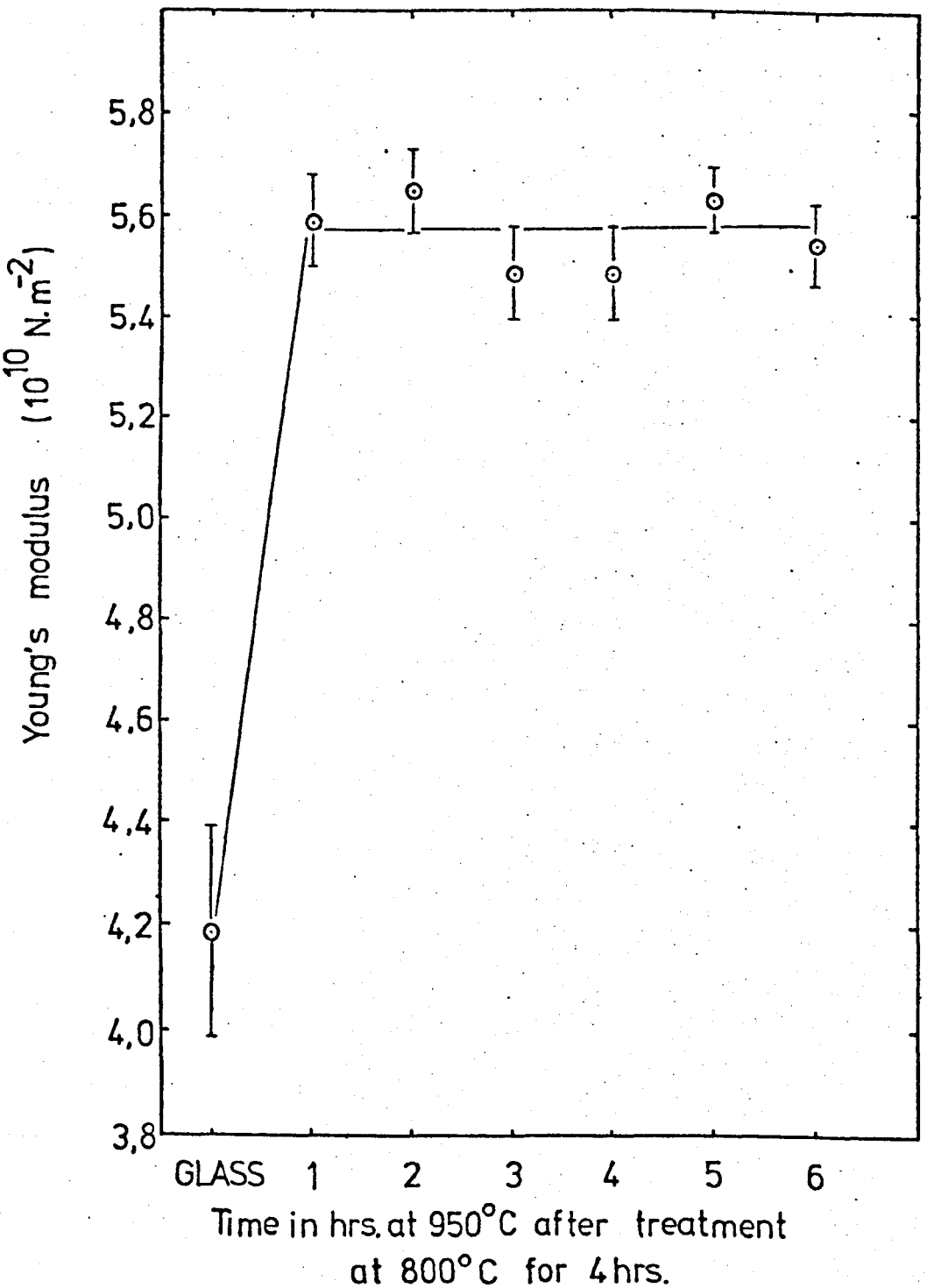

Fig. 5.14. Young's Modulus of glass 12 after various heat-treatment times.

	σ_f MNm^{-2} samples abraded for 60mins	σ_f MNm^{-2} samples abraded for 5mins	σ_f MNm^{-2} unabraded	Young's Modulus $E(10^{10}Nm^{-2})$
Glass 12	88 ± 5	108 ± 8	108 ± 8	4·1 ± 0·2
800°C 4 hrs 950°C 1 hr	93 ± 10	171 ± 12	148 ± 10	5·6 ± 0·9
800°C 4 hrs 950°C 2 hrs	78 ± 5	-	147 ± 8	5·65 ± 0·8
800°C 4 hrs 950°C 3 hrs	81 ± 4	-	143 ± 12	5·5 ± 0·9
800°C 4 hrs 950°C 4 hrs	80 ± 4	-	140 ± 9	5·5 ± 0·9
800°C 4 hrs 950°C 5 hrs	78 ± 3	173 ± 6	126·5 ± 8	5·6 ± 0·6
800°C 4 hrs 950°C 6 hrs	80 ± 3	-	126 ± 10	5·5 ± 0·8
Glass 8	-	110 ± 5	-	-
800°C 4 hrs 950°C 1 hr	-	134 ± 8	-	-
800°C 4 hrs 950°C 4 hrs	-	143 ± 7	-	-
Glass 1	-	110 ± 6	-	-
800°C 4 hrs 950°C 1 hr	-	157 ± 5	-	-
800°C 4 hrs 950°C 4 hrs	-	168 ± 12	-	-

Table 5.7. Mechanical strength measurements of selected glasses and glass-ceramics.

strength measurements.

5.5.4. Conclusion.

From the above results it can be concluded that the strength of a material is strongly dependent on the surface condition, which includes the abrasion resistance. From the data on lightly abraded specimens, the small increase in strength may result primarily from an improved abrasion resistance and not necessarily from a high inherent strength. The decrease in strength of unabraded specimens as crystallization progresses, may provide a clue to the relation between the structure and the mechanical properties of a material. With respect to the unabraded specimens, the gradual decrease of strength suggests that the material is behaving like a glass containing flaws of gradually increasing size.

The present study has not provided a clear-cut answer regarding what characteristics of the glass-ceramic lead to its hardness and strength. Bearing in mind the gradual changes in the strength and hardness, it seems possible that microcrystallinity is not, itself, the most important factor. It is suggested that the mechanical properties may be partially determined by the glassy matrix, and that gradual changes in the chemical composition of the matrix may be important factors in determining the strength properties.

5.6. Optical Properties.

The optical transmission properties were measured for glasses and glass-ceramics 1, 8, 12 and 13. The overall transparency in the near infra-red and visible regions appears to be very good.

In the infra-red region, similar spectra were obtained for all the above glasses. Figs. 5.15 - 5.18. show the percentage transmission. The main parts of interest are the absorption

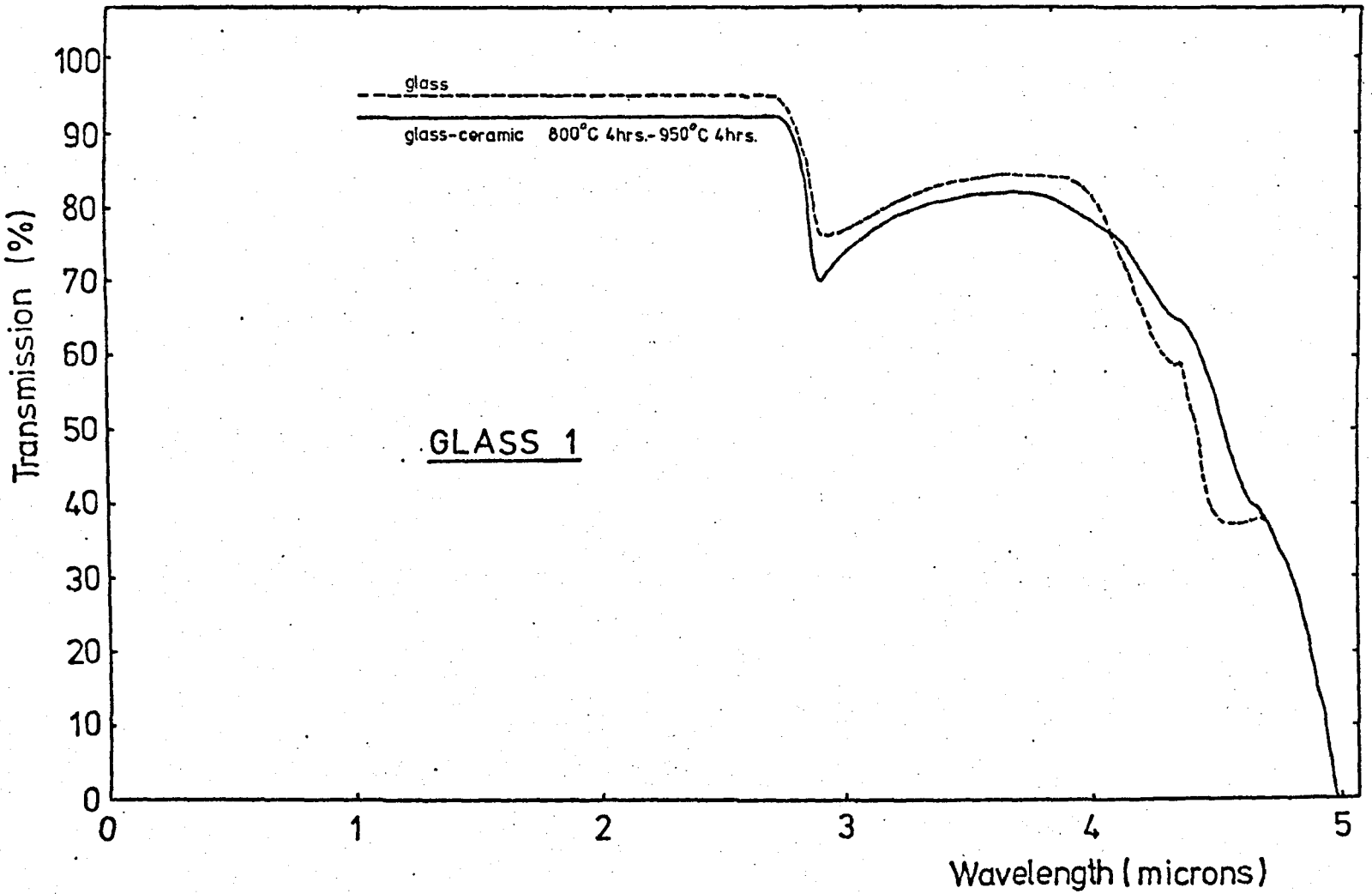

Fig. 5.15. Infra-red spectra of glass and glass-ceramic 1.

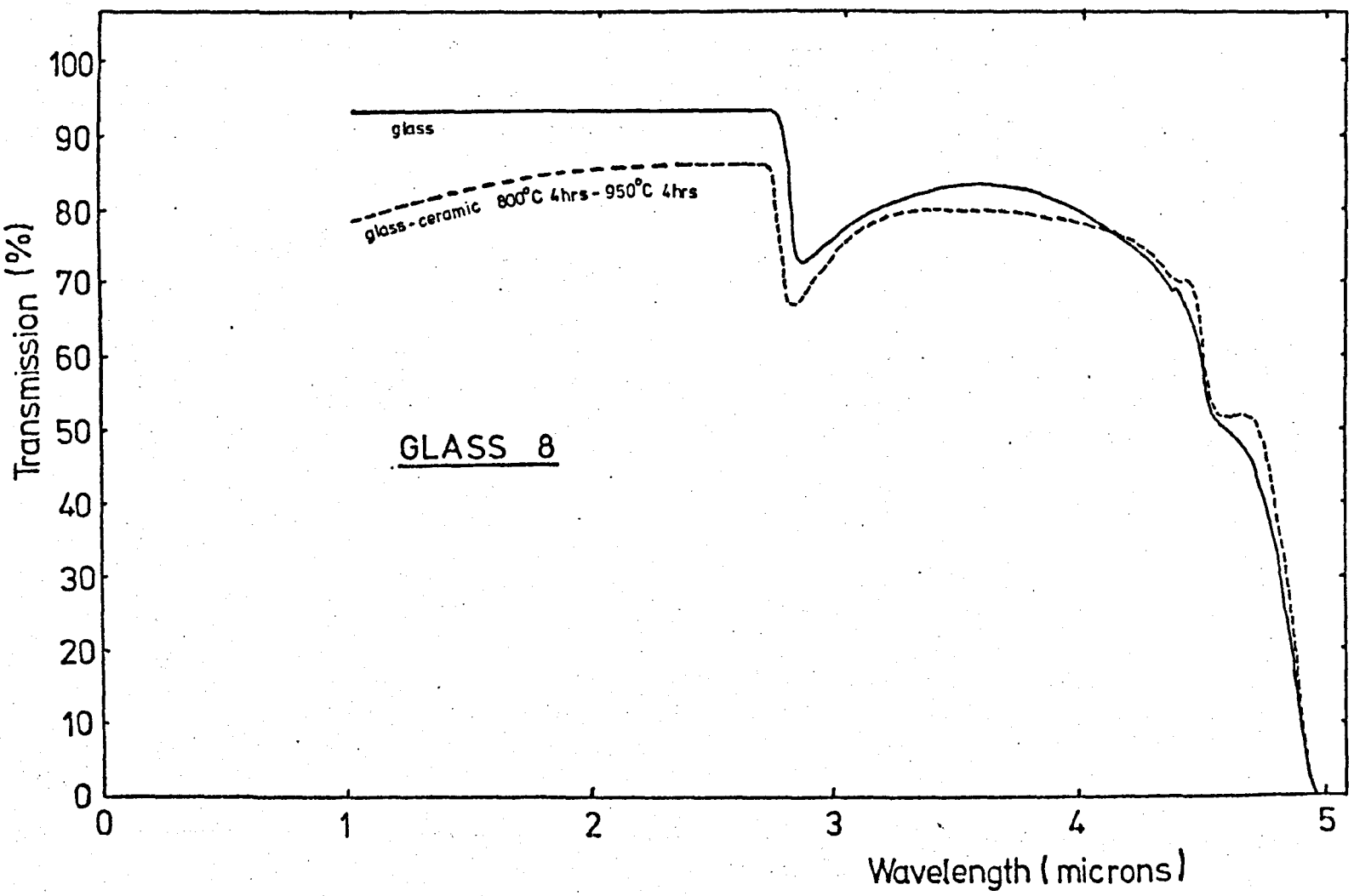

Fig. 5.16. Infra-red spectra of glass and glass-ceramic 8.

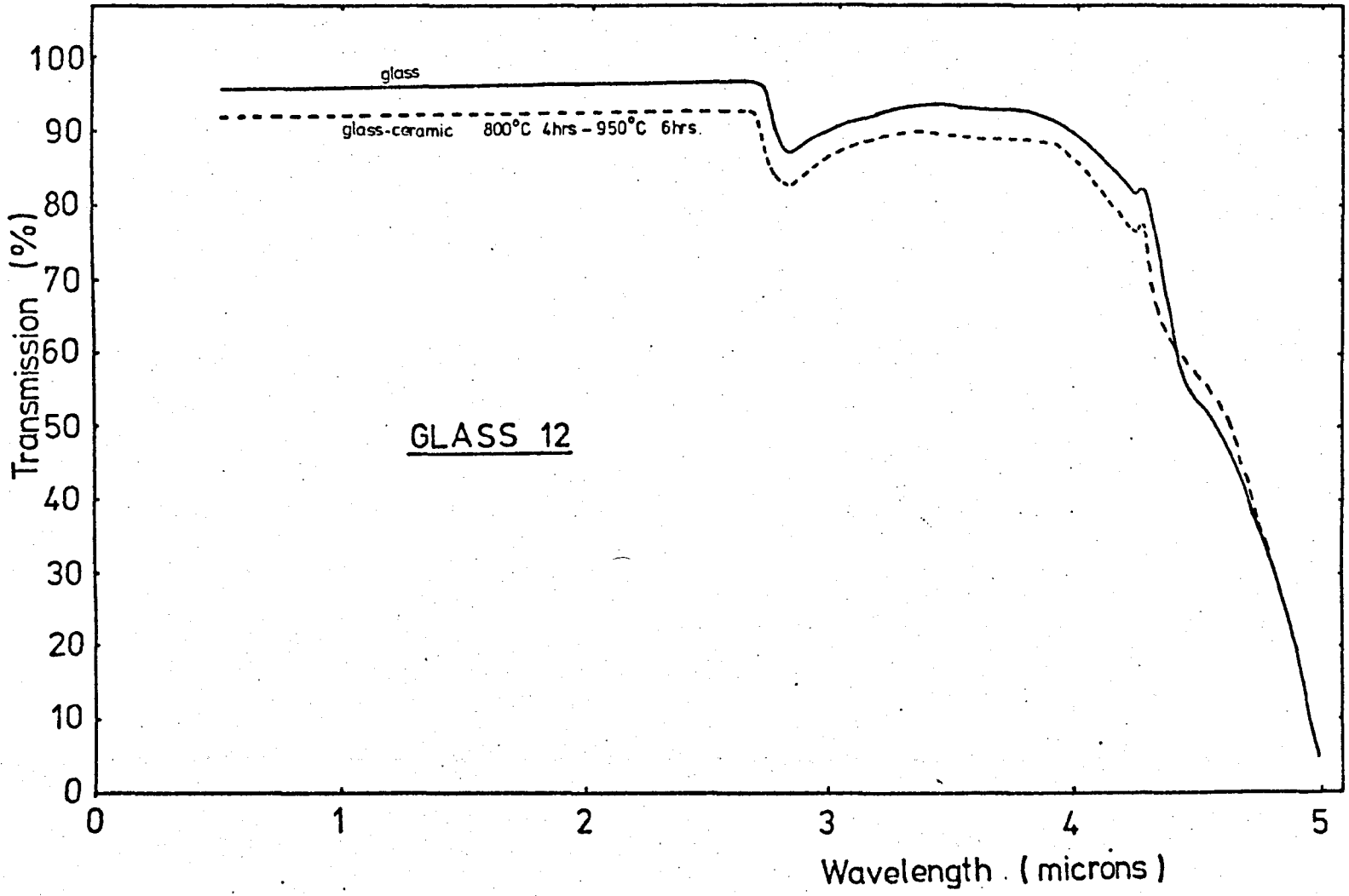

Fig. 5.17. Infra-red spectra of glass and glass-ceramic 12.

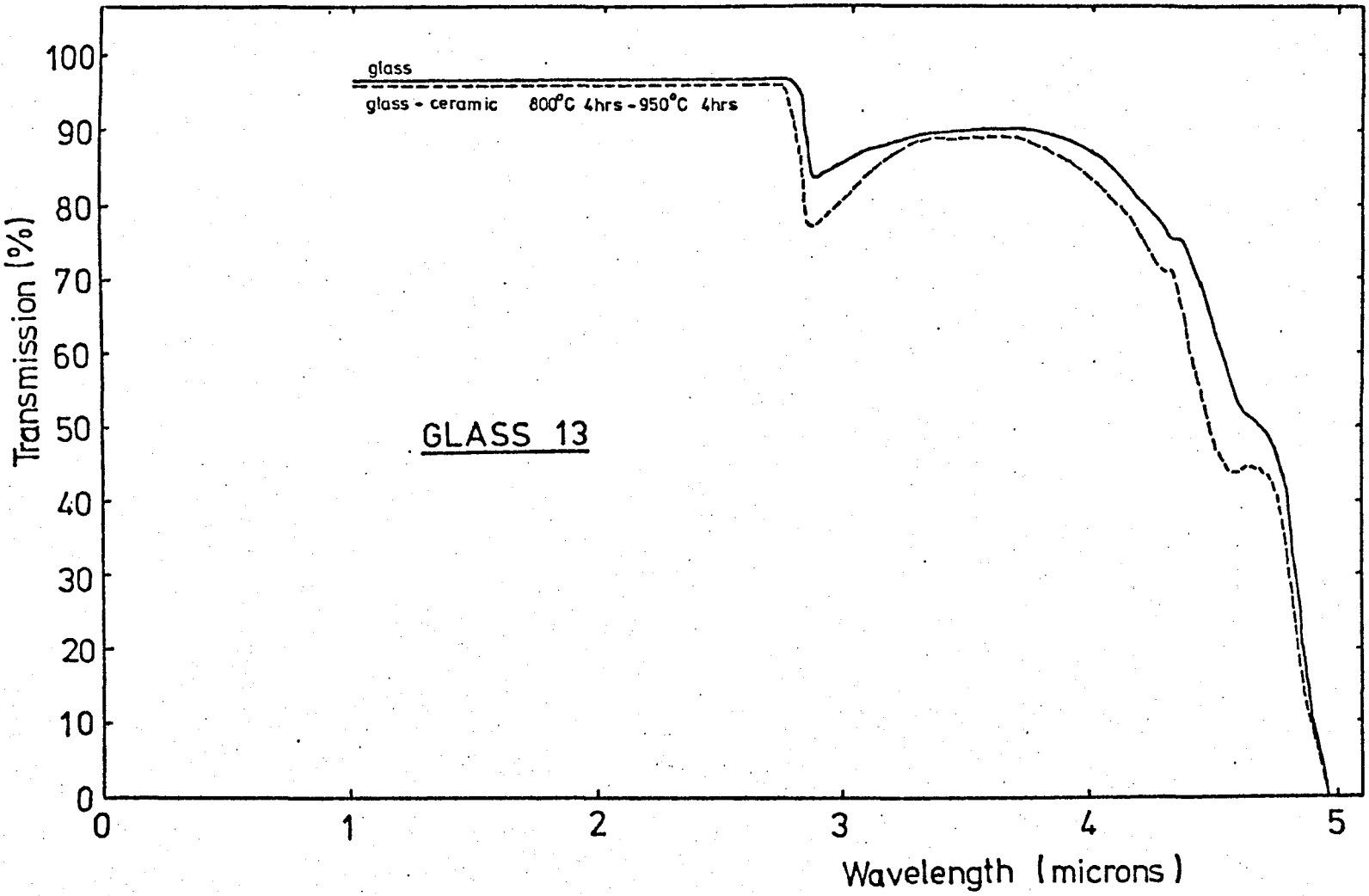

Fig. 5.18. Infra-red spectra of glass and glass-ceramic 13.

peaks at 2·8 microns and 4·25 microns.

Much work has been performed to determine the nature of these absorption bands. Spectra published by Drummond (1936) and Devers (1943) show an absorption maximum at 2·7 microns for fused silica. Drummond (1934) pointed out the wide variation of the intensity of this band in fused silica and he suggested that the 2·7 micron band was due to an impurity, namely, carbon dioxide. A series of papers followed, discussing the identity of this band. Ellis and Lyon (1936, 1937) found little or no absorption by fused silica which had an opportunity to dissolve carbon dioxide and suggested that water was the impurity. Harrison (1947) found the band at 2·7 microns in fused silica and also bands at 2·85 microns in fused boric oxide, 2·95 microns in fused sodium tetraborate, and approximately 3·2 microns in fused metaphosphoric acid. These bands were attributed to OH vibrational bands of water in the glass, and the possibility that the positions of these bands might be related to the strength of the bonding of the OH groups to the principal component of the glass was suggested. Adams and Douglas (1959) and Boulos and Kreidl (1972) reviewed the fact that the asymmetric stretching vibration in water vapour occurring at 2·6 microns becomes broader and moves to longer wavelengths when hydrogen bonding occurs, as in liquid water and ice.

Investigations by Glaze et al. (1948, 1950, 1953, 1955) were based on the results of Harrison and the authors were generally of the opinion that water is present as molecular H_2O groups. The assignments made for the most intense bands other than those due to the SiO_2 network were 2·75 microns for the OH vibrational group and 4·25 microns for the CO_2 vibrational group. Glaze and his co-workers also observed that bands due to these impurities could be substantially reduced by bubbling dry gas through the molten glass or by melting the glass under vacuum. It was found that the former method was more

efficient than the latter.

The most extensive work on the assignment of the 'water' bands in glasses was that of Scholze (1959). The only disagreement with his conclusions by Moore and McMillan (1956) and Adams (1961a,b,) occurred in the assignment of a 4·25 micron peak. Scholze (1959) and also Boulos and Kreidl (1972) claim that this peak is due to OH stretching vibrations when a hydrogen bond exists. Adams (1961a) managed to disprove this and assigned the 4·25 micron peak to $(CO_3)^{2-}$. It is now accepted, therefore, that this 4·25 micron peak is due to carbon dioxide.

In the present work the 2·8 micron peak is assigned to the OH vibrations linked to non-bridging oxygen ions, indicating a presence of physically absorbed molecular water either in the glass or on the surface. The 4·25 micron peak is due to $(CO_3)^{2-}$. The small point of inflexion at 4·5 microns is due to the overtone of the fundamental vibration of the SiO_4 tetrahedra at 9 microns. Following this the transmission cut-off at approximately 5 microns is, as expected, due to the extremely strong absorption of the Si-O network.

One particularly interesting feature is that the transmission of the glass-ceramics is very close to that of the parent glasses. The thickness of the samples used varied only slightly and not enough to give substantial differences in the overall transmission spectra. The thicknesses were measured as follows:

Glass 1	0·91 mm
Glass-ceramic 1	0·875 mm
Glass 8	0·71 mm
Glass-ceramic 8	0·67 mm
Glass 12	0·75 mm
Glass-ceramic 12	0·70 mm
Glass 13	0·71 mm
Glass-ceramic 13	0·84 mm

Fig. 5.19. shows the percentage transmission of the above glasses and glass-ceramics in the visible range 350nm to 750nm. All the parent glasses have a very similar transmission of around 80% over the complete range. The glass-ceramics vary somewhat, with glass-ceramic 8 having a more translucent appearance, and thus having the least transmission. For all the glasses and glass-ceramics, the cut-on in the ultra-violet region occurs at around 250nm, which ties in fairly well with the well-known observation that transition metal impurities commonly found in glass produce absorption in the ultra-violet region depending on the valence state of the impurity ions (Sigel and Ginther, 1968).

Glass 8, as seen in fig. 5.19., has the greater absorption towards the U.V. because the presence of impurities such as iron and manganese is greatest in the MgO compared to the other alkaline earth metal oxides such as CaO and BaO.

When attempting to compare the optical transmission properties in the visible region of the glass-ceramics to the micro-structural parameters, especially particle size, difficulty arises in explaining loss of transmission in the blue region due to light scattering. The particle size of the crystals in all the glasses 1, 8, 12 and 13, heat-treated at 800°C for 4 hours and 950°C for 4 hours, was much smaller than the wavelength of visible light, and in any case varied from 10 to 23nm. This makes the explanation of why there is such a large variation in the transmission of the glass-ceramics very difficult. Glass-ceramics 1 and 8 have the worst transmissions and it can be pointed out that after the nucleation heat-treatment, these materials had a bluish appearance, indicating light scattering was occurring. The micrographs of glass-ceramic 8 (fig. 4.9.) showed that in the nucleation stage, a background phase separation of the order of 100nm was present, but no sign of this was apparent after the crystallization

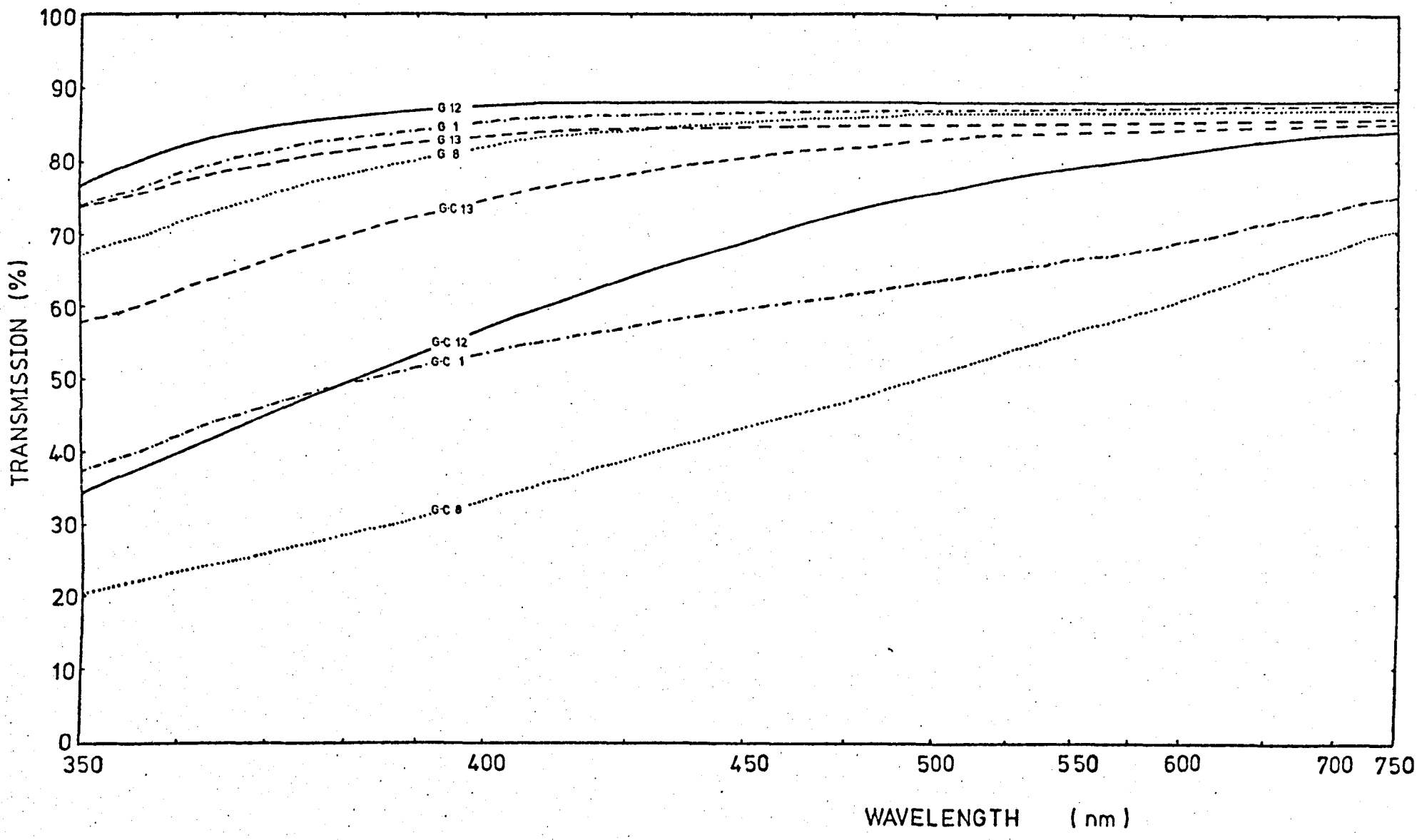

Fig. 5.19. Visible spectra of glasses and glass-ceramics 1, 8, 12 and 13.

stage. The only explanation that can be offered relates to the presence of larger quantities of impurities in the MgO in glass-ceramics 1 and 8, but this would also decrease the transmission in the parent glasses.

5.7. Discussion

The various physical properties of the glass-ceramics have in general shown to be strongly dependent on the time at the crystallization temperature. It is of interest to consider how far these variations are explainable in terms of the microstructure changes.

It is notable that a number of properties attain a maximum or minimum value for glass-ceramics produced by a crystallization heat-treatment at a temperature of 950°C for a time of 5 to 6 hours.

No distinct maximum value was noted either for the volume fraction or the particle size after this time, but microstructural analysis of the glass, after 24 hours at 950°C showed no change in the quantities. Because of the difficulty in measurement of the microstructural properties, no conclusive evidence can be given regarding direct relationships. But because of the diverse nature of the properties studied, it seems reasonable to suppose that these observations are explainable, at least partly, in terms of microstructural effects.

It should be recalled at this point that a detailed analysis of the microstructure of glass-ceramic 12 showed the volume fraction of the crystalline phase to have attained a flattened maximum and the mean free path in the residual glass phase, λ, a distinct minimum for the material heat-treated at 950°C for 5 hours, after a nucleation treatment at 800°C for 4 hours.

Firstly the density and thermal expansion of glass 12 appear to be microstructure sensitive. These properties increase just as the volume fraction of gahnite crystals increases and then

level off to a stable value after 5 to 6 hours at the crystallization temperature.

For the thermal expansion, the presence of larger alkaline earth metal ions increases the expansion coefficient quite significantly. The choice of glass 12 made it suitable for sealing to tungsten, with respect to thermal expansion matching. Subsequent crystallization resulted in a good, strong seal.

A wide range of thermal expansions can be obtained, depending on the crystalline phases and the alkaline earth metal ions present.

The microhardness of glass-ceramic 12 follows a similar pattern to that of the density in that there is an initial decrease in the value after annealing and subsequent nucleation and / or crystallization. During crystallization itself a gradual increase in microhardness occurs until a flattened maximum is reached, which again coincides with a maximum volume fraction and minimum mean free path. The microhardness has been shown to be dependent on d, which indicated that the deformation process is related to slip occurring in the glass terminated by the crystal boundaries.

The maximum strength occurs within one hour of the crystallization treatment where the minimum particle size occurs. Analysis of the results established a linear relationship between σ_f and $d^{-1/2}$ and supported the view that the strength of the glass-ceramic is controlled by microflaws present at the glass-crystal interface, due to thermal expansion mismatch producing stresses at the interface.

CHAPTER VI

Chemical Compatibility

6.1. Introduction

In this chapter details are presented of experimental techniques and results obtained in studying the chemical stability of transparent glass-ceramics in various vapours used in conventional incandescent and discharge lamps.

Details are given of the preparation of lamps and capsules containing six vapours, with investigations conducted on weight change, colour change and surface analysis by scanning electron microscopy. High temperature stability results are also considered.

Colour centres produced in sodium exposed samples were analysed by electron spin resonance and optical absorption. A model is proposed for the possible mechanism involved in the formation of such colour centres.

Radiation damage by X-rays was similarly studied, as was also the effect of another alkali vapour, lithium, on the transparent glass-ceramic.

Thermal bleaching was performed on most coloured samples to investigate the nature of colour centre destruction.

6.2. General review of colour centre in glasses.

Very little published work has been found on the attack of vapours used in lamp making on glasses, ceramics and glass-ceramics. An apparent reason for this is that, since the lamp envelope is found to be unstable, rather than studying in detail the physical cause of instability in the initial material, a better envelope is

developed. Henderson and Marsden (1972) give a general review on lamps, materials, and the technology involved in the production and utilization of light.

Elyard and Rawson (1962) studied the resistance of glasses of simple composition to attack by sodium vapour at elevated temperatures by incorporating samples of vitreous silica, binary phosphates, borates, aluminoborates, aluminates and silicates into sodium vapour lamps. The extent of attack was determined by measuring only the change in the weight of the specimens and by noting the change in the colour of the glass surface. Similarly, Burns (1965) investigated the discolouration of vitreous silica by sodium vapour by measuring the rate of discolouration at different temperatures. Here the darkening of the silica was shown to be associated with the diffusion of sodium into the silica network. No mechanism was however given for the nature of the production of light-absorbing centres.

A number of papers have appeared in the literature in which the attack of glass by sodium vapour has been used to show up defects on the glass surface. Andrade and Tsien (1937) examined glass surfaces after the reaction experiment, which was of short duration, and showed a line pattern on the glass where attack had taken place. It was believed that the exposure to sodium vapour had made visible Griffith cracks on the surface. More recent work by Ernsberger (1960) has tended to discredit this theory. The regions where the attack begins may coincide with regions in which the glass surface has been mechanically damaged, and it would not be surprising if other regions on the surface could act as nuclei for the attack process. Similar work on the attack of glass by sodium vapour to show up defects on glass surfaces has been performed by Gordon et al. (1959) and Argon (1959).

Work carried out by Wheeldon (1959) has shown that sodium penetrates some distance into the glass. There exists a

sharp boundary between the discoloured surface layer and the rest of the glass which Wheeldon took to indicate an actual chemical reaction between the sodium and the glass. If the sodium simply dissolved in the glass, one would expect to see a gradual fall off in the intensity of the discolouration with increasing distance from the surface, indicating diffusion of the sodium metal into the glass.

Much work has been performed on the study of colour centres formed in irradiated glasses. Lee and Bray (1962) studied the electron spin resonance of irradiated alumino-silicate glasses by 40kV X-rays, and concluded that they contain a paramagnetic centre consisting of a hole trapped on a bridging oxygen ion which is bonded to a substitutional aluminium ion. Sidorov and Tyul'kin (1971) investigated radiation centres in vitreous silica and established two types of centres: an electron trapped on a silicon atom, called an E_1' - centre, and a hole on the oxygen of a hydroxyl group, called an E_2' - centre. Weeks (1963) found the same E_2' - centre in crystalline quartz.

Van Wieringen and Kats (1957) studied the electron spin resonance of silicate glasses and fused silica coloured by X-rays. Again, two paramagnetic resonance peaks were found, attributed to electrons and holes. Trapped hole centres in X-irradiated alkali-silicate glasses were studied by Schreurs (1967). An electron spin resonance hole band at $g = 2{\cdot}01$ was found to actually consist of two separate hole bands, one characteristic for low-alkali silicate glasses, the other for glasses having higher concentrations of modifier ions. The model proposed for the first centre, termed HC_1, is a hole located on a Si-O tetrahedron having two non-bridging oxygens, with the hole largely restricted to these two non-bridging oxygens. The second centre, called HC_2, is a hole located on a Si-O tetrahedron with three non-bridging oxygens.

Swyler et al. (1973) studied the kinetics of

radiation induced colouring of glasses, during and after electron irradiation, by optical absorption and luminescence with no apparent conclusions as to the mechanism of colour centre formation. Tyul'kin (1971) analyzed the structure of glasses in the systems $MgO - SiO_2$ and $CaO - SiO_2$ according to data on their γ-radiation induced colour centres. Complicated mechanisms were proposed but all led to the production of a hole trapped at a non-bridging oxygen ion near which a metal ion resides.

Brekhovshikh et al.(1967) studied γ-irradiated three component glasses by electron spin resonance. Colour centres were again identified as holes trapped at the terminal, non-bridging oxygen ions.

From all the above investigations, the typical paramagnetic centres described as defects of the lattice are an electron trapped at an oxygen ion vacancy and a hole trapped at an oxygen ion.

6.3. Exposure to vapours - experimental.

Investigations were performed on glass 12 heat-treated at 800°C for 4 hours and 950°C for 6 hours, because of the closeness of the thermal expansion coefficients to tungsten and because of the successful glass-to-tungsten sealing mentioned in section 5.2.1..

Six vapours commonly used in lamps were chosen. These were sodium, scandium iodide and sodium iodide, bromine, fluorine, aluminium chloride and aluminium sodium chloride. The chloride vapours investigated are in the experimental stage in lamp production. Only iodides have been used so far.

For sodium vapour, a sample of glass-ceramic 12 measuring 8mm x 3mm x 1mm was inserted into a 35 watt arc tube containing a few torr of 99%/1% Neon/Argon and approximately 250mgm of sodium which is an excess at the arc tube operating temperature of around 250°C. Fig. 6.1 shows the arc tube with the sample inserted.

For the scandium iodide and sodium iodide vapour,

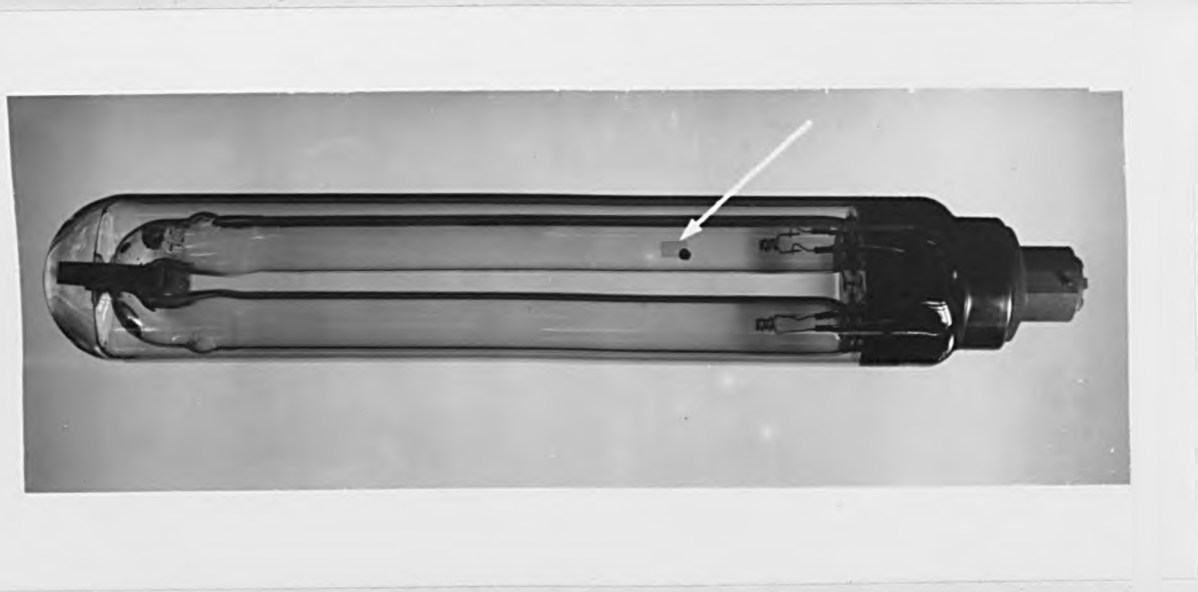

Fig. 6.1. Sodium vapour arc tube showing position of sample.

the sample measuring 8mm x 2mm x 1mm was introduced into a 250 watt arc tube containing mercury, sodium iodide and scandium iodide, small amounts of caesium iodide, thorium and 60 torr of argon. The operating temperature of the inner wall was about 730°C. Fig. 6.2. shows the complete arc tube with the sample.

For bromine and fluorine vapours, samples measuring 8mm x 3mm x 1mm were inserted into incandescent tubes. The bromine lamp was filled with an amalgam of 0.05% bromophosphonitrile $(PNBr_2)_n$ and brominated benzene $(C_6H_2Br_4)$ (in the ratio 1 : 1) in petroleum ether. The ether quickly evaporated, leaving approximately 60 gm of bromine on the tube surface. The fluorine lamp contained 1 torr NF_3, after coating of the tube with aluminium phosphate in order to prevent attack. Both the bromine and fluorine lamps contained 3.5 atmospheres of argon.

Three lamps of each vapour were produced. Of the three lamps for a particular vapour, two contained a sample each and the third lamp was left empty for running characteristics. These lamps are shown in fig. 6.3..

For the other vapours, vitreous silica capsules were made up. One contained 2mgm of aluminium chloride powder with 2mgm of aluminium wire, and the other had 2mgm of aluminium sodium chloride powder and also 2mgm of aluminium wire. A third capsule was made up with sodium iodide, scandium iodide and aluminium wire. These capsules are shown in fig. 6.3..

Into each of these a sample measuring 8mm x 2mm x 1mm was introduced. The capsules were subsequently pumped down, flushed with argon and sealed off from the exhaust tube. All the capsules were inserted into a furnace and were run at 800°C for various lengths of time.

To compare the action of sodium vapour on the

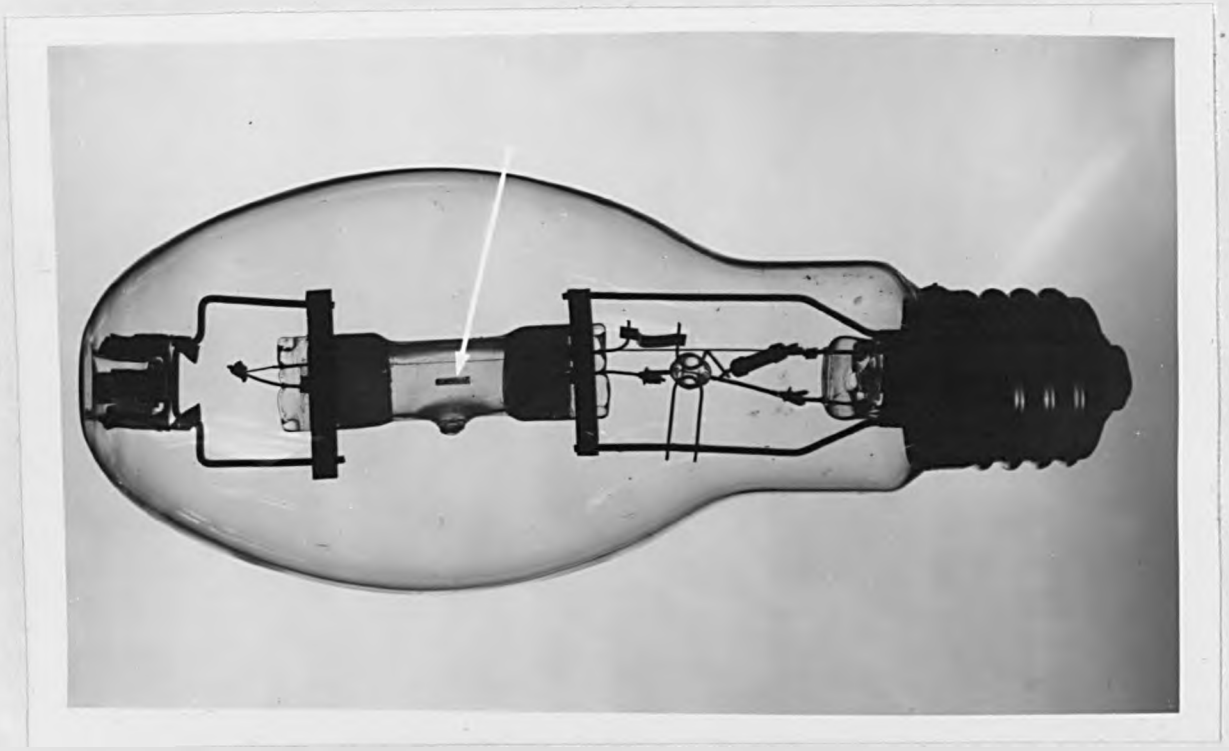

Fig. 6.2. Sodium iodide and scandium iodide vapour arc tube showing position of sample.

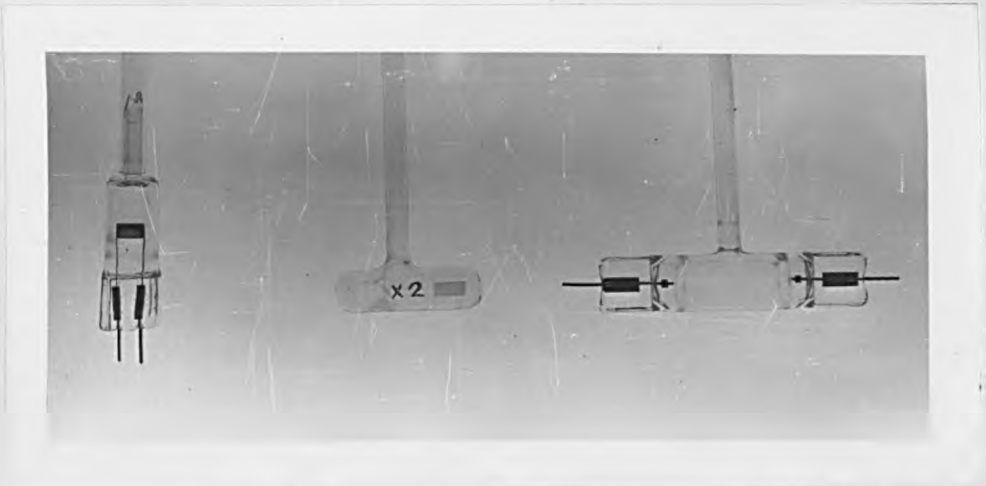

Incandescent lamp for bromine or fluorine vapour

capsule for metal halides

arc tube for sodium iodide and scandium iodide

Fig. 6.3. Photograph of preparatory stage of incandescent lamp, capsule and arc tube.

glass-ceramics, lithium vapour was also investigated.

Here, approximately 3gm of lithium metal was inserted into a thick-walled stainless steel container or 'bomb' approximately 2·5cm in internal diameter and 30cm in length as shown in fig. 6.4.. The metal was placed at the bottom of this cylindrical container, and the sample was suspended on a cradle and lowered to approximately 5cm above the lithium. The stainless steel container was placed vertically in a furnace, evacuated, and heated to 200°C to drive off any excess oil left on the lithium. The system was subsequently sealed and the temperature was raised to 400°C, at which point the lithium metal vaporised. Many attempts were made to choose the right temperature as initial runs at 700°C and above had completely destroyed the glass specimen; i.e. the attack process was too great. The optimum temperature and time to produce a significant attack without too much damage was found to be 500°C for 15 mins.

6.4. Results

For all the six vapours used, the samples were weighed before and after exposure in order to determine if any weight increase had occurred due to the absorption of the vapour. Any colour changes were noted and surface deposition of condensed vapours was distinguished from vapour absorption.

The surfaces of all the samples were subsequently washed in ether, distilled water and methanol, vacuum coated with gold-palladium and analysed under a scanning electron microscope.

6.4.1. Weight and colour changes.

Table 6.1. summarizes the initial investigations of chemical stability experiments. Any weight changes were not apparent due to the small size of the specimens used. There was, however, a great

Fig. 6.4. Stainless steel lithium bomb.

Vapour	lamp	lamp ref. no-	time of exposure	initial weight (gms) ±0·0002	final weight (gms) ±0·0002	Comments
Na	low pressure discharge	A3	20 mins	0·0324	0·0326	Browning of sample
		A1	45 mins	0·0327	0·0325	Heavier brown colouration
		A2	3 hrs	0·0458	0·0457	Heavy brown colouration
Br	incandescent	D2	183 hrs	0·0458	0·0454	No attack and no
		D1	405 hrs	0·0504	0·0504	colour change
Fl	incandescent	E1	5½ hrs	0·0496	0·0499	Blackening of sample &
		E2	20 hrs	0·0439	0·0437	lamp envelope
Metal halides $NaI + ScI_3$	Mercury low pressure halide discharge	B1	240hrs+	0·0254	-	white spotty surface deposit. Lamp left running
		B2	240 hrs	0·0130	0·0132	Black spotty surface deposit.
$AlCl_3 + Al$	enclosed with samples in silica capsules and treated in furnace at 800°C	X1	20 hrs	0·0241	0·0241	Slight darkening on surface probably due to condensed vapour
		C1	244 hrs	0·0398	0·0392	
$AlCl_3 + NaCl + Al$		Z2	20 hrs	0·0329	0·0331	Darkening of sample
		Y2	71 hrs	0·0343	0·0344	and capsule
$NaI + ScI_3 + Al$		H1	1038hrs	0·0391	0·0390	Na attack or colour change very slight surface deposit

Table 6.1. Summary of initial vapour exposure investigations.

variety of colourations and surface deposits that were noted. The more successful lamps with the least amount of colouration were, as expected, the bromine incandescent lamps and the mercury metal halide discharge lamps. Further tests were performed on these with the results of weight and colour changes given in Table 6.2..

In the case of encapsulated samples, the major cause of surface attack was the condensed vapours forming as a deposit on the surface of the glass-ceramic.

6.4.2. Scanning electron microscopy.

In most cases, scanning electron microscopy proved to be inconclusive because of the surface residue of condensed vapours screening the glass-ceramic surface. This was evident for the glass-ceramics which were encapsulated with the aluminium chloride and aluminium sodium chloride vapours. For the lamps, results could only indicate whether the surface attack was in fact a condensed vapour or whether attack of the glass had actually occurred. An attempt was made to determine the depth of penetration of certain vapours (e.g. sodium) by polishing away part of the edge of the specimen. A depth attack was encountered in the longest exposed sample (A2), as shown in fig. 6.5., but no other lamp or capsule specimens showed this. The sample (A2) exposed in the sodium lamp for 3 hours shows a microstructure the depth of which extends to about 55 microns into the glass surface. This microstructure appears to be caused by the sodium as it diffuses into the glass, although this effect could not be observed in other sodium exposed samples.

Fig. 6.6. shows the surface microstructure of certain samples exposed to all the vapours used. Fig. 6.6. also shows the surface of the original unetched glass-ceramic 12.

Vapour	lamp ref. no.	time of exposure	initial weight (gms) ± 0·0002	final weight (gms) ± 0·0002	Comments
Br	04	875hrs	0·0132	0·0133	
	01	938hrs	0·0143	0·0143	No surface attack or
	02	1043hrs	0·0173	0·0173	colour change
	03	1043hrs	0·0111	0·0111	
Metal halide NaI + ScI_3	B1	2150hrs	0·0254	0·0254	Regions of settled deposit just as for initial test

Table 6.2. Summary of further lamp vapour tests in bromine lamps and sodium iodide and scandium iodide arc tubes.

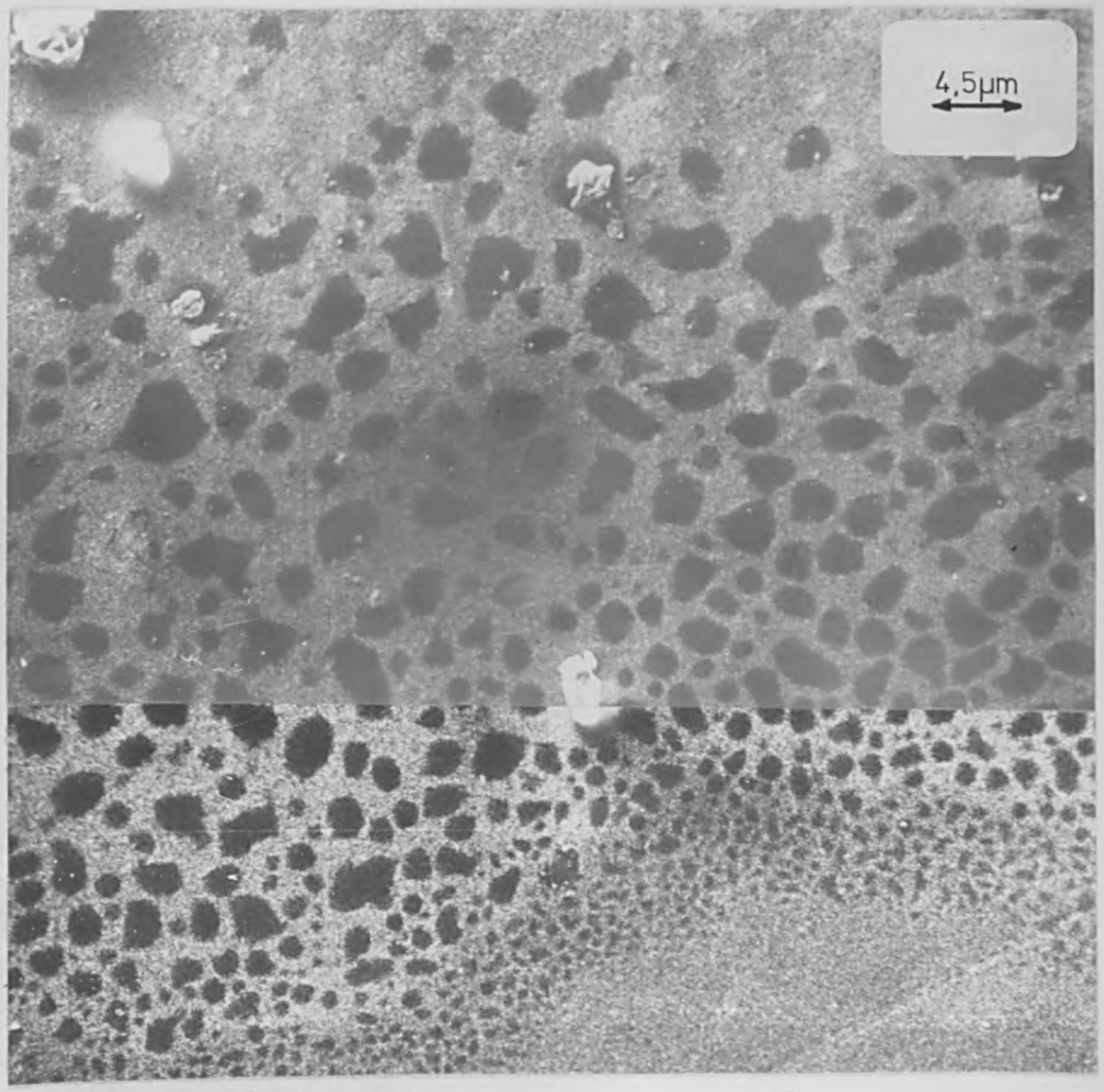

Fig. 6.5 Scanning electron micrograph showing depth attack due to sodium vapour in sample A2 (Table 6.1) The surface of the glass is approximately 5 microns above the photograph.

Unexposed glass-ceramic

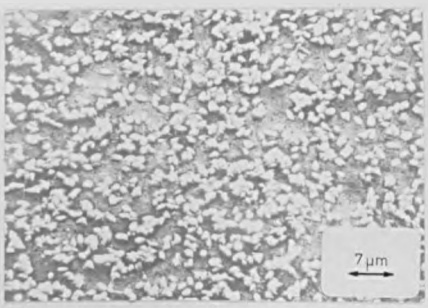

$NaI + ScI_3$ (B2)
(lamp)

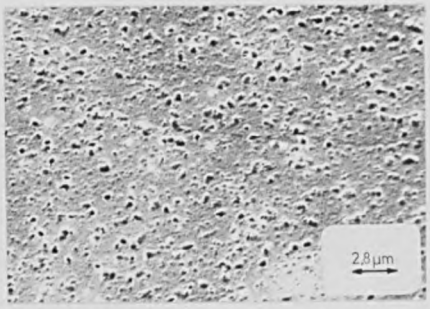

$NaI + ScI_3$ (B1)
(lamp)

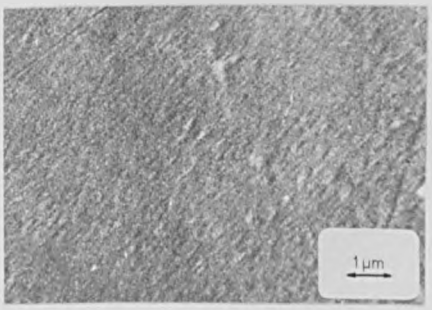

$NaI + ScI_3$ (H1)
(capsule)

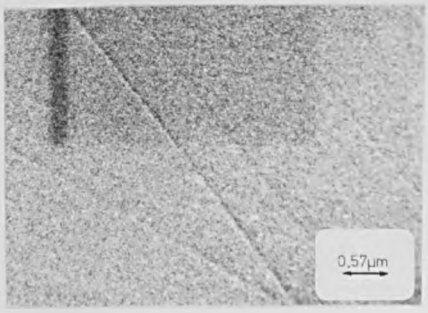

Br (lamp) (D1)

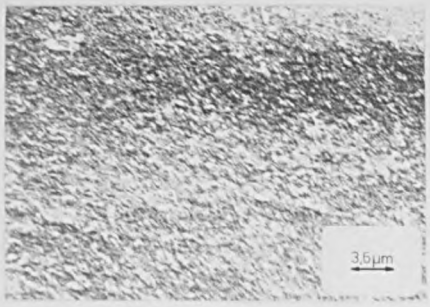

F (lamp) (E2)

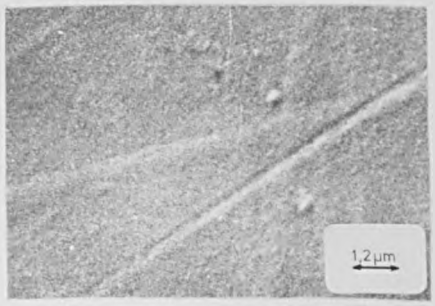

Na (lamp) (A2)

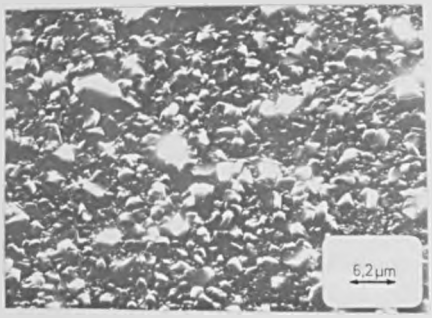

$AlCl_3$ + NaCl (Y2)
(Capsule)

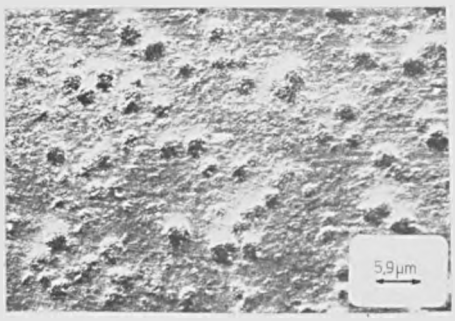

$AlCl_3$ (X1)
(Capsule)

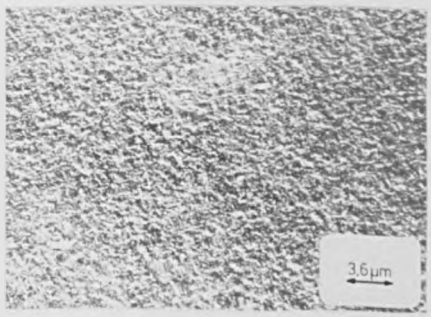

$AlCl_3$ (C1)
(Capsule)

Fig. 6.6 Scanning electron micrographs of unexposed and exposed samples of glass-ceramic 12 to various vapours. (Sample identification in brackets refers to Tables 6.1 and 6.2)

6.5. High Temperature Stability

Glass 12 heat-treated at 800°C for 4 hours and 950°C for 6 hours was chosen for high temperature investigations.

The sample measuring 8mm x 3mm x 1mm was polished in the usual way, vacuum coated with gold-palladium and analyzed in the scanning electron microscope. Fig. 6.7. shows the surface structure. The gold-palladium was removed with a lens polishing cloth and the thermal expansion was measured and was shown to be $31.8 \times 10^{-7}°C^{-1}$ (20 - 800°C).

Following this, the sample was subjected to a treatment in a furnace at 900°C for 500 hours. After exposure, the thermal expansion was again measured. The value remained at $31.8 \times 10^{-7}°C^{-1}$. The surface was again vacuum coated with gold-palladium and again examined in the scanning electron microscope. Very little microstructural change was observed, as can be seen in fig. 6.7..

When the glass-ceramic was heated above 1000°C for 100 hours, no loss in transparency was detected. The temperature was raised to 1050°C and was maintained there for 10 hours. Subsequent visual observation showed no loss in transparency, and the same treatment was performed at 1100°C. After approximately 2 hours at 1150°C, softening of the sample occurred, causing it to sag in the recrystallized alumina boat, but again no loss in transparency was noted.

The treatment was terminated at 1200°C after one hour when the sample adhered to the bottom of the boat. Even at this temperature no loss in transparency was observed.

An X-ray diffraction photograph of the specimen subjected to the above treatment showed no secondary crystallization, with no change in the peaks from the unexposed glass-ceramic.

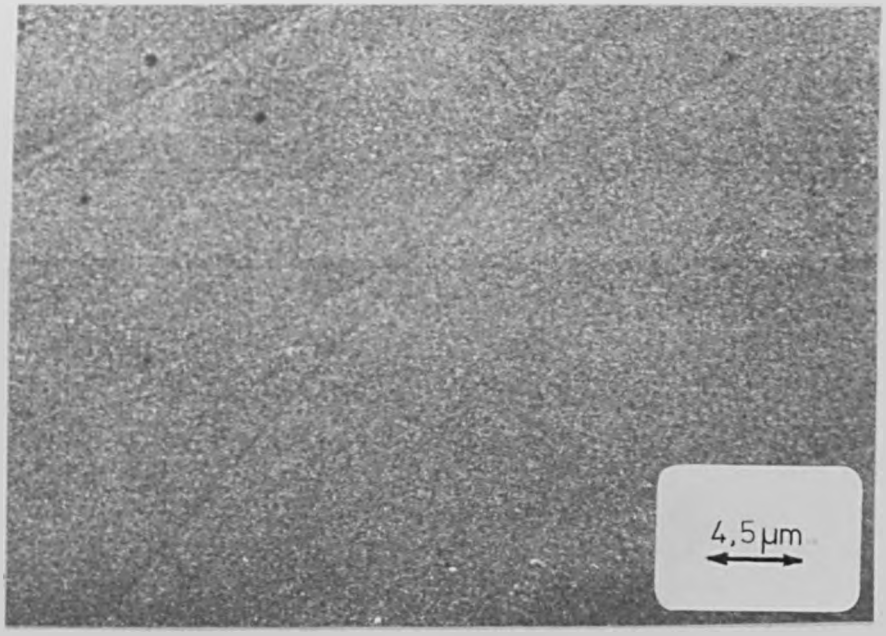

Surface before high temperature stability experiments.

Surface after high temperature stability experiments.

Fig. 6.7 Scanning electron micrographs of glass-ceramic 12 before and after high temperature stability experiments.

6.6. Colour centre formation

6.6.1. Sodium vapour exposure

After experiments had been performed on the chemical compatability of glass-ceramic 12 heat-treated at 800°C for 4 hours and 950°C for 6 hours, it was apparent that there existed the possibility of the formation of colour centres due to the sodium vapour. As mentioned in section 6.4., the sodium exposed material produced no surface damage but gave a deep-brown colouration. It was thus decided to investigate this phenomenon, using electron spin resonance and optical transmission.

The initial sample studied was one exposed to sodium vapour in an arc tube for 3 hours (sample A2 in Table 6.1.), and then compared to the unexposed glass-ceramic.

Fig. 6.8. shows the resulting spectra. The resonances appearing in the unexposed glass-ceramic are explained in Chapter IV section 4.7.. They are the six hyperfine Mn^{2+} lines centred around $g = 2$ with ΔB equal to 83 Gauss (0·0083 T), and the two Fe^{3+} resonances present at $g = 4{\cdot}27$ and $g = 3{\cdot}92$.

The sodium sample appears almost identical to this, but with an additional symmetric resonance at $g = 2$, the free electron resonance, indicating the presence of some colour centre.

It was thought that the mechanism involved in the colour centre formation was very similar to colour centres formed in radiation damaged alkali halides (Townsend and Kelly, 1973). The simplest centre studied was the F-centre which is a halogen ion vacancy plus a trapped electron.

One of the earliest reports on the discolouration of ordinary glasses by sodium vapour was by Fonda and Young (1934). They stated that the colouration was either yellow, brown or black,

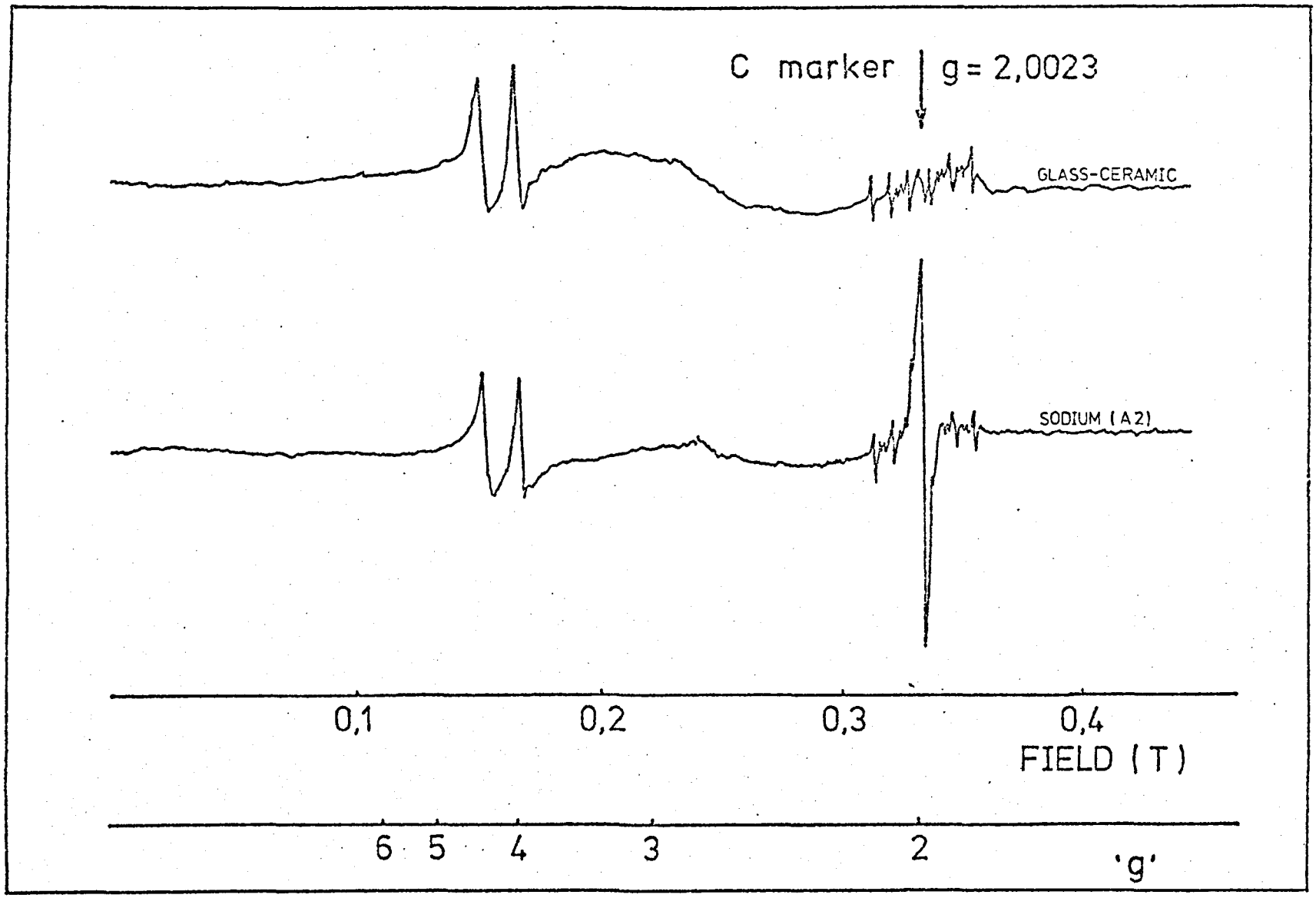

Fig. 6.8. E.S.R. spectra of glass-ceramic 12 before and after exposure to sodium vapour.

and that it was confined to a film of the glass surface in contact with the vapour, and that the extent of penetration increased with time of heating. Where black discolouration occurs, the primary cause lies in a chemical disintegration of the glass. It was questionable, however, whether the yellow discolouration that was characteristic of the more resistant glasses was due to a chemical disintegration. It seemed rather that it resulted from the diffusion of sodium atoms into the glass with possible segragation into aggregates of colloidal size. This was concluded after long tubes of the more resistant glasses were given an oven bake-out, filled with sodium and sealed off at a high vacuum. They were then heated in an oven at 350°C for 24 hours, after which time they had developed a strong yellow colour. The next and critical step consisted of placing only one half of the length of tubing into the oven at 350°C, allowing the other half to project outside, so that it was maintained at room temperature. After approximately 75 hours, the intensity of colour of the half of the tube within the furnace had become greatly reduced. It would seem that the colouration was initially caused by diffusion, and that the same process occurred, only reversed, on subsequent heating; the sodium in the glass distilling towards the cold end of the tube because of the reduced vapour pressure.

Rexer (1932) concluded that the diffusion of sodium in sodium chloride crystals did not occur through the lattice, but rather through fissures of atomic dimensions resulting from imperfections in the lattice. A similar process seems to occur in the diffusion of hot sodium in silica. No colouration or action whatever occurs with natural quartz. After fusion, however, and treatment at the same temperature in sodium, the sample is vigorously attacked, disintegrating into a black mass of reduced silicon. According to Rexer, it is expected that the effect of fusion is to disorganize the crystal lattice. It would seem apparent, therefore, that diffusion of sodium takes place readily

between the molecular aggregates so formed, and that the bonds within these aggregates are so loose that chemical reduction is possible.

A possible model for the colour centre formed in transparent glass-ceramic 12 is that a sodium atom present in the vapour penetrates or diffuses into the glass network, breaking a bridging Si - O - Si bond and the released electron orbits around the negative ion vacancy with the Na^+ ion residing in an interstitial position. This model is illustrated in fig. 6.9..

This model indicates the formation of the colour centre leading to the resonance at $g = 2$, but the colouration of the glasses and glass-ceramics may involve some other chemical reaction. According to theories by Hass (1950), Hass and Salzberg (1954) and Burns (1965), silicon monoxide could result from the reaction, i.e. the SiO_2 is reduced to SiO. Thin films of silicon and silicon monoxide have a remarkable similarity in the absorption spectra to that of sodium-attacked silica. Recalling fig. 6.5., it can be seen that the attack due to sodium vapour progresses from the surface inwards. Regions of attacked glass appear to be formed. These could be aggregates of silicon monoxide.

Theoretical calculations by Volf (1961) of the number of bridging oxygen ions around silicon in the glass can be investigated using the expression : the ratio of Si to O

$$\frac{Si}{O} = \frac{SiO_2/100}{\text{mole}_{SiO_2}\ \frac{Me_mO_n}{100}\ \frac{O_n}{\text{mole}_{Me_mO_n}}} \qquad (6.1.)$$

where SiO_2 is the weight percentage of SiO_2

mole_{SiO_2} is the molecular weight of SiO_2 = 60·06

Me_mO_n is the weight percentage of all oxides, including SiO_2 in the glass

$\text{mole}_{Me_mO_n}$ is the molecular weight of the oxides

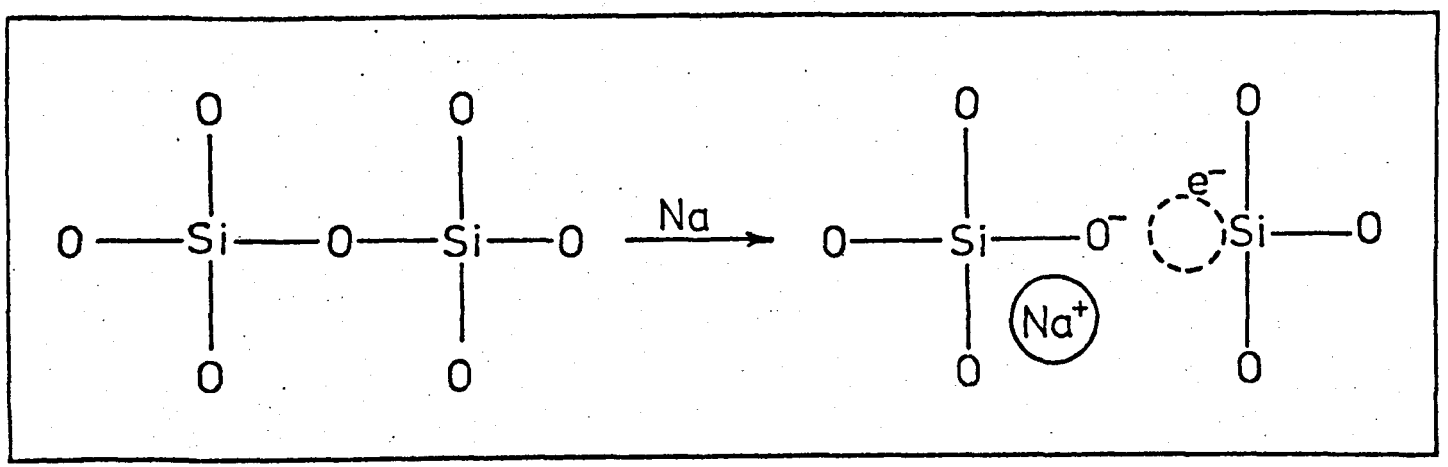

Fig. 6.9. Model for colour centre formation due to sodium exposure.

... O_n is the number of oxygens in the oxide.

The results of these calculations have shown that in the glass structure, there are two or three bridging oxygen ions per silicon ion, hence two or one non-bridging oxygen ions. It would be correct to say that in the glass-ceramic there could also be at least one non-bridging oxygen ion per silicon ion in the glass phase. Hence, the possibility exists that the sodium ion then resides on the non-bridging oxygen bond or any other nearby interstitial position.

Since the above arguments are extremely hypothetical due to the complexity of the five component glass structure, fused silica capsules each containing approximately 0·015gm 80 ; 20 (weight) mercury/ sodium amalgam and a few hundred torr of argon were made up. The capsules were exposed in a furnace for one and two hours at 400°C. A brown colouration was noted of varying intensity, the two hour capsule being darker than the one hour capsule. The capsules were broken and the fragments were analysed. The brown colouration appeared to be only on the inner surface of the capsule. This was expected since attack was only inhibited on the inner surface of the capsule. A definite boundary seemed to exist between the attacked and unattacked regions. E.S.R., however, produced no resonances. Washing the samples under warm water removed the brown colouration completely. It was noticed that the complete attacked brown surface was removed, leaving the glass surface below in an original glass state. The effect here appears to be different from that for the glass-ceramics studied, even though for the glass-ceramics the sodium vapour was all around the sample. The only common occurrence was the brown colouration. Burns (1965) studied the discolouration of vitreous silica by sodium and proposed that a sodium silicate glass is formed which is soluble in water as well as colour centre formation to produce the brown colouration. Sidorov and Tyul'kin (1971) performed E.S.R. studies on radiation centres in vitreous silica but reached no conclusion as to the nature of the

centres formed.

Further tests were thus performed on the colour centre formation. Six specimens (four of glass-ceramic 12, one of glass 12 and one of glass-ceramic 8 heat-treated at 800°C for 4 hours and 950°C for 4 hours) were introduced into each of two arc tubes containing sodium as described in section 6.3.. Glass-ceramic 8 was also introduced, since the MgO present in this material was thought to be more chemically stable than the CaO present in glass-ceramic 12 (McMillan, 1964).

One arc tube was run for one hour and the other for two hours. Fig. 6.10. shows the two lamps after each exposure. Also shown are the positions of the specimens in each lamp.

The one hour lamp produced the best results with a uniform colouration, as expected, of all four samples of glass-ceramic 12. The two hour lamp, however, produced patchy and non-uniform colourations as can be seen in fig. 6.11. The appearance of the samples was different for each material.

In the one hour lamp, glass-ceramics 8 and 12 had the same even brown colouration, whilst glass 12 appeared darker, obviously suffering a greater attack.

In the two hour lamp, all the samples had uneven colourations, and in general were lighter in appearance than in the one hour lamp.

Fig. 6.12. shows the E.S.R. results for specimens from both lamps. All the spectra show the same $g = 2$ resonance but of a varying intensity, indicating a varying number of colour centres produced. Figs. 6.13 and 6.14. show the transmission in the visible region of all the specimens labelled in fig. 6.12..

E.S.R. results match up extremely well with the transmission results in that the greater the free electron resonance at $g = 2$, the greater the absorption. Glass 12 showed a deeper colouration

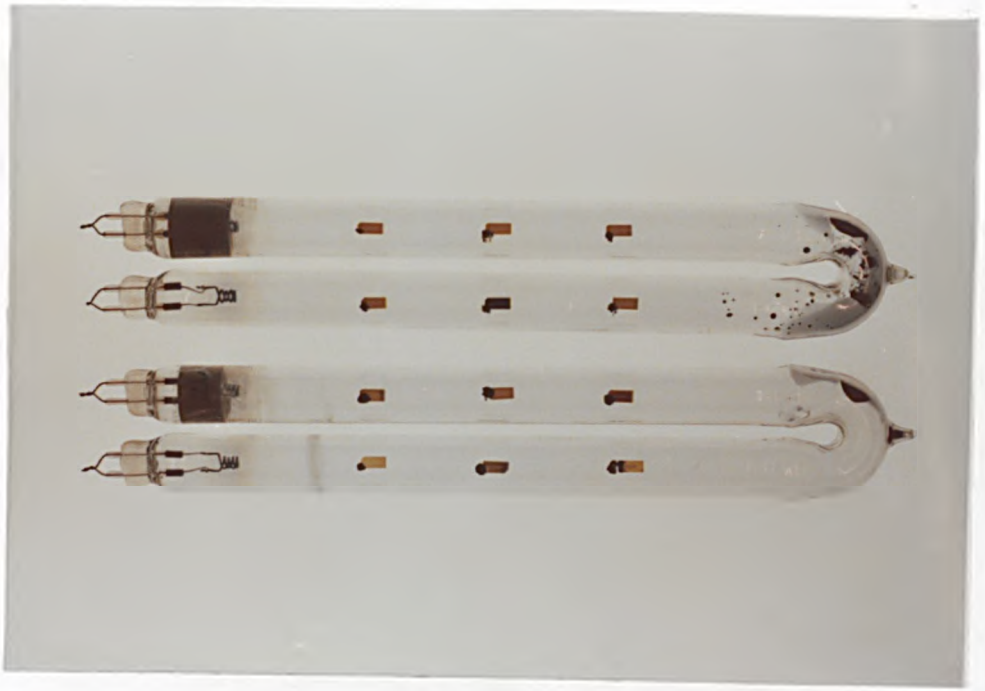

Fig. 6.10. Sodium arc tubes run for one and two hours with samples of glass 12, and glass-ceramics 8 and 12. (Upper tube - 1 hour exposure; Lower tube - 2 hours.)

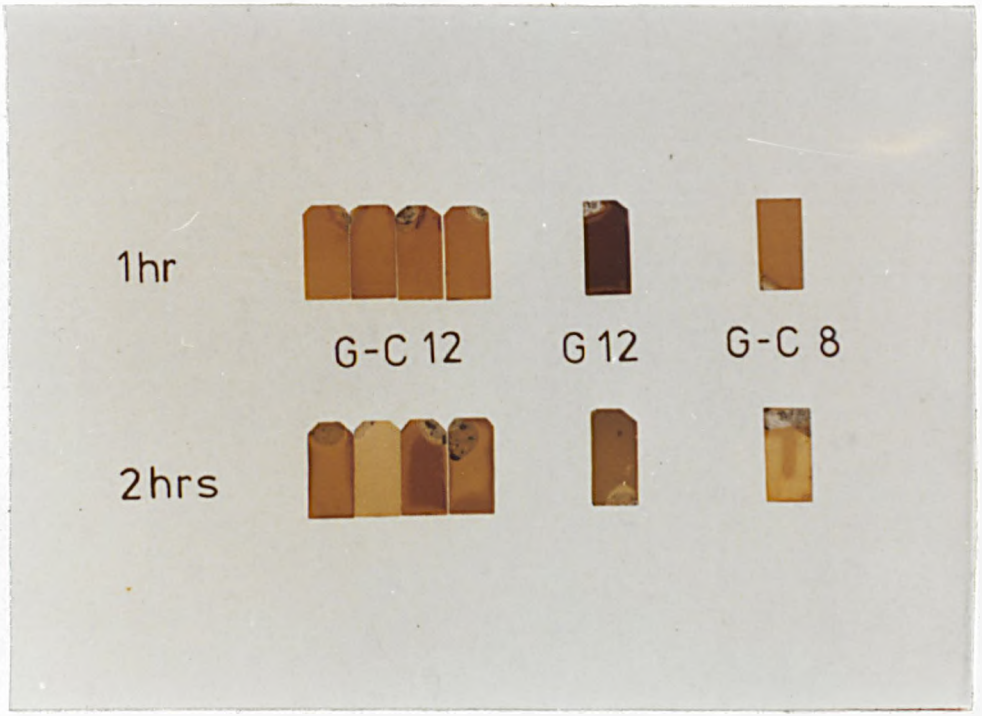

Fig. 6.11. Samples of glass 12, and glass-ceramics 8 and 12 after exposure to sodium vapour for one and two hours.

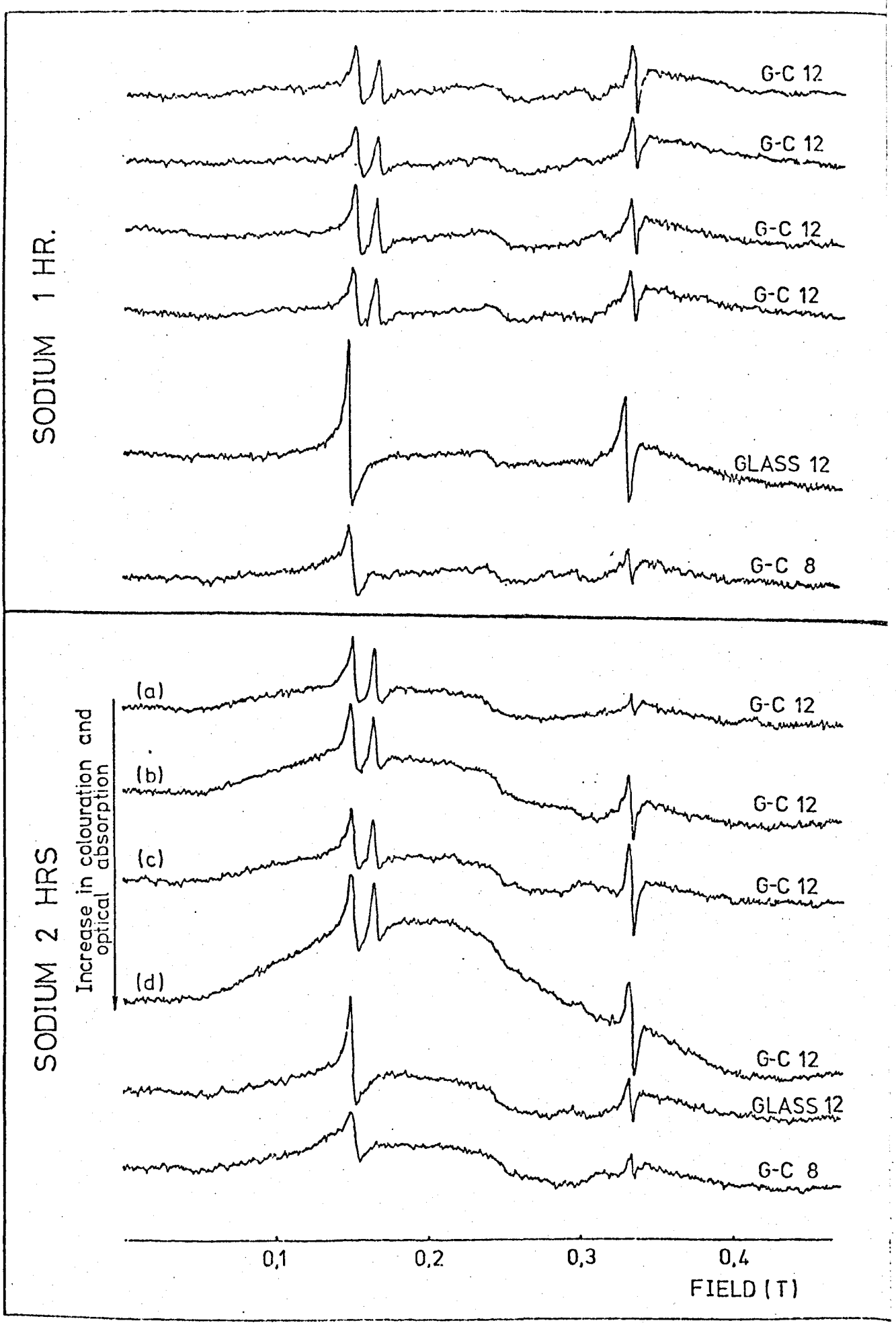

Fig. 6.12. E.S.R. spectra of all samples in fig. 6.11 exposed to sodium vapour.

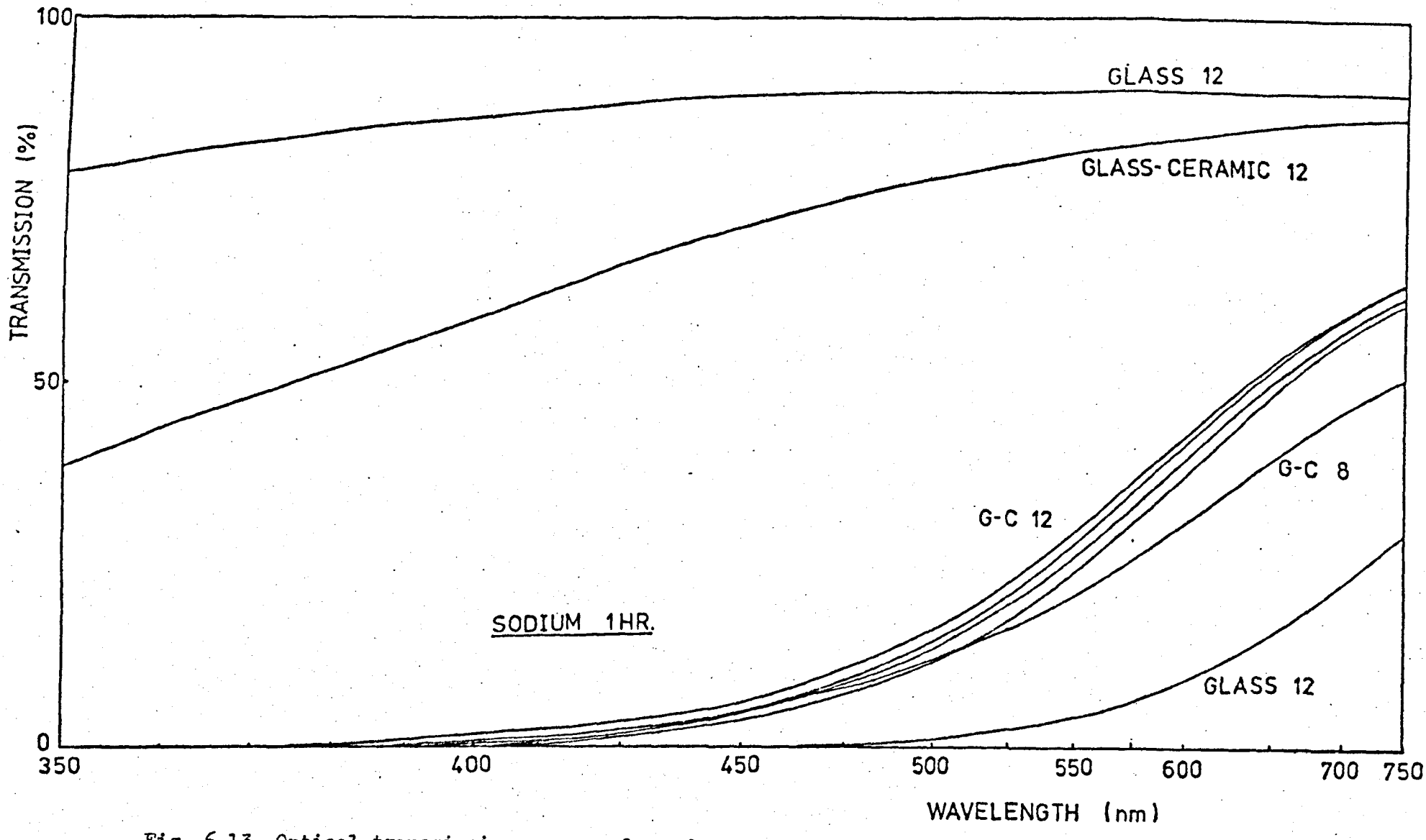

Fig. 6.13 Optical transmission curves of samples exposed in the sodium vapour lamp for 1 hour.

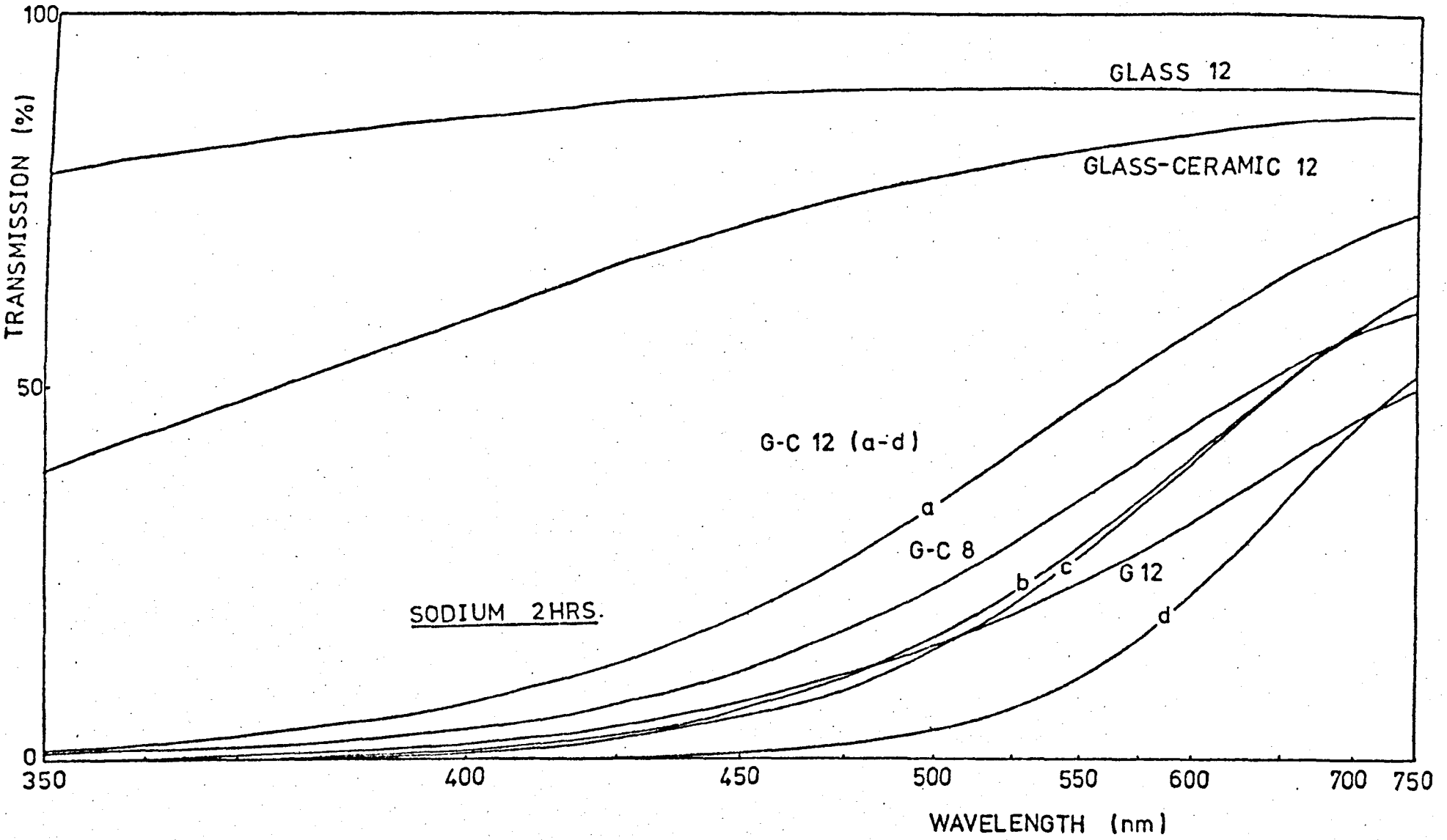

Fig. 6.14 Optical transmission curves of samples exposed in the sodium vapour lamp for 2 hours.

and a larger g = 2 resonance than glass-ceramic 12, and glass-ceramic 8 showed less effect than either, probably due to the more chemically stable MgO present.

6.6.2. X-ray irradiation

It was considered interesting to observe briefly if any colour centres could be formed, similar to those formed due to sodium vapour exposure, by subjecting samples of glass and glass-ceramic 12 to X-ray irradiation. No colouration or E.S.R. spectra were observed after exposure to CuK_{α} (40kV and 16mA) radiation for 24 hours.

Exposure to X-rays produced by synchrotron radiation (NINA synchrotron - Daresbury Laboratories) for 8 hours at 5GeV and 10mA, resulted in a brown straw-like colouration. It was noticed that the colouration began to fade very slowly within a couple of weeks.

The E.S.R. spectrum, fig, 6,15,, not only produced a very intense and narrow g = 2 resonance, but also another resonance at $g = 2{\cdot}009 \pm 0{\cdot}005$. The intensity of these lines (reduced by a factor of 20) can be compared to the height of the two Fe^{3+} peaks at g = 4·27 and g = 3·92.

Work performed by van Wieringen and Kats (1957) on the E.S.R. of silicate glasses, coloured by X-rays, showed two resonances at around g = 2·01 and g = 1·96. They suggested that the high-field peak at g = 1·96 was caused by centres having an excess of negative charge, i.e. caused by electrons, and the low-field peak at g = 2·01 was caused by centres having a lack of negative charge, i.e. caused by holes. According to these data, it would seem that the resonance of X-ray irradiated glass and glass-ceramic 12 at g = 2·009 is due to hole centres. This implies that the hole centres are non-bridging oxygen ions the charge of which is not compensated by a neighbouring metal ion but by a trapped hole. For the case of sodium exposed samples, the sodium ions are present to maintain charge neutrality, but the free electron resonance

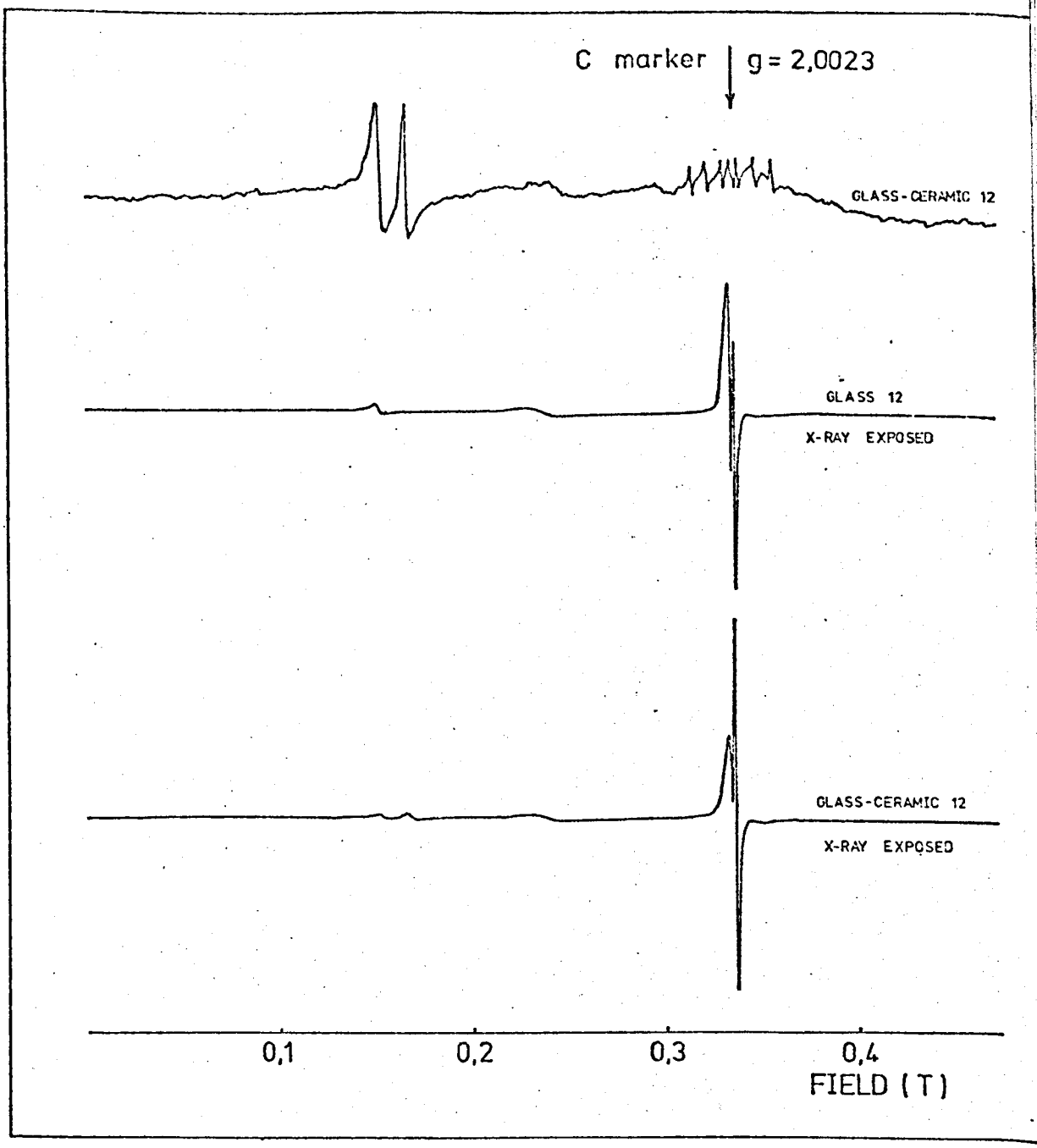

Fig. 6.15. E.S.R. spectra of X-ray exposed glass and glass-ceramic 12.

is present, indicating an electron orbiting a negative ion vacancy, which here again is the oxygen ion.

For X-ray irradiated samples therefore, two colour centres are produced, namely trapped electron centres as for sodium exposed samples, and trapped hole centres. In glass 12 the resonance produced by the hole centres is more intense than the resonance developed by the electron centres. For the glass-ceramic, the roles are reversed, whereby the resonance of the electron centres is more intense than the resonance of the hole centres. Less non-bridging oxygen ions could be available in the glass-ceramic to neighbour trapped holes, due to the re-arrangement of the structure of the glass during crystallization.

Similar work to that of van Wieringen and Kats was done by Lee and Bray (1962) and Schreurs (1967) and was discussed in section 6.2..

6.6.3. Lithium vapour exposure

After exposure to sodium vapour had produced some interesting results, it was wondered whether other alkali metal vapours would initiate the same effect of colour centre production.

The simplest metal chosen was lithium. Since lithium is a smaller ion than sodium, it would be expected that more colour centres could be produced in the same amount of time exposure. It was found , however, that exposure for one hour produced a destructive effect on the samples, and so the optimum temperature and time for the production of a significant colouration, without too much damage, was found to be 500°C for 15 mins, as described in section 6.3.. After this treatment the sample had turned brown.

The E.S.R. spectrum of this particular sample produced tha same $g = 2$ resonance as for the sodium exposed sample in fig. 6.8.. The absorption in the visible region increased towards the lower wave-

length region. Thus, the lithium behaves in a similar fashion to the sodium in developing colour centres, but in a more pronounced way.

Fig. 6.16. shows the E.S.R. spectra of lithium exposed glass-ceramic and other specimens of glass-ceramic 12 subjected to sodium vapour.

The results imply that the alkali metal vapours, sodium and lithium, both cause the same colour centres to be formed, but do not actually themselves take part in the colour centre produced. The previously proposed colour centre model due to sodium vapour (section 6.6.) appears to be in good agreement with these observations.

6.7. Thermal bleaching

The colour centres produced in the glass-ceramics by exposure to sodium and lithium vapours could be bleached by placing the glass-ceramics into a furnace and noting at what temperature and after what time the colouration began to fade. Hence, E.S.R. and optical absorption could determine whether the number of colour centres had in fact been reduced. Bleaching the samples in the resonant cavity, using the special liquid nitrogen attachment working from $-200^{\circ}C$ to $+300^{\circ}C$ produced no effect, the maximum temperature used being too low. The lowest temperature at which a noticeable fading of the colouration was observed was $400^{\circ}C$ for the sodium exposed samples.

The first sodium exposed sample (sample A2 in Table 6.1.) was bleached at $400^{\circ}C$ for one hour. It was expected that the E.S.R. resonance at $g = 2$ might revert to its original shape, that of the unexposed glass-ceramic. This, however, did not happen. An intense wide resonance was produced. It was also observed that during bleaching of the above sample, a brownish 'treacle-like' substance had formed on the lower surface of the specimen as it rested in the furnace. This substance rapidly solidified on removal from the furnace and began to craze on cooling.

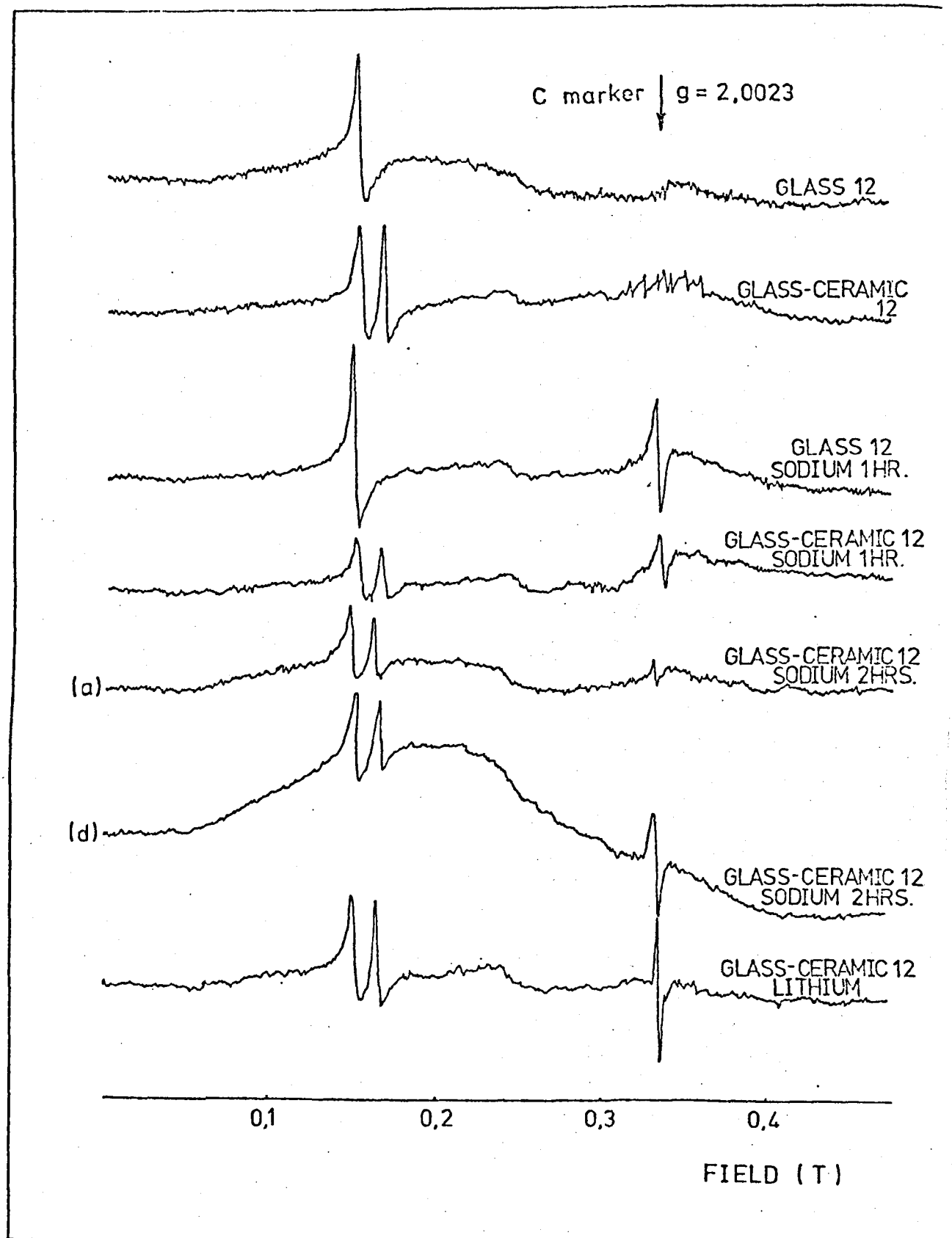

Fig. 6.16. E.S.R spectra of unexposed and exposed samples of glass and glass-ceramic 12 to sodium and lithium vapour.

This surface could not readily be identified as it was difficult to peel the layer off, but it was thought that this could have been a sodium silicate glass, caused by the reaction of the sodium and silica network during bleaching. The reason for the crazing of the 'treacle-like' substance on the surface of the sample may be a higher coefficient of thermal expansion of this substance than the glass itself. This would be consistent with the formation of a sodium silicate glass, because such a glass is likely to have a high thermal expansion coefficient.

The sample was broken into two halves and the E.S.R. was performed on each half. Results are shown in fig. 6.17.. It was now thought that some impurity had managed to adhere to the surface of one of the halves of the specimen.

Slight abrasion, for a few seconds on 600 grit Carborundum paper, of the surfaces where the 'treacle-like' substance had formed, resulted in the original glass-ceramic spectrum, with only a very small $g = 2$ resonance. It was, therefore, believed that the initial intense resonance was due to impurities and not to the bleaching process.

To analyse the thermal bleaching effect in greater detail, the four samples of glass-ceramic 12 which had been exposed to sodium vapour in the one hour arc tube, were subjected to heat-treatments of 400°C, 450°C, 500°C and 600°C for times ranging from 15 minutes to two hours.

The most significant results were obtained by optical absorption measurements, since E.S.R. results only showed a dramatic decrease in the $g = 2$ resonance even after the 15 minute bleaching time.

The optical absorption decreased as the time of bleaching increased and results are given as a ratio of the intensity at a chosen wave-length of 500nm of bleached sample, I, to unbleached sample, I_o. Fig. 6.18. shows the results for the temperatures chosen. The

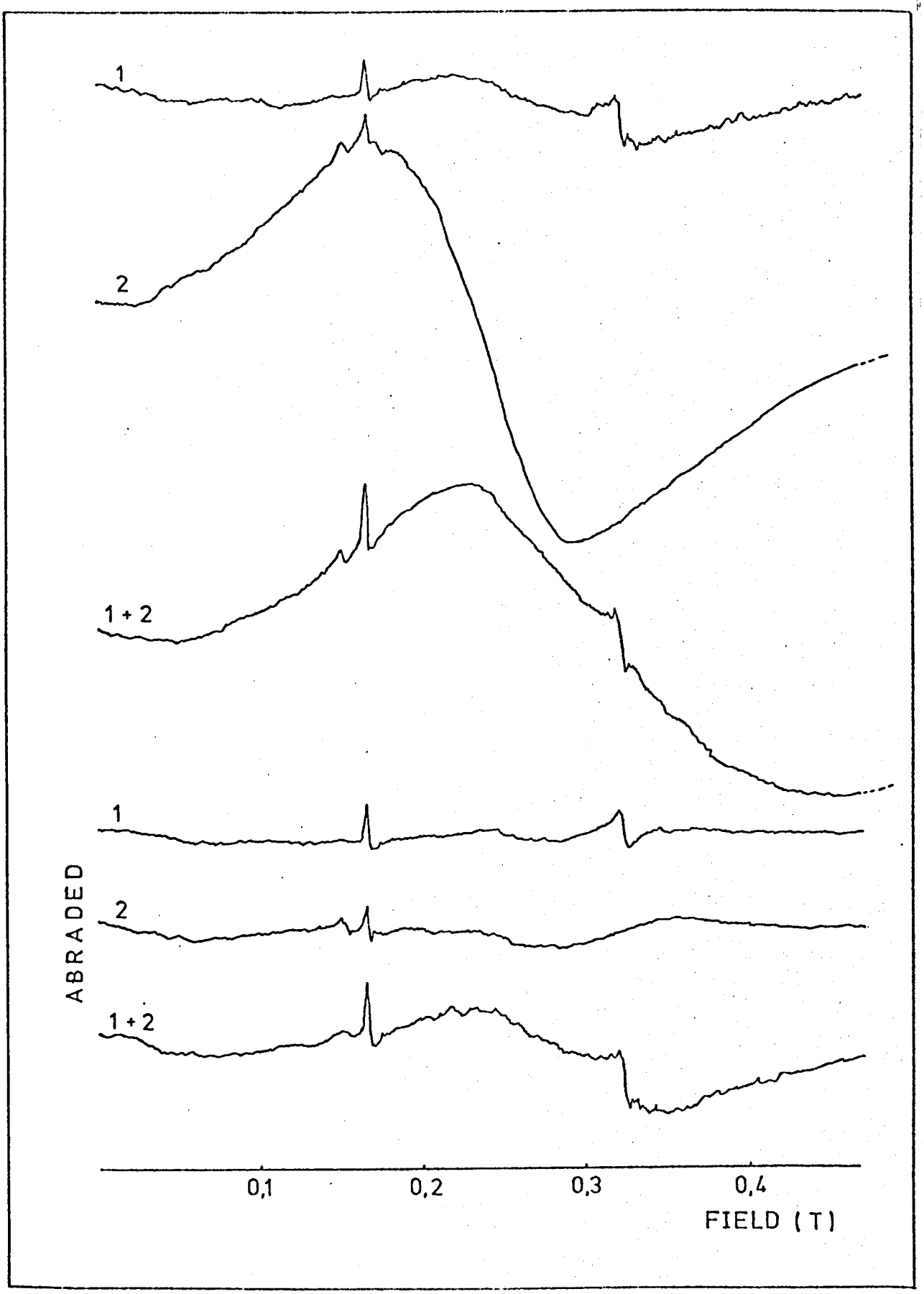

Fig. 6.17. E.S.R spectra of bleached glass-ceramic 12 before and after surface grinding to illustrate the presence of impurities.

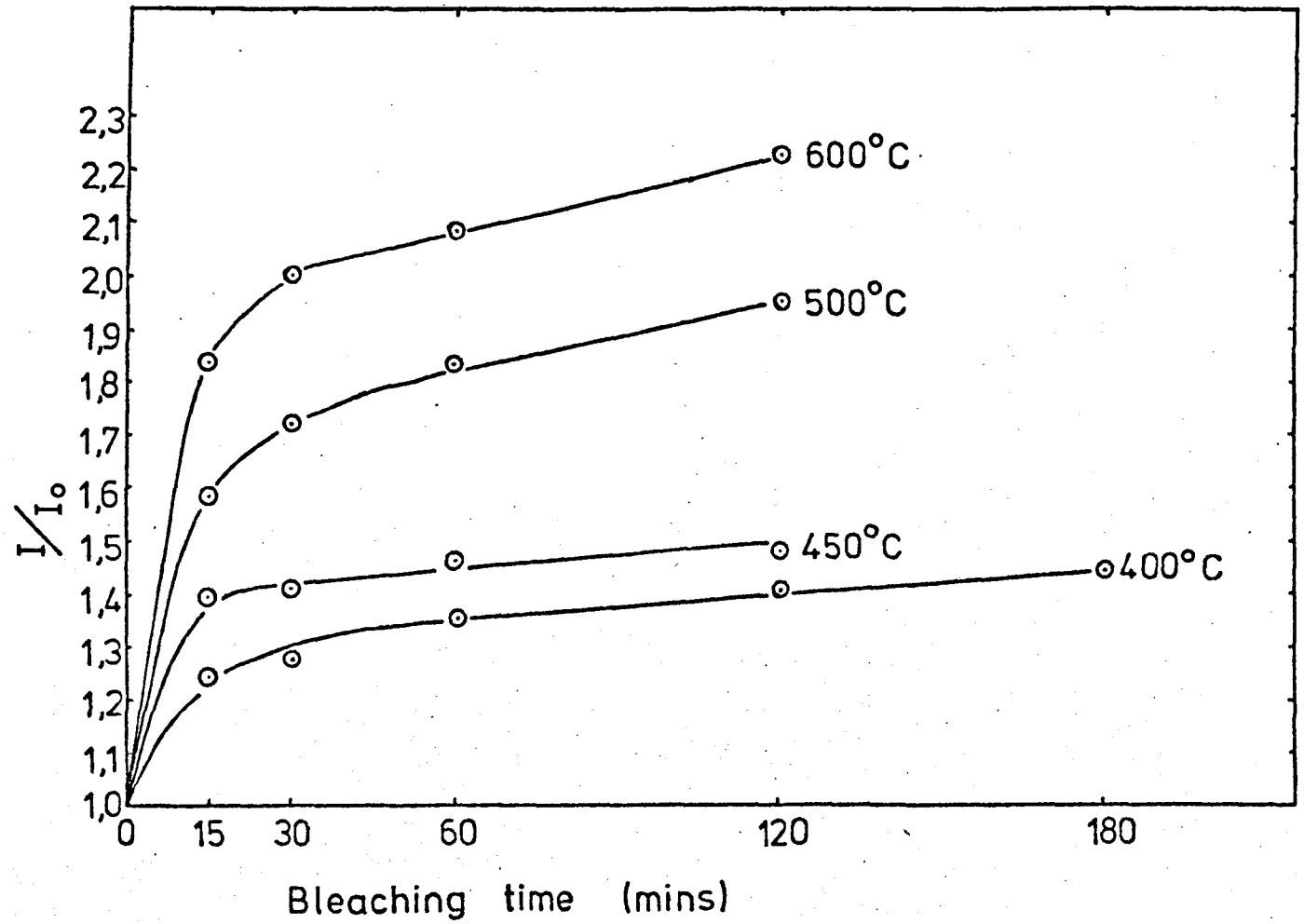

Fig. 6.18. Variation of optical transmission at 500nm with time for different bleaching temperatures.

bleaching rate increases for increasing temperatures, indicating that the rate is a function of temperature. For all temperatures, the maximum rate of bleaching is seen to be within 30 minutes at a particular temperature, after which the bleaching decreases to a very slow rate.

The rate of bleaching,

$$B = \frac{d(I/I_o)}{dt} \qquad (6.2.)$$

was plotted against temperature and was found to be proportional to the reciprocal of the absolute temperature, as seen in fig. 6.19., which implies a thermally activated process.

The rate of bleaching, B, can be related to a rate of chemical reaction which increases exponentially with the temperature. If a thermally activated diffusion process is involved,

$$B = B_o \exp\left(-\frac{E_B}{RT}\right) \qquad (6.3.)$$

or

$$\ln B = \ln B_o - \frac{E_B}{RT} \qquad (6.4.)$$

where E_B is the activation energy for the process

R is the gas constant

T is the absolute temperature

and B_o is a constant.

Calculations of the activation energy, E_B, from fig. 6.19. for the bleaching process gave a value of 6.4 kcal $mole^{-1}$.

Experiments by Burns (1965) involved heating a vitreous silica capsule containing sodium metal in a tubular furnace and measuring the optical density or transmission of light after different times of exposure at different temperatures.

His first calculation involved measuring the quantity of material diffusing across unit area, which is proportional to

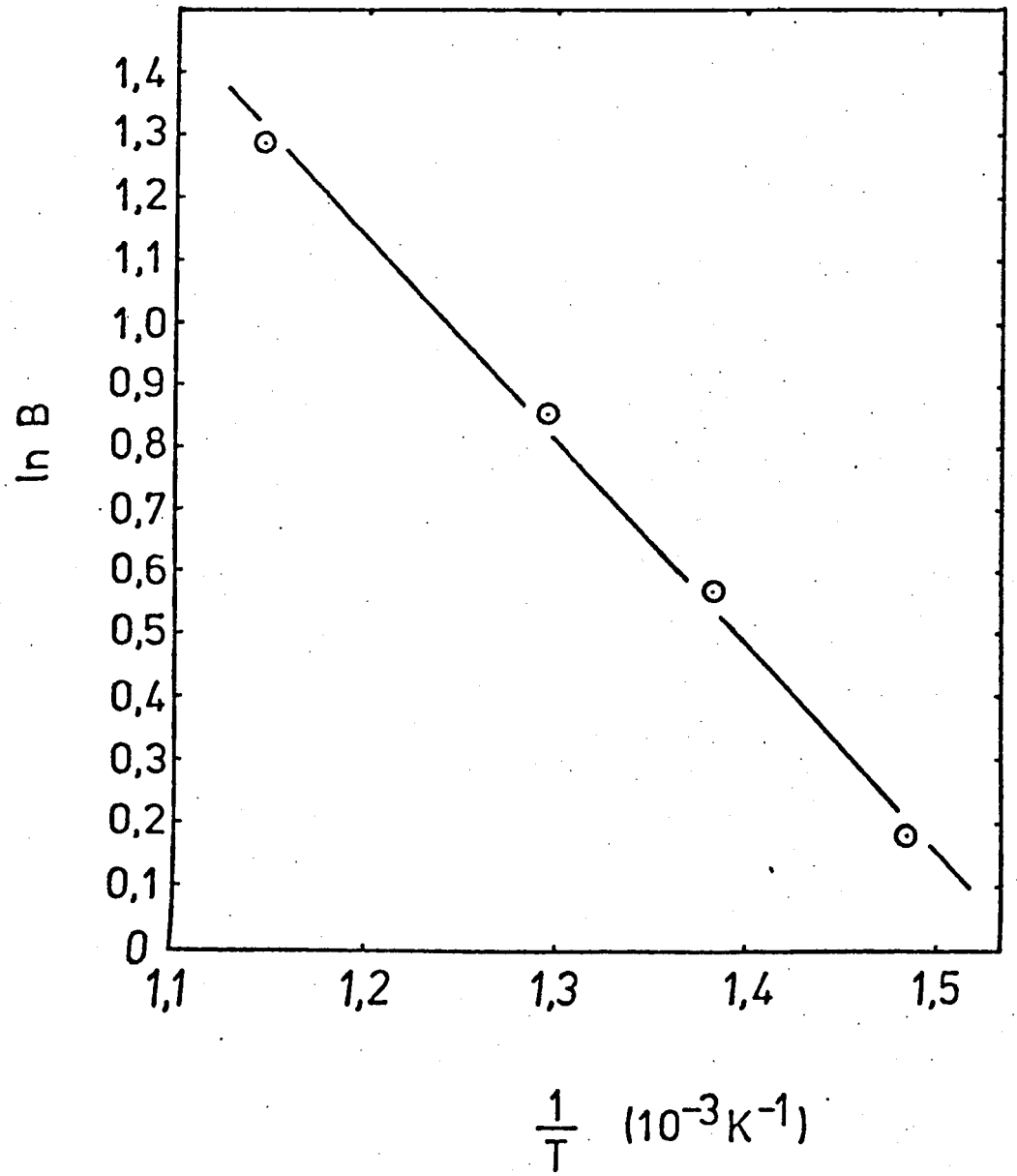

Fig. 6.19. Variation of bleaching rate with temperature.

tha square root of the diffusion coefficient, D, and the square root of the time, t. The optical density, ρ, according to Beer's law, states that it is also proportional to $D^{1/2}$ and to $t^{1/2}$.

For most diffusion processes

$$D = D_o \exp\left(-\frac{E}{RT}\right) \qquad (6.5.)$$

and so

$$\frac{d(\rho^2)}{dt} = K \exp\left(-\frac{E}{2RT}\right) \qquad (6.6.)$$

where E is the activation energy of the diffusion process

and K is a constant.

For this Burns measured the activation energy of the diffusion of sodium ions through silica to be 22 kcal $mole^{-1}$. Kamel (1953) and Frischat (1968) have shown that the diffusion of sodium ions through silica and high silica content glasses has an activation energy of between 16 and 25 kcal $mole^{-1}$.

The next calculation involved measuring the rate of decrease in the optical density with time and temperature using the relation

$$\frac{d\rho}{dt} = K_1 \exp\left(-\frac{E_B}{RT}\right) \qquad (6.7.)$$

where E_B is the activation energy for the bleaching process

and K_1 is a constant.

This was performed because Burns found that a maximum optical density had been reached during the heat-treatment of the capsules, and further heat-treatment resulted in a decrease in the optical density.

From equation (6.7.) Burns obtained a value of the activation energy E_B for the bleaching process to be 6·8 kcal $mole^{-1}$.

In the present work, the bleaching process could only be performed on sodium exposed samples, and the activation energy

for the bleaching process gave a value of 6.4 kcal mole^{-1} which matches Burns' results very closely.

Burns stated that the darkening of the silica capsule and the bleaching process occurred simultaneously but the latter occurred at a much slower rate, the two processes being governed by different laws. No explanation was given for the mechanisms of sodium diffusion and the bleaching process involved, but it is curious to know why the activation energy for the bleaching process is so low, too low to consider the diffusion of sodium out of the glass. Even the diffusion of oxygen is unlikely, since Williams (1965) showed that the activation energy for the diffusion of oxygen in fused silica is 29 kcal mole^{-1}.

Since the E.S.R. spectrum after thermal bleaching shows a disappearance of the g = 2 resonance, the electron orbiting the negative ion vacancy must be released. Since the activation energy for the bleaching process is too low for sodium or oxygen ion diffusion, it may suggest that another process is involved, requiring a higher temperature than that for colour centre formation. This may be the re-combination of the released electron and the sodium ion to form sodium metal.

With the limited information available, it is not considered possible to give a clear mechanism of the bleaching process.

6.8. Discussion

The main aspect of chemical stability experiments was to determine to what extent the transparent glass-ceramics could be chosen for particular lamp applications.

The common factor to all electric lamps is the need for a light transmitting bulb or envelope to isolate the inside of the lamp from the surrounding air, and to maintain the necessary gaseous atmosphere. It must be compatible with the gas-filling and other lamp components, and able to withstand the pressure and temperature of

the device without interfering with its operation.

The chemical stability of the transparent glass-ceramics studied behaved in a way that was expected for lamp vapours, when samples were incorporated into discharge and incandescent lamps. The least attack was encountered for lamps containing metal halides (sodium iodide and scandium iodide) and bromine. Capsules containing chlorides and also sodium iodide and scandium iodide proved inconclusive because of condensed vapours re-depositing on the surface of the specimens.

Weight change experiments showed negligible results, probably due to the small size of samples needed for insertion into the exhaust tubes in the lamps and capsules.

Scanning electron microscopy showed only a qualitative view of the nature of surface attack. The main problem, of course, was the surface deposition of condensed vapours, but all scanning electron microscopy had shown attack to a certain extent. Even for bromine exposed samples, which behaved in the best way, a slight surface effect was noticeable, but running the lamp for a thousand hours showed no real microstructural change.

For sodium vapour, the samples showed very little surface attack, but the presence of a brown colouration throughout the material meant that colour centres were formed.

The only satisfactory method of determining whether a material is suitable for lamp construction is to expose it for long periods of time, even for the running life of the lamp itself, and noting any change in lamp characteristics and any substantial changes in the structure of the sample.

It has been shown that samples introduced into bromine and sodium iodide and scandium iodide lamps produced very little degradation. The bromine lamp ran for the maximum life of the lamp, and the sodium iodide and scandium iodide lamp ran for about half the maximum

life.

The observations of colour centres produced by metal vapours such as sodium and lithium, have shown that similar colour centres are formed no matter what the alkali metal vapour, i.e. the metal vapour produces the colour centre but does not take part in the actual colour centre formed. The colour centres produced are of the free electron type with an E.S.R. free electron resonance at g = 2. A model was proposed for the colour centre analogous to an F- centre in alkali halide crystals, whereby the vapour of the alkali metal diffuses into the glass structure, breaking a bridging Si - O - Si bond, and the released electron orbits the negative ion vacancy, with the alkali metal ion residing in an interstitial position not far from the non-bridging oxygen ion.

The attack of the various alkali metal vapours occurs in the glassy phase only, since no change was observed in the E.S.R. resonances of the two Fe^{3+} peaks after attack. This attack is therefore limited to the phase where silica is present and not to other crystal phases, such as in this case, tetragonal zirconia or gahnite.

For colour centres produced by X-ray irradiation, two colour centres were thought to be formed; trapped electron centres and trapped hole centres. The possibility exists that the same colour centre is produced as for the sodium exposed samples, except that instead of the sodium ion being present, a trapped hole is situated at the non-bridging oxygen ion.

Thermal bleaching showed that the mechanism of colour centre destruction involves a different process to the mechanism of colour centre formation. Diffusion of sodium ions or oxygen ions is not possible because the calculated activation energy of 6·4 kcal $mole^{-1}$ for the bleaching process is too low for consideration of this type of mechanism.

CHAPTER VII

General Conclusions

In the zinc-aluminosilicate systems investigated, it has been shown that nucleation and crystallization is possible in order to achieve extremely fine-grained transparent glass-ceramics. Three stages were involved during the crystallization of the glasses, namely phase separation which involved the diffusion of zirconium ions into zirconium rich regions, nucleation whereby crystals of tetragonal zirconia were precipitated, and finally the crystallization of small crystals of β-quartz s.s. or gahnite. To produce transparent glass-ceramics with a spinel-type phase, i.e. gahnite, a minimum amount of 9.1 wt.% ZrO_2 was required for subsequent crystallization of the gahnite phase.

Transmission electron microscopy has shown that the crystal size was extremely small, not exceeding 28nm and that a low volume fraction of crystals was present, 22% for glass-ceramics containing gahnite as the primary phase, and 34% for glass-ceramics where β-quartz s.s. was the main phase, the glassy phase being mainly siliceous. During nucleation in all glasses the tetragonal zirconia crystals reached a size of 90nm and a maximum volume fraction of 9%.

Three glass-ceramics where gahnite was the main crystalline phase produced, but with different alkaline earth metal oxides, were analysed. It was found that the alkaline earth metal ions acted as interstitial ions, and did not take part in crystal formation. Microstructurally, glass-ceramics with the alkaline earth metal oxides, MgO, CaO, or BaO were identical when considering crystal volume fractions and particle sizes. The only apparent difference was noted in the glass-ceramic with CaO where an initial spherical morphology, common to all

the other glass-ceramics was transformed into a rod-shaped morphology. A detailed analysis of this glass-ceramic showed that microstructural parameters such as particle size, volume fraction and mean free path were strongly dependent on the heat-treatment schedule, the optimum microstructure being achieved after a heat-treatment of 800°C for 4 hours and 950°C for 5 hours.

Electron spin resonance proved invaluable in monitoring the crystallization process in that the presence of impurity ions of Fe^{3+} shows a four-fold coordination in the glass phase and a six-fold coordination in the gahnite phase in the glass-ceramic. Thus in the glass phase, only one Fe^{3+} resonance was observed with the appearance and growth in intensity of the second Fe^{3+} resonance on crystallization, until no further increase occurred after the samples had been heat-treated for 800°C for 4 hours and 950°C for 5 hours. This showed that the maximum number of crystals had formed, which is in good agreement with the particle size and volume fraction measurements mentioned above.

When considering physical properties, the remarkable fact is that the presence of such a low volume fraction of crystalline species can have such a marked influence on the physical properties when the glass is transformed into a glass-ceramic.

The thermal expansion coefficients varied over a wide range from low to moderate expansion, depending on whether the primary crystal phase was a β-quartz s.s. (glass-ceramic expansion $12 \times 10^{-7}{}^{\circ}C^{-1}$) or gahnite (glass-ceramic expansion 26 to 38 $\times 10^{-7}{}^{\circ}C^{-1}$). Variations also occurred for the gahnite glass-ceramics, where the presence of larger alkaline earth metal oxides increased the expansion coefficient. Glass 12 has been shown to seal quite rigidly to tungsten, and the seal remained strong when the glass was converted into a glass-ceramic. In general, the expansion coefficient of glass-ceramic 12 chosen for detailed study followed the additive relationship with an increase in expansion

coefficient as the volume fraction of gahnite crystals increased.

Density measurements have also been shown to follow the additive relationship, as well as microhardness values.

The densities of the glasses and glass-ceramics varied by only small quantities. The average value of the density for all the glass-ceramics was $2{\cdot}6 gm.cc.^{-1}$.

The microhardness values between different glass-ceramics containing the gahnite crystalline phase varied very slightly around 750 VHN($kgmm^{-2}$). The microhardness of the glass-ceramic containing β-quartz crystals reached a value of around 900 VHN($kgmm^{-2}$) because of the higher volume fraction of crystals present here than in the gahnite containing glass-ceramics.

Microhardness results have been in good agreement with theoretical work in that the hardness is proportional to the particle size, d, indicating that the fracture mechanism occurs at grain boundaries. These conclusions were hard to justify because of the large errors associated with the measurement of the particle size.

Modulus of rupture values for the transparent glass-ceramics were generally high, ranging from $110MNm^{-2}$(16,000 p.s.i.) to $150MNm^{-2}$(22,000 p.s.i.).

Mechanical strength results were also in accordance with theoretical evidence in that strength is proportional to $d^{-1/2}$ when the stresses introduced at the crystal-glass boundaries are compressive in the circumferential direction, due to the higher expansion coefficient of the crystalline phase than the glassy phase.

Optical properties have been shown to be good, both in the near infra-red region up to about 4 microns, and the visible region down to about 400nm where light scattering and absorption due to transition metal impurities come into play.

The chemical stability of glass-ceramic 12 in

certain lamp-making vapours proved very interesting. The material was compatible with bromine vapour and with sodium iodide and scandium iodide vapours when introduced into the corresponding lamps and exposed for periods of up to 1000 hours. When exposed to sodium vapour, the material turned dark brown without any sign of surface attack and colour centres were found to be involved, due to the diffusion of sodium into the glass network.

Electron spin resonance produced a resonance at the free electron g = 2 value, and a model was proposed for the colour centre whereby sodium diffuses into the glass network, breaks an Si-O-Si bond and the released electron orbits the negative ion vacancy with Na^+ ion residing in an interstitial position.

X-ray irradiation showed that trapped electron centres and trapped hole centres were involved. Thermal bleaching led to the conclusion that a different mechanism was occurring than for the colour centre formation. Diffusion of sodium ions or oxygen ions could not be considered because of the low activation energy calculated (6.4 kcal $mole^{-1}$) for the bleaching process.

Future Work

Proposals for future work would be to investigate more fundamental characteristics of microstructure, using evidence from small angle X-ray scattering on the phase separation and nucleation of the glasses. X-rays could similarly be used to measure such properties as thermal expansion, particle size and volume fraction in much more detail and relating to results performed by dilatometric measurements and counting techniques from transmission electron micrographs.

A more detailed investigation on the mechanical strength of transparent glass-ceramics would prove very useful in attempting to gain a better understanding of the mechanisms involved.

Because of limitations of time only limited experiments were performed using E.S.R. on transition metal ion impurities present in the glasses. This field could be greatly expanded as a useful technique for monitoring crystallization processes. Similarly, more fundamental work needsto be done on colour centres by working on very simple glass compositions, so as to be able to provide concrete evidence on colour centre formation and destruction.

It would also prove invaluable to be able to produce and study the properties of silica-free transparent glass-ceramics for lamp purposes, especially sodium vapour lamps. A very useful area here would be in the aluminoborate system, because of the known resistance of this to sodium vapour.

Finally, it should be pointed out that tubes of glass 12 are being drawn to produce an experimental lamp to be run with sodium iodide and scandium iodide vapour.

REFERENCES

ABRAGAM A. and PRYCE M.H.L. (1951) Proc. Roy. Soc. A205, 135

ADAMS R.V. and DOUGLAS R.W. (1959) J. Soc. Glass Tech. 43, 147T

ADAMS R.V. (1961)a Phys. Chem. Glasses 2, 39

ADAMS R.V. (1961)b Phys. Chem. Glasses 2, 101

AINSWORTH L. (1954) J. Soc. Glass Tech. 38, 478

AKHMED-ZADE K.A., ZAKREVSKII V.A. and YUDIN D.M. (1974) Sov. Phys.-Sol.St 16, 241

AMATO I., NEGRO A. and BACHIORRINI A. (1975) Rev. Int. Htes. Temp et Réfract. 12, 241

ANDRADE E.N. and TSIEN L.C. (1937) Proc. Roy. Soc. A159, 346

ARAFA S., ASSABGHY F., FAHMY H, ALLAM M. and SABEK D. (1975) J. Amer. Ceram. Soc. 58, 203

ARGON A.S. (1959) Proc. Roy. Soc. 250, 472

BABASOVA A.K., JININA P.A. and SKRYPKO G.G. (1974) Steklo Sitally i Silikatnye Materialy 3, 42

BAILAR J.C., EMELEUS H.J., NYHOLM R. and TROTMAN-DICKENSON A.F. (1973)a "Comprehensive Inorganic Chemistry" vol. 1 (Pergamon Press)

BAILAR J.C, EMELEUS H.J., NYHOLM R. and TROTMAN-DICKENSON A.F. (1973)b "Comprehensive Inorganic Chemistry" vol. 3 (Pergamon Press)

BARRY T.I. (1969) J. Mater. Sci. 4, 485

BEALL G.H., KARSTETTER B.R. and RITTER H.L. (1967) J. Amer. Ceram. Soc. 50, 181

BEALL G.H. and DUKE D.A. (1968) J. Mater. Sci. 4, 340

BEREZHNOI A.I. (1970) "Glass-Ceramics and Photo-Sitalls" (Plenum Press, New York

BINDER K. and STAUFFER D. (1976) Adv. in Physics 25, 343

BIRCHALL T. and REID A.F. (1973) J. Solid State Chem. 6, 411

BISHAY. A.M. and HASSAN F. (1967) "Interaction of Radiation with Solids" (Plenum Press, New York)

BISHAY A.M. and MAKAR L. (1968) J. Amer. Ceram. Soc. 52, 605

BISHAY A.M. (1970) J. Non Cryst. Solids 3, 54

BLAU H.H. (1933) Ind. Eng. Chem. 25, 848

BLEANEY B.I. and BLEANEY B. (1968) "Electricity and Magnetism" (Oxford University Press)

BOULOS E.N. and KREIDL N.J. (1972) J. Canad. Ceram. Soc. 41, 83

BOWERS K.D. and OWEN J. (1955) Rep. Prog. Phys. 18, 304

BRADLEY D.E. (1954) Brit. J. Appl. Phys. 5, 65

BREARLEY W. and HOLLOWAY D.G. (1963) Phys. Chem. Glasses 4, 69

BREKHOVSKIKH S.M., SIDOROV T.A. and TYUL'KIN V.A. (1967) Inorg. Mater. (Consultants Bur. Transl) 3, 1994

BRIGGS J. and CARRUTHERS T.G. (1976) Phys. Chem. Glasses 17, 30

BUERGER M.J. (1954) Amer. Mineral. 39, 600

BURNS J.A. (1965) Glass Tech. 6, 17

CASTNER T., NEWELL G.S., HOLTON W.C. and SLICHTER C.P. (1960) J. Chem. Phys. 32, 668

CLINTON D.J. (1972) Micron 3, 358

CONRAD M.A. (1972) J. Mater. Sci. 7, 527

CORNING GLASS WORKS (1960) Brit. Pat. 857367

CORNING GLASS WORKS (1965) Dutch Pat. 6,413,978

CORNING GLASS WORKS (1972) U.S. Pat. 3,681,102

COTTERILL R.M.J., JENSEN E.J., KRISTENSEN W.D. and PAETSCH R. (1975) J. de Physique 36, C2

CULLITY B.D. (1959) "Elements of X-ray Diffraction" (Addison-Wesley, Reading, Massachusetts)

DEVERS P.K. (1943) Magazine of Light 2, 15

DICKSON B.L. and SRIVASTAVA K.K.P. (1976) J. Phys. Chem. Solids 37, 447

DOHERTY P.E. and LEOMBRUNO R.R. (1964) J. Amer. Ceram. Soc. 47, 368

DOREMUS H. (1973) "Glass Science" (Wiley, New York)

DOUGLAS R.W. (1958) J. Soc. Glass Tech. 42, 145

DRUMHELLER J.E., LOCHER K. and WALDNER F. (1964) Helv. Phys. Acta 37, 626

DRUMMOND D.G. (1934) Nature 134, 739

DRUMMOND D.G. (1936) Proc. Roy. Soc. 153, 328

DUKE D.A., BEALL G.H., MACDOWELL J.F. and KARSTETTER B.R. (1967) Industrie Chimique Belge 32, 528

DUKE D.A. and CHASE G.A. (1968) Appl. Optics 7, 813

ELLIS J.W. and LYON W.K. (1936) Nature 137, 1031

ELLIS J.W. and LYON W.K. (1937) Nature 139, 70

ELYARD C.A. and RAWSON H. (1962) Adv. in Glass Tech., VIth Int. Congress on Glass (Plenum Press, New York)

ERNSBERGER F.M. (1960) Phys. Chem. Glasses 1, 37

ERNSBERGER F.M. (1961) Progr. Ceram. Sci. 3, 57

FOLEN V.J. (1962) J. Appl. Phys. 33, 1084

FONDA R. and YOUNG A. (1934) Gen. Electr. Rev. 37, 331

FREIMAN S.W. and HENCH L. (1972) J. Amer. Ceram. Soc. 55, 86

FRISCHAT G.H. (1968) J. Amer. Ceram. Soc. 51, 528

FULLMAN R.L. (1953) Trans. AIME 197, 447

GARIF'YANOV N.S. and TOKAREVA L.V. (1964) Sov. Phys.-Sol.St. 6, 1137

GLADMAN T. and WOODHEAD J.H. (1960) J. Iron Steel Inst. 194, 189

GLADMAN T. (1963) J. Iron Steel Inst. 201, 1044

GLAVERT A.M. (1974) "Practical Methods in Electron Microscopy", vol. 1 (North Holland Pub. Co.)

GLAZE F.W., FLORENCE J.M., HAHNER C.H. and STAIR R. (1948) J. Amer. Ceram. Soc. 31, 328

GLAZE F.W., ALLHOUSE C.C., FLORENCE J.M. and HAHNER C.H. (1950) J. Res. Nat. Bur. Stand. 45, 121

GLAZE F.W., BLACH M.H. and FLORENCE J.M. (1953) J. Res. Nat. Bur. Stand 50, 187

GLAZE F.W. (1955) Bull. Amer. Ceram. Soc. 34, 291

GORDON J.E., MARSH D.M. and PARRATT M.E. (1959) Proc. Roy. Soc. A249, 65

GRISCOM D.L. (1973) Proc. Nato. Adv. Study Inst., p 209

GUINIER A. (1963) "X-ray Diffraction" (W.H. Freeman and Co.)

HALL E.O. (1951) Proc. Phys. Soc. London B64, 747

HARPER H., JAMES P.F. and McMILLAN P.W. (1970) Disc. Farad. Soc. 50, 206

HARRISON A.J. (1947) J. Amer. Ceram. Soc. 30, 362

HASS G. (1950) J. Amer. Ceram. Soc. 33, 353

HASS G. and SALZBERG C.D. (1954) J. Opt. Soc. Amer. 44, 181

HASSELMAN D.P.H. and FULRATH R.M. (1966) J. Amer. Ceram. Soc. 49, 68

HAWARD R.N. (1949) "Strength of Plastics and Glass" (Cleaver-Hume Press, London

HAYDEN H.W., MOFFATT W.G. and WULFF J. (1965) "The Structure and Properties of Materials", vol. 3 (Wiley, New York)

HENDERSON S.T. and MARSDEN A.M. (1972) "Lamps and Lighting" (Edward Arnold, London)

HERBERT J. (1963) Genie Chim. 90, 135

HILLIARD J.E. and CAHN J.W. (1964) Trans. AIME 221, 344

HING P. and McMILLAN P.W. (1973) J. Mater. Sci. 8, 340

HING P. and McMILLAN P.W. (1973) J. Mater. Sci. 8, 1041

HIRAYAMA C., CASTLE J.G. and KURIYAMA M. (1968) Phys. Chem. Glasses 9, 109

HOPPER R.W., SCHERER G. and UHLMANN D.R. (1974) J. Non Cryst. Solids 15, 45

HOWARD R.T. and COHEN M. (1947) AIME Technical Publication No. 2215

HUGGINS M.L. and SUN K.H. (1943) J. Amer. Ceram. Soc. 26, 4

JA Y.H. (1970) Aust. J. Phys. 23, 299

JACKSON K.A. (1974) J. of Crystal Growth 24/25, 130

JAMES P.F. and McMILLAN P.W. (1968) Phil. Mag. 18, 863

JAMES P.F. and McMILLAN P.W. (1971) J. Mater.Sci. 6, 1345

JAMES P.F. and KEOWN S.R. (1974) Phil. Mag. 30, 789

JAMES P.F. (1974) Phys. Chem. Glasses 15, 95

JANAKIRAMRAO B.V. (1964) Glass Tech. 5, 67

KALININ M.I. and PODUSHKO E.V. (1964) "The Structure of Glass", vol. 3 (Consultants Bureau, New York) p. 172

KAMEL R. (1953) J. Appl. Phys. 24, 1308

KARAPETYAN G.O., TSEKHOMSKII V.A. and YUDIN D.M. (1963) Sov. Phys-Sol.St. 5, 456

KARAPETYAN G.O., KONDRAT'EV Yu.N. and YUDIN D.M. (1964) Sov. Phys-Sol.St. 6, 1219

KAY J.F. and DOREMUS R.H. (1974) J. Amer. Ceram. Soc. 57, 480

KINGERY W.D. (1958) "Ceramic Fabrication Processes" (Wiley, New York)

KONDRAT'EV Yu.N. (1965) "The Structure of Glass" vol 7, (Consultants Bureau, New York) p.221

KURKJIAN C.R. and SIGETY E.A. (1968) Phys. Chem. Glasses 9, 73

LANCASTER G. (1967) J. Mater. Sci. 2, 489

LANDOLT-BÖRNSTEIN (1950) "Numerical Data and Functional Relationships" (Springer-Verlag, Berlin)

LEE S. and BRAY P.J. (1962) Phys. Chem. Glasses 3, 37

LONGHURST R.S. (1970) "Geometrical and Physical Optics" (Longman, London)

LOVERIDGE D. and PARKE S. (1971) Phys. Chem. Glasses 12, 19

LOW W. and OFFENBACHER E.L. (1965) Solid State Phys. 17, 135

LUNTER S.G., KARAPETYAN G.O., BOKIN N.M. and YUDIN D.M. (1968) Sov.Phys-Sol.St. 9, 2259

MACDOWELL J.F. and BEALL G.H. (1969) J. Amer. Ceram. Soc. 52, 17

MATUSITA K., SAKKA S., MAKI T. and TASHIRO H. (1975) J. Mater.Sci. 10, 94

McINTOSH R.M., TURNOCK A. and WILBURN F.W. (1974) Trans. J. Brit. Ceram.Soc. 73, 117

McMILLAN P.W. (1964) "Glass-Ceramics" (Academic Press,New York)

McMILLAN P.W., HODGSON B.P. and BOOTH R.E. (1969) J. Mater. Sci 4, 1029

McMILLAN P.W. (1974) Proc. Xth Int. Cong. on Glass 14, 1

MIE G. (1908) Ann. Physik 25, 377

MOON D.W., AITKEN J.M., MacCRONE R.K. and CIELOSZYK G.S. (1975) Phys. Chem. Glasses 16, 91

MOORE H. and McMILLAN P.W. (1956) Trans. Soc. Glass Tech. 40, 139T

MOREY G.W. (1954) "Properties of Glass" (Reinhold Pub. Co. New York)

NATIONAL RESEARCH COUNCIL (1926) "International Critical Tables" (McGraw-Hill, New York)

NAVARRO F. (1976) Glastech. Berichte 49, 82

NEILSON G.F. (1970)a Final Scientific Report, Owens-Illinois Inc.

NEILSON G.F. (1970)b Disc. Farad. Soc. 50, 145

NEILSON G.F. (1971) Adv. in Nucl. and Cryst. in Glasses, Am. Ceram. Soc. p73

NEILSON G.F. (1972) J. Appl. Phys. 43, 3728

NEUROTH N. (1975) U.S. Pat. 3,928,229

OCKAWA A. (1975) "Crystal Growth and Characterization", ed. Ueda R. and Mullin J.B.(North Holland Pub. Co., Amsterdam) p.5

OROWAN E. (1949) Rep. Prog. Phys. 12, 185

ORR C. and DALLAVALLE J.M. (1959) "Fine Paticle Measurement" (MacMillan Co., New York)

ORTON J.W. (1968) "Electron Paramagnetic Resonance" (London Iliffe Books Ltd.)

PARTRIDGE G. and McMILLAN P.W. (1963) Glass. Tech. 4, 173

PAVLUSHKIN N.M. and ELIERN G.A. (1974) Trudy No. 55 Moscow Khimiko-Tekhno. Inst. im. Mendeleyeva p.74

PAVLUSHKIN N.M., KHODCKOVSKAYA R.J. and ORLOVA L.A. (1971) 1Xth Int. Cong. on Glass. Scientific and Technical Communication vol 2. (ed. Institut du Verre, France)

PAVLUSHKIN N.M., KHODCKOVSKAYA R.J., ORLOVA L.A. and ORLOV V.V. (1974) Izv. Akad. Nauk SSR-Neorganicheskie Materialy 10, 1852

PETCH N. (1953) J. Iron Steel Inst. 174, 25

PETROVSKII G.T., KRESTNIKOVA E.N. and GREBENSHCHIKOVA N.I. (1964) "The Structure of Glass", vol. 3. (Consultants Bureau, New York) p.77

PETROVSKII G.T., KRESTNIKOVA E.N., GREBENSHCHIKOVA N.I. and PROSKURYAKOV M.V. (1965) "The Structure of Glass", vol.7. (Consultants Bureau, New York) p.150

PETZOLDT J.(1970) Glastech. Berichte 43, 127

PROD'HOMME M. (1968) Phys, Chem. Glasses 9, 101

RAMPLEY D.N. (1973) Lab. Practice (Nov. 1973) p.676

RAWSON H. (1967) "Inorganic Glass-Forming Systems" (Academic Press, New York)

RAY N.H. and STACEY M.H. (1969) J. Mater. Sci. 4, 73

RAYLEIGH (1871) Phil. Mag. 4(XLI) 274,447

RAYLEIGH (1881) Phil. Mag. 4(XII) 81

RAYLEIGH (1899) Phil. Mag. 4(XLVII) 375

de REAUMUR M. (1739) Mem. Acad. Sci. p.370

REXER E. (1932) Z. Phys. 76, 735

ROGERS P.S. (1970) Mineral. Mag. 37, 741

SANDS R.H. (1955) Phys. Rev. 99, 1222

SCHLIEFER P., JARZMIK B. and KUCHARSKI J. (1968) Szklo i Ceramika 19, 97

SCHMOCKER V., BOESCH H.R. and WALDNER F. (1972) Phys. Letters 40A, 237

SCHOLES S. (1975) J. Non. Cryst. Solids 19, 167

SCHOLES S., WILKINSON F.C.F., ROGERS P.S., TIPPLE A.J. and WILLIAMSON J. (1975) J. Non Cryst. Solids 19, 145

SCHOLZE H. (1959) Glastech. Berichte 32, 81, 142,and 278

SCHREURS J.W.H. (1967) J. Chem. Phys. 47, 818

SELLERS C.M. and SMITH A.F. (1967) J. Mater. Sci. 2, 521

SEWARD T.P., UHLMANN D.R. and TURNBULL D. (1967) J. Amer. Ceram. Soc. 50, 25

SHAFFER J.S., FARACH H.A. and POOLE C.P. (1976) Phys. Rev.B. 13, 1869

SIDDALL G. (1960) European Regional Conf. on Electron Microscopy 1, 584

SIDOROV T.A. and TYUL'KIN V.A. (1971) Inorg. Mater. (Consultants Bureau Transl.) 7, 47

SIGEL G.H. and GINTHER R.J. (1974) J. Non Cryst. Solids 13, 372

SMOTHERS W.J. and CHIANG Yao (1958) "Differential Thermal Analysis: Theory of Practice" (Chem. Pub. Co. Inc., New York)

STANWORTH J.E. (1950) "Physical Properties of Glass" (Oxford Univ. Press)
STEELE F.N. and DOUGLAS R.W. (1965) Phys. Chem. Glasses 6, 246
STEVELS J.M. (1948) "Progress in the Theory of the Physical Properties of Glass" (Elsevier Pub. Co., Amsterdam)

STOOKEY S.D. (1953) Ind. Eng. Chem. 45, 115

STOOKEY S.D. (1954) Ind. Eng. Chem. 51, 805

STOOKEY S.D. (1962) Symposium on Nucl. and Cryst. in Glasses and Melts, Amer. Ceram. Soc. p.1

STRATTON J.A. (1944) "Electromagnetic Theory" (McGraw-Hill, New York)

STROH A.N. (1955) Phil. Mag. 46, 968

SUGIURA Y. (1960) J. Phys. Soc. Japan. 15, 1217

SWYLER K.J., HARDY W.H. and LEVY P.W. (1973) Brookhaven Nat. Lab. Report 20253

TAMMANN G. (1925) "The States of Aggregation" (D.van Nostrand Co., New York)

TASHIRO M. and SAKKA S. (1964) Inst. of Chem. Research, Kyoto Univ. Bull. 42, 351 351

TASHRO M. and SAKKA S. (1966) Glass Ind. 47, 428

THOMSON E. (1930) J. of Geology 38, 193

TOROPOV N.A. and SIRAZHIDDINOV N.A. (1966) Inorg. Mater. (Consultants Bureau Transl.) 2, 633

TOWNSEND P.D. and KELLY J.C. (1973) "Colour Centres and Impurities in Insulators and Semiconductors" (Sussex Univ. Press)

TUCKER R.F. (1962) Adv. in Glass Tech., VIth Int. Congress on Glass p.103

TUDOROVSKAYA N.A. and SHERSTYUK A.I. (1964) "The Structure of Glass" vol 3. (Consultants Bureau, New York) p.126

TURCHINOVICH L.M. and ADLER Yu.P. (1973) Fiziko Khim. Mekh. Mat. 9, 27

TURKALO A.M. (1968) J. Amer. Ceram. Soc. 51, 470

TYUL'KIN V.A. (1971) Inorg. Mater. (Consultants Bureau Transl.) 7, 1986

UHLMANN D.R. (1971) Adv. in Nucl. and Cryst. in Glasses, Amer. Ceram. Soc. p.91

UTSUMI Y. and SAKKA S. (1970) J. Amer. Ceram. Soc. 53, 286

VAISFELD N.M. (1971) J. Non Cryst. Solids 6, 283

VARGIN V.V. and MILYUKOV E.M. (1968) J. Appl. Chem. USSR (Consultants Bureau Transl.) 41, 177

VOLF M.B. (1961) "Technical Glasses" (Pitman and Sons Ltd., London)

VREESWIJK J.C.A., GOSSINK R.G. and STEVLES J.M. (1974) J. Non Cryst. Solids 16, 15

WATENABE M., CAPORALI R.V. and MOULD R.E. (1962) Symp. on Nucl. and Cryst. in Glasses and Melts, Amer. Ceram. Soc. p.23

WEEKS R.A. (1963) Phys. Rev. 130, 570

WEYL W.A. and MARBOE E.C. (1962) "The Constitution of Glasses", vol. 1. (Wiley, New York)

WHEELDON J.W. (1959) Brit. J. Appl. Phys. 10, 295

WICKMAN H., KLEIN M.P. and SHIRLEY D.A. (1965) J. Chem. Phys. 42, 2113

van WIERINGEN J.S. and KATS A. (1957) Philips Res. Rep. 12, 432

WILLIAMS E.L. (1965) J. Amer. Ceram. Soc. 48, 190

WONG J. and ANGELL C.A. (1971) Appl. Spectr. Revs. 4, 200

YAMANE M. and MACKENZIE J.D. (1974) J. Non Cryst. Solids 15, 153

YAMANE M. and SAKAINO T. (1974) Glass Tech. 15, 134

ZARZYCKI J. (1973) Recent Adv. Sci. Tech. Mater. (Proc. Cairo Solid State Conf.-Plenum Press, New York) p.193

ZDANIEWSKI W. (1975) J. Amer. Ceram. Soc. 58, 163

ZENER C.M. (1952) "Elasticity and Anelasticity of Metals" (Univ. Chicago Press) p.154